A Framework for A Risk Assessment of the Delineation of Wellhead Protection Areas

by

Dougall James Miln Harvey, M.Eng., P.Eng.

A thesis
presented to the University of Waterloo
in fulfilment of the
thesis requirement for the degree of

Doctor of Philosophy
in
Civil Engineering

Waterloo, Ontario, Canada, 1999

© Dougall James Miln Harvey, 1999

National Library of Canada
Acquisitions and Bibliographic Services
395 Wellington Street
Ottawa ON K1A 0N4
Canada

Bibliothèque nationale du Canada
Acquisitions et services bibliographiques
395, rue Wellington
Ottawa ON K1A 0N4
Canada

Your file Votre référence

Our file Notre référence

The author has granted a non-exclusive licence allowing the National Library of Canada to reproduce, loan, distribute or sell copies of this thesis in microform, paper or electronic formats.

L'auteur a accordé une licence non exclusive permettant à la Bibliothèque nationale du Canada de reproduire, prêter, distribuer ou vendre des copies de cette thèse sous la forme de microfiche/film, de reproduction sur papier ou sur format électronique.

The author retains ownership of the copyright in this thesis. Neither the thesis nor substantial extracts from it may be printed or otherwise reproduced without the author's permission.

L'auteur conserve la propriété du droit d'auteur qui protège cette thèse. Ni la thèse ni des extraits substantiels de celle-ci ne doivent être imprimés ou autrement reproduits sans son autorisation.

0-612-44764-2

Canada

The University of Waterloo requires the signatures of all persons using or photocopying this thesis. Please sign below, and give address and date.

ABSTRACT

Groundwater protection has become an important component of regional planning and engineering as a result of the large risk that is associated with the contamination of groundwater aquifers, their values as a resource to society and the high cost associated with remediation. One of the methods that has been proposed for the protection of regional groundwater aquifers is to zone a boundary around current production wells as a groundwater conservancy area in order to restrict risky industrial practises within the hydrogeologic environment from which public water supply wells draw their groundwater. The USEPA has detailed a methodology for generating the boundary around a production well and designated the area within this boundary as a wellhead protection area (WHPA). However, all of the methods that are currently consider acceptable for WHPA delineation do not necessarily provide the best alternative for determining the WHPA boundary when approached from a benefit-cost-risk perspective. The risk associated with WHPA delineation is related to the improper zoning of land that is not necessary for groundwater protection under the criteria and constraints set out in the Wellhead Protection Plan.

The present research developed a Wellhead Protection (WHP) Plan for the community of Pleasant Plains, New Jersey using information from State WHP plans that have submitted to the USEPA for approval. The Pleasant Plains WHP Plan sets out the criteria and constraints that are necessary for WHPA delineation at the municipal wellfields, and will be used as a basis for determining the best methodology for WHPA delineation. The delineation methods that were compared include arbitrary and calculated fixed radii, analytical methods, analytical and numerical models as detailed by the USEPA, as well as random walk numerical modeling. The research compared these methodologies to determine the best alternative for WHPA delineation, and the regret associated with not using the most scientifically defensible method of delineating groundwater protection areas. The results indicate that the best alternative for generating wellhead protection areas is based on numerical modeling that includes the affects of both advection and dispersion. The results also show that there is a reduction in risk associated with being closer to the "true" WHPA boundary based on the constraints set out in the WHP Plan.

Uncertainty analysis was then performed on the numerical WHPA models to determine the value of information associated with the uncertainty in the input parameters of the conceptual model of the groundwater environment around the study site. This value of information represents the maximum exploration and sampling budget that should be put toward obtaining new data to reduce input uncertainty to the numerical model for delineating WHPA boundaries. Finally, the transient nature of hydrologic stresses on the groundwater flow field was investigated to determine their effect on the WHPA boundaries. These transient effects include changes to the pumping rates for existing wells, the addition of new wells to the wellfield, and the decommissioning of contaminated wells in an existing wellfield. The results show that the best option for WHPA delineation uses sustainable well rates to reduce the effects of changing pumping rates, that new wells having an effect on existing WHPA boundaries must be analysed using the same methods that were used to generate the existing boundaries, and that the decommissioning of existing well should not be used to change existing boundaries.

ACKNOWLEDGEMENTS

The author would like to thank the Department of Civil Engineering for providing me with the resources and direction that were necessary to fully develop the research that I have been persuing for the past 5 years. I would also like to express my sincere thanks to Dr. J.F. Sykes for his guidance and patience during my tenure at the University of Waterloo. I would like to thank the Natural Sciences and Engineering Research Council of Canada for partial funding of this research project.

Finally, I am eternally grateful to my wife Kimberley Ann Thompson and my son Seamus Dougall Miln Harvey for their moral support, encouragement, patience and understanding, without which I would not have been able to complete the work that I undertook.

"It is the mark of an instructed mind to rest satisfied with the degree of precision which the nature of the subject permits, and not to seek an exactness where only an approximation of the truth is possible"

Aristotle

TABLE OF CONTENTS

Title	Page No.
TITLE PAGE	i
ABSTRACT	iv
ACKNOWLEDGEMENTS	v
TABLE OF CONTENTS	vii
LIST OF TABLES	x
LIST OF FIGURES	xi
LIST OF APPENDICES	xv
CHAPTER 1 - INTRODUCTION	**1**
1.1 General	1
1.2 Rationale	1
1.3 Scope	4
CHAPTER 2 - BACKGROUND AND LITERATURE REVIEW	**6**
2.1 Risk Assessment of Groundwater Contamination	6
2.1.1 Introduction	6
2.1.2 Risk-Based Screening Models	7
2.1.3 Hydrogeologic Decision Analysis	8
2.1.4 Uncertainty in Hydrogeologic Analysis	11
2.1.5 Expected Opportunity Loss	14
2.2 Wellhead Protection Areas	16
2.2.1 Introduction	16
2.2.2 Groundwater Capture Zone Research	17
2.2.3 Wellhead Protection Area Research	19
2.3 Exposure Assessment Modeling	21
2.3.1 Groundwater Flow and Contaminant Transport	21
2.3.2 Advective Particle Tracking	26
2.3.3 Random Walk Particle Tracking	27
2.3.4 Transient Modeling	29
2.4 Summary	29
CHAPTER 3 - REICH FARM SUPERFUND SITE	**31**
3.1 Introduction	31
3.2 The Reich Farm Superfund Site	31
3.3 Model Sensitivity	44
3.3.1 Groundwater Head as a Performance Measure	47
3.3.2 Groundwater Head Through Each Wellfield	50

3.3.3 Capture Zone Area as a Performance Measure 53
3.4 Summary 56

CHAPTER 4 – DECISION ANALYSIS FOR WHPA DELINEATION 58

4.1 Introduction 58
4.2 The Philosophical Basis Underlying Groundwater Protection 58
4.3 Wellhead Protection Plan 61
4.4 Environmental Decision Making for Delineating WHPAs 63
4.4.1 The Benefits and Costs of WHPA Delineation 63
4.4.2 The Risk of WHPA Delineation 64
4.4.2.1 The Cost of Failure for WHPA Delineation 66
4.4.2.2 The Probability of Failure for WHPA Delineation 70
4.5 Methods of WHPA Delineation 74
4.5.1 Introduction 74
4.5.2 USEPA Delineation Techniques 74
4.5.3 Numerical Modeling Delineation Techniques 77
4.6 WHPA Decision Making 77
4.6.1 Delineation of All Potential WHPA Boundaries 78
4.6.2 Zone I, II and III WHPA Boundaries 78
4.6.2.1 The Zone I WHPA Boundary 94
4.6.2.2 The Zone II and Zone III WHPA Boundaries 99
4.7 Discussion 109
4.8 Summary 109

CHAPTER 5 - REGRET ANALYSIS FOR WHPA DELINEATION 112

5.1 Introduction 112
5.2 Regret Analysis of WHPA Delineation 112
5.2.1 The Zone I WHPA Boundary 112
5.2.2 The Zone II and Zone III WHPA Boundaries 115
5.3 Discussion 129
5.4 Summary 130

CHAPTER 6 – NUMERICAL WHPA MODEL UNCERTAINTY 131

6.1 Introduction 131
6.2 First Order Second Moment Analysis 131
6.3 Stochastic Analysis 136
6.3.1 Analysis of STLINE Modeling 141
6.3.2 Analysis of RWAPT Modeling 149
6.4 Summary 159

CHAPTER 7 - TRANSIENT ANALYSIS OF WHPA DELINEATON **161**

7.1 Introduction 161
7.2 The Transient Nature of Groundwater Caputer Zones 161
7.3 Transient Capture Zone Analysis 169
7.4 Sustainable Well Yield Analysis 170
7.5 Addition of New Wells to the Wellfield 176
7.6 Decommissioning of an Existing Well at the Wellfield 180
7.7 Discussion 183
7.8 Summary 183

CHAPTER 8 - DISCUSSION **184**

8.1 Introduction 184
8.2 The Flexibility of the Decision Making Paradigm 184
8.3 The Robustness of the Decision Making Paradigm 185
8.4 Application to Three-Dimensional Groundwater Flow Analysis 187
8.5 Application of WHPA Boundaries to Other Environmental Decisions 188
8.6 Accounting for Contaminants in the Decision Making Process 188
8.7 Accounting for Non-Point Source Pollutants 190
8.8 The Use of Geographic Information Systems for Decision Making 191
8.9 Summary 191

CHAPTER 9 - CONCLUSIONS AND RECOMMENDATIONS **193**

CHAPTER 10 - REFERENCES **197**

LIST OF TABLES

Table 3.1: Model Layers for SWIFT Modeling of the Cohansey Aquifer 33
Table 3.2: Average Annual Well Pumping Rates for UWTR Wells (1971-1995) 37
Table 3.3: Well Pumping Rates for the Sensitivity Analysis of Model Performance 50
Table 3.4: The Sensitivity of Capture Zone Area as a Performance Measure 56
Table 4.1: The Number of State WHP Plans Using Each Method of Delineation 62
Table 4.2: Distances Used For Applying Arbitrary Fixed Radius Modeling 62
Table 4.3: Travel Times Used for Applying Analytical and Numerical WHPA Modeling 62
Table 4.4: Types and Costs of Failure for WHPA Delineation 69
Table 4.5: Probability of Model Failure for Each WHPA Modeling Technique 72
Table 4.6: Probability of Failure for Each Arbitrary Fixed Radius Distance 73
Table 4.7: Probability of Criterion Choice for Each Particle Time of Travel 73
Table 4.8: Probability of Failure for Time of Travel Based Modeling Techniques 73
Table 4.9: Average Parameter Values for Uniform Flow Equation Analysis 76
Table 4.10: Parameter Values for RESSQC, GPTRAC and MWCAP Analysis 76
Table 4.11: The WHPA Boundary Area for Each Potential Zone I Boundary 97
Table 4.12: Failure Areas (ZDUs) for Each Zone I Boundary 97
Table 4.13: The Net Present Worth Costs of Delineating Zone I WHPAs 98
Table 4.14: The WHPA Boundary Areas for Potential Zone II and III Boundaries 107
Table 4.15: Failure Areas (ZDUs) for Each Zone II and Zone III Boundary 107
Table 4.16: The Net Present Worth Costs of Delineating Zone II and Zone III WHPAs 108
Table 5.1: Failure Areas for Regret Analysis of the Zone I Boundary 124
Table 5.2: The Regret Associated with Using Non-Optimal Boundaries to Delineate Zone I WHPAs 125
Table 5.3: Failure Areas for the Zone II and Zone III Boundary 126
Table 5.4: Failure Areas for the Zone II and Zone III Boundary 127
Table 5.5: Regret Analysis of Methods for Zone II and III Boundary Delineation 128
Table 5.6: Failure Areas for the Zone II and Zone III Boundaries 129
Table 6.1: Statistical Moments for Uncertain Parameter Values at the Study Site 132
Table 6.2: Contributions of Input Uncertainty to Total Capture Zone Area Variance 136
Table 6.3: A Summary of the Statistical Parameters from STLINE Uncertainty 141
Table 6.4: A Summary of the Statistical Parameters from RWAPT Uncertainty 155
Table 7.1: Capture Zone Areas Based on Yearly Values of Well Pumping Rates 169
Table 7.2: A Comparison of WHPA Areas Based on Transient Analysis 170
Table 7.3: A Comparison of WHPA Areas Based on Sustainable Well Yield 173
Table 7.4: A Comparison of WHPA Areas Based on the Addition of Well 44 176

LIST OF FIGURES

Figure 2.1: Boundary Conditions for the Conceptual Model of a Study Site 22
Figure 2.2: Grid Block Discretization in the X Direction 24
Figure 3.1: Location of the Hydrogeologic and Hydrologic Features of the Study Site 32
Figure 3.2: Finite Difference Grid of the Conceptual Model of the Study Site 34
Figure 3.3: The Location of the Pumping Wells for the UWTR Wellfields 35
Figure 3.4: Steady State Hydraulic Head Field at the Study Site Prior to Pumping 36
Figure 3.5: Forward Particle Tracking to Identify Prepumping Contaminant Particle Pathways 38
Figure 3.6: Annual Pump Rates for the United Water Toms River Wellheads (1970 - 1995) 39
Figure 3.7: Calibrated Steady State Hydraulic Head Field for the Study Site (feet) 41
Figure 3.8: Forward Particle Pathlines Emanating from the Study Site Under the Influence of Advection 42
Figure 3.9: The 180 Day, 5 Year and 10 Year STLINE Capture Zones for the UWTR Wellfields 43
Figure 3.10: Forward Particle Pathlines Using RWAPT Modeling of Advection-Dispersion 45
Figure 3.11: The 10 Year STLINE and RWAPT Capture Zones for the UWTR Wellfields 46
Figure 3.12: Normalized Sensitivity of Groundwater Head to Well 20 Pumping Rate 48
Figure 3.13: Normalized Sensitivity of Groundwater Head to Parkway Wellfield Pumping Rate 49
Figure 3.14: Normalized Sensitivity of Groundwater Head to Net Infiltration 51
Figure 3.15: Normalized Sensitivity of Groundwater Head to Hydraulic Conductivity 52
Figure 3.16: Location of the Transect Lines and Associated Grid Block Centers 54
Figure 3.17: The Normalized Sensitivity Values for Grid Block Head Along Transect 1 55
Figure 3.18: The Normalized Sensitivity Values for Grid Block Head Along Transect 2 55
Figure 4.1: The ZOC, ZDU and ZOU Parameters That Define WHPA Uncertainty 66
Figure 4.2: Failure Areas for a Three-Tiered Approach to WHPA Zoning 67
Figure 4.3: The Zone I WHPA Boundaries Using Arbitrary and Calculated Fixed Radii 79
Figure 4.4: The Zone II WHPA Boundaries Using Calculated Fixed Radii 80
Figure 4.5: The Zone II WHPA Boundaries Using the Uniform Flow Analytical Model 81
Figure 4.6: The Zone II WHPA Boundaries Using GPTRAC, RESSQC and MWCAP 82
Figure 4.7: The Zone II WHPA Boundaries Using STLINE and RWAPT 83

Figure 4.8: The Zone III WHPA Boundaries Using Calculated Fixed Radii 84
Figure 4.9: The Zone III WHPA Boundaries Using the Uniform Flow Analytical Model 85
Figure 4.10: The Zone III WHPA Boundaries Using GPTRAC, RESSQC and MWCAP 86
Figure 4.11: The Zone III WHPA Boundaries Using STLINE and RWAPT 87
Figure 4.12: Potential Zone I WHPA Boundaries Around Well 20 88
Figure 4.13: Potential Zone I WHPA Boundaries Around the Parkway Wellfield 89
Figure 4.14: Potential Zone II WHPA Boundaries Around Well 20 90
Figure 4.15: Potential Zone II WHPA Boundaries Around the Parkway Wellfield 91
Figure 4.16: Potential Zone III WHPA Boundaries Around Well 20 92
Figure 4.17: Potential Zone III WHPA Boundaries Around the Parkway Wellfield 93
Figure 4.18: The Zone of Confidence (ZOC) for Protection Zones II and III 95
Figure 4.19: The Interaction Between the 1000 foot Zone I Boundary and ZOC II and III 96
Figure 4.20: Wellhead Protection Area Decision Making for Calculated Fixed Radii 100
Figure 4.21: Wellhead Protection Area Decision Making for The Uniform Flow Equation 101
Figure 4.22: Wellhead Protection Area Decision Making for the GPTRAC Model 102
Figure 4.23: Wellhead Protection Area Decision Making for the MWCAP Model 103
Figure 4.24: Wellhead Protection Area Decision Making for the RESSQC Model 104
Figure 4.25: Wellhead Protection Area Decision Making for the STLINE Model 105
Figure 4.26: Wellhead Protection Area Decision Making for the RWAPT Model 106
Figure 4.27: The Best Alternative for Zone I, II and III Groundwater Protection Zones 110
Figure 5.1: The Standard RWAPT WHPA Boundaries for Regret Analysis 113
Figure 5.2: Failure Associated with the Zone I Calculated Fixed Radius Boundary 114
Figure 5.3: The Interaction Between Non-Optimal and Optimal Zone I WHPA Boundaries 116
Figure 5.4: The Interaction Between Non-Optimal and Optimal Zone I WHPA Boundaries 117
Figure 5.5: Failure Areas for the Zone II and III Calculated Fixed Radii Around Well 20 118
Figure 5.6: Regret Analysis of the WHPA Boundaries Using the Uniform Flow Equation 119
Figure 5.7: Regret Analysis of the WHPA Boundaries Using the RESSQC Model 120
Figure 5.8: Regret Analysis of the WHPA Boundaries Using the GPTRAC Model 121
Figure 5.9: Regret Analysis of the WHPA Boundaries Using the MWCAP Model 122
Figure 5.10: Regret Analysis of the WHPA Boundaries Using the STLINE Model 123
Figure 6.1: The Steady State Hydraulic Head Field in the Cohansey Aquifer 133
Figure 6.2: The Variance in Head Which Results from the FOSM Method 134
Figure 6.3: The Contribution of Parameter Variance to Total Variance For Transect 1 135
Figure 6.4: The Contribution of Parameter Variance to Total Variance

For Transect 2 135
Figure 6.5: A Single Realization of a Random Hydraulic Conductivity Field 138
Figure 6.6: Normalized Probability Density of Zone III STLINE Boundary Location 140
Figure 6.7: Three Hundred Latin Hypercube Simulations of the Zone II STLINE Boundary 142
Figure 6.8: Three Hundred Latin Hypercube Simulations of the Zone III STLINE Boundary 143
Figure 6.9: The ZOC, ZOU and 50th Percentile Boundaries for 300 Zone II STLINE Simulations 144
Figure 6.10: The ZOC, ZOU and 50th Percentile Boundaries for 300 Zone III STLINE Simulations 145
Figure 6.11: A Comparison of the Deterministic and 50th Percentile Zone II STLINE Boundaries 146
Figure 6.12: A Comparison of the Deterministic and 50th Percentile Zone III STLINE Boundaries 147
Figure 6.13: A Comparison of the 50th and 95th Percentile STLINE Boundaries 148
Figure 6.14: One Hundred Latin Hypercube Simulations of the Zone II RWAPT Boundary 150
Figure 6.15: One Hundred Latin Hypercube Simulations of the Zone III RWAPT Boundary 151
Figure 6.16: Probability Density of the Zone II RWAPT WHPA Boundary 152
Figure 6.17: Probability Density of the Zone III RWAPT WHPA Boundary 152
Figure 6.18: The ZOC, ZOU and 50th Percentile Boundaries for 100 Zone II RWAPT Simulations 153
Figure 6.19: The ZOC, ZOU and 50th Percentile Boundaries for 100 Zone III RWAPT Simulations 154
Figure 6.20: A Comparison of the Deterministic and 50th Percentile Zone II RWAPT Boundaries 156
Figure 6.21: A Comparison of the Deterministic and 50th Percentile Zone III RWAPT Boundaries 157
Figure 6.22: A Comparison of the 50th and 95th Percentile RWAPT Boundaries 158
Figure 7.1: The Zone III WHPA Boundary for Well 20 Based on the 1971 Pumping Rate 162
Figure 7.2: The Zone III WHPA Boundaries Based on the 1972 Pumping Rates 163
Figure 7.3: The Zone III WHPA Boundaries Based on the 1973 Pumping Rates 164
Figure 7.4: The Zone III WHPA Boundaries Based on the 1974 Pumping Rates 165
Figure 7.5: The Zone III WHPA Boundaries Based on the 1975 Pumping Rates 166
Figure 7.6: The Zone III WHPA Boundaries Based on the 1985 Pumping Rates 167
Figure 7.7: The Zone III WHPA Boundaries Based on the 1995 Pumping Rates 168
Figure 7.8: The Zone II STLINE Boundaries using Transient Particle Tracking Analysis 171
Figure 7.9: The Zone III STLINE Boundary using Transient Particle

Tracking Analysis 172
Figure 7.10: The Zone II STLINE Boundaries Based on Sustainable Well Yield Analysis 174
Figure 7.11: The Zone III STLINE Boundaries Based on Sustainable Well Yield Analysis 175
Figure 7.12: The Location of Additional Well 44 in Proximity to the UWTR Wellfields 177
Figure 7.13: The Zone II STLINE Boundary Based on Sustainable Well Yields for 7 Wellheads 178
Figure 7.14: The Zone III STLINE Boundary Based on Sustainable Well Yields for 7 Wellheads 179
Figure 7.15: The Change in the Zone III WHPA Boundary With the Addidion Of Well 44 181
Figure 7.16: A Comparison of the WHPA Boundaries Based on the Decommissioning of Well 26 182

LIST OF APPENDICES

APPENDIX I	FORTRAN Code for CAPZON.FOR	203
APPENDIX II	FORTRAN Code for RWAPT.FOR	209
APPENDIX III	FORTRAN Code for CZAREA.FOR	217
APPENDIX IV	FORTRAN Code for UNIFORM.FOR	219
APPENDIX V	FORTRAN Code for CZSTAT.FOR	222

CHAPTER 1
INTRODUCTION

1.1 General

Over the past twenty years it has become increasingly evident that the groundwater environment is being contaminated by hazardous chemicals from a variety of anthropogenic activities. These activities include point sources of pollution (municipal solid waste landfills, industrial waste transport, storage and treatment facilities, underground storage tanks, private septic systems) and non-point sources of pollution (pesticide, herbicide and fertilizer application to agricultural land, feedlots, sludge application to land). The contaminants that have evolved from these sources, in many instances, have caused complex contaminant plumes as a result of advection, diffusion, dispersion and reaction in the groundwater environment.

These groundwater contaminant plumes pose a risk to human health through public water supply systems that rely on sensitive aquifers as the source of their drinking water. Groundwater is a principle source of water for many communities in North America including the Regional Municipality of Waterloo, which uses groundwater for approximately 92% of its drinking water. As a result of the potential for contamination of sensitive aquifers, municipal supply wells located in these aquifers are at risk and this could potentially place the public at risk if any contaminants were to enter a water distribution system. As a result of this risk of contamination, it has become important for municipalities to protect drinking water aquifers using groundwater protection initiatives.

1.2 Rationale

In order to protect sensitive aquifers from contamination it has been suggested that the area surrounding each municipal supply well be protected by a conservancy area, called a wellhead protection area, in which industrial development is highly regulated. The process of delineating wellhead protection areas (WHPAs) was first introduced in North America as a part of the Wellhead Protection Program by the United States Environmental Protection Agency (USEPA). The three main objectives of the Wellhead Protection Program are the delineation of WHPAs for all supply wells within a region, the identification of any potential contaminant sources and the identification of any methods that may be used to control the possibility of groundwater contamination (USEPA, 1991).

In order to delineate a wellhead protection area around a municipal wellfield there are a number of methods that are considered acceptable and these methods range from the use of circles of an arbitrary radius around the wellhead to the use of complex computer models to simulate

groundwater flow and transport. For the numerical modeling of WHPAs, these computer models define the groundwater flow field around the wellhead, and using advective groundwater time of travel and a reverse particle tracking model, they determine the boundary of a capture zone associated with a specific particle travel time. However, advective particle tracking is the simplest form of contaminant transport modeling. A more complex transport model, which uses both advection and dispersion to implement particle tracking, is the random walk model. The use of the random walk model to implement WHPA modeling adds one more piece of information about the hydrogeologic environment to the process of delineating WHPA boundaries.

Steady state groundwater flow modeling is the simplest form of modeling in the hydrogeologic environment. At many municipal wellfields there are multiple wells under production for water supply, and other wells that have been developed but are assigned for future use. The total pumped volume on a monthly basis fluctuates significantly for individual wells in the network, and for the entire wellfield, depending on consumer demand and changes in the hydrologic stresses to the system. If capture zones were produced based on the average pumping rate for each month of a year they would encompass different areas. This indicates that the sizes of the capture zones around a wellfield are dependent on the length of the pumping records for each wellhead. It is, therefore, necessary to look at transient fluctuations in the groundwater flow field as a part of the definition of a WHPA boundary for a wellfield. Another application for transient modeling of wellhead protection areas lies in the analysis of temporal changes in the number of wells and the associated well pumping rates that are applied to a wellfield. As new wells are developed changes occur to the pumping stresses that affect the hydraulic gradient around the wellfield. This produces transient particle pathlines and, as a result, the use of steady state reverse particle pathline analysis is inappropriate. In order to model changes in the size and shape of a capture zone it is necessary to perform a transient analysis of the hydrologic stresses placed on the groundwater flow regime.

One of the problems that must be dealt with in groundwater modeling is the determination of the confidence that can be attributed to model prediction. Over the past 20 years it has become evident that there is uncertainty in the value of many of the input parameters for groundwater flow and transport models. This uncertainty is related to the methods used to determine parameter values and the methods used to distribute these values within the conceptual model of a study site. Parameter values are determined from field testing, but field tests provide only point measurements of these values. They must be averaged and distributed spatially to determine the parameter values for each of the grid blocks within the spatial discretization of a conceptual model. Because of measurement error and spatial distribution methods, the value for each grid block parameter is not

known with certainty. A common technique for analyzing uncertainty is stochastic analysis, which assumes an *a priori* probability density function for each of the uncertain input parameters, repeatedly samples each input distribution and simulates groundwater flow and transport. The results of model simulation provide a probability density function for important output variables, which provides a measure of the uncertainty in model prediction.

The ultimate decision that must be made to protect the water quality of an aquifer is the choice of where to zone a wellhead protection area boundary. The designation of an area as a WHPA has many ramifications on the way that municipal development may occur, and the way that industries will conduct business, within the vicinity of the WHPA. There will be the need to monitor the quality of groundwater around industrial sites and there may be a need to implement remedial action if a contamination event occurs. In theory there is a unique set of hydrogeologic parameters, represented by the conceptual model of a study site, which will result in the delineation of the optimal capture zone boundary. This optimal capture zone would encompass every particle pathline related to the specific time of travel that was modeled and would result in the delineation of the optimal WHPA. However, as a result of the uncertainty in defining the conceptual model of a study site the results of any single numerical model simulation may be non-optimal. The use of a non-optimal capture zone boundary for the delineation of the wellhead protection area will result in extra cost to industries that are found within the WHPA or to the municipality which must regulate development within the region. If the WHPA is too conservative, as a result of an overestimation of the groundwater time of travel, the industries on the periphery of the WHPA would incur extra costs of doing business associated with extra protection against groundwater contamination. If the WHPA is not conservative enough, as a result of an underestimation of the groundwater time of travel, the municipality would incur extra costs associated with monitoring and remediation of groundwater contaminants from industries outside of the WHPA which should have been found within it.

In order to compare the risk that is associated with various engineering decisions related to industrial development within a wellhead protection area it is necessary to use an economic decision making tool. Environmental decision making, or benefit-cost-risk analysis, provides such a tool in that it compares the benefits, costs and risks of an engineering decision. Determination of the risk associated with an engineering decision involves the calculation of the probability of failure and the cost of failure of the engineered system. The difference between the worth of the optimal engineering decision and a non-optimal decision is the opportunity loss, or regret, associated with choosing a non-optimal alternative.

An example of the need for WHPA delineation is provided by the aquifer system beneath the Reich Farm Superfund site. A number of water supply wells, owned and operated by United Water Toms River, are completed in a phreatic aquifer near Pleasant Plains, New Jersey. A source of trichloroethene (TCE) and tetrachloroethene (PCE) contamination was discovered at Reich Farm upgradient of these wells within the ultimate capture zone of the wellfield. From this contaminant source, a plume of TCE and PCE migrated over 1500 meters to the supply wellfield. Analysis of the groundwater flow system using reverse particle tracking may be used to identify the limits of groundwater capture and thereby identify the time related sources of groundwater for these production wells. This has implications on future development within the capture zones for the United Water Toms River wellfields.

1.3 Scope

The primary objectives of the proposed research are fourfold. The first objective is to develop a decision making model that may be used to compare groundwater protection alternatives for public water supply wells. The second objective is to apply the decision making model to a set of wellhead protection area boundaries to choose the best alternative for groundwater protection. The third objective is to determine the regret associated with using a non-optimal technique for WHPA delineation and the fourth objective is to determine the value of information on model uncertainty for the numerical modeling WHPA boundaries.

These objectives will be achieved using a number of specific undertakings. In Chapter 3, the first undertaking involves choosing a suitable study site for the application of the decision making model. A steady state groundwater flow analysis is performed to reveal the hydrogeology below the study site for the application of WHPA modeling techniques. A sensitivity analysis is performed to determine the most sensitive parameter for the performance measure of groundwater head and capture zone area. Finally, a random walk model is developed for delineating WHPA boundaries using both advective and dispersive components of transport to provide an improved WHPA delineation model.

In Chapter 4, the concept of the risk of failure of wellhead protection areas is developed to provide a basis for decision making. A Wellhead Protection Plan is developed for the study site to provide the criteria and constraints that will be used for applying all methods of WHPA delineation. A set of WHPA boundaries is then generated by applying all potential WHPA delineation techniques to the wells at the study site. Finally, the decision making model is used to choose the best alternative for groundwater protection.

In Chapter 5, regret analysis is used to determine the opportunity loss, or regret, associated with choosing the non-optimal delineation technique, using the same decision making model that was developed in Chapter 4. In Chapter 6, uncertainty analysis is applied to the numerical WHPA models to determine the uncertainty associated with location of the WHPA boundary. In Chapter 7, a transient analysis is performed to determine the effect that transient pumping rates have on the best alternative for groundwater protection. Finally, a sustainable well yield analysis is performed to determine whether a more appropriate well rate can be determined for implementing WHPA delineation. In Chapter 8, a number of issues that are associated the application of decision making to WHPA delineation are discussed to place this analysis tool in the broader context of municipal planning and industrial development.

CHAPTER 2
BACKGROUND AND LITERATURE REVIEW

2.1 Risk Assessment of Groundwater Contamination

2.1.1 Introduction

Risk assessment is defined as the process of characterizing the adverse health effects of human exposure to environmental chemicals (Reichard *et al.*, 1990) and is comprised of hazard identification, exposure assessment, dose-response assessment and risk characterization. Hazard identification involves the classification of environmental chemicals that are hazardous to human health. It entails performing toxicological studies (e.g. human epidemiological studies, animal testing, *in vitro* testing, etc.) to determine the toxicity of environmental chemicals. Exposure assessment involves determining the extent to which an individual at a point of interest may be exposed to a hazard due to all potential pathways of exposure. It usually involves modeling the transport of contaminants from the potential source of a contaminant to the point of interest where there is a direct connection to human exposure. Dose-response assessment involves quantifying the increased effect of an environmental hazard due to increased exposure to an individual. It usually involves short term animal laboratory studies (e.g. rodent exposure experiments), which are used to extrapolate human exposure levels. Risk characterization is the process of summarizing the total risk from the separate components of a risk assessment.

Exposure assessment determines the level of exposure to a particular chemical or array of chemicals at a point of interest. The two primary exposure pathways that may cause the uptake of an environmental hazard are airborne transport and groundwater transport. Human uptake resulting from either of these pathways may occur as a result of inhalation, dermal absorption or ingestion. The primary means of analysis for exposure assessment from groundwater transport involves groundwater flow and transport modeling from a contaminant source to a point of compliance. This type of modeling defines the concentration of a chemical as a function of time at a point of compliance and the time of travel from the source to the point of compliance.

Risk assessment of groundwater contamination has been approached from two perspectives with respect to the time of travel from a contaminant source to a point of compliance. The first perspective involves forward particle tracking from the contaminant source. A number of different source types have been investigated including soil contamination sites, landfill sites and leaky underground tanks. The purpose of this type of modeling is to analyze the contamination of sensitive aquifers that may serve as potential groundwater resources in the future. For this type of study a

regulatory limit is set at a point of compliance, for example, the boundary of a sensitive aquifer, and the time dependent concentration of an indicator contaminant is determined at this point. The second perspective involves reverse particle tracking from the point of compliance back to the particle source based on a specific time of travel. When particles are released from the periphery of a pumping well, the particle pathline points delineate the volume of subsurface media from which the wellhead withdraws its water. The endpoints of each pathline, when they reach the ground surface may be connected to form a capture zone boundary. The area encompassed by this boundary is called a wellhead protection area if it is zoned by the municipality for groundwater protection. For this perspective, municipal wellfields have been investigated as the point of particle release and wellhead protection areas as the points of compliance.

There are a large number of potential contaminant sources in North America. For virtually all of these sources groundwater modeling could be required to identify the potential risk that these sources pose to groundwater resources and the potential that exists for the remediation of these contaminated sites (National Research Council, 1990). The benefit of groundwater modeling is that it provides a systematic methodology for analyzing many aspects of the risk associated with groundwater contamination. As a result, the use of groundwater models in this context is presently encouraged by regulatory agencies like the United States Environmental Protection Agency.

2.1.1 Risk-Based Screening Models

A number of authors have developed methodologies to assess the risk of contamination due to existing or planned activities on the hydrogeologic environment. Many of these methodologies are qualitative in nature and have been developed for the purpose of ranking pollutant sources within a zone of protection around a wellfield. The term used for these methodologies is risk-based screening models.

In 1980 under the Comprehensive Environmental Response, Compensation and Liability Act (CERCLA) the USEPA set up the National Priorities List, or Superfund List, and a Hazardous Ranking System that could be used by states to rank hazardous waste sites. Wu and Hilger (1984) evaluated the hazardous ranking system and found that it provided an expedient and consistent procedure for evaluating the hazard potential at uncontrolled waste sites, but that it was lacking in its use of local hydrogeologic conditions for the analysis. Zaporozec (1985) developed a system that uses overlay maps including a soils map, a subsurface map and a groundwater flow map for assessing the attenuative capacity of the hydrogeology within a capture zone. Wellhead protection areas were discussed as a part of the groundwater flow map though no quantitative method was given for their determination. Jennings and Suresh (1986) developed a risk penalty function for the management of

hazardous waste. This method was designed to use risk ranking and rating techniques to choose the best technology to manage a stream of industrial waste. Olivieri *et al.* (1986) developed a risk matrix system using a site sensitivity factor and a contaminant severity factor to rank potential sources of contaminants. An extension of the risk matrix system was developed by the USEPA to present a comprehensive method for determining risk numbers associated with particular contaminant sources within a capture zone (USEPA, 1991). As a part of this method contaminant transport was represented by a likelihood of release and a likelihood of reaching the well, both of which were determined using qualitative indices in the ranking system. Shook and Grantham (1993) developed a hazard ranking system specific to the state of Idaho for the protection of the Snake Plain Aquifer that is the state's largest groundwater source. The system included risk factors that related to the existence of groundwater quality management programs, the severity of the potential impact of a pollutant source and the toxicity of the pollutant to human health. DelVecchio and Haith (1993) introduced the application of Monte Carlo methods to matrix ranking techniques for comparing groundwater contamination sites. Jennings *et al.* (1994) updated their hazard ranking system to take into account parameter uncertainty by applying probabilistic distributions to the criteria weightings. The authors used Monte Carlo analysis to generate output distributions for the rating scores of each alternative. Hamed *et al.* (1995) develop a probabilistic model for screening groundwater contamination sources that used first and second order reliability methods in place of Monte Carlo analysis.

2.1.3 Hydrogeologic Decision Analysis

Risk assessment has been defined as a modeling paradigm that is used to determine the potential impact of modern industrial practises on the natural environment. Risk-based screening models represent a qualitative approach to achieve this purpose. From a quantitative perspective risk assessment has also been applied to the analysis of the impact of engineering design on the natural environment. The ultimate goal of all environmental modeling is to make the best decision based upon the information that is available. This has been accomplished using a risk-based economic decision making tool called environmental decision making.

Environmental decision making is a methodology that is used for selecting the best alternative among several acceptable design options for an engineering decision that affects the environment. Hydrogeologic decision analysis, as a subset of environmental decision making, is a form of decision making that was developed specifically to deal with the unique qualities of the subsurface environment. For the remediation of a contaminated site, acceptable design alternatives are usually related to the choice of remedial technologies to contain and/or remediate a contaminant

plume. For land use zoning, acceptable planning alternatives often relate to the choice of sites for the development of specific land-use classes. For the case of siting a high risk industry within a wellhead protection area, these alternatives are related to the design of remedial structures to prevent contaminant release into the groundwater flow system and the choice of a location for the industry.

The general form of the relationship that has been developed for hydrogeologic decision making is a benefit-cost-risk function. This function, as developed by Massmann and Freeze (1987a), is given by the following relationship:

$$NPW_j = \sum_{t=0}^{T} \frac{1}{(i+1)^t} \left[B_j(t) - C_j(t) - R_j(t) \right] \tag{2.1}$$

where: NPW_j = the net present worth of engineering project j [$]

$B_j(t)$ = benefits of project j in year t [$]

$C_j(t)$ = costs of project j in year t [$]

$R_j(t)$ = risk of failure of project j in year t [$]

i = the interest rate defining the time value of money

For a project involving groundwater contamination the risk of failure is given by:

$$R_j(t) = P_f(t) * C_f(t) * \gamma(C_f) \tag{2.2}$$

where: $P_f(t)$ = probability of failure of a monitored facility in year t [dimensionless]

$C_f(t)$ = cost of failure in year t [$]

$\gamma(C_f)$ = normalized utility function [dimensionless]

The probability of failure can be reduced by detecting a potential groundwater plume before it actually causes failure:

$$P_f(t) = P_f^u(t) * (1 - P_d) \tag{2.3}$$

where: $P_f^u(t)$ = probability of failure of an unmonitored facility in year t

P_d = probability of detection of a contaminant plume

The probability of failure is an explicit recognition of the role of uncertainty in the decision making process. It may be determined using historical data relating to the frequency of occurrence of a specific failure event, or it may be delineated using a computer model to predict system behavior. However, as a result of the lack of adequate statistics relating to the failure of most environmental designs and the diversity of factors affecting failure, computer modeling of system behavior is most commonly used to predict probable failure outcomes for an environmental system. The probability of failure, with respect to groundwater contamination, is generally defined as the probability that a contaminant plume is detected at a regulatory point of compliance.

The cost of failure involves the costs associated with the remediation of the groundwater to below health-based water quality standards at the point of compliance. These costs might include remediation costs, groundwater pumping costs or regulatory penalties and legal costs associated with the management of cleanup operations. The normalized utility function reflects the owner's aversion to causing a groundwater contaminant plume that would require remediation (Freeze *et al.*, 1990). For risk averse decision making the normalized utility function would be assigned a value greater than one resulting in a conservative estimate of the risk of failure. For risk neutral decision making the normalized utility function would be assigned a value of one.

Environmental decision making arose in water resources management as a result of the need to estimate the benefits and costs of an engineering design that could have an impact on the environment. Tschannerl (1971) looked at decision making from the perspective of reservoir design and operation based on hydrologic modeling using limited streamflow records. Baecher *et al.* (1980) applied benefit-cost-risk analysis to dam construction for which the probability of failure and the consequences of failure were determined from historical records. The concept of risk-based decision making in the groundwater environment was first introduced by Raucher (1983) with the presentation of a conceptual framework for benefit-cost analysis of groundwater protection including a discussion of the social benefits and probabilistic risks of preventing groundwater contamination. This concept was expanded upon by Massmann and Freeze (1987a; 1987b) in the context of the design of waste management facilities within the adversarial environment of regulatory compliance and market economics. The authors developed the benefit-cost-risk relationship for the purpose of designing leachate containment facilities for a waste management site. Wolka and Austin (1988) described a method for estimating the benefits of groundwater remediation based on the distribution of contaminant concentration at a potential exposure site and the duration of exposure. Marin *et al.* (1989) and Medina *et al.* (1989) used environmental decision making to assess the permitting of waste management sites under parameter uncertainty. Reichard and Evans (1989) used a form of benefit-cost-risk analysis to investigate the choice between remediating a contaminant plume and installing point-of-use groundwater treatment at potential receptor sites to reduce risk levels to homeowners with residential wells downgradient of the plume.

In a series of papers on decision making that affects the hydrogeologic environment Freeze *et al.* (1990), Massmann *et al.* (1991), Sperling *et al.* (1992) and Freeze *et al.* (1992) presented a comprehensive development of hydrogeologic decision analysis in the face of parameter uncertainty. Decision making was applied to two field situations: the siting of a waste management facility and the operation of dewatering facilities at an open-pit mine. LeGrand and Rosen (1992) discussed the

advantages of using a risk-based approach to decision making at groundwater contamination sites. James and Freeze (1993) applied hydrogeologic decision analysis to determining the need for extra borehole locations for estimating aquitard continuity below a soil contamination site. James *et al.* (1996a; 1996b) discussed the use of hydrogeologic decision analysis as a tool for choosing between continued groundwater monitoring and contaminated soil remediation at a site containing a plume of radioactive waste. Jardine *et al.* (1996) applied hydrogeologic decision analysis to the design of a groundwater monitoring network at a waste management facility located above a fracture bedrock aquifer.

2.1.4 Uncertainty in Hydrogeologic Analysis

The process of modeling the natural environment can be defined as the science of collecting a discrete set of observations and making predictions about system behavior. Model predictions are uncertain because of uncertainties about existing and future sources of contaminants, conceptual uncertainties of the modeling process and parameter uncertainty associated with the sampling process (Carrera, 1993). There is also uncertainty in modeling the natural environment because of the natural randomness of real systems, measurement error in sampling, and the limited number of observations that are used in modeling a highly variable natural system (National Research Council, 1990). To translate uncertainty in input parameters into uncertainty in output predictions the most common technique is stochastic analysis using direct parameter sampling.

For stochastic analysis it is assumed that each uncertain input parameter is a random variable that may be described by a probability density function. Each random variable is assigned an *a priori* probability density function described by the mean, variance and correlation scale of measured data values. For example, the hydraulic conductivity of each lithologic unit is usually assigned a lognormal distribution calculated from the statistics of sample measurements taken during the field testing program. The lognormal distribution is not the only distribution that may be used to describe environmental variables but it is commonly used to describe many hydrogeologic parameters (Freeze and Cherry, 1979). The uncertainty in an output parameter may then be investigated by sequential random sampling of each uncertain input parameter probability density function and computer model simulation. The uncertainty in the output is measured by the statistical moments of the output parameter probability density function.

Two parameter sampling techniques that are commonly used in stochastic analysis are Monte Carlo sampling and Latin Hypercube sampling. For Monte Carlo sampling the whole input probability density function is randomly sampled while for Latin Hypercube sampling the input probability density function is divided into equally probable increments and each increment is

randomly sampled. The use of Latin Hypercube sampling necessitates fewer model simulations to represent an equivalent output probability density function generated by Monte Carlo sampling (Iman and Conover, 1979). The chosen value of the input parameter must then be distributed spatially within the conceptual model to prepare the input for a computer model simulation. Two methods that are often used to represent the spatial distribution of a model parameter are block correlated parameter fields and random parameter fields. Block correlated parameter distribution assumes that the randomly sampled input value is applied to all of the finite difference blocks within a large area of the conceptual model. However, this is not indicative of the actual random nature of parameter distribution within the soil strata (Mantoglou and Wilson, 1982; Hoeksema and Kitanidis, 1985; Dagan, 1986). A method that generates a more realistic field of parameter values uses a random field generator. A number of methodologies exist to generate random fields of model parameter including the turning bands method, the covariance matrix method and the discrete Fourier transform method (Mantoglou and Wilson, 1982; Williams and El-Kadi, 1986; Robin *et al.*, 1993). These methodologies provide random parameter values for each grid block within a study area that are based on the mean value, variance and the correlation scale of the *a priori* probability distribution.

A number of researchers have developed stochastic techniques for the analysis of uncertainty in hydrogeologic modeling. Freeze (1975), in a seminal study on groundwater flow analysis, identified two types of uncertainty associated with deterministic modeling. The first type was associated with the "nonuniformity of the porous media" and the difficulties involved in modeling natural processes, and the second type was associated with limited information on the parameters that are inputs to the model. Smith and Schwartz (1981) identified a number of sources of uncertainty in contaminant transport modeling and used Monte Carlo sampling to investigate the uncertainty in contaminant time of travel and contaminant concentration at a receptor within a hypothetical aquifer. Mercer *et al.* (1983) applied uncertainty analysis to contaminant transport modeling of the groundwater below the Love Canal Superfund Site to determine the risk of contamination to the lower confined Lockport Dolomite aquifer. Gorelick (1983) discussed the need to address parameter uncertainty in groundwater management models that combine the use of distributed parameter groundwater hydraulic models and optimization techniques. Sykes *et al.* (1985) developed adjoint sensitivity equations for two dimensional steady state flow in an unconfined aquifer to calculate the sensitivity of nuclear waste repository performance to parameter uncertainty in modeling the groundwater flow system. Gelhar (1986) discussed the use of stochastic techniques for studying parameter uncertainty in hydrogeologic modeling and found that stochastic theory provided a unified approach that incorporates the effect of natural heterogeneity to predict both groundwater flow and

contaminant transport. La Venue *et al.* (1989) discussed the use of the first order second moment method to analyze the uncertainty in groundwater travel times for a proposed nuclear waste isolation facility and found that stochastic methods are more appropriate when the hydrogeologic system responds in a non-linear way to parameter variation. Tiedeman and Gorelick (1993) applied stochastic simulation to the optimization of plume containment of a TCE plume. Numerical groundwater modeling was used to assess the uncertainty in the design of a groundwater capture well network with particle tracking and solute transport modeled under Monte Carlo simulation to verify the validity of the optimal solution. Sykes and Harvey (1996) used random field generation of hydraulic conductivity and distribution coefficient to investigate the uncertainty in contaminant cleanup times for a Superfund site under pump and treat cleanup scenarios.

The role of parameter uncertainty in engineering decision analysis in the hydrogeologic environment was developed by Massmann and Freeze (1987a; 1987b) and later expanded upon by Freeze *et al.* (1990) and Massmann *et al.* (1991). An objective function for basing engineering decisions was developed to include a risk component that was based on computer modeling of groundwater flow and contaminant transport. The inherent uncertainty in the input parameter values to the model led the authors to conclude that the probability of failure could be reduced with increased field sampling of flow and transport parameter values. This approach to uncertainty analysis was subsequently used as a component of hydrogeologic decision analysis by a number of authors (Freeze *et al.*, 1992; James and Freeze, 1993; Wijedasa and Kemblowski, 1993; James and Gorelick, 1994; Jardine *et al.*, 1996; James *et al.*, 1996a).

Stochastic analysis necessitates the use of an algorithm to sample random values of all uncertain input parameters. Several algorithms have been developed that generate random parameter fields that are used for stochastic analysis including the spectral method, the nearest neighbor method, the turning bands method, the matrix decomposition method and the power spectral elimination method. One of the first random field generators was developed by Mejia and Rodriquez-Iturbe (1974) based on the spectral method and was intended for use in the generation of spatially varied rainfall records. Smith and Freeze (1979) developed a random field generator that produced an independent random field of values at all nodes in the field and then replaced each nodal value by a weighted average of the original nodal value and its four "nearest neighbors". The turning bands method was developed by Mantoglou and Wilson (1982) to generate two-dimensional random parameter fields. Several arbitrary points chosen within the parameter field were used to generate random numbers for all nodes in the field using a turning band line, such that each node was assigned a parameter value equal to the average of the ensemble of random values. Williams and El-Kadi

(1986) developed a method of generating two-dimensional random fields using matrix decomposition. The covariance matrix, representing the spatial structure of the parameter field, was decomposed into the lower triangular matrix, multiplied by a random vector and added to the mean value to produce one realization of the random field. Robin *et al.* (1993) developed a method that uses discrete Fourier transforms to generate two-dimensional and three-dimensional cross-correlated random fields on a regular grid. The algorithm generates random fields by applying an inverse Fourier transform to the random spectral field.

2.1.5 Expected Opportunity Loss

For every engineering decision that has an effect on the environment there is an optimal design alternative. The optimal design is associated with the value of each design variable or modeling parameter that would result in the lowest net social cost for both implementation and remediation of the contaminant plume. If perfect knowledge of the hydrogeologic system were available it would be possible to choose the optimal design. However, as a result of uncertainty in describing the physical system that represents the study site, perfect knowledge of model parameter values is not available. The ultimate decision of choosing a specific design alternative will result in either an overdesign or an underdesign. As a result there is economic regret associated with making a non-optimal decision that was first introduced by Tschannerl (1971) as the concept of expected opportunity loss.

With respect to the siting of high risk industries within a wellhead protection area, benefit-cost-risk analysis can be used to analyze the expected opportunity loss associated with a specific design alternative. This will be important in assessing the feasibility of industrial development within a wellhead protection area from the perspective of both the proponent of development and the municipality. The optimal design alternative will be the design that prevents the migration of contaminants to the WHPA boundary or that minimizes the cost of remediation. The expected opportunity loss associated with an engineering design in the hydrogeologic setting may be described by the following relationship:

$$OL_j = \left\{ C^{op} + \sum_{t=0}^{T} R^{op}(t) \right\} - \left\{ C_j^n + \sum_{t=0}^{T} R_j^n(t) \right\} \qquad (2.4)$$

where: OL_j = the opportunity loss for design j [$]

C^{op} = cost of the optimal design [$]

$R^{op}(t)$ = risk of failure for the optimal design [$]

C_j^n = cost of non-optimal design j [$]

$R_j^n(t)$ = risk of failure for the non-optimal design j [$]

In the case of underdesign, the containment structure would allow chemicals to leak into the groundwater zone subjecting the wellhead to the potential risk of contamination. This would result in extra cost to remediate the contaminant plume. In the case of overdesign, the containment structure would be designed such that there was added cost associated with the construction of a more conservative containment structure. The use of expected opportunity loss in conjunction with groundwater modeling techniques will provide decision makers with more information about the consequences, both physical and economic, of decisions that are made about siting risky industrial development within an area designated for groundwater protection.

Tschannerl (1971) established the principle of expected opportunity loss in water resources engineering by determining the loss in net benefits associated with the design of surface water storage reservoirs using limited streamflow records. It was shown that, as additional data were collected, there was a trade-off between the cost of data collection and its worth in reducing uncertainty and expected opportunity loss. Davis *et al.* (1972) analyzed expected opportunity loss for bridge design and applied it to Rillito Creek in Tucson, Arizona using short lengths of measured flow data. Reichard and Evans (1989) assessed the value of hydrogeologic information for health risk-based decision making in the context of expected opportunity loss. Net benefits of a decision were calculated using a combination of the economic cost of the decision and the social cost associated with the residual health risk that was determined from a combination of the risk of failure and the cost of failure. The authors provided a methodology for determining each of the components of net social benefit and applied it to a study case of a contaminant plume impinging upon the potable water supply for a number of homeowner wells.

Freeze *et al.* (1992) introduced the concept of opportunity loss in data worth analysis for hydrogeologic decision making. Regret was defined as "the price that must be paid for selecting the non-optimal alternative given perfect knowledge of the state". Regret was applied to the decision of building a landfill liner in the presence of uncertainty in the information regarding the continuity of an aquitard protecting a lower municipal aquifer. James and Gorelick (1994) extended the analysis of regret in hydrogeologic decision analysis with the development of a Monte Carlo based methodology for calculating regret, and used this to determine the optimal sampling program for remediation of contaminated aquifers. Regret was analyzed in terms of the difference between the cost of remediation for a project based on perfect sample information and the cost of the project based on imperfect *a priori* information. The costs involved in the objective function were calculated using the probability of plume capture and the total volume of pumped water using Monte Carlo simulation of the MODFLOW groundwater flow model.

2.2 Wellhead Protection Areas

2.2.1 Introduction

The concept of the wellhead protection area (WHPA) in North America was first detailed as part of the Wellhead Protection Program administered by the United States Environmental Protection Agency (USEPA, 1987). The Wellhead Protection Program was established under 1986 Amendments to the Safe Drinking Water Act. The Wellhead Protection amendment was designed to assist local and state authorities in the protection of groundwater resources against contamination by chemicals and microorganisms that could have adverse health effects on humans. To achieve this objective the USEPA provided a methodology that included such elements as the determination of a WHPA boundary for each well or wellfield, the identification of all anthropogenic sources of contaminants within each protection area and contingency plans for alternative water supplies in the case that contamination occurs.

The definition of a wellhead protection area is "the surface and subsurface area surrounding a water well or wellfield, supplying a public water system, through which contaminants are reasonably likely to move toward and reach such water well or wellfield" (U.S. Environmental Protection Agency, 1987). The USEPA provided a set of criteria that could be adopted by state authorities for determining the extent of the WHPA boundary. These criteria refer to the conceptual standards that form the technical basis for WHPA delineation. The five criteria that were identified include distance, drawdown, time of travel, flow boundaries and assimilative capacity. The distance criterion refers to the use of a specified radius around the wellhead. The drawdown criterion refers to the extent that the pumping well lowers the water table for an unconfined aquifer and the potentiometric surface for a confined aquifer. The time of travel criterion refers to the maximum time for a groundwater contaminant to reach the well. The flow boundary criterion refers to the location of groundwater divide or other hydrogeologic features that control groundwater flow. The assimilative capacity criterion refers to the concept of using the ability of the unsaturated and saturated zones to attenuate the concentration of contaminants within the capture zone to acceptable levels before they reach the supply well. Guidelines were provided for reasonable threshold values for each of these criteria.

The USEPA also defined a number of methods that could be used to "translate the selected criteria ... into mappable delineation boundaries" (USEPA, 1987). The six methods that were identified include arbitrary fixed radii, calculated fixed radii, simplified variable shapes, analytical methods, hydrogeologic mapping, and numerical flow and transport models. The use of arbitrary

fixed radii involves drawing circles of a specified radius around the wellfield being protected. The use of calculated fixed radii involves drawing circles representing a specified time of travel around the wellfield. The use of simplified variable shapes involves applying analytical models to generate "standardized forms" using time of travel and flow boundary criteria. The use of analytical methods involves applying hydrogeologic input parameters to calculate the groundwater divide using an analytical model such as the uniform flow equation. The use of hydrogeologic mapping involves geological and geophysical mapping to delineate the WHPA. The use of numerical flow and transport models involves applying computer models to approximate groundwater flow and transport numerically. Of these methods, numerical modeling provides the highest degree of accuracy but involves the greatest amount of time and cost for the delineation of wellhead protection areas.

2.2.2 Groundwater Capture Zone Research

One of the first research studies to delineate capture zones around pumping wells was performed by Keely and Tsang (1983). The authors defined a capture zone as "the aerial limits of the zone of the aquifer actually yielding waters to a pumping well". Drawdown effects for a well were analyzed using an analytical solution to the groundwater flow equation that was based on the assumption of a homogeneous isotropic unconfined aquifer. By imposing well drawdown results on the regional aquifer flow condition it was possible to analyze the effect of the well pumping rate on the size of the capture zone. The theoretical model development formed the basis for the RESSQ model that was subsequently applied to a study case of a pumping well near a waste injection well. RESSQ was used to solve contaminant plume movement as a function of time and the contaminant concentration breakthrough curve for the water supply well.

A number of researchers have used the USEPA definition of a capture zone to develop particle tracking codes that are either incorporated into a groundwater flow model or that use the results of a groundwater flow model to perform particle tracking. GWPATH (Shafer, 1987) uses the results of the groundwater flow model of McWhorter and Sunada to perform particle tracking. STLINE (GeoTrans Inc., 1987) is a three-dimensional particle tracking program that uses the results of both SWIFT III (Sandia Waste Isolation Flow and Transport model) and MODFLOW (Modular Flow model) to perform forward and reverse particle tracking and particle time of travel calculations. MODPATH (Pollock, 1988) and PATH3D (Zheng, 1989) are three-dimensional particle tracking codes that use the results of MODFLOW. FLOWPATH (Guiguer and Franz, 1991) is a two-dimensional steady state groundwater flow model that incorporates particle tracking and time of travel calculations. Schafer-Perini and Wilson (1991) presented a computer algorithm to delineate particle pathlines and time related capture zones based on a bilinear velocity interpolator that uses

the same five point finite difference grid block system that was used in the development of MODFLOW. Cordes and Kinzelbach (1992) developed a particle tracking program for use with a finite element flow model that maintains fluid continuity between finite element patches for the calculation of the velocity field. The USEPA developed a model, called WHPA, which contains four computer programs that delineate wellhead protection areas. These four models include: two analytical models (RESSQC and MWCAP), a semi-analytical model (GPTRAC), and an uncertainty analysis model (MONTEC) for the analytical solution to the groundwater flow equation (Blandford and Huyakorn, 1990).

Bair and Roadcap (1992) compared the ability of a number of these models to delineate capture zones in a variety of hydrogeologic environments. The authors compared three types of models (analytical, semi-analytical and numerical models) for delineating capture zones, each consisting of a component that solves the flow equation and a component that performs reverse particle tracking. The analytical model consisted of CAPZONE and GWPATH, the semi-analytical model consisted of RESSQC and DREAM, and the numerical model consisted of MODFLOW and MODPATH. Each model was applied to a fractured carbonate aquifer in Richwood, Ohio to delineate time related capture zones. MODFLOW and MODPATH were found to provide the best reliability for delineating capture zones. Springer and Bair (1992) continued the research of Bair and Roadcap (1992) by applying three types of models to a stratified drift buried valley aquifer in Wooster, Ohio, and Bates and Evans (1996) applied them to the municipal wellfield at Elmore, Ohio.

Other authors have used these models to delineate time related capture zones for specific municipal pumping wells. Eberts and Bair (1990) used MODFLOW to model capture zones for the South wellfield in Columbus, Ohio. Bair *et al.* (1990) extended this study to include particle tracking of hypothetical spills within the 2000 day capture zone for the South wellfield. Bair *et al.* (1991) used CAPZONE and GWPATH to delineate the 1 year capture zone for the municipal wellfields of North Canton, Ohio. Buxton *et al.* (1991) used MODFLOW and MODPATH to analyze the recharge areas for Long Island, New York under a number of development conditions. Barlow (1994) used MODFLOW and MODPATH to delineate areas of contribution to public water supply wells for Cape Cod, Massachusetts. Ramanarayanan *et al.* (1995) used GPTRAC and the method of characteristics to delineate the 10 year capture zones for the two municipal supply wells of Tipton, Oklahoma. Wuolo *et al.* (1995) presented an application of the analytic element method to delineate the 10 and 20 year capture zones for Brooklyn Park, Minnesota, while Bakker and Strack (1996) used the analytic element method for the delineation of time related capture zones boundaries around multiple pumping wells.

Uncertainty in the size and shape of a time related capture zone has been analyzed in a number of research studies. Bair *et al.* (1991) used Monte Carlo sampling of hydraulic conductivity and effective porosity to determine the uncertainty in the delineation of WHPAs using CAPZONE and GWPATH. The 75th and 95th percentile capture zones were chosen to represent the confidence interval for the expected value of the capture zone boundary where the 75th percentile capture zone encompasses 75% of the end points from the complete set of Monte Carlo input data points. Varljen and Shafer (1991) studied the uncertainty of the 1 and 10 year capture zones using MONTEC and GWPATH for a hypothetical aquifer and used Monte Carlo sampling of hydraulic conductivity to determine uncertainty of the 95th percentile capture zone using 300 pathlines. They found that uncertainty in a capture zone was affected by both natural hydrogeologic conditions and the pattern of sampling points for aquifer properties. Rifai *et al.* (1993) used the MONTEC model to assess uncertainty in the size and shape of the 5 year capture zones for the municipal wellfields of Houston, Texas using the 50th, 75th and 95th percentile capture zones as measures of model uncertainty. Harmsen *et al.* (1991a; 1991b) used Monte Carlo sampling of hydrogeologic parameters of the Central Wisconsin sand plain, using MODFLOW and PATH3D, to analyze uncertainty in the three-dimensional separation distance between a septic tank drainage field and a water supply well.

Akindunni *et al.* (1995) analyzed the problem of pumping a vertically stratified contaminant plume from an unconfined aquifer. Many current models used to delineate the extent of groundwater contamination are based on a two-dimensional plan view conceptualization. The authors developed a three-dimensional groundwater flow and solute transport model using the finite element method. The model assumes solute transport by advection only using a forward particle tracking algorithm. The authors found that the model appears to be an effective means of investigating three-dimensional contaminant transport to wells in an unconfined aquifer at the local scale around the well, but that because of the radial geometry used in modeling flow, the model could not include superposition of the regional flow on the drawdown data.

2.2.3 Wellhead Protection Area Research

A number of research studies have discussed the delineation of wellhead protection areas based on time related capture zones. Whittemore *et al.* (1987) used an analytic model to delineate time related capture zones for Harvey County, Kansas as a part of their proposed wellfield protection plan. Coe *et al.* (1989) delineated the 5 year capture zones for Columbus, Ohio as a part of their Wellhead Protection Program. Griswold and Donohue (1989) delineated the State of Massachusetts Zone II (180 day time of travel) protection areas for the Bondsville Fire and Water District wellfield. Guiguer and Franz (1991) used FLOWPATH to delineate the wellhead protection area for one of the

supply wells for Littleton, Massachusetts. Rifai *et al.* (1993) delineated the 5 year time of travel wellhead protection area for Houston, Texas using the MONTEC model. Baker *et al.* (1993) used MWCAP to delineate the dividing streamline for each well. It was combined with the results of the one mile radius upgradient of the wellfield and hydrogeologic map information to determine the minimum size of area to be delineated as the wellhead protection area as a part of the Wellhead Protection Program for Rhode Island.

Several research studies have looked into the delineation of wellhead protection areas as a component of a geographic information system for aquifer protection. Whittemore *et al.* (1987) discussed the use of ERDAS, a GIS mapping system, as a component of the groundwater protection program for Harvey County, Kansas. The authors proposed overlaying the results of capture zone analysis and the results of DRASTIC analysis, the National Water Well Association's system of evaluating groundwater protection potential, using GIS mapping. The capture zone boundaries overlain on the DRASTIC results would identify which portions of the capture area were more susceptible to contamination. Rifai *et al.* (1993) used a GIS system to provide model input data to determine the size and shape of time related capture zones for Houston, Texas using the MONTEC model. Baker *et al.* (1993) used the Rhode Island GIS system to provide data input for wellhead protection area delineation using the MWCAP analytical groundwater flow model. Adams and Foster (1992) discuss the use of land surface zoning techniques for the protection of groundwater resources. They suggest that land surface zoning may be managed using a GIS system with a number of layers of information including a soil vulnerability index, the soil lithology, the depth to the water table and the size of a wellhead protection area.

Subsequent to using an analytic technique to determine the size of a potential WHPA, the next step in a WHP Program is to zone the calculated boundary as a WHPA. DeHan (1986) presented the methodology proposed by the state of Florida for zoning and protecting wellhead protection areas using state legislation. Linquiti and Harvey (1989) and Coughnawohr *et al.* (1989) discussed methods that could be used by local governments to control land-use to protect the groundwater within a WHPA. These controls include land use zoning and subdivision control, site plan review, source control for new industrial developments and the purchase of property. Cleary and Cleary (1991) presented a discussion of the methods that are used to delineate WHPAs with reference to European nations where many Wellhead Protection Programs date back to the 1950's. Neufeld and Mulamootil (1991) discussed groundwater management practices in Canada and compared these practices with the Wellhead Protection Program instituted in the United States by the Environmental Protection Agency. They found that a concern of groundwater protection is the encroachment of urban

development on wellfields and that land use zoning could be effective as a control for WHPA management. Rudolph (1991) discussed the concept of wellhead protection within the Region of Waterloo. The general hydrogeology of the region was presented and three major wellfields were analyzed with respect to the potential for contamination. The author concluded that a Wellhead Protection Program is needed in the Region of Waterloo to protect these groundwater resources. Schleyer *et al.* (1992) discussed the delineation and management of wellhead protection zones in Germany where there are potentially 13,050 WHPAs of which 72% have already been designated. These zones were first developed in the 1930's and are delineated based on the time of travel criterion where the prohibition and restriction of risky activities increase with proximity to the wellhead. Mull *et al.* (1992) discussed groundwater protection for Hanover, Germany where there is widespread contamination from both point source and non-point source pollution. The authors suggest that, due to the extremely high cost of restoration, contaminants must be ranked such that lower maximum tolerable concentration is equated to higher ranking. The ranking system would correlate the source of contamination with the type of contamination in the remediation scheme. Heubner (1992) prepared a survey of U.S. state groundwater regulation and found that almost half of the states had some form of wellhead or recharge-area protection programs that was either in place or in progress, but that only 18 of these proposed programs had been approved by the USEPA.

2.3 Exposure Assessment Modeling

2.3.1 Groundwater Flow and Contaminant Transport

Exposure assessment for groundwater contaminant risk analysis involves chemical fate and transport modeling in the hydrogeologic environment. The fundamental equation defining three-dimensional transient groundwater flow in a heterogeneous, saturated, anisotropic porous media is given by:

$$\frac{\partial}{\partial x_i}\left(K_{ij}\frac{\partial h}{\partial x_j}\right)+\sum q(x_i,t)\delta(x_i-\bar{x}_i)=S_s\frac{\partial h}{\partial t} \qquad \mathbf{i,j=1,3} \qquad (2.5)$$

where: h = the hydraulic head [L]

K_{ij} = the hydraulic conductivity tensor [L/T]

$q(x_i,t)$ = source/sink term at any point in the system [T^{-1}]

$\delta(x_i-\bar{x}_i)$ = is the Dirac Delta function

x_i = Cartesian coordinate parameters [L]

$\bar{x}_i$ = source/sink location [L]

S_s = specific storage [L^{-1}]

This equation defines the potentiometric surface within the aquifer that contains point sources and sinks of groundwater flow. Groundwater flow follows Darcy's law such that:

$$q_i = -K_{ij}\frac{\partial h}{\partial x_j} \tag{2.6}$$

where: q_i = the specific discharge [L/T]

$\frac{\partial h}{\partial x_j}$ = hydraulic gradient in the x_j direction [L/L]

Average linear groundwater velocity is given by:

$$v_i = \left(\frac{q_i}{n}\right) \tag{2.7}$$

where: v_i = average linear velocity [L/T]

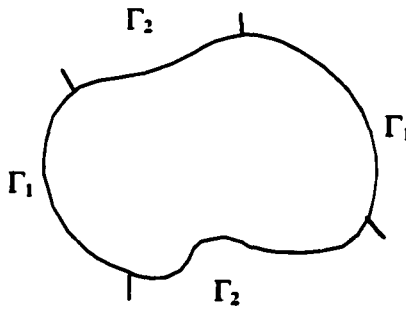
n = porosity [L/L]

Boundary conditions for any system must be specified to identify the interaction between the system and the external environment. There are two general types of boundary conditions as presented in Figure 2.1. The first type is a prescribed potential, or Dirichlet boundary condition, on boundary 1. The second type is a prescribed flux, or Neumann boundary condition, on boundary 2. The sum of all boundary conditions is the system boundary, Γ. These boundary conditions are defined as follows:

$$h(\Gamma_1) = \hat{h} \qquad \text{on } \Gamma_1 \tag{2.8}$$

$$q_n(\Gamma_2) = -K_{ij}\left(\frac{\partial \hat{h}}{\partial x_j}\right)\cdot n_i \qquad \text{on } \Gamma_2 \tag{2.9}$$

where: n_i = the unit normal to Γ_2



$\Gamma = \Gamma_1 + \Gamma_2$

Figure 2.1: Boundary Conditions for the Conceptual Model of a Study Site

Contaminant transport in the groundwater regime, involving the movement of dissolved solutes within groundwater, is affected by advection, mechanical dispersion, molecular diffusion and

reaction. Advection is the movement of dissolved solutes along with the flow of groundwater. Mechanical dispersion and molecular diffusion are two components of the process of hydrodynamic dispersion that result in the dilution of contaminant concentration due to the spreading of the plume as a result of the convoluted path that it takes through the porous media. Contaminant reaction results in the reduction in contaminant concentration due to a number of physical-chemical processes that may include adsorption-desorption, solution-precipitation, oxidation-reduction, acid-base reaction and microbial transformation.

The fundamental equation that defines contaminant transport in groundwater as a result of these processes is given by:

$$\theta \frac{\partial C}{\partial t} = \frac{\partial}{\partial x_i}\left(\theta D_{ij} \frac{\partial C}{\partial x_j}\right) - \theta v_i \frac{\partial C}{\partial x_i} + q(x_i, t) C_s + r_c \qquad (2.10)$$

where: C = aqueous phase concentration of a contaminant [M/L^3]

C_s = concentration in the source/sink [M/L^3]

θ = fluid content [L^3/L^3]

D_{ij} = hydrodynamic dispersion tensor [L^2/T]

v_i = linear velocity [L/T]

r_c = rate of all reactions occuring in the aqueous phase [M/L^3T]

Hydrodynamic dispersion is given by:

$$D_{ij} = (\alpha_l - \alpha_t)\frac{v_i v_j}{|v|} + \alpha_t \delta_{ij}|v| + \tau D_m \qquad (2.11)$$

where: α_l = longitudinal dispersivity [L]

α_t = transverse dispersivity [L]

$|v|$ = magnitude of the velocity vector [L/T]

δ_{ij} = Kronecker Delta function

τ = tortuosity of the porous media [L/L]

D_m = the coefficient of molecular diffusion [L^2/T]

The previous equations provide the basis for the numerical modeling of groundwater flow and transport in porous aquifer material. They define the contaminant concentration at any point in the groundwater regime at any point in time. Numerical models are the most general tools for the quantitative analysis of groundwater applications. They are not bound by the restrictive assumptions of analytical solutions. Numerical solutions normally involve approximating partial differential equations with a set of discrete equations in time and space. The region of space, often called the

conceptual model of the site, is discretized in three dimensions to produce a set of spatial subregions. The equations of groundwater flow are applied to each subregion resulting in a set of equations that may be applied to each step in time. The two major techniques that are used to perform spatial and temporal discretization are the finite difference method and the finite element method.

The finite difference method approximates the differential equations that are characteristic of groundwater flow and transport using a differential approach. The conceptual model of the study site is first discretized into a three-dimensional grid. A fluid balance is applied to the discretized grid to define the finite difference equations. Each equation is written in differential form and applied to each grid block. The development of the differential form of Equation 2.1 is presented below and refers to the grid block representation presented in Figure 2.2.

The Taylor Series expansion for the fluid potential at point x+Δx is given by the following expression:

$$\phi(x+\Delta x)=\phi(x)+\Delta x\phi'(x)+\frac{\Delta x^2}{2}\phi''(x)+... \tag{2.12}$$

Truncating equation 2.12 to first order yields the following:

$$\frac{d\phi}{dx}\approx\frac{\phi(x+\Delta x)-\phi(x)}{\Delta x} \tag{2.13}$$

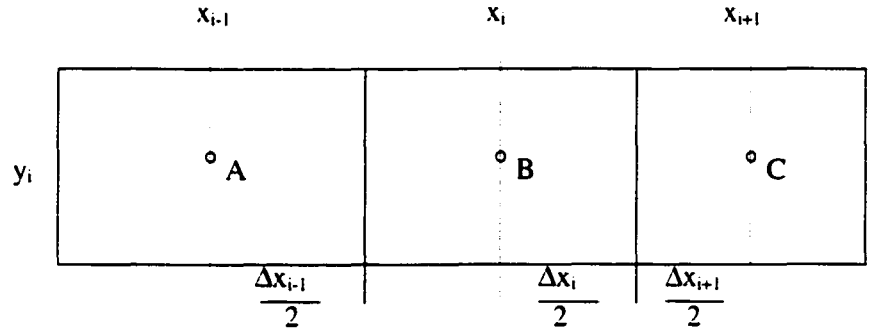


Figure 2.2: Grid Block Discretization in the X Direction

Thus Darcy's flux, q, may be written by the following:

$$q=-K\frac{dh}{dx}\approx-K\frac{h(x+\Delta x)-h(x)}{\Delta x} \tag{2.14}$$

The groundwater flux may be written, from the interface of blocks B and C to the center of block C, as:

$$q_{i+1/2}=-K\frac{\partial h}{\partial x}=\frac{2(h_{i+1}-h_{i+1/2})}{\left(\frac{\Delta x_{i+1}}{K_{i+1}}\right)} \qquad \text{or,}\ (h_{i+1}-h_{i+1/2})=\frac{q_{i+1/2}}{2}\left(\frac{\Delta x_{i+1}}{K_{i+1}}\right) \tag{2.15}$$

It may also be written, from the center of block B to the interface of blocks B and C, as:

$$q_{i+1/2} = \frac{2(h_{i+1/2} - h_i)}{\left(\frac{\Delta x_i}{K_i}\right)} \qquad \text{or,} (h_{i+1/2} - h_i) = \frac{q_{i+1/2}}{2}\left(\frac{\Delta x_i}{K_i}\right) \tag{2.16}$$

Adding equations 2.15 and 2.16, the flux between block B and C is given by:

$$q_{i+1/2} = \frac{2(h_{i+1} - h_i)}{\left(\frac{\Delta x_i}{K_i}\right) + \left(\frac{\Delta x_{i+1}}{K_{i+1}}\right)} \qquad \text{or,} q_{i+1/2} = T_{i+1/2}(h_{i+1} - h_i) \tag{2.17}$$

$$\text{where: } T_{i+1/2} = \frac{2}{\left(\frac{\Delta x_{i+1}}{K_{i+1}}\right) + \left(\frac{\Delta x_i}{K_i}\right)} \tag{2.18}$$

where: $T_{i+1/2}$ = the transmissivity between blocks i and i+1 [T^{-1}]

Δx_i = the length increment of grid block A in the x direction [L]

K_i = hydraulic conductivity of block i [L/T]

h_i = the head at the center of block i [L]

The Taylor Series expansion of equation 2.12 may also be written as:

$$\phi(x - \Delta x) = \phi(x) - \Delta x \phi'(x) + \frac{\Delta x^2}{2}\phi''(x) - \ldots \tag{2.19}$$

Truncating equations 2.12 and 2.19 to second order and adding the resultant equations provides an expression for the change in the fluid flux in the x direction as given by:

$$\phi(x + \Delta x) + \phi(x - \Delta x) \approx 2\phi(x) + \Delta x^2 \phi''(x) \tag{2.20}$$

Thus, the second order differential of the potential is given by:

$$\frac{\partial^2 \phi}{\partial x^2} = \frac{\phi(x + \Delta x) - 2\phi(x) + \phi(x - \Delta x)}{\Delta x^2} \tag{2.21}$$

The change in flux, q_x, may be written as:

$$\frac{\partial q_x}{\partial x} = \frac{\partial}{\partial x}\left(K_x \frac{\partial h}{\partial x}\right) = \frac{1}{\Delta x}\left(K_x \frac{\Delta h}{\Delta x}\right) = \frac{T_{i+1/2}(h_{i+1} - h_i) - T_{i-1/2}(h_i - h_{i-1})}{\Delta x_i} \tag{2.22}$$

Therefore the finite difference representation of the groundwater flow equation may be written as:

$$\frac{T_{i+1/2}(h_{i+1,jk} - h_{ijk}) - T_{i-1/2,jk}(h_{ijk} - h_{i-1,jk})}{\Delta x_i} + \frac{T_{j+1/2}(h_{i,j+1,k} - h_{ijk}) - T_{j-1/2}(h_{ijk} - h_{ij-1,k})}{\Delta y_j}$$

$$+ \frac{T_{k+1/2}(h_{ijk+1} - h_{ijk}) - T_{k-1/2}(h_{ijk} - h_{ijk-1})}{\Delta z_k} + Q(i,j) = S_s \frac{(h_{ijk}^m - h_{ijk}^{m-1})}{(t^m - t^{m-1})} \tag{2.23}$$

Writing a linear equation in differential form for each of the N grid blocks in the conceptual model results in N equations with N unknowns. These N equations can then be solved using matrix techniques to determine the steady state hydraulic head field for the study site.

2.3.2 Advective Particle Tracking

Another method that has been used to represent solute transport through the groundwater regime is particle tracking. Particle tracking calculates the pathline taken by an infinitely small imaginary particle by following its movement when it is placed in the flow field. Solute transport is assumed to occur by advective transport only and as a result does not take into account other contaminant transport process that may be important in some hydrogeologic settings. When the velocity field is reversed, particle tracking may be used to determine the source of groundwater flow based on average water particle travel times. Pathline endpoints from particles placed on the periphery of a supply well within the groundwater flow field define a time related capture zone associated with a specific time of travel. A groundwater capture zone refers to the portion of a flow field that contributes water to a well or a surface body of water such as a river or lake. The ultimate capture zone for a well is the region of an aquifer from which a pumping well ultimately draws all of its water. A time related capture zone draws water only from a portion of this volume in a fixed amount of time (Townley and Davidson, 1988).

Particle tracking codes are post-processors to groundwater flow models. They use the head field or velocity field from a flow model to trace out particle pathlines. There are a number of methods that may be used to define particle pathlines. For a finite difference groundwater model a numerical pathline generation scheme based on a bilinear velocity interpolator provides consistent and accurate results (Schafer-Perini and Wilson, 1991). Using a two-dimensional five grid block arrangement of heads, conservation of fluid mass may be used to define the following relationship:

$$q_{x,i+1/2}\Delta y_j - q_{x,i-1/2}\Delta y_j + q_{y,j+1/2}\Delta x_i - q_{y,j-1/2}\Delta x_i = Q_{ij}/b \qquad (2.24)$$

where: $q_{x,i+1/2}$ = right block face Darcy velocity in the x direction [L/T]

$q_{x,i-1/2}$ = left block face Darcy velocity in the x direction [L/T]

$q_{y,j+1/2}$ = upper block face Darcy velocity in the y direction [L/T]

$q_{y,j-1/2}$ = lower block face Darcy velocity in the y direction [L/T]

Δx_i = grid block discretization in the x direction [L]

Δy_j = grid block discretization in the y direction [L]

Q_{ij} = the net flux out of grid block (i,j) [L^3/T]

b = aquifer thickness [L]

Applying Darcy's Law across the grid block face, as shown in equation 2.14, results in the following:

$$q_{x,i+1/2} = -2K_{i+1/2,j}\frac{h_{i+i,j} - h_{i,j}}{\Delta x_{i,j} + \Delta x_{i+1,j}} \tag{2.25}$$

A similar relationship can be applied to each of the other block faces resulting in the calculation of velocities for each of the block faces. Applying linear velocity interpolation across the grid block in the x direction results in the following relationship:

$$q_x = q_{x,i-1/2} + \left[\frac{q_{x,i+1/2} - q_{x,i-1/2}}{\Delta x_{i,j}}\right](x - x_o) \tag{2.26}$$

where: x = final particle position [L]

x_o = initial particle position [L]

Assuming that the porosity of the porous media is constant over a grid block, the Darcy velocity defined above can be equated to the time derivative of particle displacement:

$$q_x = a + b(x) = n\frac{dx}{dt} \tag{2.27}$$

where: n = the porosity of grid block (i,j) [L/L]

Integrating Equation 2.23, by separation of variables, yields the following:

$$\Delta t = \frac{n}{b}\ln\left[\frac{a + bx}{a + bx_o}\right] \tag{2.28}$$

where: Δt = the differential particle travel time [T]

Equation 2.28 relates the particle travel time, Δt, to the new particle position in the x direction based on the current particle position. A similar relationship can be derived for the y direction allowing the determination of a new particle position in two-dimensional space. Thus, in order to track a particle through a flow field it is necessary to determine the velocity at each block face around a grid block and then to determine where a particle enters and exits the grid block.

Particle tracking for the present research was developed in a two-dimensional sense because of the fact that the aquifer that is being analzed is phreatic. However, these principles may be extended to 3 dimensions to represent particle movement in more complex hydrogeologic settings.

2.3.3 Random Walk Particle Tracking

Advective particle tracking does not take into account hydrodynamic dispersion that is associated with solute transport in the groundwater environment. One method that has been used to include dispersion in particle tracking is the random walk method that models longitudinal and transverse dispersion as a combination of a random number and the dispersion coefficient. The basic relationships for advective particle tracking were presented above, and are based on a field of block

face values of velocity. For random walk it is necessary to define a field of block face values of dispersion. These values of dispersion are derived from equation 2.11 using the velocity field that defines advective particle tracking. Longitudinal and transverse dispersion, respectively, are given by:

$$D_l = \alpha_l \frac{v_x v_x}{|v|} + \alpha_t \frac{v_y v_y}{|v|} + D^* \tag{2.29}$$

$$D_t = \alpha_l \frac{v_y v_y}{|v|} + \alpha_t \frac{v_x v_x}{|v|} + D^* \tag{2.30}$$

where: D_l = the longitudinal dispersion[L^2/T]

D_t = the transverse dispersion[L^2/T]

α_l = the longitudinal dispersivity[L]

α_t = the transverse dispersivity [L]

v_x = the velocity in the x-direction [L/T]

v_y = the velocity in the y-direction [L/T]

v = the velocity at the point of interest [L/T]

D^* = the coefficient of molecular diffusion [L^2/T].

Random walk particle tracking in two dimensions is given by the following relationships (Walton, 1991):

$$x_p(t+\Delta t) = x_p(t) + v_x^{'}\Delta t + R_1(2\alpha_l v_{xy}\Delta t)^{1/2}\left(\frac{v_x}{v_{xy}}\right) + R_2(2\alpha_t v_{xy}\Delta t)^{1/2}\left(\frac{v_y}{v_{xy}}\right) \tag{2.31}$$

$$y_p(t+\Delta t) = y_p(t) + v_y^{'}\Delta t + R_1(2\alpha_l v_{xy}\Delta t)^{1/2}\left(\frac{v_y}{v_{xy}}\right) - R_2(2\alpha_t v_{xy}\Delta t)^{1/2}\left(\frac{v_x}{v_{xy}}\right) \tag{2.32}$$

where:

$$v_x^{'} = v_x + \frac{\partial D_x}{\partial x} \tag{2.33}$$

$$v_y^{'} = v_y + \frac{\partial D_y}{\partial y} \tag{2.34}$$

$$v_{xy} = (v_x^2 + v_y^2)^{1/2} \tag{2.35}$$

$$R_1, R_2 = -6 + \sum_{i=1}^{12} RN_i \tag{2.36}$$

and, the variables R_1 and R_2 are normally distributed random numbers with zero mean and unit standard deviation (Press *et al.*, 1992).

2.3.4 Transient Modeling

Steady state modeling in groundwater hydrology defines the average condition of the water table based on average input conditions of groundwater sinks and sources. However, the natural hydrogeologic environment is more complex as a result of temporal changes to these input conditions. Transient groundwater modeling defines the change in the elevation of the groundwater potential based on temporal changes to the hydrologic stresses on the system. For example, groundwater recharge from infiltration and from river recharge change from season to season depending on the amount of precipitation, runoff, evapotranspiration and river flow that occurs. As well, in the simulation of pumping stresses from a municipal wellfield, the well pumping rates change on a daily, weekly and monthly basis depending on consumer demand. Transient modeling allows input conditions to change on a temporal basis. This can be accomplished with a number of groundwater flow models including SWIFT and MODFLOW that can be used to solve both the steady state and transient hydraulic head fields for complex hydrogeologic environments (Reeves *et al.*, 1985; McDonald and Harbaugh, 1988).

2.4 Summary

A great deal of research has been conducted on the risk assessment of environmental contamination, protection of sensitive aquifers, and environmental decision making as an economic analysis tool for comparing engineering designs that affect the natural environment. Risk assessment research has looked at both qualitative assessment of the ranking of contaminant sites as to their impact on the hydrogeologic environment and quantitative assessment of the effect that specific contaminant sites will have on production wellheads and sensitive aquifers. Groundwater protection research has looked at the management of protection zones from a planning perspective and the implementation of WHPAs from a practical perspective using the criteria and methods promoted by the USEPA. Much of this research has involved the use of computer models to delineate WHPAs with some investigation into parameter uncertainty and its effect on the location of the final WHPA boundary. However, environmental decision making has not been applied to the question of what is the best alternative for WHPA delineation around municipal wellheads, or the question of what is the economic regret of choosing the non-optimal delineation alternative. Nor has it been applied to the economic impact of uncertainty on WHPA delineation modeling and related issues of the effect of transient changes to hydrologic stress on numerical modeling of WHPA boundaries. The delineation

of wellhead protection area boundaries has implications on municipal planning in that wellhead protection areas are zoned to prevent industries that present a high risk of groundwater contamination from locating within the area that has been zoned as a drinking water supply area. The proposed research may help to provide a methodology for communities, which are currently debating the issue of source water protection, to make a more informed choice for wellhead protection.

CHAPTER 3
REICH FARM SUPERFUND SITE

3.1 Introduction

To compare the techniques that are used to delineate wellhead protection areas, it was necessary to choose a study site that includes a water supply wellfield and a contaminant source that poses a risk of contamination to a sensitive aquifer. The study site that was chosen was the municipal wellfields owned by United Water Toms River (UWTR) located near the town of Pleasant Plains, New Jersey directly downgradient of the Reich Farm Superfund site (see Figure 3.1). The purpose of this chapter is to introduce the conceptual model of the groundwater flow system at the site that was used for numerical modeling. This conceptual model was originally developed by Sykes (1985) to model contaminant transport from the Superfund site. It was updated for groundwater protection modeling, and a sensitivity analysis was performed to provide a basis for an uncertainty analysis of groundwater protection modeling.

3.2 The Reich Farm Superfund Site

A conceptual model was developed for the groundwater flow system in the Pleasant Plains area of Dover Township, Ocean County, New Jersey. This conceptual model is an updated version of the groundwater flow model developed by Sykes (1995). The resulting groundwater flow field contains a municipal wellfield, which is completed in the shallow water table aquifer, and the Reich Farm Superfund site, as shown in Figure 3.1. From a hydrogeologic perspective Dover Township is underlain by the Cohansey-Kirkwood aquifer system. The Cohansey Formation is the upper phreatic aquifer that is defined by a fine sand that is locally cemented with iron oxide and interbedded with clay and gravel lenses. This shallow phreatic aquifer is the principle source of water for Dover Township. The Cohansey Formation is underlain by the Kirkwood Formation, which is a silty sand aquifer. Between these two aquifer systems is a transitional zone that is defined by low vertical hydraulic conductivity, which results in negligible recharge from the lower Kirkwood to the upper Cohansey aquifer (EBASCO Services Inc, 1988). As a result, the conceptual model that was developed to represent the upper Cohansey is essentially two-dimensional in nature.

The Cohansey aquifer was modeled using three distinct sand layers to allow for vertical gradients in the vicinity of the wells. These layers are described in Table 3.1. It was assumed that the bottom of the Cohansey Formation represents the lower boundary of the conceptual model. The

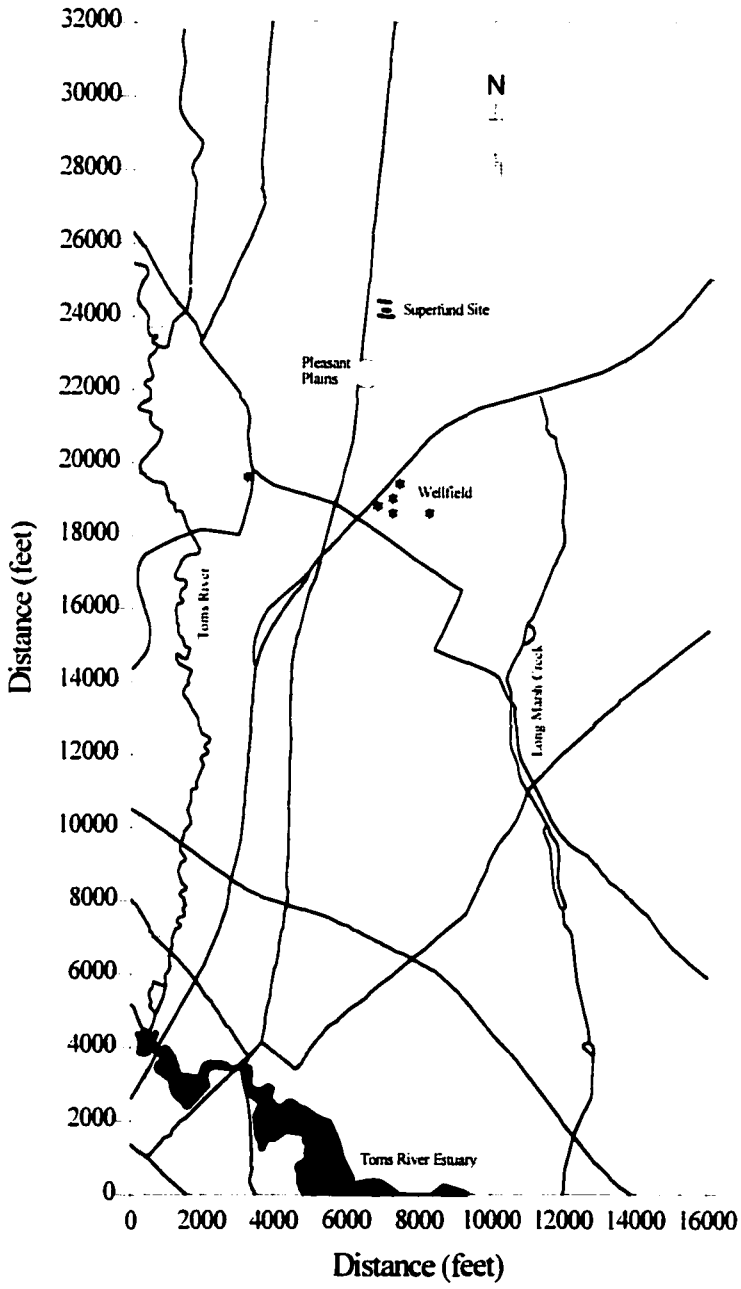


Figure 3.1: Location of the Hydrogeological and Hydrologic Features of the Study Site

study site was discretized into a finite difference grid with 44 grid blocks in the east-west direction and 64 grid blocks in the north-south direction as presented in Figure 3.2.

Layer	Layer Depth	Soil Lithology
1	From the water table to 12.2 meters above the bottom of the Cohansey Aquifer	Sand
2	From 12.2 meters to 6.1 meters above the bottom of the Cohansey Aquifer	Sand
3	From 6.1 meters above the bottom to the bottom of the Cohansey Aquifer	Sand

Table 3.1: Model Layers for SWIFT Modeling of the Cohansey Aquifer

The boundary conditions for the system are specified as follows. The west, north and east boundaries of the site are located below divides in the surface water system as shown in Figure 3.1. To the southwest the Toms River is assumed to have no underflow and was assigned a constant head. leakage boundary condition. The southern boundary of the site was given prescribed values of head to allow groundwater outflow to the Toms River estuary. The upper boundary of the system was assigned either prescribed heads or prescribed recharge rates. Surface water sources, including the Toms River, the Toms River estuary and Long Marsh Creek were assigned prescribed head values associated with long term, average surface water elevation. The rest of the surface blocks were assigned a spatially uniform net infiltration rate.

The values of the hydrogeologic input parameters and the boundary conditions are set as follows. Average uniform hydraulic conductivity values for K_x, K_y and K_z, for layers 1 and 2, were chosen to be 45.7 meters/day, 45.7 meters/day and 9.1 meters/day, respectively. Average K_x, K_y and K_z, for layer 3, was chosen to be 15.2 meters/day, 15.2 meters/day and 3.0 meters/day. Spatially uniform net infiltration was calibrated to 0.00132 meters/day (Sykes, 1995). Average sand porosity was estimated to be 0.30. The locations of wells 20, 22, 24, 26, 28 and 29 at the UWTR wellfield are presented in Figure 3.3. Well rates were determined from 25 years of average annual pumping data that are presented in Table 3.2. Daily pumping rates for these 6 wells are 1823.6 m^3/day (64400 ft^3/day), 2137.9 m^3/day (75500 ft^3/day), 1874.6 m^3/day (66200 ft^3/day), 1767.0 m^3/day (62400 ft^3/day), 1769.8 m^3/day (62500 ft^3/day) and 1806.6 m^3/day (63800 ft^3/day), respectively.

A steady state groundwater flow analysis of the Cohansey aquifer was prepared using SWIFT v2.29 (GeoTrans Inc., 1989). Figure 3.4 presents the hydraulic head field in the Cohansey aquifer prior to the operation of the wells at the UWTR wellfields. The regional hydraulic gradient is approximately 0.0030 meter/meter, sloping from the northeast to the

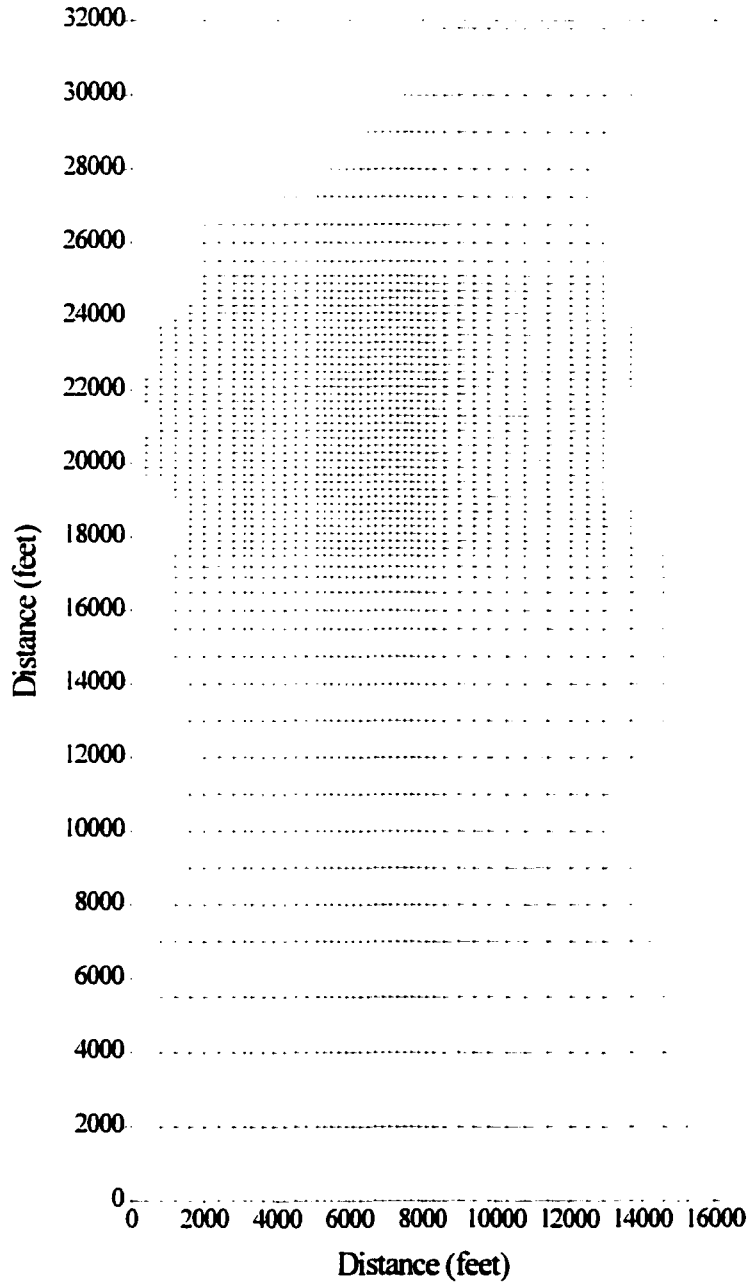


Figure 3.2: Finite Difference Grid of the Conceptual Model of the Study Site

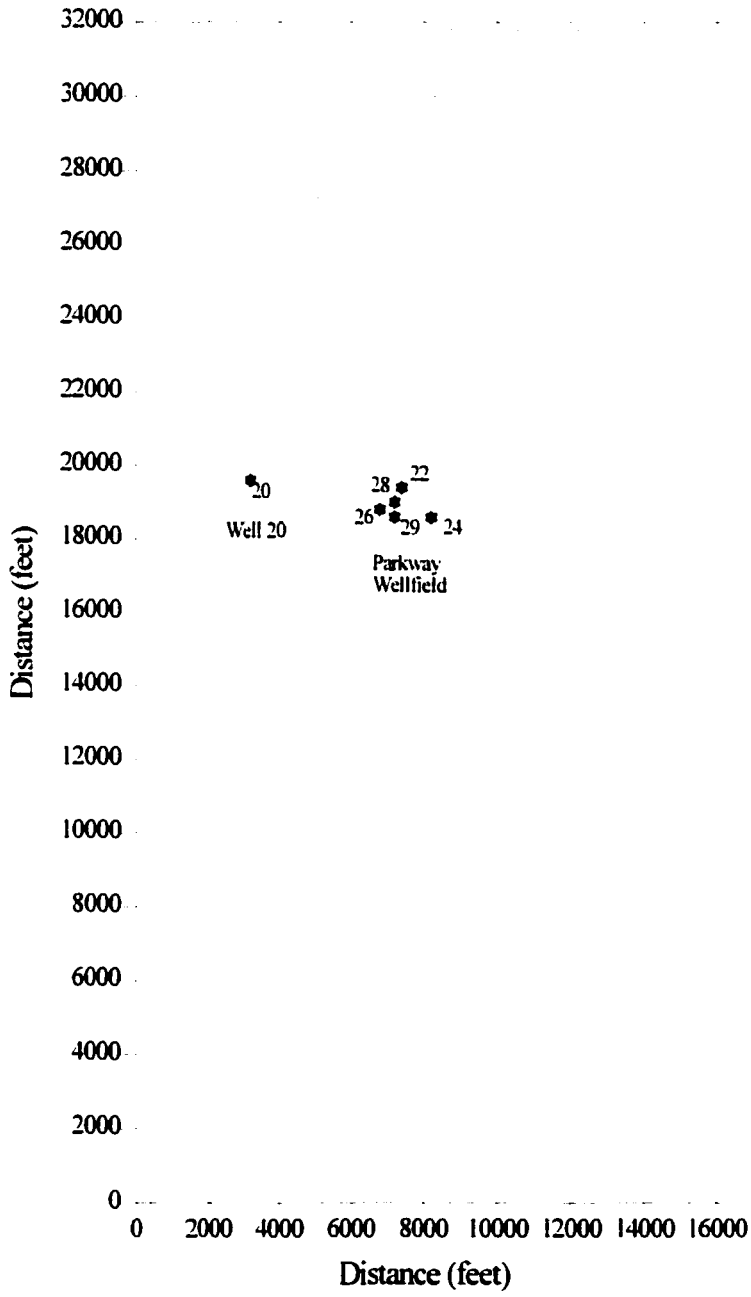


Figure 3.3: The Location of the Pumping Wells for the UWTR Wellfields

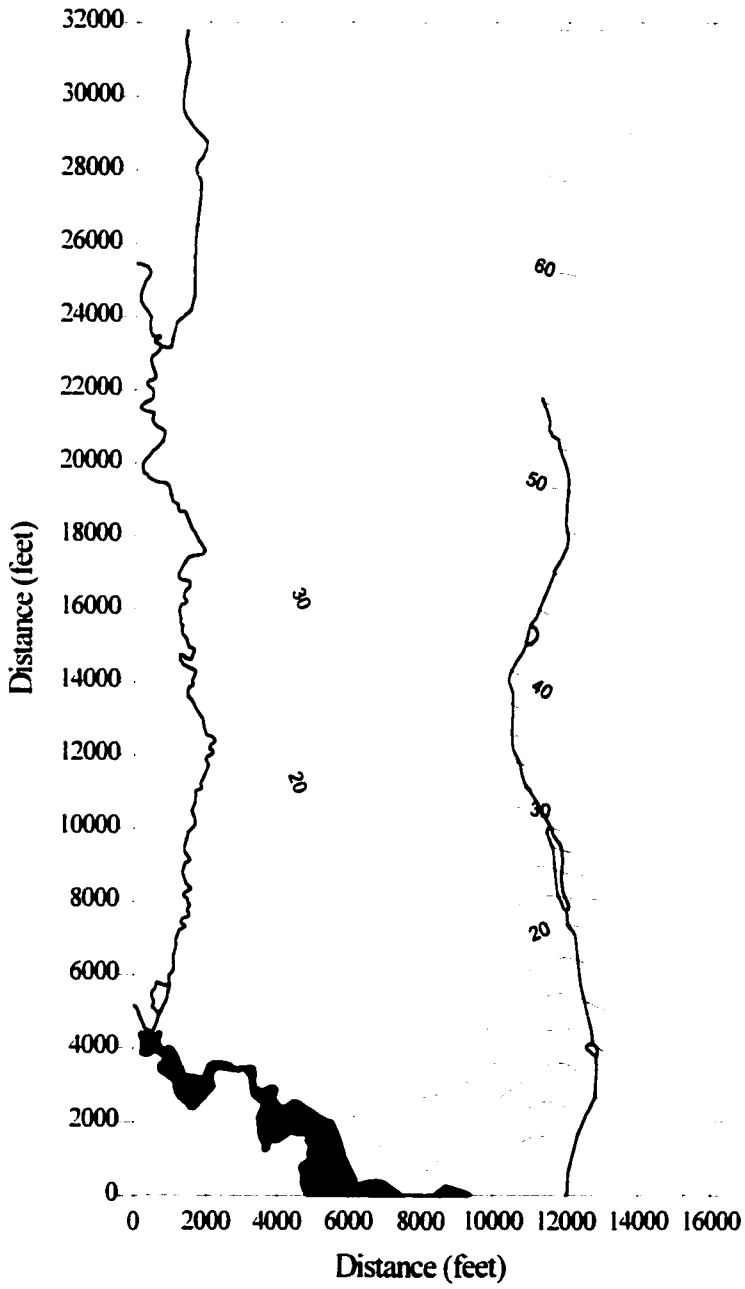


Figure 3.4: Steady State Hydraulic Head Field at the Study Site Prior to Pumping

southwest of the watershed. Forward particle tracking was performed using STLINE v1.9 (GeoTrans, Inc., 1987) from a starting location of the TCE contaminated soil at the Reich Farm Superfund site as presented in Figure 3.5. Particles released from the Superfund site migrate down the regional hydraulic gradient to the Toms River to the west of the site missing the future UWTR wells by more than 600 meters.

Year	Well 20	Well 22	Well 24	Well 26	Well 28	Well 29
1971	50000	0	0	0	0	0
1972	43000	16000	0	13000	0	0
1973	53000	65000	52000	65000	0	0
1974	82000	72000	64000	76000	0	0
1975	81000	66000	57000	32000	41000	41000
1976	79000	58000	52000	49000	52000	52000
1977	77000	81000	49000	41000	48000	53000
1978	74000	47000	68000	50000	53000	67000
1979	79000	77000	65000	63000	68000	68000
1980	83000	68000	46000	67000	60000	63000
1981	77000	65000	69000	60000	60000	66000
1982	75000	56000	55000	56000	39000	47000
1983	75000	77000	60000	77000	61000	55000
1984	84000	83000	71000	83000	50000	53000
1985	75000	81000	72000	66000	59000	65000
1986	78000	82000	74000	66000	70000	77000
1987	75000	71000	78000	59000	61000	69000
1988	66000	69000	59000	54000	52000	60000
1989	61000	78000	65000	59000	72000	64000
1990	58000	59000	70000	68000	69000	68000
1991	40000	80000	72000	64000	71000	64000
1992	35000	74000	54000	58000	73000	64000
1993	46000	85000	64000	54000	75000	68000
1994	57000	88000	66000	46000	59000	64000
1995	64000	85000	64000	66000	67000	73000

Table 3.2: Average Annual Well Pumping Rates for UWTR Wells (1971-1995)

The UWTR municipal wellfields began operating with the development of well 20. By 1971 well 20 was operating at its average annual steady state pumping value. The Parkway wellfield began operating in 1972 with the development of wells 22 and 26, well 24 began operating in approximately 1973, and wells 28 and 29 began operating in approximately 1975. Average yearly pumping rates for the UWTR wells are given in Figure 3.6. The operation of these production wells

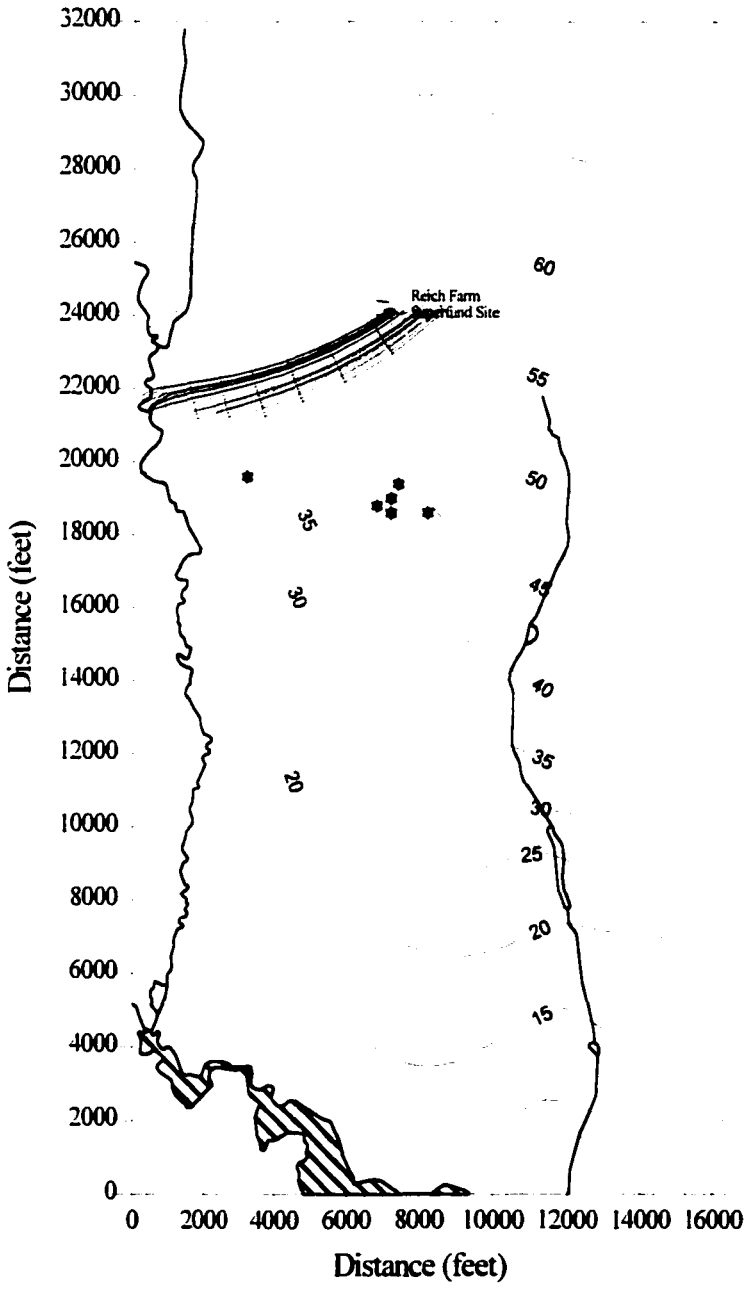


Figure 3.5: Forward Particle Tracking to Identify Prepumping Contaminant Particle Pathways

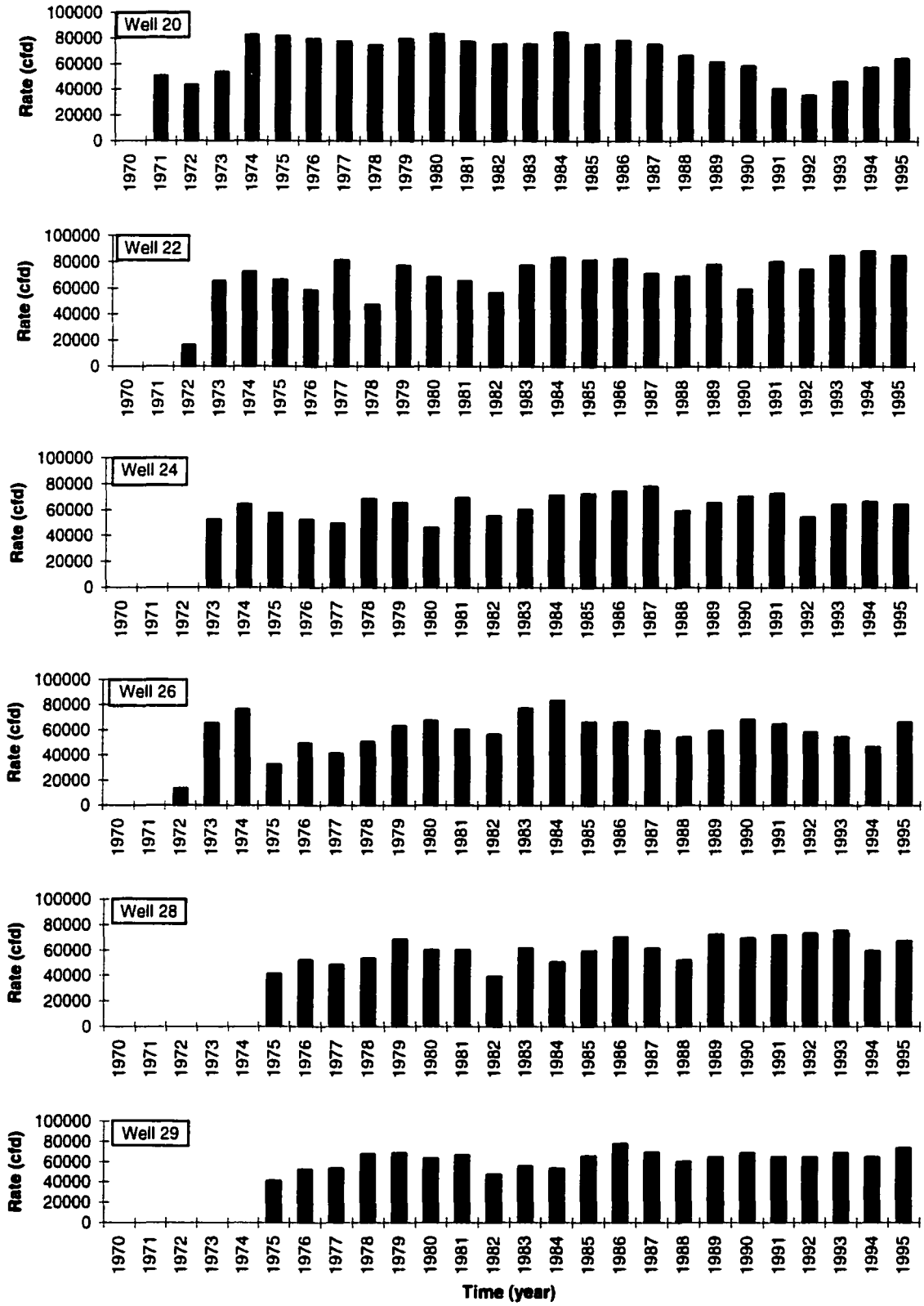


Figure 3.6: Annual Pump Rates for the United Water Toms River Wells (1970 - 1995)

in the Cohansey aquifer has had a profound effect on the direction and magnitude of the regional hydraulic gradient in the middle of this flow field. Figure 3.7 presents the calibrated steady state hydraulic head field based on average model input parameters and the wellhead pumping rate presented in the previous paragraph (Sykes, 1995).

The effect that the UWTR wellfields have had on this groundwater flow system and their relationship to the Reich Farm contamination site may be shown using contaminant transport simulation. Contaminant transport was implemented using advective particle tracking to determine the results of releasing particles from the soil contamination site. Figure 3.8 presents the results of forward particle tracking from the west side of the Reich Farm where some of the highest concentrations of TCE and PCE were found. Under the influence of the UWTR wellfields, particles released from the Reich Farm site only enter well 20.

Advective particle tracking was also used to define the time related capture zones for the two UWTR wellfields. A set of particles were released from around each wellhead and tracked backward in time to their pathline endpoints based on a specific travel time. A computer model called CAPZON was written to draw the boundary of a capture zone around the outer extent of these reverse particle pathlines originating from a well. CAPZON reads all the pathline points generated by the STLINE particle tracking model and creates a convex hull from the set of points that are farthest away from the center of mass of all the pathline points. The FORTRAN computer code for CAPZON is presented in Appendix I. Figure 3.9 shows the 180 day, 5 year and 10 year time of travel capture zones around well 20 and the Parkway wellfield. From this figure it is evident that the Reich Farm contamination site is within the 10 year capture zone for well 20.

Another method of implementing contaminant transport, which includes advection and dispersion, is random walk particle tracking analysis. The random walk method uses the velocity field from a groundwater flow model and a field of contaminant dispersion values to track particles through the groundwater system, according to equations 2.31 to 2.35. RWAPT is a computer model that was developed to implement random walk particle tracking. The model was written in FORTRAN and the code is presented in Appendix II. The model accepts the block-centered hydraulic head field that is output from SWIFT. Groundwater velocities and dispersion values are calculated at each grid block face. Particles may be tracked either forward or backward in time using the random walk equations.

To implement forward RWAPT modeling a set of particle was released from the same location as the source location for STLINE simulation. The model was run 10 times using different

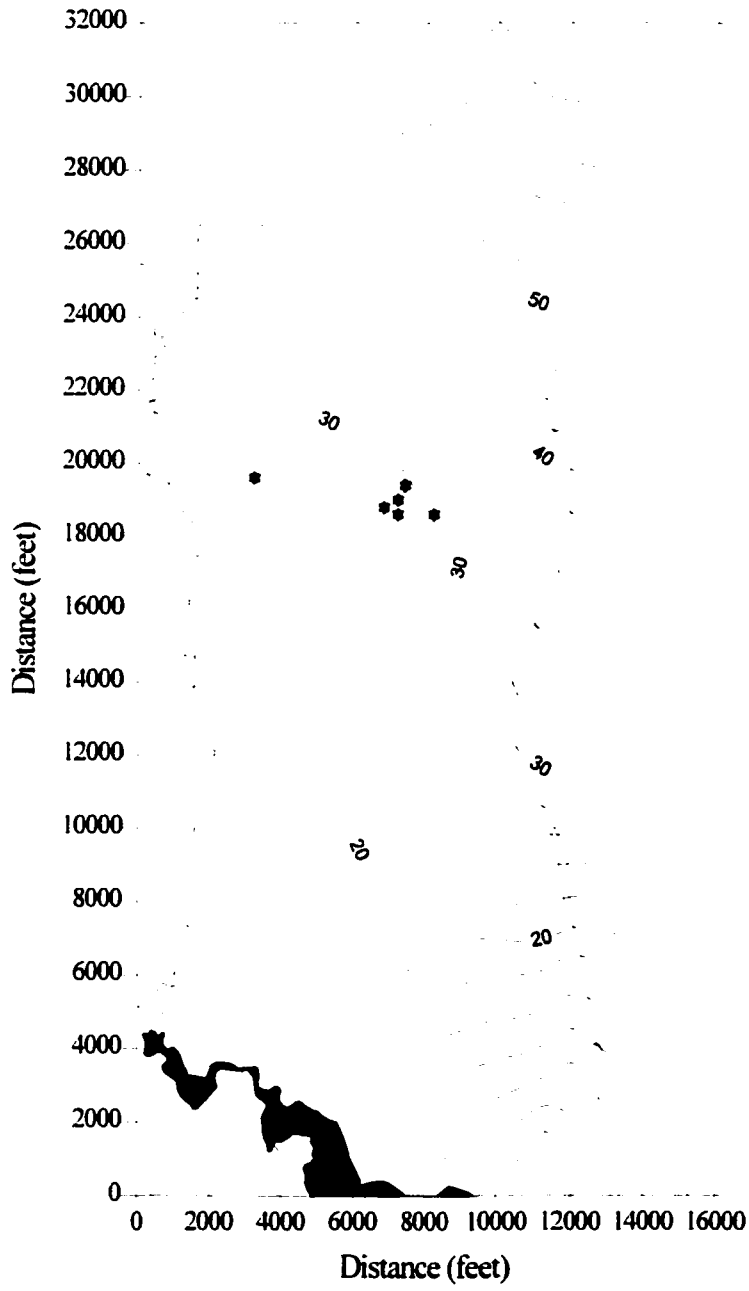


Figure 3.7: Calibrated Steady State Hydraulic Head Field for the Study Site (feet)

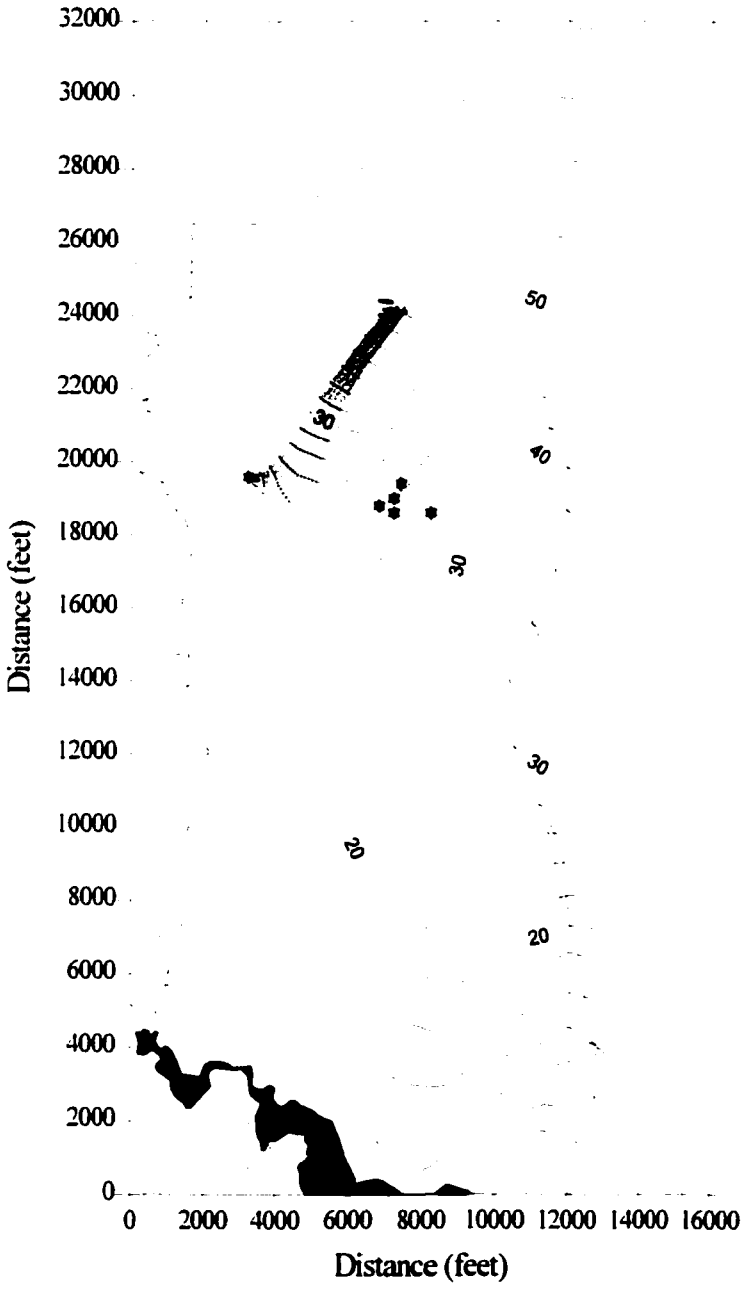


Figure 3.8: Forward Particle Pathlines Emanating from the Study Site Under the Influence of Advection

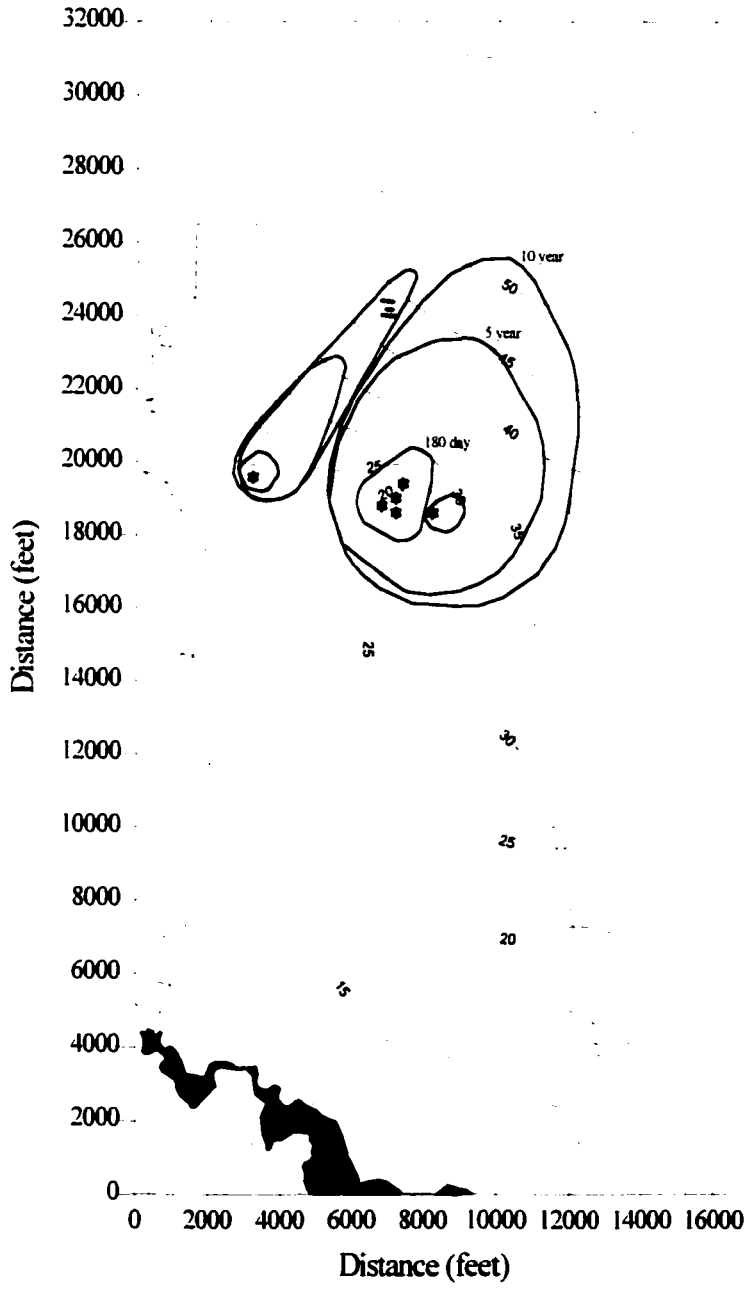


Figure 3.9: The 180 Day, 5 Year and 10 Year STLINE Capture Zones for the UWTR Wellfields

initial seeds, and longitudinal and transverse dispersion values of 20.0 meters and 2.0 meters, respectively. This was done to determine the full extent of particle dispersion produced by the random walk model. Figure 3.10 presents the results of the ensemble of particle pathlines. The effects of dispersion are evident in that the solute particles enter both wellfields.

RWAPT was also used to generate reverse particle pathlines, and CAPZON was used to delineate time related capture zones. To implement reverse RWAPT modeling a set of particles was released from the periphery of the wellfields. An analysis was performed to determine the minimum number of simulations, using different initial seeds, to assess the effect of dispersion on the size of the RWAPT capture zone. Ten random seeds were chosen to produce the set of particle pathlines. Figure 3.11 presents the 10 year time of travel capture zones around well 20 and the Parkway wellfield using both RWAPT and STLINE reverse particle tracking. The effect of dispersion is evident in that the RWAPT capture zones, for the same time of travel, encompass a greater area than the STLINE capture zones. It is also evident that the capture zones for well 20 and the Parkway wellfield overlap showing that a contaminant source at the periphery of the ultimate capture zone may enter the capture zone for another well as a result of dispersion. Another point that arose in the random walk analysis is that the size of the resulting capture zone increased with a greater number of initial seeds used to start the RWAPT simulation. However, the increase in the size of the capture zone was inconsequential for simulations that used greater than 11 initial seeds.

3.3 Model Sensitivity

Sensitivity analysis is a technique used to measure the sensitivity of model output to changes in model input. One method that may be used to perform a sensitivity analysis is direct parameter sampling (Skaggs and Barry, 1996). Direct parameter sampling is implemented using a low value and a high value of a specific input parameter. The difference between model output values divided by the difference in the input parameter values is the marginal sensitivity of the output performance measure. The marginal sensitivity values can be compared for different input parameters to determine which model parameters are most sensitive for a given conceptual model. Direct parameter sampling will be used to perform sensitivity analysis of the groundwater flow model.

The sensitivity of model performance is a local derivative of the performance measure function that may be approximated numerically using a forward difference approach, a backward difference approach or centered difference approach. The equations that represent these approaches are presented in the following equations:

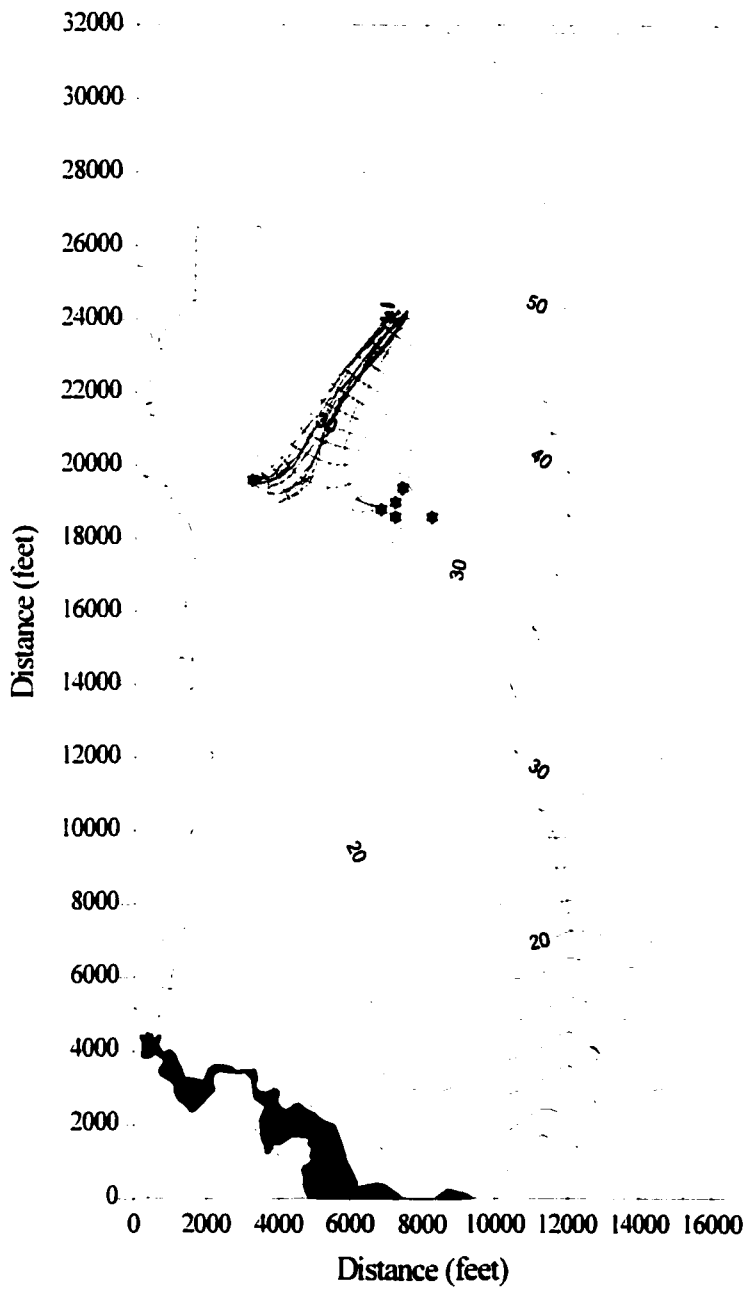


Figure 3.10: Forward Particle Pathlines Using RWAPT Modeling of Advection-Dispersion

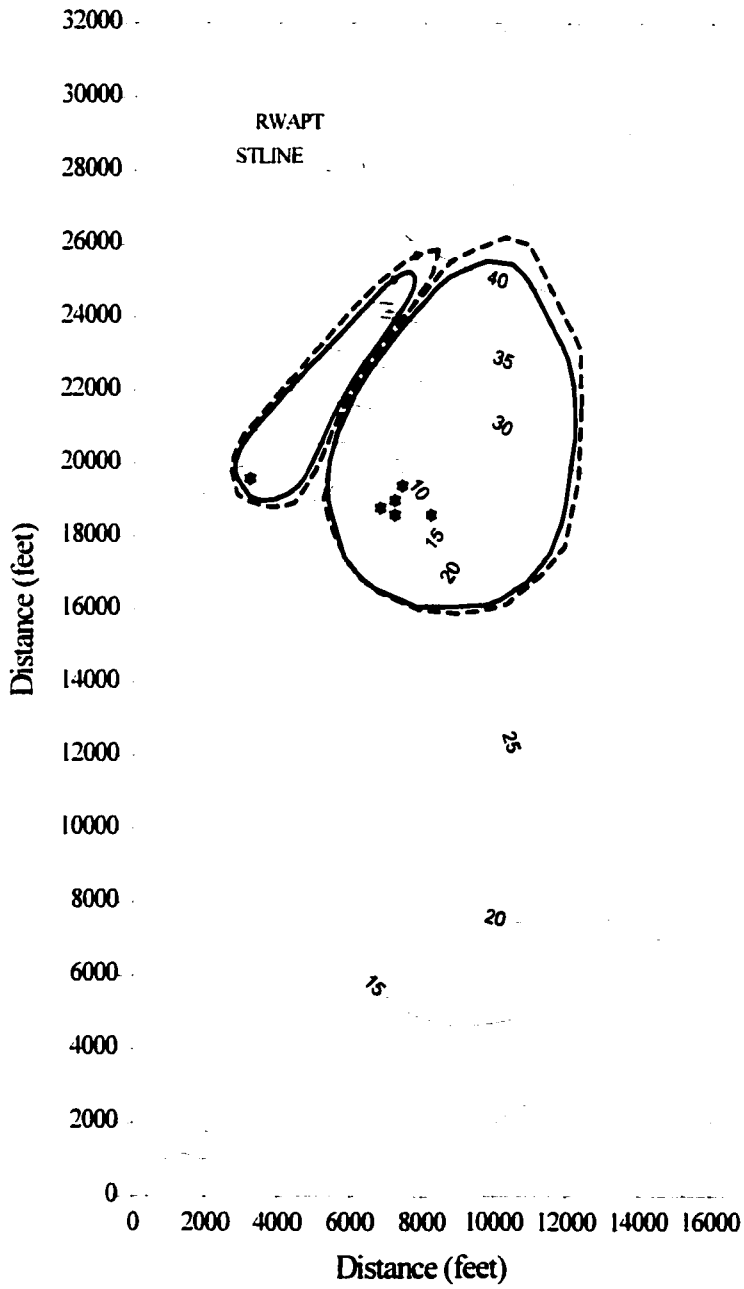


Figure 3.11: The 10 Year STLINE and RWAPT Capture Zones for the UWTR Wellfields

Forward Difference Method: $$S_m = \frac{dP}{d\alpha} = \left[\frac{P^{high} - P^{ave}}{\alpha^{high} - \alpha^{ave}}\right] \quad (3.1)$$

Backward Differences Method: $$S_m = \frac{dP}{d\alpha} = \left[\frac{P^{ave} - P^{low}}{\alpha^{ave} - \alpha^{low}}\right] \quad (3.2)$$

Centered Difference Method: $$S_m = \frac{dP}{d\alpha} = \left[\frac{P^{high} - P^{low}}{\alpha^{high} - \alpha^{low}}\right] \quad (3.3)$$

where: P = system performance measure

α = the system parameter

The marginal sensitivity coefficient may be normalized to allow different sensitivity coefficients to be compared on an equal basis. The normalized sensitivity coefficient associated with the centered difference approach is given by the following:

$$S_m = \left[\frac{P^{high} - P^{low}}{\alpha^{high} - \alpha^{low}}\right]\left(\frac{\alpha^{ave}}{P^{ave}}\right) \quad (3.4)$$

The centered difference method will be used to generate marginal sensitivity coefficients for 8 model input parameters that include net infiltration rate, hydraulic conductivity and wellfield pumping rates for the 6 production wells in this study. The performance measures that were chosen for analysis include spatially distributed hydraulic head, specific grid block values of hydraulic head, and capture zone area. The perturbation of the system parameters away from the average input value was chosen to be ±1% of the average parameter value.

3.3.1 Groundwater Head as a Performance Measure

The low, average and high values of pumping rate for the 6 production wells at the UWTR wellfields considered in this study were determined using the data from 1981 to 1995 and are presented in Table 3.3. The analysis was divided into the sensitivity of model output to the pumping rate for well 20 (Q_{20}) and the sensitivity of model output to the total pumping rate for the Parkway wellfield ($Q_{parkway}$). The distribution of normalized sensitivity coefficients of groundwater head to perturbations in Q_{20} is presented in Figure 3.12, and to perturbations in $Q_{parkway}$ is presented in Figure 3.13. The significance of these sensitivity plots is that the groundwater heads are highly sensitive to pumping rate in the vicinity of the both wellfields. An increase in wellhead pumping rate results in a decrease in the value of head, which leads to the negative values of sensitivity coefficient. These plots also indicate that groundwater head is much more sensitive to the Parkway wellfield pumping rate because the Parkway wellfield has a greater influence on drawdown of the water table around both wellfields.

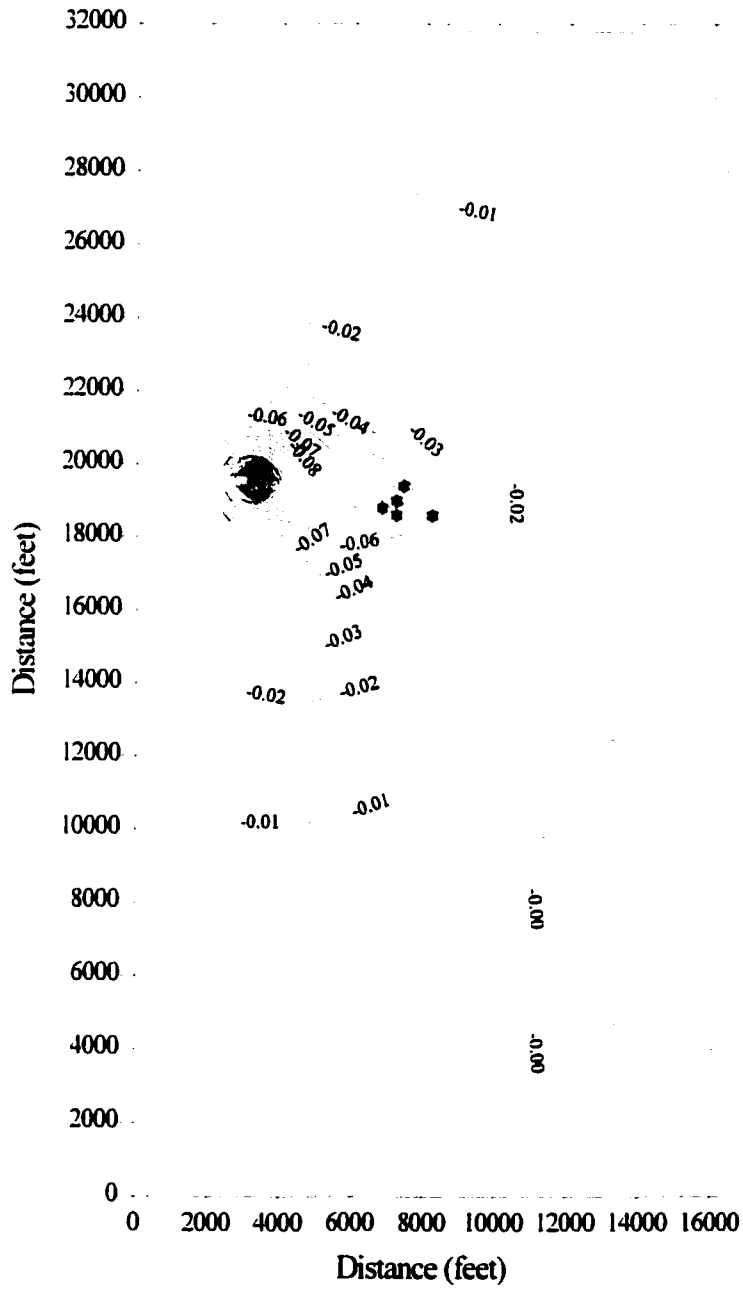


Figure 3.12: Normalized Sensitivity of Groundwater Head to Well 20 Pumping Rate

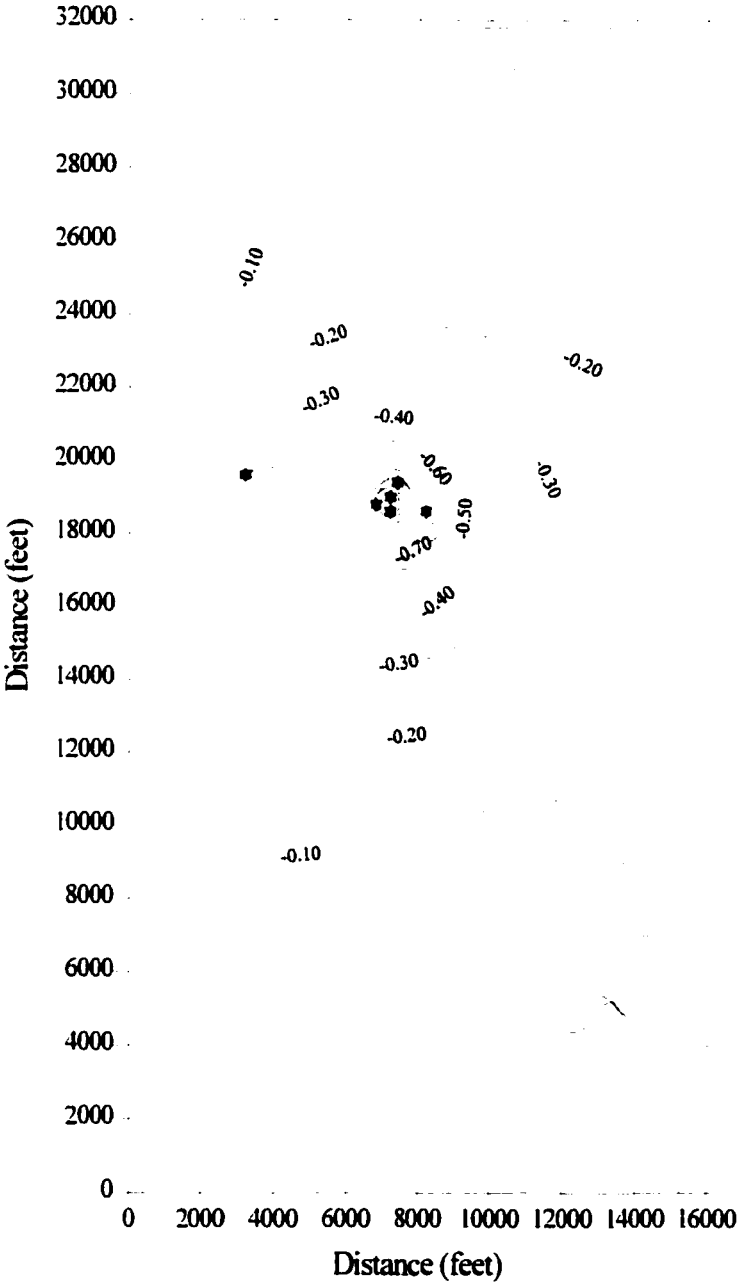


Figure 3.13: Normalized Sensitivity of Groundwater Head to Parkway Wellfield Pumping Rate

The average value of recharge used to model the flux of water into the upper boundary is 0.00132 meters/day. The perturbed values of recharge, 0.001307 meters/day and 0.001335 meters/day, were distributed uniformly within the conceptual model for simulation. The distribution of normalized sensitivity of groundwater head to net infiltration is presented in Figure 3.14. The significance of this sensitivity plot is that groundwater head increases with an increase in net infiltration. It is also evident that, for the Reich Farm site, groundwater head is more sensitive to infiltration than to any of the other model parameters. This is a result of the fact that the largest source of water for this flow system comes from net infiltration.

The average value of hydraulic conductivity, for K_x and K_y, in the conceptual model of the Reich Farm site is 45.7 meters/day. This value was perturbed to obtain 45.3 meters/day for the α^{low} value and 46.2 meters/day for the α^{high} value of the input parameter. These values were distributed within the conceptual model of the site to perform two simulations of model output. The distribution of normalized sensitivity of groundwater head to hydraulic conductivity is presented in Figure 3.15. The significance of this plot is that groundwater head decreases with an increase in hydraulic conductivity because groundwater flow through each grid block is more easily accommodated. This sensitivity is more prevalent in areas of the conceptual model that are far away from the pumping wellfields and prescribed boundaries. This is a result of the fact that the increase in flow has a greater effect in areas where the average flow is the smallest, and this occurs farthest away from the prescribed boundaries.

UWTR Well	Q^{low} (ft^3/day)	Q^{ave} (ft^3/day)	Q^{high} (ft^3/day)
Well 20	63,756	64,400	65,044
Well 22	74,745	75,500	76,255
Well 24	65,538	66,200	66,862
Well 26	61,776	62,400	63,042
Well 28	61,875	62,500	63,125
Well 29	63,162	63,800	64,438

Table 3.3: Well Pumping Rates for the Sensitivity Analysis of Model Performance

3.3.2 Groundwater Head Through Each Wellfield

The spatially distributed plots of normalized sensitivity coefficients provide an understanding of how the sensitivity varies within the conceptual model for a specific parameter. To determine which parameters are most important, specific model grid blocks were selected to compare normalized sensitivity coefficients. Two transect lines were generated. The first one intersects well 20 and the second one intersects the Parkway wellfield. The orientation of these transect lines was

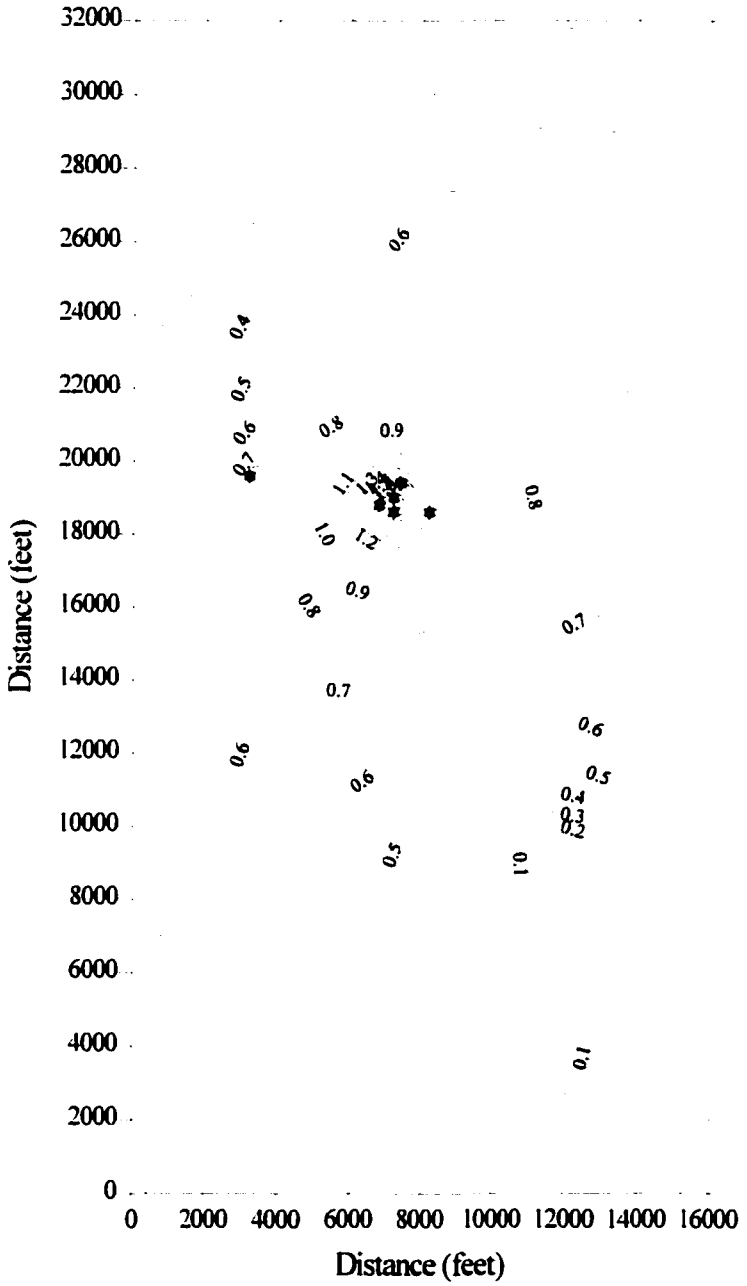


Figure 3.14: Normalized Sensitivity of Groudwater Head to Net Infiltration

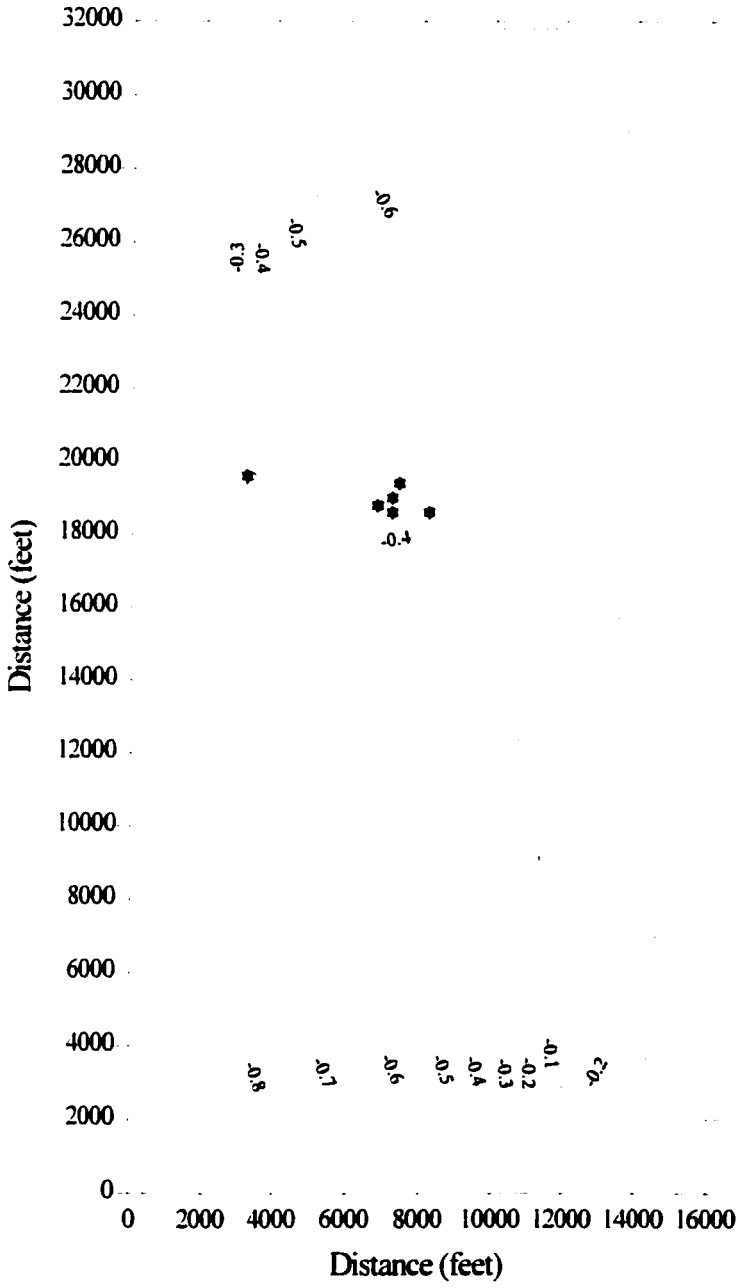


Figure 3.15: Normalized Sensitivity of Groundwater Head to Hydraulic Conductivity

chosen to coincide with the regional hydraulic gradient through the UWTR wellfields. These two lines are presented in Figure 3.16 along with the grid block centers that intersect each transect line. The value of normalized sensitivity coefficient as it varies with distance away from the wellfield for each of these two transect lines is presented in Figures 3.17 and 3.18.

From these figures a number of points are evident about the sensitivity of the numerical model to changes in the input parameters. As the net infiltration to the upper layer increases there is more water available to the groundwater flow system and the elevation of the water table increases, and thus the marginal sensitivity of hydraulic head to infiltration is positive. In contrast, as pumping rate and hydraulic conductivity increase the water table is lowered, and the marginal sensitivities of hydraulic head to pumping rate and hydraulic conductivity are negative. Figure 3.17 and 3.18 also show that, for both components of the United Water Toms River wellfield, the net recharge rate to the upper layer of the conceptual model is the most sensitive parameter. This is a result of the fact that the major source of water for this flow system is the net infiltration. With less infiltration there is less water available to the pumping wells, and the drawdown effects are larger, creating larger zones of influence around the wellheads.

3.3.3 Capture Zone Area as a Performance Measure

Another measure of the sensitivity of a groundwater model used to generate capture zones is the size of the area contained within the capture zone. A computer program, called CZAREA, was written in FORTRAN to calculate the area within a convex hull capture zone generated from the output from the STLINE particle tracking program. The computer code for this program is found in Appendix III. Table 3.4 summarizes the area contained within the 5 year capture zone and the normalized sensitivity of capture zone area to each of the input parameters.

From this table a number of points are evident about the sensitivity of capture zone area to the parameters in the groundwater model. The most sensitive input parameter is well pumping rate; for well 20 it is the well 20 pumping rate and for the Parkway wellfield it is the average Parkway wellfield pumping rate. This is a result of the fact that increased pumping has the greatest impact on decreasing the head field in the vicinity of the well that results in an increased magnitude of groundwater velocity around the wellhead. The increase in velocity results in longer particle pathlines emanating from the wellhead for a specific travel time and thus results in a larger capture zone area. The marginal sensitivity of capture zone area to both hydraulic conductivity and pumping rate are positive because an increase in each parameter causes a decrease in the hydraulic head field that results in a larger velocity field and an increase in the size of the resulting capture zone. The

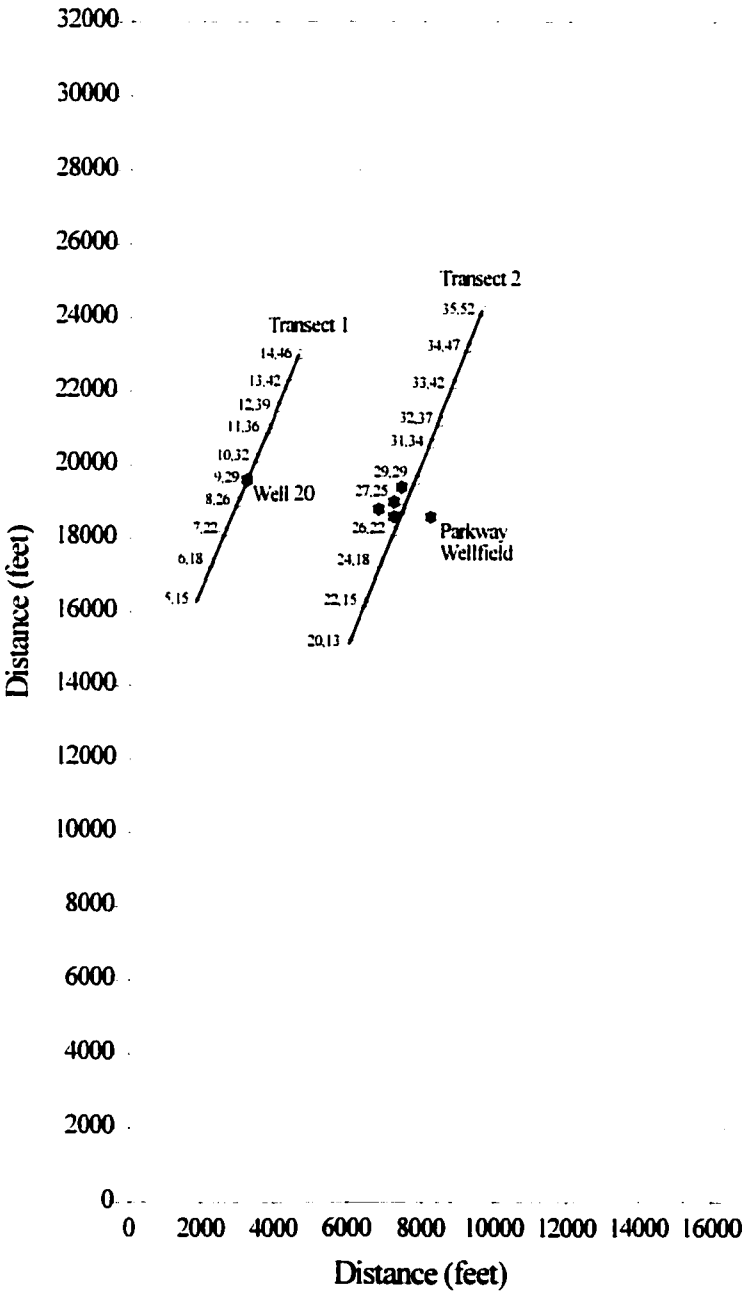


Figure 3.16: Location of the Transect Lines and Associated Grid Block Centers

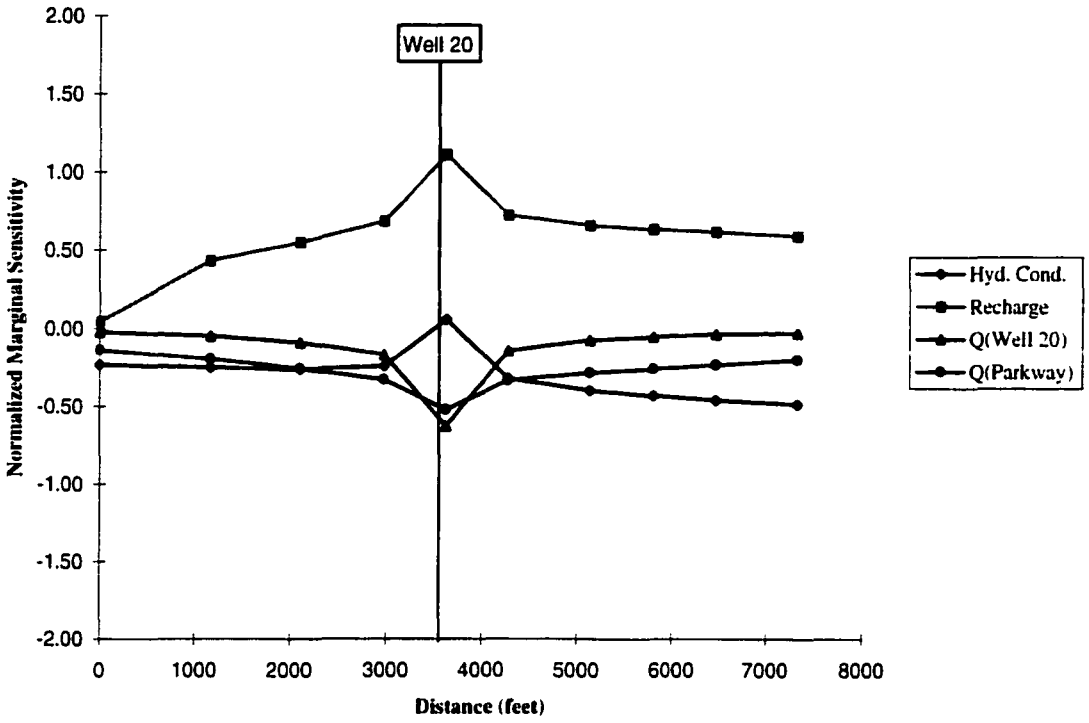


Figure 3.17: The Normalized Sensitivity Values for Grid Block Head Along Transect 1

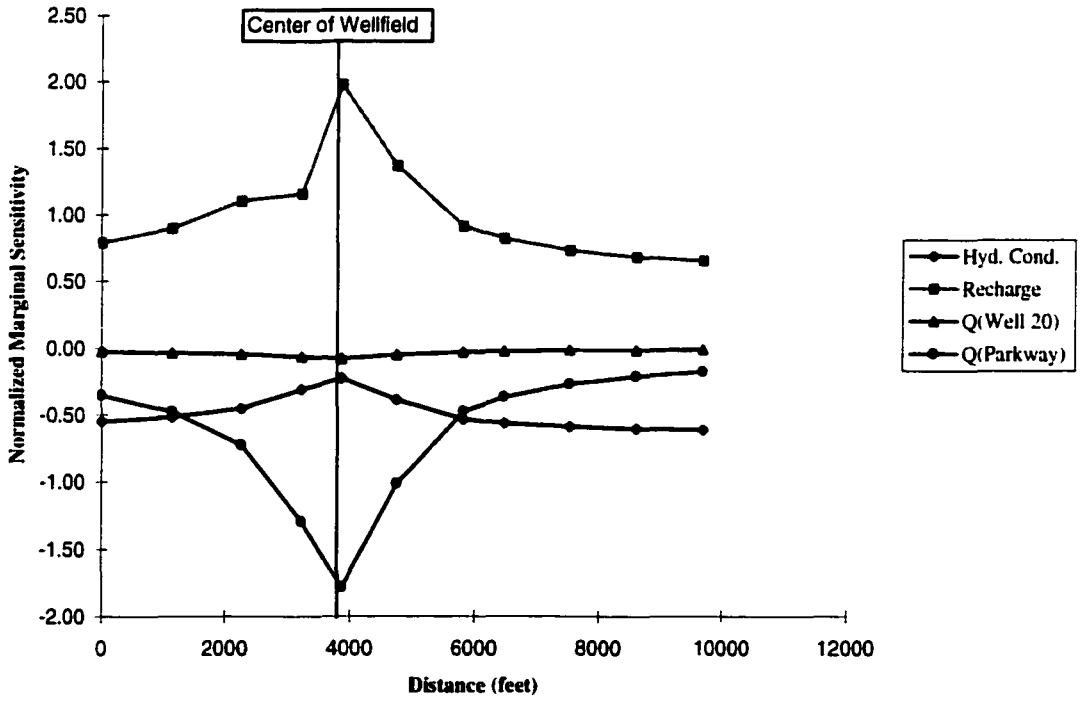


Figure 3.18: The Normalized Sensitivity Values for Grid Block Head Along Transect 2

least sensitive parameter for capture zone area is net infiltration. This is in direct contrast to the groundwater head performance measure. The marginal sensitivity of capture zone area to infiltration is negative because increased infiltration provides more water to the flow system resulting in a higher potentiometric surface in the aquifer, shorter time related particle pathlines, and a smaller capture zone area around the wellfield.

Simulation	Capture Zone Area (Parkway Wellfield) [sq.ft.]	Normalized Sensitivity Coefficient	Capture Zone Area (Well 20) [sq.ft.]	Normalized Sensitivity Coefficient
K(low)	31 695 101.2		6 591 093.1	
K(high)	31 826 907.8	0.207498	6 608 204.1	0.129636
I(low)	31 952 376.5		6 656 399.1	
I(high)	31 653 591.1	-0.050967	6 566 943.5	-0.073400
Q20(low)	31 758 057.4		6 525 017.0	
Q20(high)	31 765 649.1	0.011951	6 690 366.9	1.251193
Qp(low)	31 409 330.8		6 596 575.3	
Qp(high)	32 134 445.9	1.140782	6 628 328.3	0.240027

Table 3.4: The Sensitivity of Capture Zone Area as a Performance Measure

3.4 Summary

The steady state analysis of groundwater flow in the Cohansey aquifer beneath the United Water Toms River wellfields has revealed a number of points that relate to the risk of contamination of these wellheads. The imposition of the wellfields on the prepumping groundwater flow field has changed the flow of groundwater within the aquifer and as a result as changed the flow of potential contaminants. Prior to pumping, contaminants from the Reich Farm Superfund site migrated to the Toms River to the west of the site. After the wellfields began operating, some of the contaminant pathlines changed directions and part of the contaminants began to migrate directly toward the wellfields. A numerical modeling analysis of solute transport using advective particle tracking was not as revealing about the effect of the contaminant source on the wellheads as a transport analysis using advective-dispersive particle tracking. The advective transport analysis showed contaminant pathlines entering well 20 to the west, while a random walk analysis showed contaminant pathlines entering both wellfields. Random walk particle tracking uses more information about the interaction between the solute particles and the hydrogeologic environment in determining the effect that the contaminant source has on this sensitive aquifer. As a result, the RWAPT model will be used as a numerical model for generating WHPAs around the municipal wellheads, and will be one of the models compared in the benefit-cost-risk analysis in Chapter 4.

From the sensitivity analysis, the most sensitive parameter in the conceptual model for the performance measure of groundwater head is net infiltration. This hydrologic stress is the most important source of water for the Cohansey aquifer system. For the performance measure of capture zone area the most sensitive parameter in the conceptual model is wellhead pumping rate. Wellhead pumping rate has the greatest effect on the groundwater flowfield near the wellhead at the starting points for reverse particle tracking analysis. The information from the sensitivity analysis will be helpful in determining parameter distributions for the uncertainty analysis of numerical modeling of WHPA boundaries in Chapter 6.

CHAPTER 4
DECISION ANALYSIS FOR WHPA DELINEATION

4.1 Introduction

There are many modeling alternatives that may be used to generate a WHPA boundary. The criteria and constraints that are used to detail the acceptable alternatives are set out in a Wellhead Protection Plan. The process of WHPA delineation ultimately results in zoning the area encompassed by each WHPA boundary as a special land-use class. The municipal ordinance accompanying the zoning process places restrictions on industrial development within each groundwater protection zone. The purpose of Chapter 4 is to introduce environmental decision making as a method for choosing the best model among all acceptable alternatives for delineating wellhead protection areas for groundwater protection.

4.2 The Philosophical Basis Underlying Groundwater Protection

Groundwater is an important yet vulnerable resource in North America. Groundwater aquifers represent a major economic source of potable water. Once contaminated, groundwater is very costly to remediate. The most cost-effective means of ensuring a safe groundwater supply is to prevent contamination from occurring in the first place, and this can be accomplished using groundwater protection initiatives. The most practical means of groundwater protection occurs at the municipal level through the implementation of site-specific groundwater protection planning. The purpose of land-use planning is the division of a jurisdiction into districts to enable the regulation of land to promote the orderly development of the area and to provide for the protection of public health, safety and welfare.

The philosophical principle underlying groundwater protection is to prevent contamination, which might have an adverse effect on human health, from entering public water systems. To implement this principle, a number of basic steps need to be addressed. These steps include:

1. the development of policies for changing land-use patterns to implement groundwater protection initiatives
2. the determination of the level of protection that is to be applied to each groundwater protection district
3. the development of a methodology for choosing the best method for implementing groundwater protection

4. the hydrogeologic analyses necessary to form an understanding of the groundwater flow system in sensitive aquifers
5. the delineation of the regions of space, or planning districts, which overlay a sensitive aquifer, to which the principles of groundwater protection will be applied
6. the identification of all sources of contamination within each planning district that could have a potential impact on water quality at the wellheads
7. the development of policies to manage potentially risky land-use practices in sensitive areas of the community
8. the specification of contingency plans for an alternative supply of water in case the municipal wellheads become contaminated
9. the development of strategies to monitor groundwater quality in protection districts to assess the effectiveness of protection initiatives
10. the development of education programs to increase public awareness of groundwater protection issues

The standard methodology for applying these principles in North America has been developed by the USEPA as a result of the Wellhead Protection Amendments to the Safe Drinking Waters Act. The purpose of the present research is to determine the best alternative for modeling the location of the WHPA boundaries using the USEPA methodology. To achieve this goal it is necessary to complete steps 1 through 5 presented above. This will be accomplished in the following manner.

Step 1 Policies for changing land-use patterns will be developed in a community Wellhead Protection Plan. State Wellhead Protection Plans, submitted to the USEPA for approval by each state, provide the range of acceptable criteria and constraints for developing the Wellhead Protection Plan.

Point 1.1 A WHP Plan will be formulated for Pleasant Plains, New Jersey to delineate the set of acceptable WHPA alternative boundaries.

Step 2 The level of protection for each protection zone will be developed using a combination of groundwater monitoring and the minimization of industrial development.

Point 2.1 A set of zoning controls will be developed for each groundwater protection zone, which will increase protection with proximity to the wellhead.

Step 3 A comparison of WHPA boundary alternatives will be performed using a benefit-cost-risk approach.

Point 3.1 Determine the benefits of each WHPA model.

Point 3.2 Determine the costs of each WHPA model, which will consist of the engineering and planning costs of zoning a modeled WHPA boundary.

Point 3.3 Determine the risk of each WHPA model.

Point 3.3.1 Define failure of a WHPA model by choosing a standard for comparing WHPA models. This standard was chosen to be the Zone of Confidence for multiple WHPA boundaries. It will be used to define the size of the failure area associated with each WHPA boundary.

Point 3.3.2 Determine the type of failure. The total failure area may be comprised of a number of different types of failure based on the interaction between the ZOCs and the set of WHPA alternatives.

Point 3.3.3 Determine the probability of failure. The present research will use data on the WHPA models found in State WHP Plans, and compare the application of each model using a weighted attributes matrix.

Point 3.3.3.1 Choose the evaluation criteria for comparing WHPA models from the USEPA guidance document on WHPA delineation.

Point 3.3.3.2 Choose the weighting for each evaluation criterion.

Point 3.3.3.3 Rate each model for each evaluation criterion.

Point 3.3.3.4 Multiply the rating and weighting values to determine the score for each model. Calculate the probability of model failure.

Point 3.3.3.5 Determine a probability of choosing a criterion value for implementing WHPA modeling in each protection zone (e.g. values for distance or time of travel) based on the State WHPA Plans.

Point 3.3.4 Determine the cost of failure. This will be based on the economic factors that affect municipal planning within a community. The present research will focus on industrial development as the most important non-agricultural point source that threatens groundwater quality. The cost of failure will be the cost of preventing existing and future industrial development from locating within each of the different groundwater protection zones.

Point 3.3.4.1 Define the economic constraints associated with being located within a failure zone. They will include some, or all, of the following: the cost of purchasing land, the cost of facility relocation and the cost of groundwater monitoring within each protection zone.

Point 3.3.4.2 Apply these costs of failure to each type of failure.

Point 3.3.5 Define the risk of failure to be probability of failure times cost of failure.

Step 4 Develop a conceptual model of the groundwater flow system and use this model to implement WHPA delineation. The most scientifically defensible method of accomplishing this is to develop a numerical model of the flow system, which should include an understanding of:

Point 4.1 The extent and permeability of hydrogeologic units.

Point 4.2 The major surface water features of the watershed, and their interaction with the groundwater system.

Point 4.3 The natural, physical boundaries of the flow system.

Point 4.4 The water balance of the flow system.

Step 5 Delineate a complete set of WHPA alternatives for each municipal wellfield. All of the WHPA models presented in the WHP Plan will be used to delineate the WHPA boundaries. For each groundwater protection zone the net present cost of delineation will be calculated using the following steps:

Point 5.1 Delineate the complete set of WHPA boundaries on a single figure.

Point 5.2 Compare each boundary to the ZOCs to determine the total failure area.

Point 5.3 Determine the types of failure within the total failure area.

Point 5.4 Calculate the cost of failure for each type of failure.

Point 5.5 Sum the total cost of failure for each boundary alternative.

Point 5.6 Determine the risk of failure by multiply the cost of failure and the probability of failure.

Point 5.7 Add the cost of delineation and the risk of failure to determine the net present cost of using each WHPA model.

4.3 Wellhead Protection Plan

The Wellhead Protection Plan for the UWTR wellfields was formulated using information from a paper produced by the USEPA (Job, 1997). This paper summarizes the criteria, constraints and methods used by 46 states to prepare State Wellhead Protection Plans that were submitted to the USEPA for approval. Tables 4.1, 4.2 and 4.3 present a summary of the information found in these State Wellhead Protection Plans.

The Wellhead Protection Plan for the UWTR wellfields uses a three-tiered approach to groundwater protection. It includes a Zone I, Zone II and Zone III WHPA boundary for each wellfield. The Zone I boundary is closest to the wellheads. No development will be allowed within the Zone I boundary. The Zone II boundary will be next farthest away from the wellhead, and for

industry located within this boundary an intense program of annual groundwater monitoring will be required. The Zone III boundary will be farthest away from the wellhead, and for industry within this boundary a less intense program of annual groundwater monitoring will be required.

Delineation Method	Number of State WHP Plans
Arbitrary Fixed Radii	31
Calculated Fixed Radii	26
Simplified Variable Shapes	6
Analytical Modeling	26
Numerical Modeling	17
Hydrogeologic Mapping	31

Table 4.1: The Number of State WHP Plans Using Each Method of Delineation

Zone I Arbitrary Radii	Number of State WHP Plans
250 foot	1
500 foot	4
1000 foot	6
1500 foot	6
2000 foot	1
½ mile	1
3000 foot	1
1 mile	4

Table 4.2: Distances Used For Applying Arbitrary Fixed Radius Modeling

Zone II and III Travel Times	Number of State WHP Plans
2 year	1
3 year	1
5 year	16
2500 day	1
10 year	11

Table 4.3: Travel Times Used For Applying Analytical and Numerical WHPA Modeling

The Zone I WHPA boundary uses the distance criterion in combination with arbitrary fixed radii, the 180 day (½ year) time of travel calculated fixed radius and the ½ year numerical modeling (RWAPT) boundaries. The Zone II WHPA boundary uses the 5 year time of travel criterion in combination with calculated fixed radii, analytical methods and numerical models. The Zone III WHPA boundary uses the 10 year time of travel criterion in combination with calculated fixed radii, analytical methods and numerical models. The uniform flow equation is the analytical method of WHPA delineation. The three analytical models include RESSQC, GPTRAC and MWCAP, which

are components of WHPA version 2.2 (Blandford and Huyakorn, 1990). The numerical flow model is a combination of SWIFT, which is used to define the groundwater flow regime, STLINE for advective particle tracking and RWAPT for random walk particle tracking.

4.4 Environmental Decision Making for Delineating WHPAs

4.4.1 The Benefits and Costs of WHPA Delineation

To choose the best placement of a WHPA boundary using environmental decision making it is necessary to determine the benefits, costs and risks of delineating a groundwater protection zone. This will be achieved using the approach developed by Massmann and Freeze (1987a). The benefits of a WHPA boundary are the societal benefits of a clean source of potable water. These benefits are the same for all groundwater protection alternatives, regardless of the land encompassed by the final boundary, as long as the wellhead continues to pump groundwater that meets appropriate drinking water quality objectives. Since these benefits do not aid in differentiating between WHPA delineation alternatives they will be left out of the analysis, and decision making will be based on minimizing the costs and risks of each WHPA model.

For typical engineering ventures the costs of a project are those that are incurred during the design and implementation of the final structure. For delineating a WHPA boundary these costs include the engineering time involved in delineating the WHPA boundary and the cost of producing a Wellhead Protection Report. An estimate of these costs was made based on the cost of producing similar civil engineering consulting reports. These costs were developed with a relatively simplistic, two-dimensional conceptual model in mind, and therefore, they would increase with an increase in the complexity of the hydrogeologic environment beneath the study site. The cost of producing the arbitrary fixed radius WHPA boundary and completing a WHP report, which takes approximately 1 person-week of engineering time, is $5,000 and for the calculated fixed radii boundary this cost is $7,500. The cost of producing a WHPA boundary using the uniform flow equation, which takes approximately 2 person-weeks of engineering time, is $10,000. The cost of using an analytical model, which takes approximately 3 weeks for a groundwater modeler, is $15,000. The cost of producing a calibrated and verified groundwater map of the area around a pumping well, and to perform advective particle tracking of the WHPA boundary, which takes approximately 8 person-weeks for a groundwater modeler, is $40,000. The time to extend the groundwater flow analysis to include random walk particle tracking would involve one extra person-week for a groundwater modeler resulting in a cost of $45,000 for the RWAPT boundary.

4.4.2 The Risk of WHPA Delineation

For each WHPA boundary, for example the Zone I protection boundary, there is only one true placement for it on the ground surface. This true placement of the WHPA boundary is based on the delineation criteria presented in the Wellhead Protection Plan. Each method used to model a WHPA boundary determines only an approximation of its true placement because of the uncertainty in modeling the hydrogeologic environment. The risk associated with modeling a WHPA boundary is a combination of the cost of failure and probability of failure for the modeled boundary. These two components of the environmental decision making paradigm are determined by choosing a performance standard for WHPA modeling so that each alternative may be compared to the standard to determine the extent of failure.

Determining the extent of failure for WHPA delineation is not straightforward because no performance standard currently exists. In other environmental decision making situations, performance measures are prevalent. For example, the analysis of contaminant plume migration from an industrial property uses the applicable Water Quality Guidelines for the analysis of groundwater quality. These guidelines are compared to the concentration of contaminants in groundwater samples taken from monitoring wells at the property line of the industrial facility. The Water Quality Guidelines provide a measurable scale against which the extent of failure may be assessed. There is no equivalent performance standard for determining the failure of a wellhead protection area.

A useful basis for developing a performance standard for WHPA delineation comes from a paper by Evers and Lerner (1998). The authors proposed that a reasonable parameter that may be used to describe the certainty in WHPA modeling is the zone of confidence (ZOC) that is generated by multiple numerical model simulations of the WHPA boundary. The authors defined the ZOC to be the area "which falls within all reasonable estimates of the catchment" which result from Monte Carlo simulation of a specific numerical WHPA model. The purpose of environmental decision making is to choose the best alternative for WHPA delineation using a number of different models. The ZOC will be re-defined, for the present research, to be the area that falls within all reasonable modeling estimates of the WHPA boundary for each groundwater protection zone. For each delineation model, the area that falls within the WHPA boundary but outside of the common ZOC will be defined as the zone of delineation uncertainty (ZDU). The area contained within the borders of all modeled boundaries, but outside of the ZOC, will be defined as the zone of uncertainty (ZOU). Figure 4.1 presents three potential WHPA boundaries and the ZOC contained within these boundaries, and shows the ZOU boundary that contains all three WHPAs, and the ZDU for the first WHPA boundary.

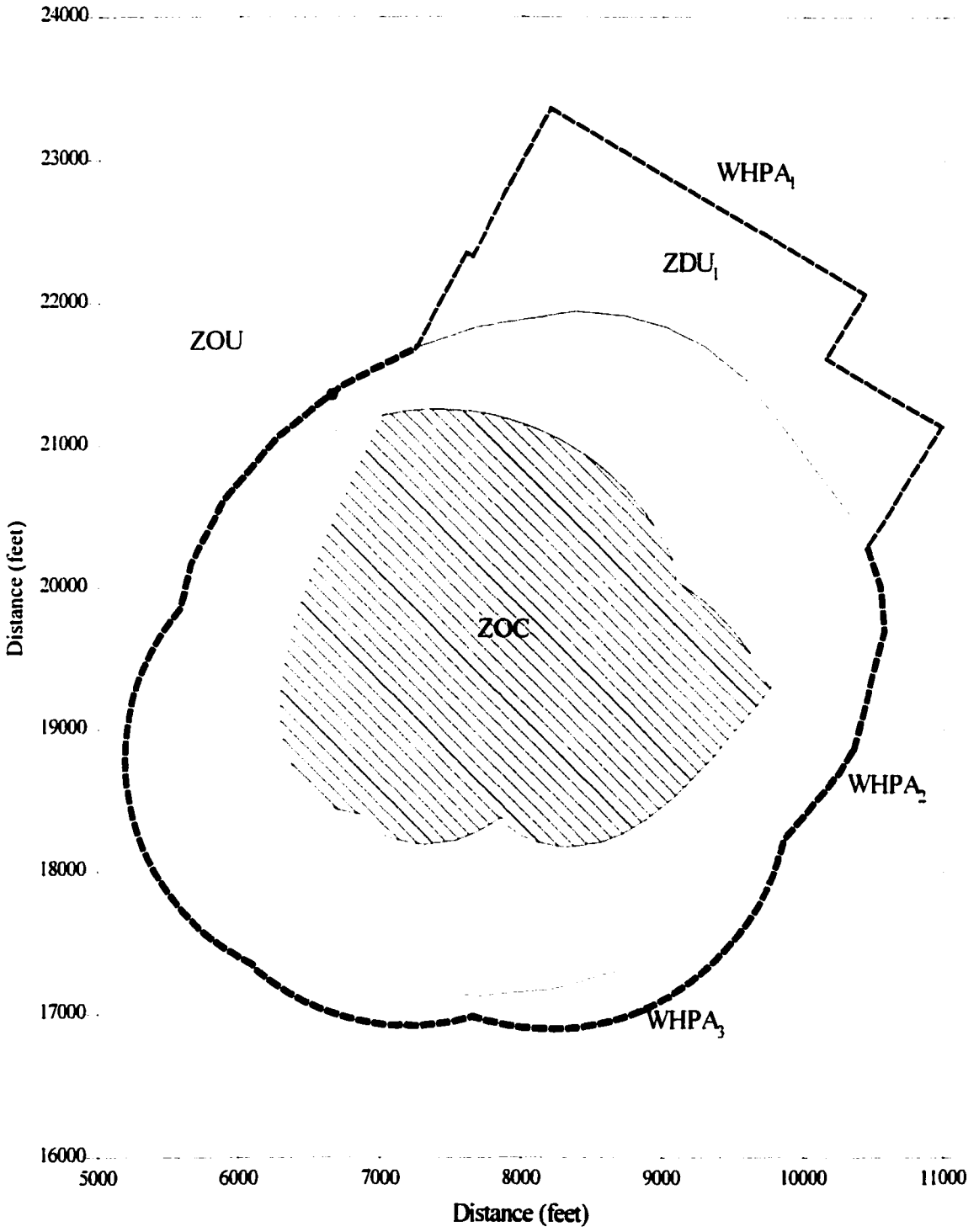


Figure 4.1 The ZOC, ZDU and ZOU Parameters That Define WHPA Uncertainty

The ZOC, as a performance standard, was developed to compare WHPA delineation methods that use scientific principles to model the location of the WHPA boundary. The time of travel based techniques represent the only delineation methods that use some scientific basis to model the hydrogeologic environment. As a result, the ZOC will only be applied to the analysis of the time of travel based methods of WHPA delineation. For the present research this entails the analysis of the Zone II and Zone III WHPA boundaries. The distance-based techniques represent a more arbitrary basis for WHPA boundary delineation, and therefore, will be compared using the total area that is contained within each potential boundary.

4.4.2.1 The Cost of Failure for WHPA Delineation

The cost of failure depends on how the groundwater protection zones are modeled relative to the true WHPA boundary. To illustrate this point, Figure 4.2 shows a three-tiered WHPA boundary placement around a hypothetical wellhead. The set of WHPA boundaries labelled "Real WHPAs" represent the true placement of the three protection boundaries. The set of WHPA boundaries labelled "Modeled WHPAs" represent the location of the boundaries that were produced by a hypothetical groundwater model. Because the Wellhead Protection Plan specifies a three-tiered approach to WHPA boundary delineation there are 15 potential areas of intersection between the "Real" and "Modeled" WHPA boundary sets.

The potential cost of failure within each intersecting area depends on the restrictions that are placed on industrial activity, as detailed in the Wellhead Protection Plan, and the relationship between the "Modeled" and "Real" WHPA boundaries. These costs of failure are specific to each groundwater protection zone, and therefore, each protection zone will be discussed separately.

Within Zone I, the USEPA recommends that the public water supply company, or local planning authority, control activity. They suggest that this be achieved by adopting a special zoning status for Zone I and purchasing the property within the WHPA boundary. They also recommend that signs be posted at all intersections between local roads and the WHPA boundary indicating the special zoning status and restricted activity within the Zone I boundary. Industrial activity will be prohibited within Zone I and the only acceptable use of this area will be parkland or natural open space.

The cost of failure will be based on the amount of developable land between the Zone I boundary and the ZOC boundary, and the average purchase price of this land. For companies that want to locate within a community the Zone I boundary is not available for development. For undeveloped land within the Zone I failure area, the cost of failure is the forgone revenue associated with not selling this land as industrial land. For companies which are already located within the Zone

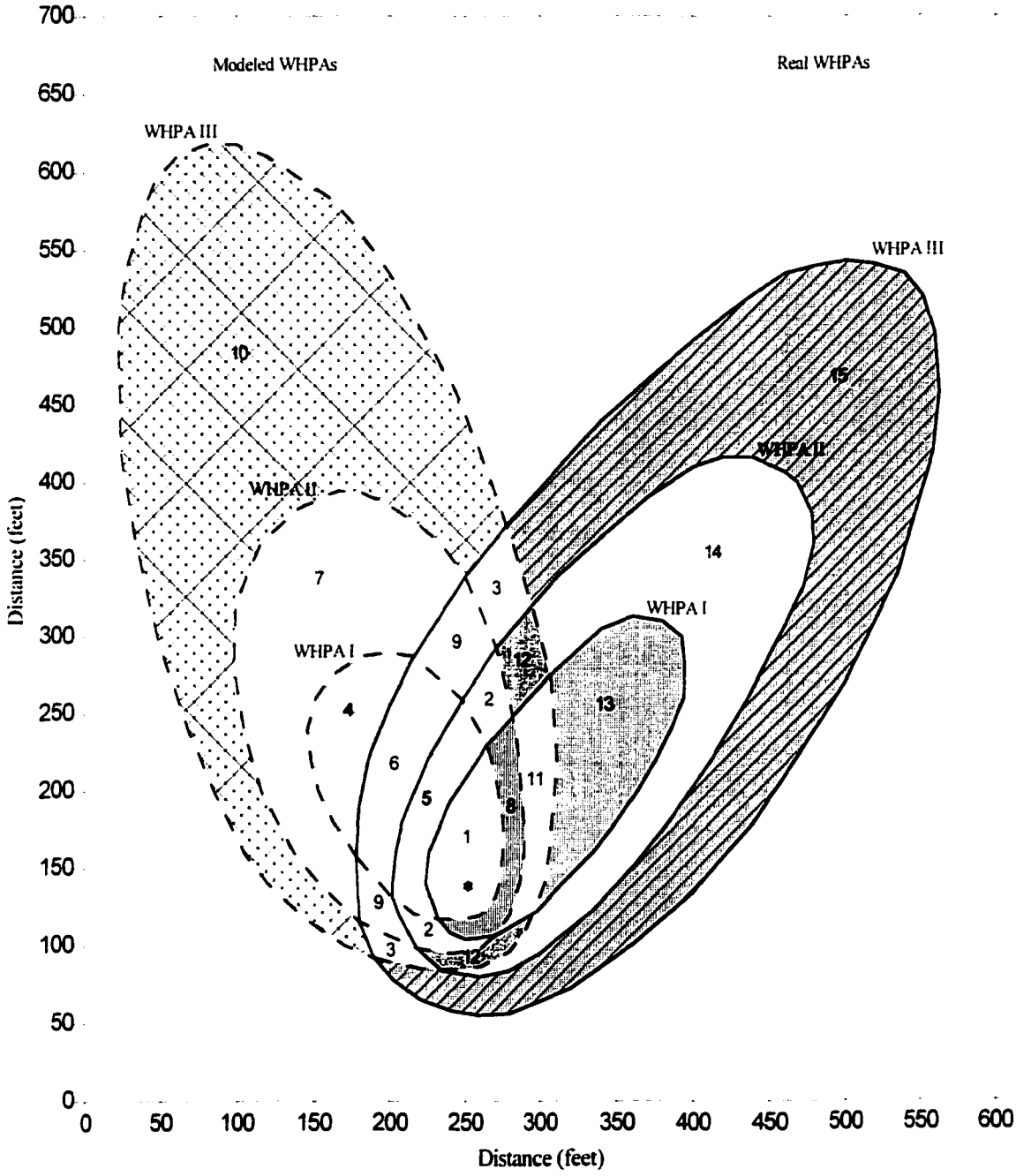


Figure 4.2: Failure Areas for a Three-Tiered Approach to WHPA Zoning

I failure area it will be necessary to relocate them to another industrial property, and thus the cost of failure for the town is the cost of purchasing the land and the cost of relocating the facility. The average cost of industrial land was estimated to be $40,000 per acre and the average cost of facility relocation was estimated to be $1,000,000 per industry.

Restricted industrial activity will be allowed within the Zone II boundary. The cost of failure will be the extra cost associated with the annual groundwater monitoring program for facilities located in the failure area associated with the Zone II boundary. A typical annual monitoring program consists of water quality testing on 3 wells downgradient of the facility at a frequency of 4 times per year (Reichard *et al.*, 1990). The annual cost of groundwater monitoring is approximately $60,000 per year per industrial facility for sample analysis and a written report. This extra cost of $60,000 per year is the cost of guaranteeing that a specific industrial facility within the Zone II boundary does not contaminate the groundwater within the protection zone.

Less severe restrictions will be applied to industrial activity within the Zone III boundary, and the cost of failure will also be less severe. Groundwater monitoring is required within the Zone III boundary but only 2 downgradient wells need to be sampled on an annual basis (Reichard *et al.*, 1990). The annual cost of groundwater monitoring is $10,000 for each industrial property within Zone III. The cost of failure will be the extra cost associated with the annual groundwater monitoring program for facilities located in the failure area associated with the Zone III boundary.

To determine the risk associated with each groundwater protection zone, it is necessary to develop a number of engineering factors that relate to the amount of industrial development that could exist within the area surrounding the supply wells. In Dover Township, approximately 50% of the land is available for development, and approximately 25% of this land has already been developed. There are approximately 2.0 acres of developable land per industrial facility in New Jersey. These engineering factors were estimated from site maps of the Ocean County area of New Jersey.

These engineering factors are community specific. A better source for this data would be the zoning maps for the area above the sensitive aquifer, and a survey of industrial and residential lots around each wellhead within the community. This type of survey is generally performed as part of implementing wellhead protection during the analysis to identify all anthropogenic sources of contaminants within the watershed (USEPA, 1991). However, this information was not available for the Pleasant Plains area at the time that the present research was performed.

It is now possible to identify the cost of failure for each of the intersecting areas in Figure 4.2. Table 4.4 presents the type of failure and identifies the cost of failure associated with these 15

areas of intersection. To understand this table it is necessary to define a number of terms. The numbers in column 1 refer to the areas in Figure 4.2. The capitalized Roman numerals in columns 2 and 3 refer to WHPAs I, II and III. "Moving" is a cost parameter that refers to the cost of moving an existing facility to a new location, which has been set at $1,000,000 for the building and $40,000 per acre for the land. "Monitoring (II)" and "Monitoring (III)" are cost parameters that refer to the cost of groundwater analysis associated with industrial properties located in WHPAs II and III, respectively. These cost parameter have been set at $60,000 and $10,000 per facility per year, respectively. "Land" is a cost parameter that refers to the cost of purchasing a parcel of land, which has been set at $40,000 per acre.

Failure Type	Modeled WHPA Zone	Real WHPA Zone	Cost of Failure	
			Existing Facilities	New Development
1	I	I	none	none
2	II	II	none	none
3	III	III	none	none
4	I	none	moving	land
5	I	II	[moving – monitoring (II)]	[land - monitoring (II)]
6	I	III	[moving – monitoring (III)]	[land - monitoring (III)]
7	II	none	monitoring (II)	monitoring (II)
8	II	I	[moving – monitoring (II)]	[land - monitoring (II)]
9	II	III	[monitoring (II) – monitoring (III)]	[monitoring (II) - monitoring (III)]
10	III	none	monitoring (III)	monitoring (III)
11	III	I	[moving – monitoring (III)]	[land - monitoring (III)]
12	III	II	[monitoring (II) – monitoring (III)]	[monitoring (II) – monitoring (III)]
13	none	I	moving	land
14	none	II	monitoring (II)	monitoring (II)
15	none	III	monitoring (III)	monitoring (III)

Table 4.4: Types and Costs of Failure for WHPA Delineation

To compare these failure costs on an equal basis, all failure costs were converted into their equivalent net present worth. An engineering life of 30 years and a nominal rate of return of 6% were used to generate a value of 13.765 for the present worth factor for annual disbursements. The cost of failure, in terms of net present worth, will be determined using the following relationships:

$$\text{moving} = [\$40{,}000(X) + \$1{,}000{,}000(Z)] \quad (4.1)$$

$$\text{land} = [\$40{,}000(Y)] \quad (4.2)$$

$$\text{monitoring(II)} = [\$60{,}000(Z) * 13.76483] = [\$825{,}889.8(Z)] \quad (4.3)$$

$$\text{monitoring(III)} = [\$10{,}000(Z) * 13.76483] = [\$137{,}648.3(Z)] \quad (4.4)$$

where: X = amount of developed industrial land [acre]

Y = amount of undeveloped industrial land [acre]

Z = number of industrial facilities [facility]

To illustrate the interpretation of Table 4.4, failure type 8 will be explained. Failure type 8 refers to the failure associated with zoning the area contained within it as "WHPA II" when it should in reality have been zoned as "WHPA I". For a facility that currently exists within this area, the cost of failure is the difference between the cost of moving the facility (which would have occurred if the area had been designated as Zone I) and the cost of monitoring the groundwater (which is appropriate for Zone II). For undeveloped land within this area, the cost of failure is the difference between the unrealized sale of the land (which would have occurred if the area had been designated as Zone I) and the cost of monitoring the groundwater (which is appropriate for new facilities in Zone II).

4.4.2.2 The Probability of Failure for WHPA Delineation

The probability of failure for WHPA delineation represents the probability that the WHPA boundary that has been modeled has failed to determine the true location of the theoretical WHPA boundary. For groundwater protection using the distance criterion, the purpose of modeling is to ensure that the WHPA boundary is large enough to prevent any immediate contamination to the wellhead. There is a compromise between increasing the size of the WHPA to reduce the immediate risk of contamination, and reducing the size of the WHPA to reduce the impact of preventing development within this protection zone. As a result, the probability of failure will tend to decrease as the area contained increases. For time of travel based methods, the underlying principle is to attempt to model the true location of the theoretical WHPA boundary. Since it is impossible to determine the true boundary location there will be some failure associated with the area that is delineated. This failure area is reflected in the size of the ZDU that was determined for each delineation technique.

It is also important to ensure that the function that represents the probability of failure is based on both the choice of model (probability of model failure) and the choice of the criterion value that is used to implement the model (probability of criterion choice). The function that was developed is presented below:

$$P_f = (P_{mf} * P_{cc}) \qquad (4.5)$$

where: P_f = probability of failure

P_{cc} = probability of criterion choice

P_{mf} = probability of model failure

The probability of model failure was determined by evaluating the scientific effectiveness of each model for determining the true location of the WHPA boundary. Costanza and Sklar (1985)

developed a methodology for ranking scientific models and applied it to the evaluation of 87 freshwater wetland models. This ranking methodology evaluated each wetland model based on three factors: articulation (model size and complexity), accuracy (ability to describe the behavior of the system), and effectiveness (ability to explain articulation and accuracy). This method of ranking models proved to be a useful tool for researchers who planned to develop models for other freshwater wetland sites.

A similar evaluation system was developed herein to rate WHPA delineation models, which is based on the ranking methodology described above. This evaluation system is presented in the form of a weighted attributes matrix, which will subsequently be used to determine the probability of model failure. The weighted attributes matrix is commonly used in environmental assessment for comparing design alternatives. The present system evaluates each WHPA model using three evaluation criteria: model complexity, model flexibility and model facility. These evaluation criteria were derived from the technical evaluation factors that were developed by the USEPA to help states make a qualitative assessment of which delineation model (USEPA, 1987). Model complexity reflects the complexity of the scientific relationships in the model used to represent the hydrogeologic environment. Model flexibility reflects the ability of the model to simulate different hydrogeologic settings including the ability to model two-dimensional and three-dimensional settings. Model facility reflects the ease of gathering input data for the application of the model, which is a representation of the modeler's knowledge of hydrogeology for obtaining accurate results. The technical basis behind each of these models that will be compared is presented in Section 4.4.

The weighted attributes matrix for the WHPA models is presented in Table 4.5. Each of the evaluation criteria were assigned a weight such that the sum of the weights was 1.0, and each WHPA model was rated with a value between 0.0 and 10.0 for each of the evaluation criteria. The best method of determining these weighting and rating values is a survey of a number of experts familiar with the WHPA models and the groundwater protection issues. The results of this survey would be averaged to provide a better assessment of the true value of each model rating. The criterion weights were multiplied by the rating values for each evaluation criterion. The results were summed to provide a total score for each delineation model. Based on this system, the maximum score is a value of 10.0. The probability of model failure will be determined by dividing the total score for each model by 10.0, and subtracting the result from 1.0.

The function that was developed to represent the probability of criterion choice was produced from the information presented in Tables 4.2 and 4.3. For the arbitrary fixed radius method the implementation criterion is distance and its' values range from 250 feet to 1 mile.

For the analytical and numerical models the implementation criterion is time of travel and its' values range from ½ year to 10 years. Values for each of these criteria were chosen by decision makers during the preparation of the WHP Plan. From these ranges of values, it was possible to determine a probability of choosing a criterion.

Delineation Model	Evaluation Criteria			Total Score [10]	Probability of Model Failure
	Complexity [0.4]	Flexibility [0.4]	Facility [0.2]		
Arbitrary Fixed Radii	0.5	1.0	1.0	0.8	**0.920**
Calculated Fixed Radii	2.0	2.0	2.5	2.1	**0.790**
Simplified Shapes	3.5	2.5	3.5	3.1	**0.690**
Uniform Flow Equation	4.0	3.0	4.5	3.7	**0.630**
Analytical (MWCAP)	4.5	5.0	5.5	4.9	**0.510**
Analytical (RESSQC)	5.0	5.0	5.5	5.1	**0.490**
Analytical (GPTRAC)	5.5	5.0	5.5	5.3	**0.470**
Numerical (STLINE)	8.0	8.5	8.5	8.3	**0.170**
Numerical (RWAPT)	9.0	9.5	9.5	9.3	**0.070**

Table 4.5: Probability of Model Failure for Each WHPA Modeling Technique

For the distance criterion, the smallest value that was used is 250 feet. This implies that all decision makers agreed that the arbitrary fixed radius distance should be at least 250 feet, and therefore, the probability of criterion choice was assigned a value of 1.000. The next largest value was 500 feet. Since only 1 WHP Plan used a value of 250 feet, there were 23 of 24 decision makers who believed that the distance should be at least 500 feet, and therefore, the probability of criterion choice for this distance was assigned a value of $^{23}/_{24}$, or 0.985. Since there were 4 WHP Plans which used a value of 500 feet, there were 19 of 24 decision makers who agreed that the distance should be at least 1000 feet resulting in a weighting factor of 0.792. This reasoning was applied to all of the distances in Table 4.2, and multiplied by the probability of model failure for the arbitrary fixed radius method, to achieve the overall probabilities of failure. These probabilities of failure are presented in Table 4.6.

A similar development was used to determine the probability of criterion choice for travel times. The smallest value of this criterion is the ½ year time of travel. When this value was included with the values from Table 4.3 there were 31 WHP Plans from which to sample probability of criterion choice. All decision makers agreed that the travel time should be at least ½ years, and therefore, probability of criterion choice was given a value of 1.000. Since there is only 1 WHP Plan which used a value of ½ year, there were 30 of 31 decision makers who agreed that the travel time should be at least 2 years resulting in a probability of 0.968. Since there was only 1 WHP Plan which used a value of 2 years, there were 29 of 31 decision makers who agreed that the travel time should

be at least 3 years resulting in a probability of 0.935. This reasoning was applied to all of the potential travel times to achieve the probabilities presented in Table 4.7. These values for probability of criterion choice were applied to each of the travel time based WHPA delineation models. Probability of criterion choice was multiplied by probability of model failure to achieve the overall probabilities of failure. The probabilities of failure for the ½ year, 5 year and 10 year travel times are presented in Table 4.8.

Zone I Distance Criterion	Number of State WHP Plans	Probability of Criterion Choice		Probability of Failure
		Fractional Value	Decimal Value	[P_f]
250 foot	1	24/24	1.000	**0.920**
500 foot	4	23/24	0.958	**0.881**
1000 foot	6	19/24	0.791	**0.728**
1500 foot	6	13/24	0.541	**0.498**
2000 foot	1	7/24	0.291	**0.268**
½ mile	1	6/24	0.250	**0.230**
3000 foot	1	5/24	0.208	**0.191**
1 mile	4	4/24	0.166	**0.153**

Table 4.6: Probability of Failure for Each Arbitrary Fixed Radius Distance

Time of Travel Values	Number of WHP Plans	Probability of Criterion Choice	
		Fractional Value	Decimal Value
½ year	1	31/31	1.000
2 year	1	30/31	0.968
3 year	1	29/31	0.935
5 year	16	13/31	0.903
2500 day	1	12/31	0.387
10 year	11	11/31	0.354

Table 4.7: Probability of Criterion Choice for Each Particle Time of Travel

Delineation Technique	Probability of Model Failure	Probability of Failure		
		½ Year	5 Year	10 Year
Calculated Fixed Radii	0.790	**0.790**	**0.564**	**0.280**
Uniform Flow Equation	0.630	**0.630**	**0.569**	**0.223**
Analytical (MWCAP)	0.510	**0.510**	**0.461**	**0.181**
Analytical (RESSQC)	0.490	**0.490**	**0.442**	**0.173**
Analytical (GPTRAC)	0.470	**0.470**	**0.424**	**0.166**
Numerical (STLINE)	0.170	**0.170**	**0.154**	**0.060**
Numerical (RWAPT)	0.100	**0.100**	**0.090**	**0.035**

Table 4.8: Probability of Failure for Time of Travel Based Modeling Techniques

4.5 Methods of WHPA Delineation

4.5.1 Introduction

The basis for all current techniques for delineating groundwater capture zones, promoted by the USEPA, is steady state analysis of the groundwater flow field, which will use some or all of the information detailed in the conceptual model of groundwater flow system presented in Chapter 3. Average hydrogeologic parameter values are determined for all necessary input variables and the steady state groundwater head field and velocity field are used as input to capture zone analysis techniques. The following section will describe the technical basis for each of these delineation models.

4.5.2 USEPA Delineation Techniques

The first technique suggested by the USEPA for WHPA delineation involves the use of arbitrary fixed radii. An arbitrary fixed radius is a circle of a specified radius that is drawn around each wellhead. The specific radius may be chosen based on federal, state or regional guidance on groundwater protection. Common specified radii which have been used to delineate WHPAs are 250 foot, 500 foot, 1000 foot, 1500 foot, 2000 foot, 3000 foot, ½ mile and 1 mile radii around the wellhead.

The second technique suggested by the USEPA is the calculated fixed radius method. Calculated fixed radii are circles that are drawn around each wellhead of a specific radius that is based on a specified time of travel to the wellhead. The specified time of travel and the average flowrate from the wellhead are related to the volume of groundwater withdrawn from the flowfield using the volumetric flow equation (USEPA, 1987). The volumetric flow equation determines the radius, r, as follows:

$$r = \sqrt{\frac{Qt}{\pi n H}} \qquad (4.6)$$

where: Q = the pumping rate for the well [L^3/T]

n = aquifer porosity [L/L]

H = well screen length [L]

t = travel time from the well to the WHPA boundary [T]

To illustrate the use of this delineation method the following parameter values will be used. A 180 day time of travel in combination with a pumping rate of 665,616 meters^3/year (64,400 feet^3/day) for well 20, a porosity of 0.30 and a well screen length of 15.24 meters (50 feet) will result in a calculated fixed radius of 151.2 meters (496.0 feet).

Simplified variable shapes are standard forms, or boundary shapes, which are generated using a combination of analytical methods and the hydrogeologic parameters of the wellfield. The standard form for the delineation of WHPAs in Southern England uses the time of travel criterion to calculate the upgradient extent of the capture zone and the uniform flow equation to calculate the downgradient extent of the capture zone (USEPA, 1987). Since these are combinations of other delineation techniques already under analysis they will not be explicitly analyzed in the current research.

There are a number of analytical methods that may be used to delineate travel times within the groundwater regime. The simplest method uses the uniform flow equation to generate the flow divide for the wellhead under the assumption of a homogeneous, isotropic flow field (USEPA, 1987). The uniform flow equation is presented below:

$$-\frac{Y}{X} = \tan\left(\frac{2\pi Kbi Y}{Q}\right) \tag{4.7}$$

where: Y = distance of the divide from the well in the y-direction [L]

X = distance of the divide from the well in the x-direction [L]

K = hydraulic conductivity [L/T]

b = aquifer thickness [L]

i = regional hydraulic gradient [L/L]

The location of the downstream stagnation point (X_L) is given by:

$$X_L = \left(\frac{-Q}{2\pi Kbi}\right) \tag{4.8}$$

The location of the maximum boundary limit in the y-direction (Y_L) is given by:

$$Y_L = \pm\left(\frac{Q}{2Kbi}\right) \tag{4.9}$$

The uniform flow equation delineates the divide between groundwater that flows to the well and groundwater that flows past the well. The stagnation point is the location of the divide directly downgradient of the well. The maximum boundary limit is the maximum distance in the y-direction of the flow divide away from the centreline particle streamline. The uniform flow equation does not take into account the influence of other wells near a specific wellfield and thus within a wellfield containing multiple wellheads there may be error in applying this relationship separately to each well if the flow divides overlap. However, it does illustrate the potential influence of adjacent pumping wells on each other by showing the overlap between flow divides. A FORTRAN computer program, called UNIFORM, was written to implement the uniform flow equation that is presented as Equation

4.7. The model transposes the results of the uniform flow equation to the coordinate system of the conceptual model for each well at the UWTR Wellfield under the input conditions presented in Table 4.9. The computer code for UNIFORM is found in Appendix IV.

Well Parameter	Units	w-20	w-22	w-24	w-26	w-28	w-29
Transmissivity (Kb)	$feet^2/day$	7500	7500	7500	7500	7500	7500
Regional Gradient (i)	feet/feet	0.0030	0.0035	0.0035	0.0035	0.0035	0.0035
Flowrate (Q)	$feet^3/day$	64400	75500	66200	62400	62500	63800
X-coordinate	feet	3200	7400	8200	6800	7200	7200
Y-coordinate	feet	19600	19400	18600	18800	19000	18600
Angle of Gradient	deg	225	225	225	225	225	225

Table 4.9: Average Parameter Values for Uniform Flow Equation Analysis

Analytical methods may also be incorporated into computer models like RESSQC, which is an analytical model for delineating wellhead protection areas and is part of the WHPA set of computer models. WHPA version 2.2 is the USEPA computer code for delineating capture zones (USEPA, 1993). The hydrogeologic information that was used to model capture zones at the UWTR wellfield is presented in Table 4.10. GPTRAC is a second analytical model that is a part of the WHPA code. GPTRAC delineates capture zones for pumping wells in homogeneous aquifers with steady and uniform ambient groundwater flow. MWCAP is a third analytical model that is part of the WHPA code. MWCAP delineates capture zones for multiple pumping wells in a homogeneous aquifer with steady and uniform ambient groundwater flow.

Aquifer Parameter	Units	Average Value
Transmissivity	$feet^2/day$	7500
Porosity		0.30
Thickness	feet	50
Hydraulic Gradient	feet/feet	0.003
Angle of Flow	deg	225
Simulation Time	days	1825 & 3650

Table 4.10: Parameter Values for RESSQC, GPTRAC and MWCAP Analysis

Hydrogeologic information may also be used to delineate, or map, components of a WHPA. The most common hydrogeologic information that is used to map WHPAs is the location of an upstream divide for the groundwater flow system. An upstream flow divide may be identified as a no flow boundaries such as the boundary of the watershed which overlays the groundwater system. A flow divide may also be a surface water source for the groundwater flow regime such as a river or lake. This information has been presented on the Reich Farm site map, shown in Figure 3.1, as the northern and eastern boundaries of the conceptual model of the site. These hydrogeologic boundaries may be superimposed over other WHPA delineation boundaries to better identify the extents of the ultimate capture zone boundary for a groundwater flow system.

4.5.3 Numerical Modeling Delineation Techniques

Numerical models are the last, and most versatile, delineation technique proposed by the USEPA for WHPA delineation. There are a wide diversity of numerical models that simulate groundwater flow and particle tracking. These models are complex in the way they represent the flow region within a hydrogeologic unit, and as a result numerical models require the greatest amount of information of all of the WHPA delineation techniques. SWIFT version 2.29 is a numerical model which will be used as the basis for delineating time related capture zones around a pumping wellfield. SWIFT will be used to model the groundwater flow field for the Cohansey aquifer and STLINE version 1.9 will be used to model reverse advective particle tracking. The numerical convex hull program CAPZON will be used to delineate time related capture zones from the output pathlines generated by STLINE. For random walk particle tracking simulation, the output hydraulic head field from SWIFT and the particle tracking program RWAPT will be used to generate reverse particle pathlines and the CAPZON model will be used to generate capture zone boundaries.

4.6 WHPA Decision Making

The purpose of this section is to use environmental decision making to determine the best alternative for groundwater protection of the UWTR wellfields. There are two wellfields under consideration (well 20 to the west and the Parkway wellfield to the east) and three protection zones (Zone I, II and III) for each wellfield. Decision making will be approached in a different manner for Zone I as compared to Zone II and III. Within Zone I, WHPA delineation is based primarily on the distance criterion, and therefore, decision making will be directed toward optimizing the size of the area encompassed by the WHPA boundary and the probability of failing to encompass the true WHPA boundary. Within Zone II and Zone III, WHPA delineation is based on the time of travel criterion, and therefore, decision making will be directed toward comparing each delineation technique to the ZOC standard to determine the best modeling alternative.

Environmental decision making for WHPA delineation will be implemented as follows. For each protection zone, all of the potential WHPA boundaries will be delineated in the same figure. The zone of confidence for time of travel based WHPA boundaries will be determined. Environmental decision making will be implemented in Zone I to choose WHPA I. WHPA I is the best boundary alternative for Zone I protection. For each travel time based method of WHPA delineation, the Zone II and Zone III boundaries are presented on the same figure as WHPA I, ZOC II and ZOC III to determine the risk of failure for the delineation method. Environmental decision making will then be implemented in Zone II and III to choose WHPA II and WHPA III.

4.6.1 Delineation of All Potential WHPA Boundaries

Prior to making any decisions about the best alternative for WHPA boundary it is necessary to use all delineation methods described in Section 4.4 to generate all of the possible WHPA boundary alternatives at the UWTR wellfields. This will provide an understanding of the engineering design constraints involved in generating these WHPA boundaries. The Zone I WHPA boundaries, using the 1000 foot arbitrary fixed radius and the 180 day calculated fixed radius around each wellfield, are presented in Figure 4.3. Figure 4.4 presents the Zone II boundary using calculated fixed radii. Figure 4.5 shows the Zone II boundary delineated using the uniform flow equation. Figure 4.6 shows the Zone II boundary delineated using GPTRAC, RESSQC and MWCAP. Figure 4.7 shows the Zone II boundary delineated using the SWIFT groundwater flowfield, and STLINE and RWAPT particle tracking. Figure 4.8 presents the Zone III boundary using calculated fixed radii. Figure 4.9 shows the Zone III boundary using the uniform flow equation. Figure 4.10 shows the Zone III boundaries using GPTRAC, RESSQC and MWCAP in conjunction with the groundwater flow divide to the east of the site. Figure 4.11 shows the Zone III WHPA boundary using the SWIFT steady state groundwater flowfield and STLINE and RWAPT particle tracking.

4.6.2 Zone I, II and III WHPA Boundaries

The Zone I boundary was based primarily on the distance criterion in combination with the arbitrary fixed radius technique. Figure 4.12 shows 10 potential Zone I boundaries for well 20. These include the 250, 500, 1000, 1500, 2000 and 3000 foot, ½ mile and 1 mile arbitrary fixed radii, as well as the 180 day calculated fixed radius and RWAPT numerical modeling boundaries. Figure 4.13 presents these same WHPA boundaries for the Parkway Wellfield.

Seven delineation techniques were investigated for determining the Zone II and III WHPA boundaries. These techniques include calculated fixed radii, the uniform flow equation, analytical models (GPTRAC, RESSQC and MWCAP) and numerical models (STLINE and RWAPT). Figures 4.14 and 4.15 show the seven potential Zone II WHPA boundaries and the ZOC around well 20 and the Parkway Wellfield, respectively. Figures 4.16 and 4.17 show seven potential Zone III WHPA boundaries and the ZOC around each wellfield. For both Zone II and III, the ZOC for well 20 is a combination of the calculated fixed radius, uniform flow equation, RESSQC and STLINE boundaries, and the ZOC for the Parkway wellfield is a combination of the UNIFORM, MWCAP and GPTRAC boundaries. For well 20, the Zone II and Zone III ZOC boundaries encompass areas of 2,330,200 ft^2 and 3,020,200 ft^2, respectively. For the Parkway wellfield, the Zone II and Zone III ZOC boundaries encompass areas of 7,400,600 ft^2 and 9,418,400 ft^2.

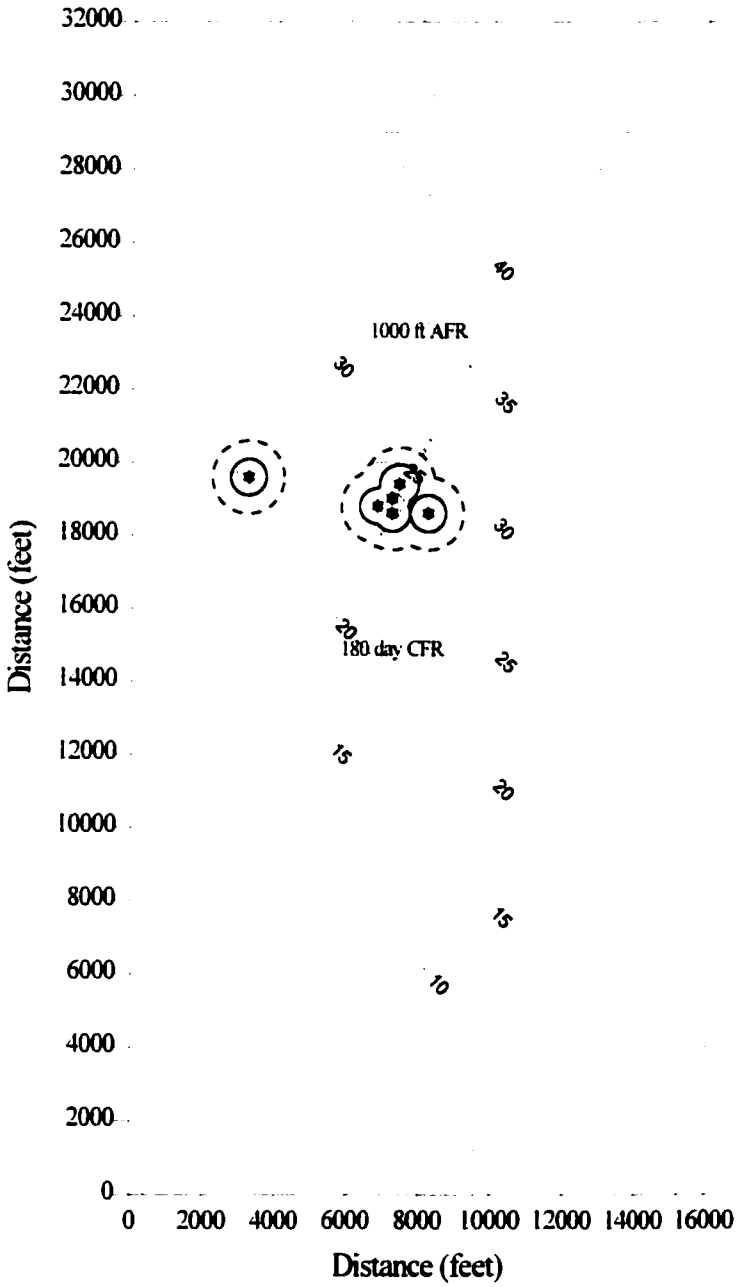


Figure 4.3: The Zone I WHPA Boundaries Using Arbitrary and Calculated Fixed Radii

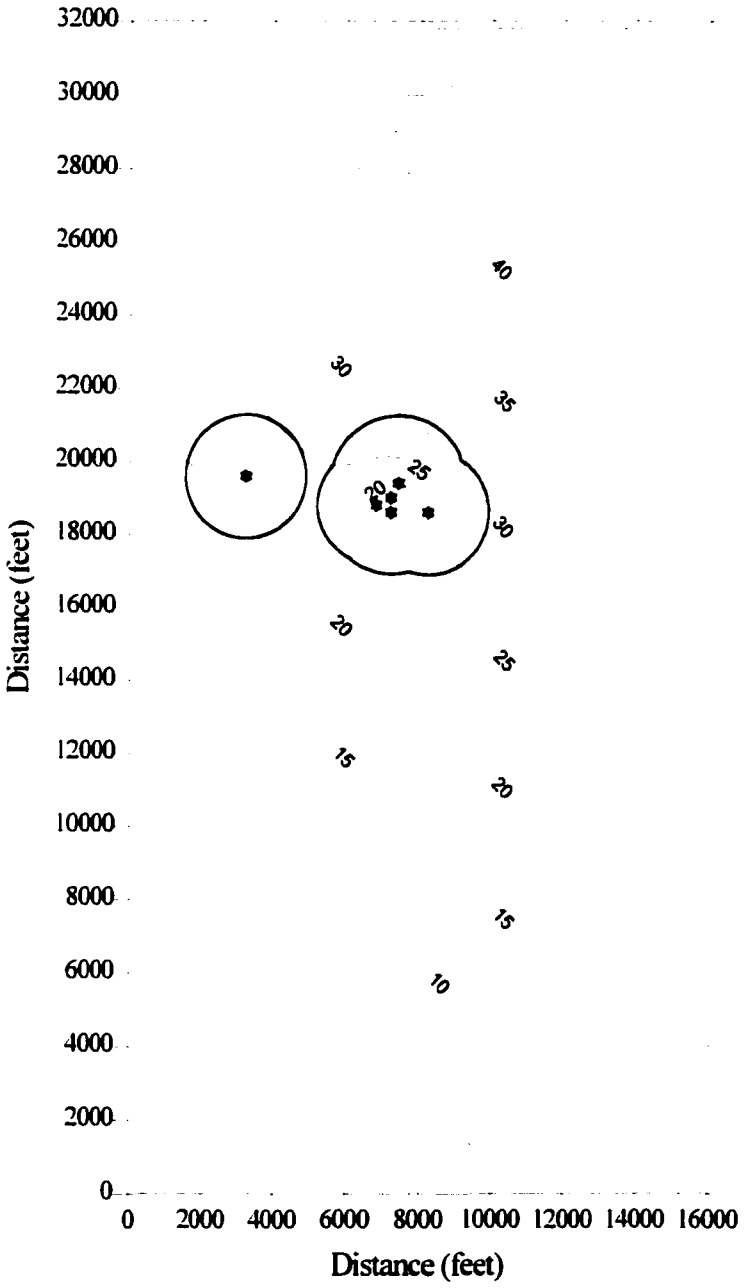


Figure 4.4: The Zone II WHPA Boundaries Using Calculated Fixed Radii

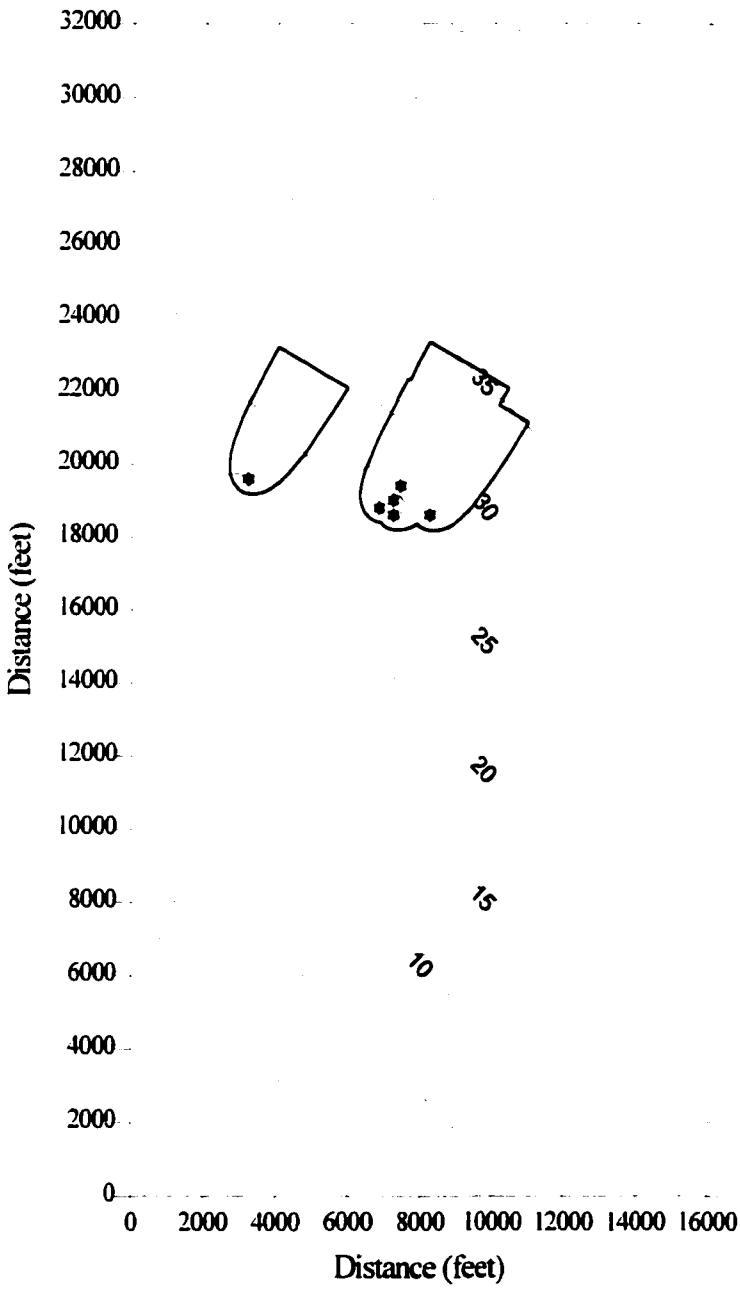


Figure 4.5: The Zone II WHPA Boundaries Using the Uniform Flow Analytical Model

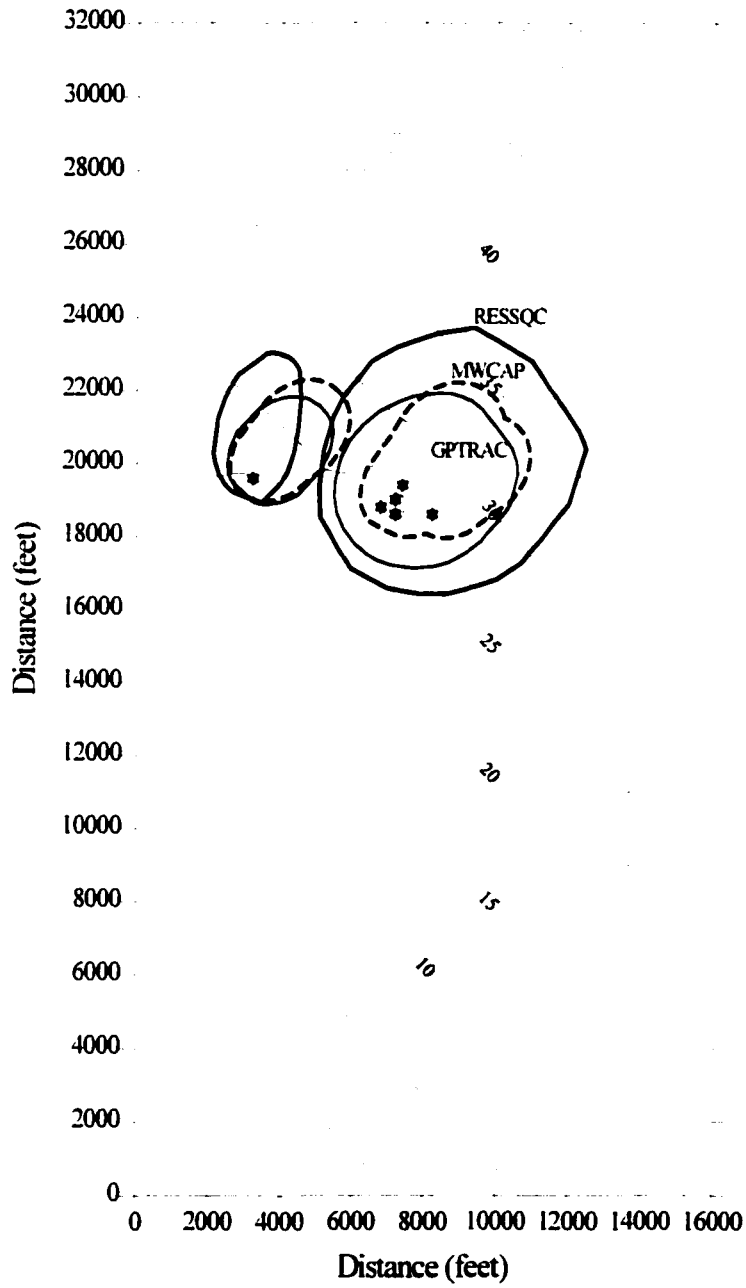


Figure 4.6: The Zone II WHPA Boundaries Using GPTRAC, RESSQC and MWCAP

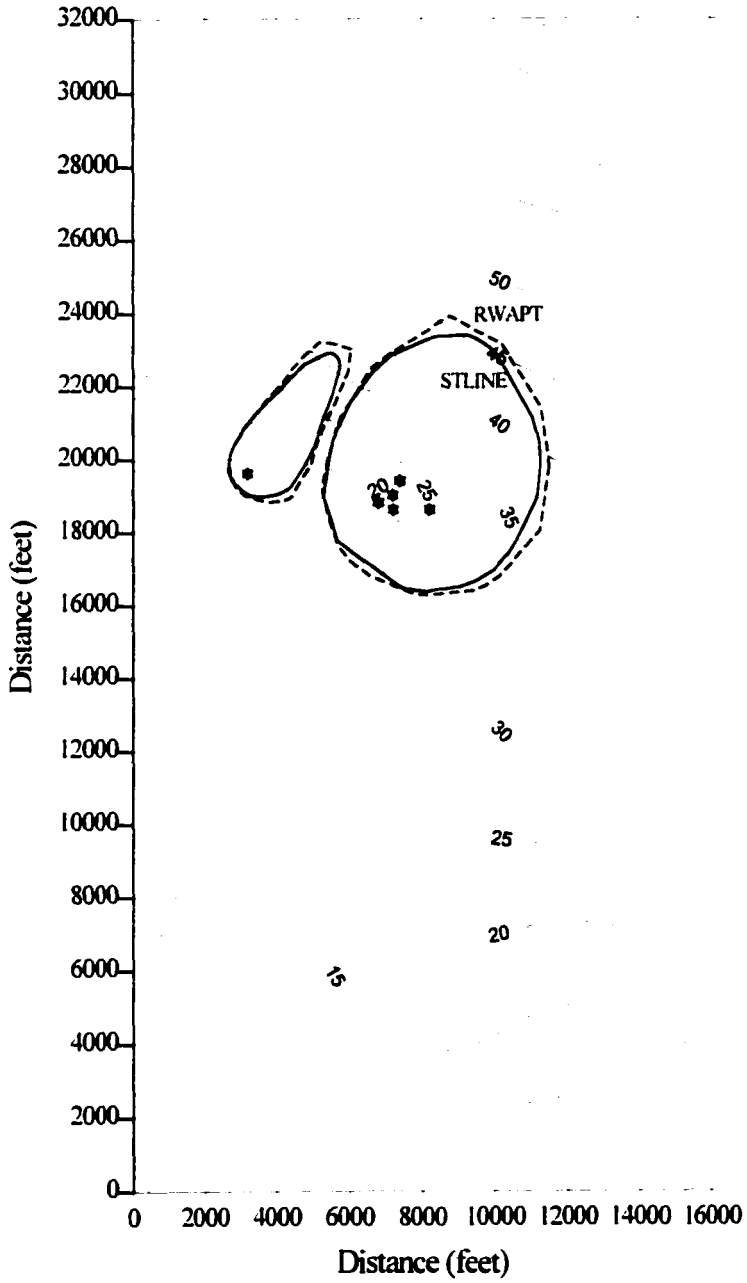


Figure 4.7: The Zone II WHPA Boundaries Using STLINE and RWAPT

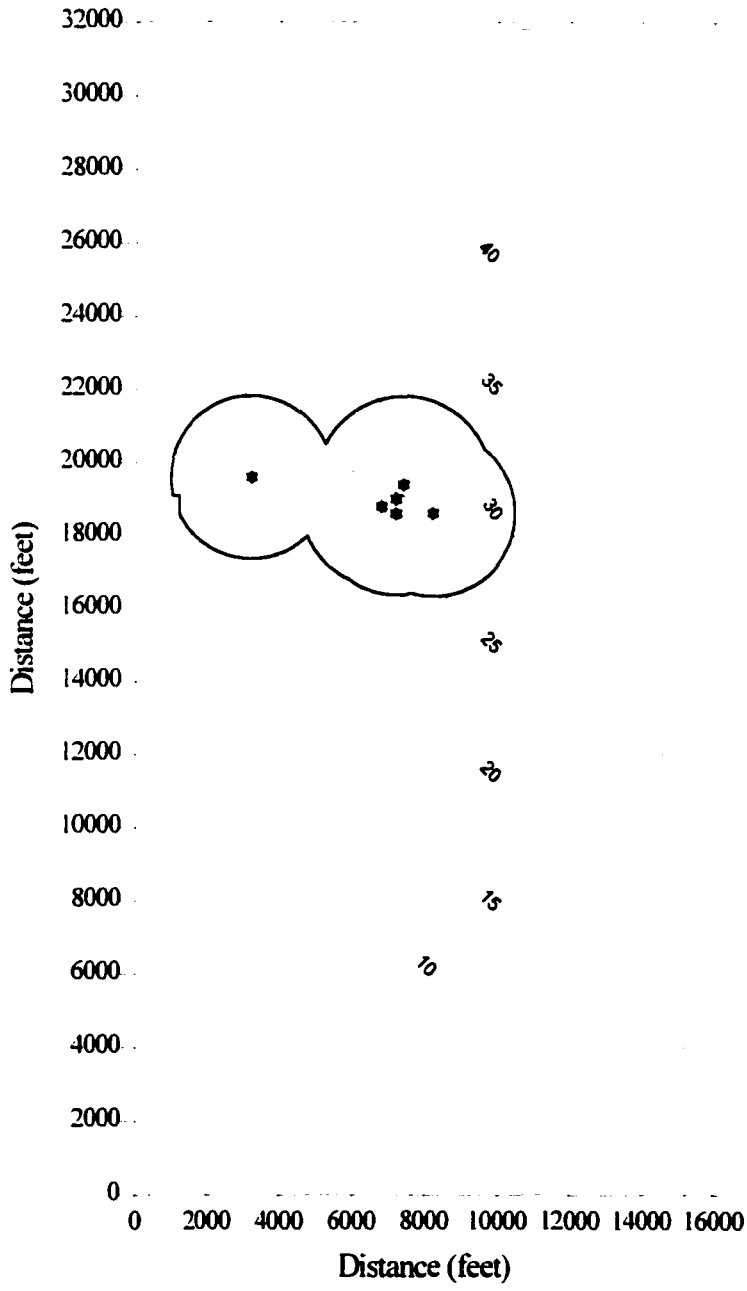


Figure 4.8: The Zone III WHPA Boundaries Using Calculated Fixed Radii

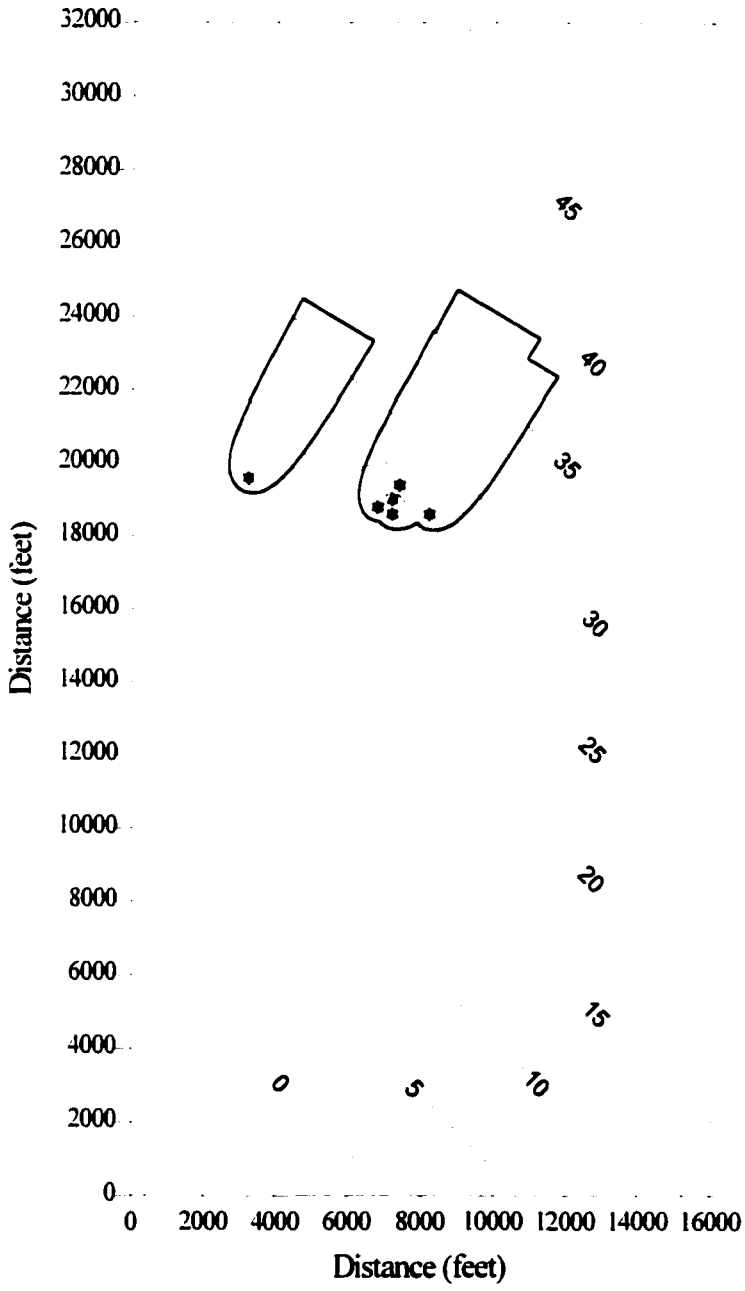


Figure 4.9: The Zone III WHPA Boundaries Using the Uniform Flow Analytical Model

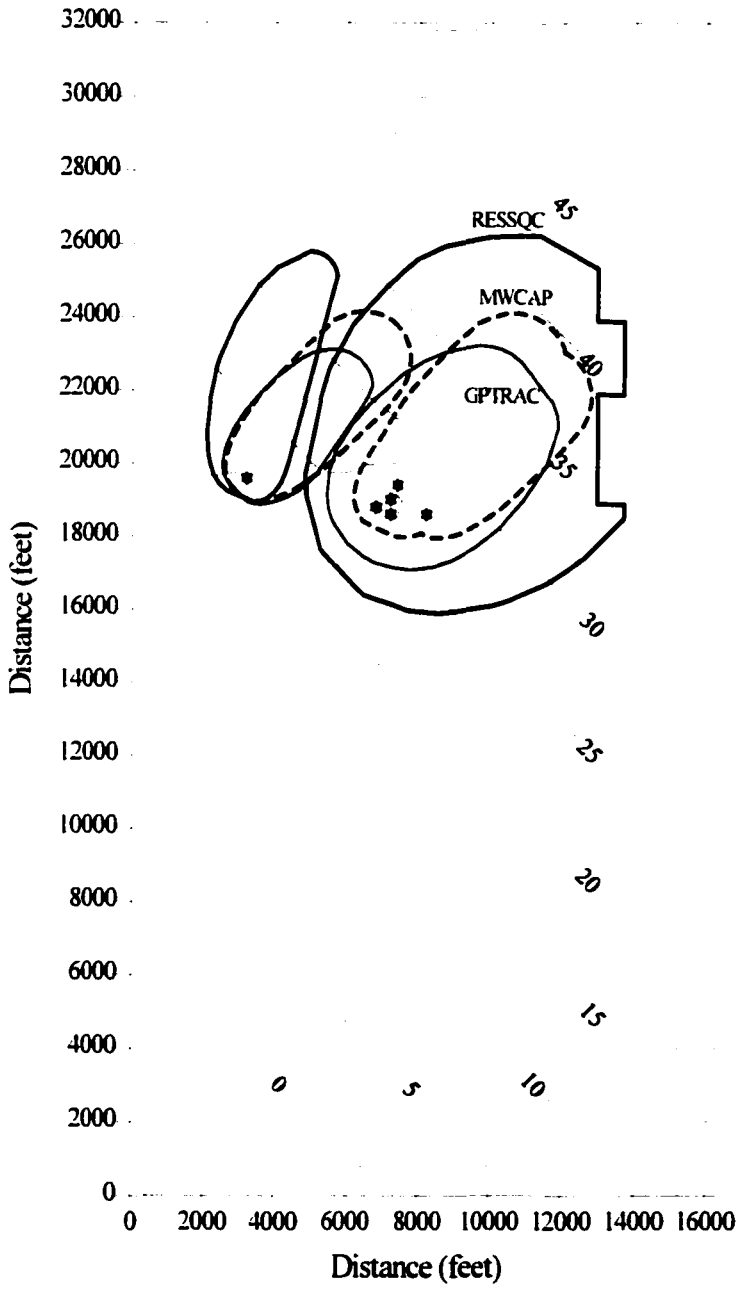


Figure 4.10: The Zone III WHPA Boundaries Using GPTRAC, RESSQC and MWCAP

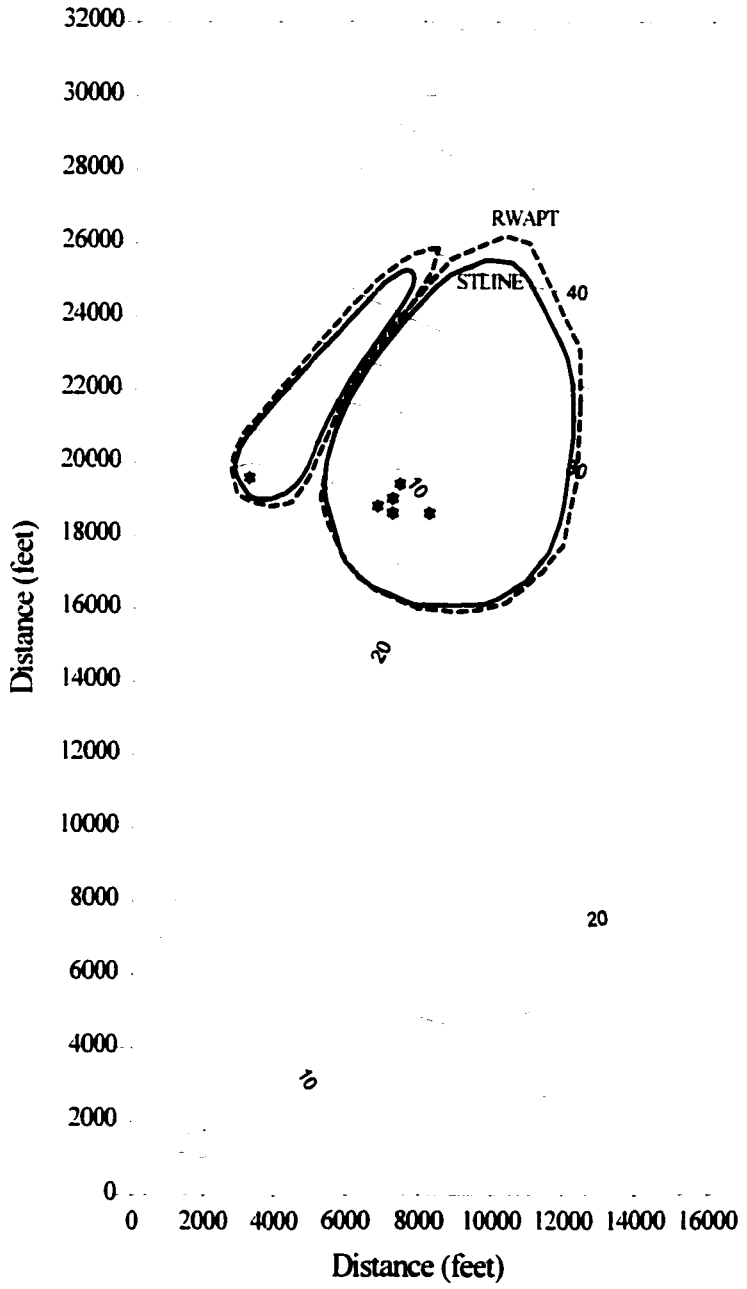


Figure 4.11: The Zone III WHPA Boundaries Using STLINE and RWAPT

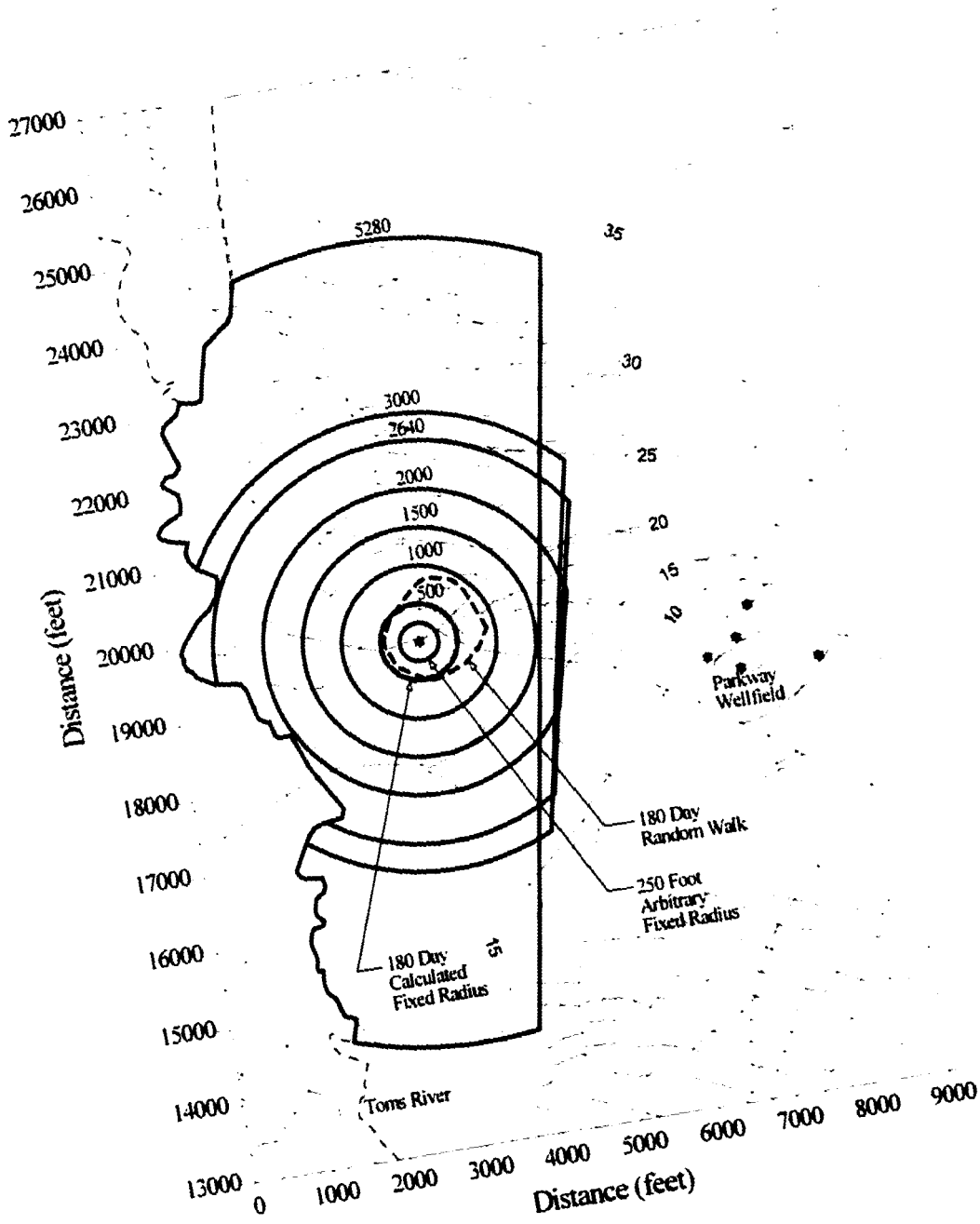


Figure 4.12: Potential Zone I WHPA Boundaries Around Well 20

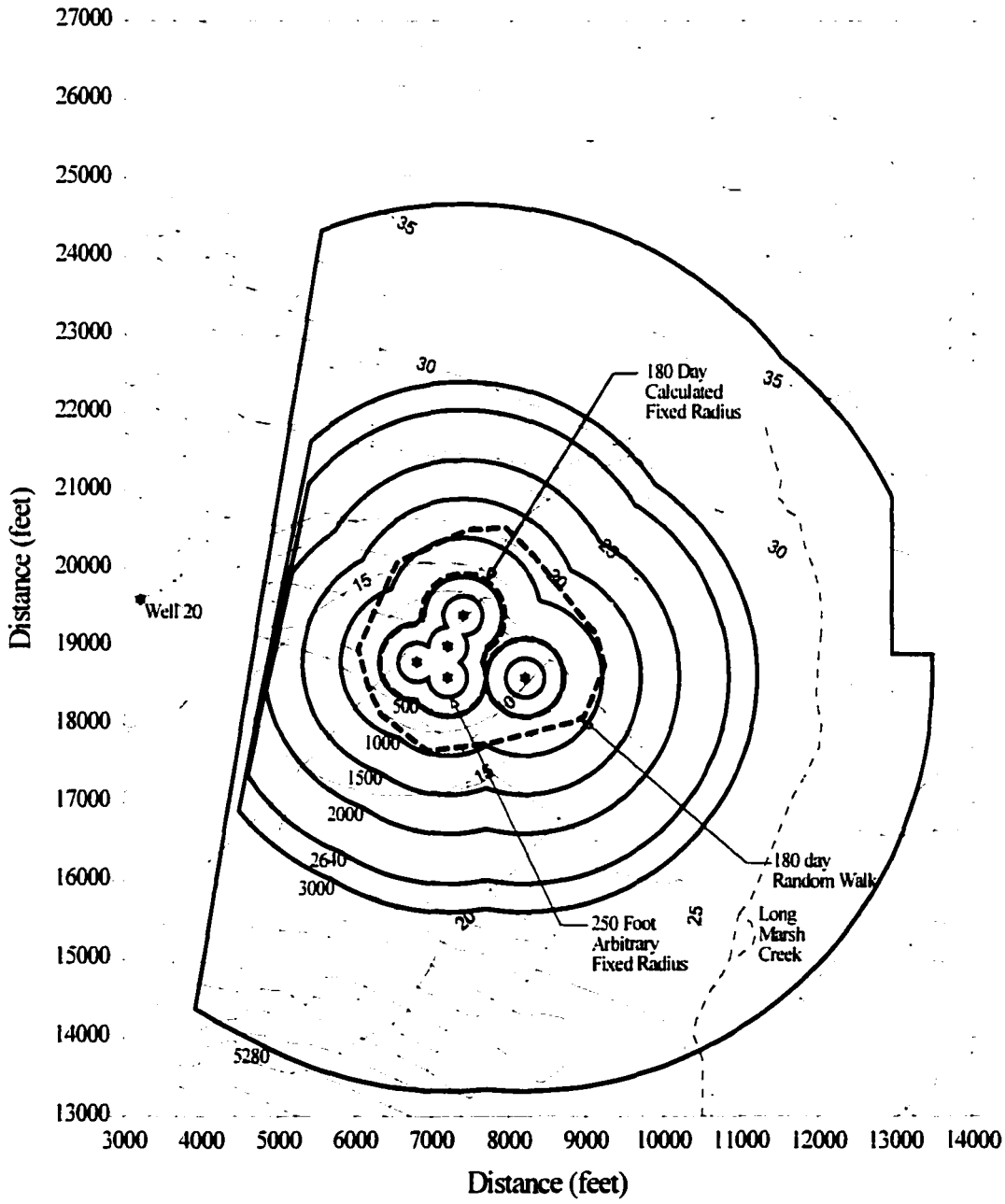


Figure 4.13: Potential Zone I WHPA Boundaries Around the Parkway Wellfield

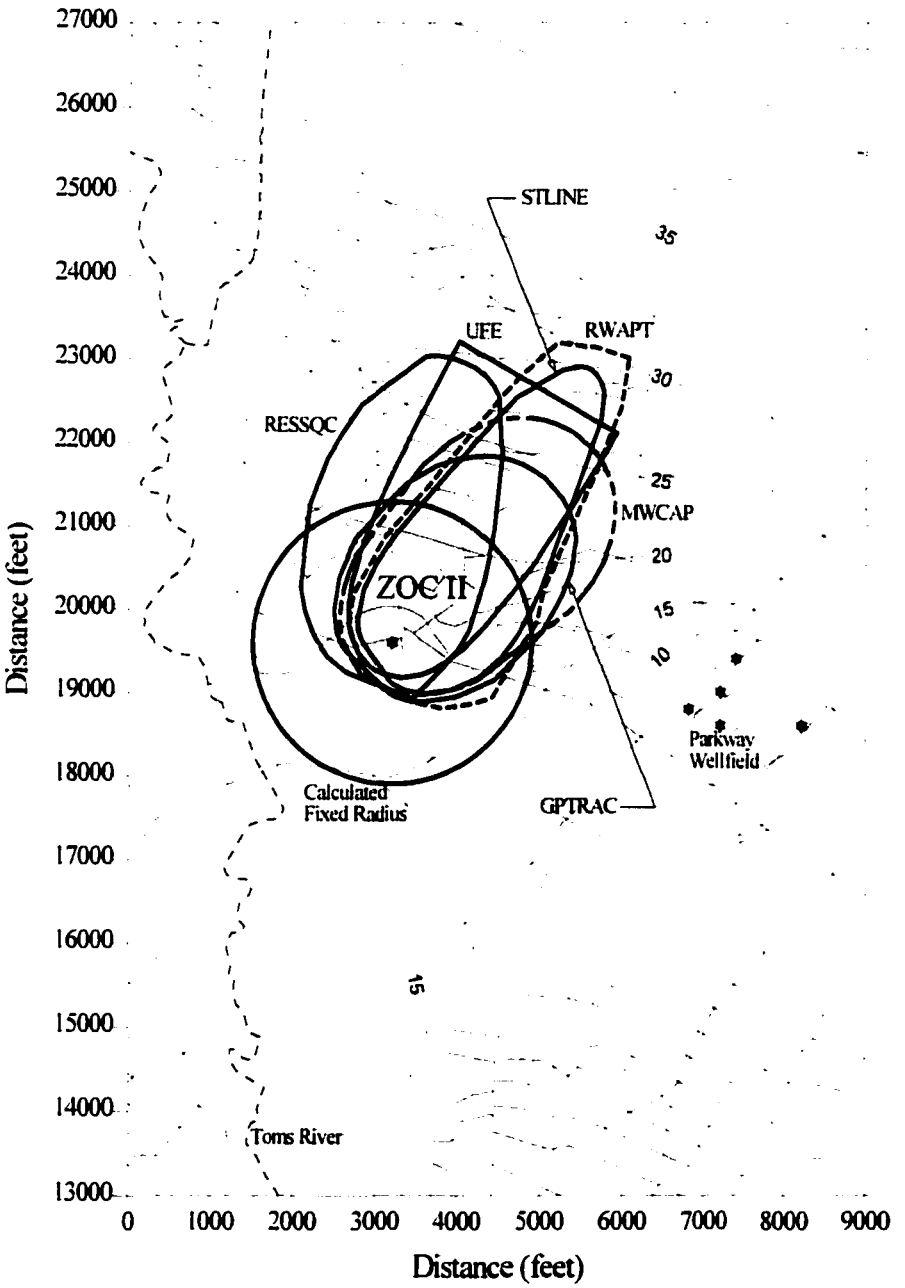


Figure 4.14: Potential Zone II WHPA Boundaries Around Well 20

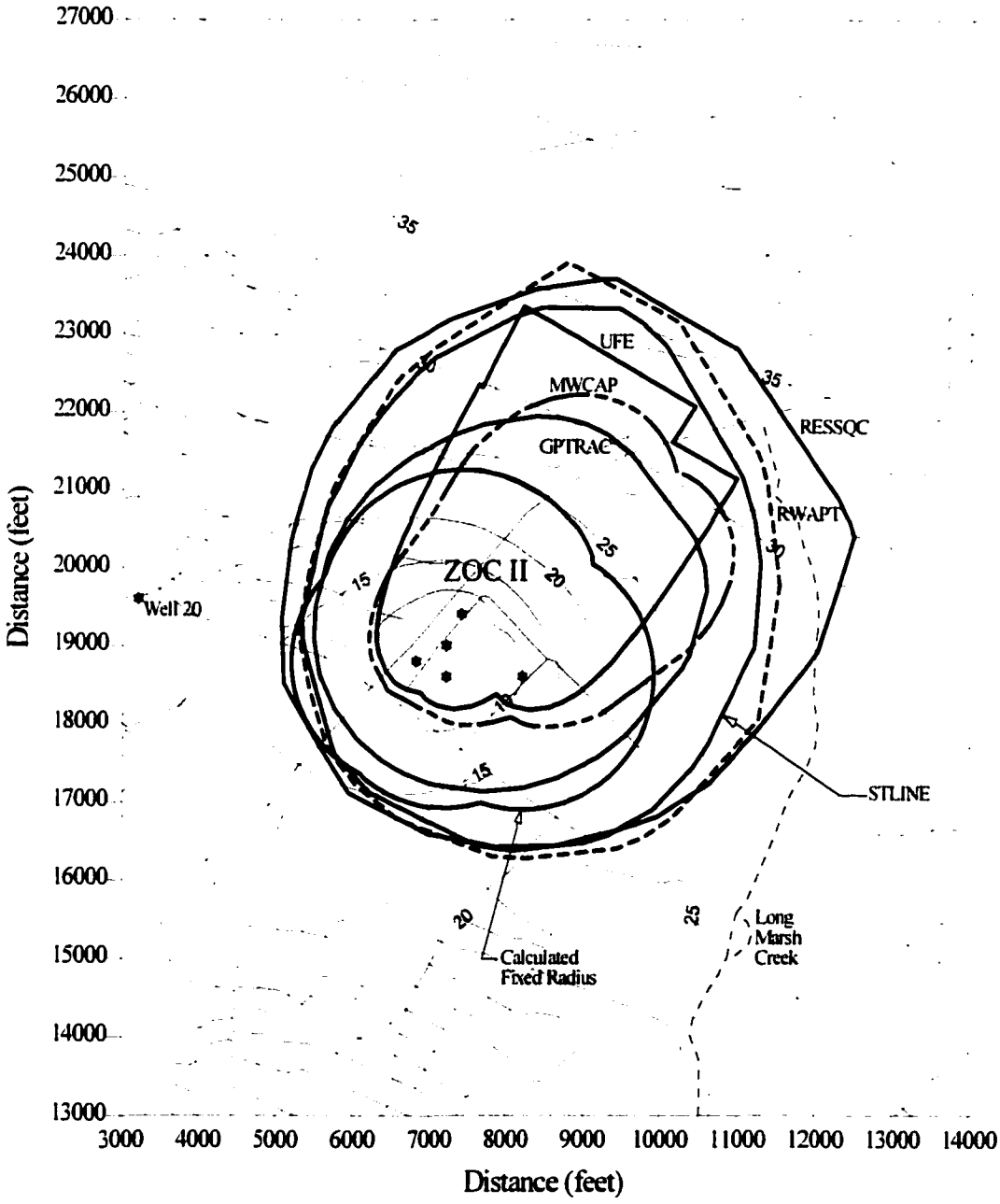


Figure 4.15: Potential Zone II WHPA Boundaries Around the Parkway Wellfield

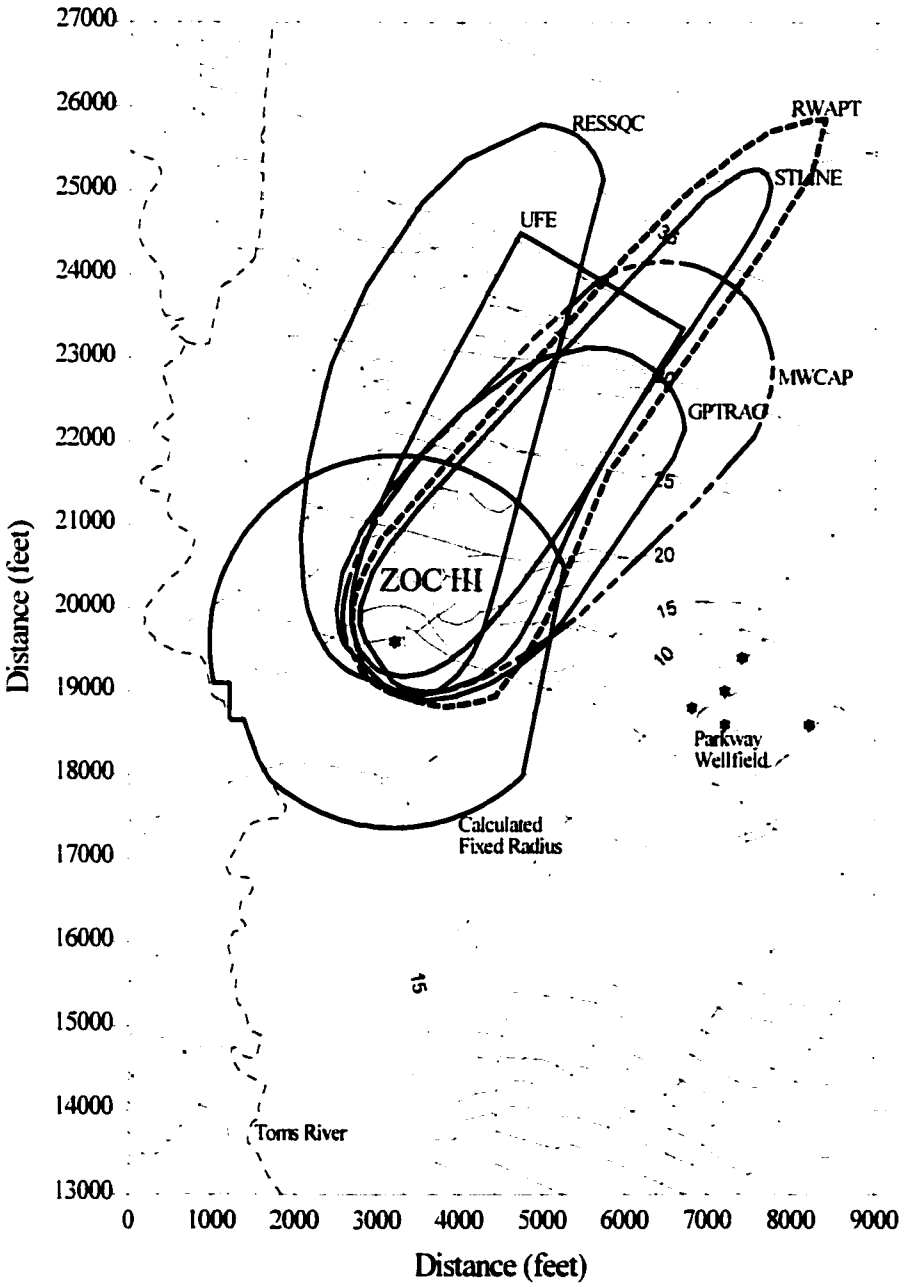


Figure 4.16: Potential Zone III WHPA Boundaries Around Well 20

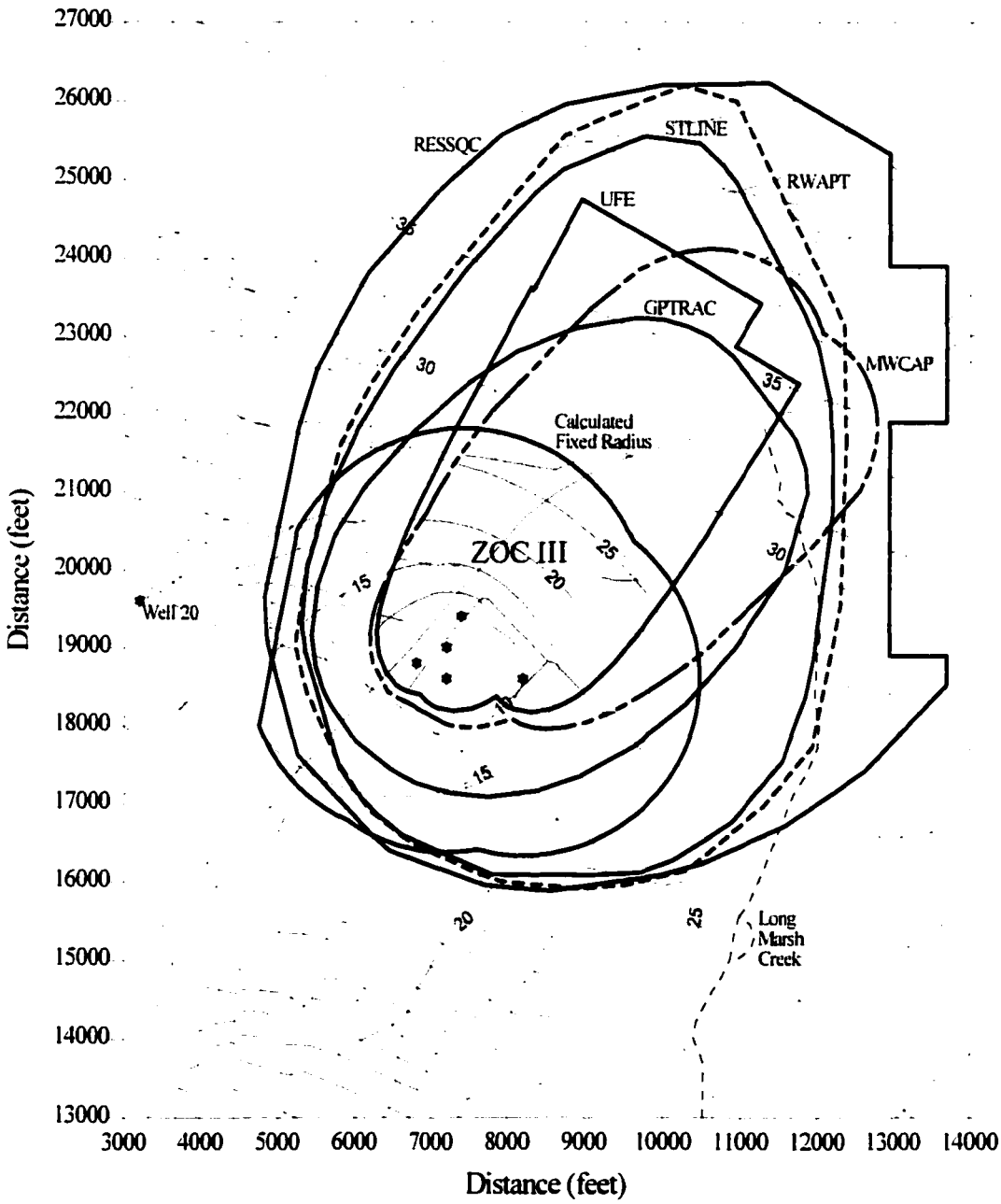


Figure 4.17: Potential Zone III WHPA Boundaries Around the Parkway Wellfield

The ZOC boundaries for Zone II and III represent the standard against which each potential WHPA delineation technique will be compared. Figure 4.18 presents a summary of the Zones of Confidence for each of the groundwater protection zones around the UWTR wellfields. These ZOC boundaries will be used for an environmental decision making analysis of the methods and criteria for delineating wellhead protection areas around the UWTR wellfields.

4.6.2.1 The Zone I WHPA Boundary

WHPA decision making, for protection Zone I, will be based on determining the areas associated with the intersection between the potential WHPA boundary and the ZOC II and III boundaries. Each of these intersecting areas was considered a failure area, according to the presentation in Table 4.4. To illustrate the decision making process, Figure 4.19 shows the location of the 1000 foot Zone I WHPA boundary and the ZOC II and ZOC III around well 20. This figure also presents the areas of intersection associated with the 1000 foot boundary and the type of failure that each of these areas represent. The size of failure area types 4, 5 and 6, for well 20, are 1,657,200 ft^2, 1,461,100 ft^2 and 22,600 ft^2, respectively. Decision making will be based on the cost of failure associated with each of these failure areas and the probability of failure of the specific WHPA model.

Table 4.11 presents the areas encompassed by each of the potential Zone I boundaries. Table 4.12 presents the failure areas that are associated with the interaction between each of these potential Zone I boundaries and the ZOC boundaries. The failure areas are differentiated based on the type of failure identified in Table 4.4 to associate each failure area with a cost of failure. Table 4.13 presents the net present worth of the cost of producing each potential Zone I boundary. When comparing these methods for WHPA delineation, the best alternative for delineating the Zone I boundary is the 250 foot AFR because it has the lowest net present cost of $791,400. The next best alternative for delineating the Zone I boundary is the ½ year RWAPT boundary, which has a net present cost of $858,800.

The net present worth of each Zone I WHPA boundary result from the interaction between the size of the area contained within the boundary and the probability of failure to contain the true WHPA boundary. It is evident that the probability of containing the true WHPA boundary increases as the area in Zone I increases, but the probability of failure increases, and therefore the risk of failure increases as well. An obvious conclusion from this analysis is that the use of the arbitrary fixed radius method can lead to very high risk of failure for some of the distances which have been compared. The use of anything above a distance of 500 feet has an environmental risk of greater than $10 million dollars. This indicates that arbitrary fixed radius method should only be used in the simplest of hydrogeologic settings where there is a low probability of failure.

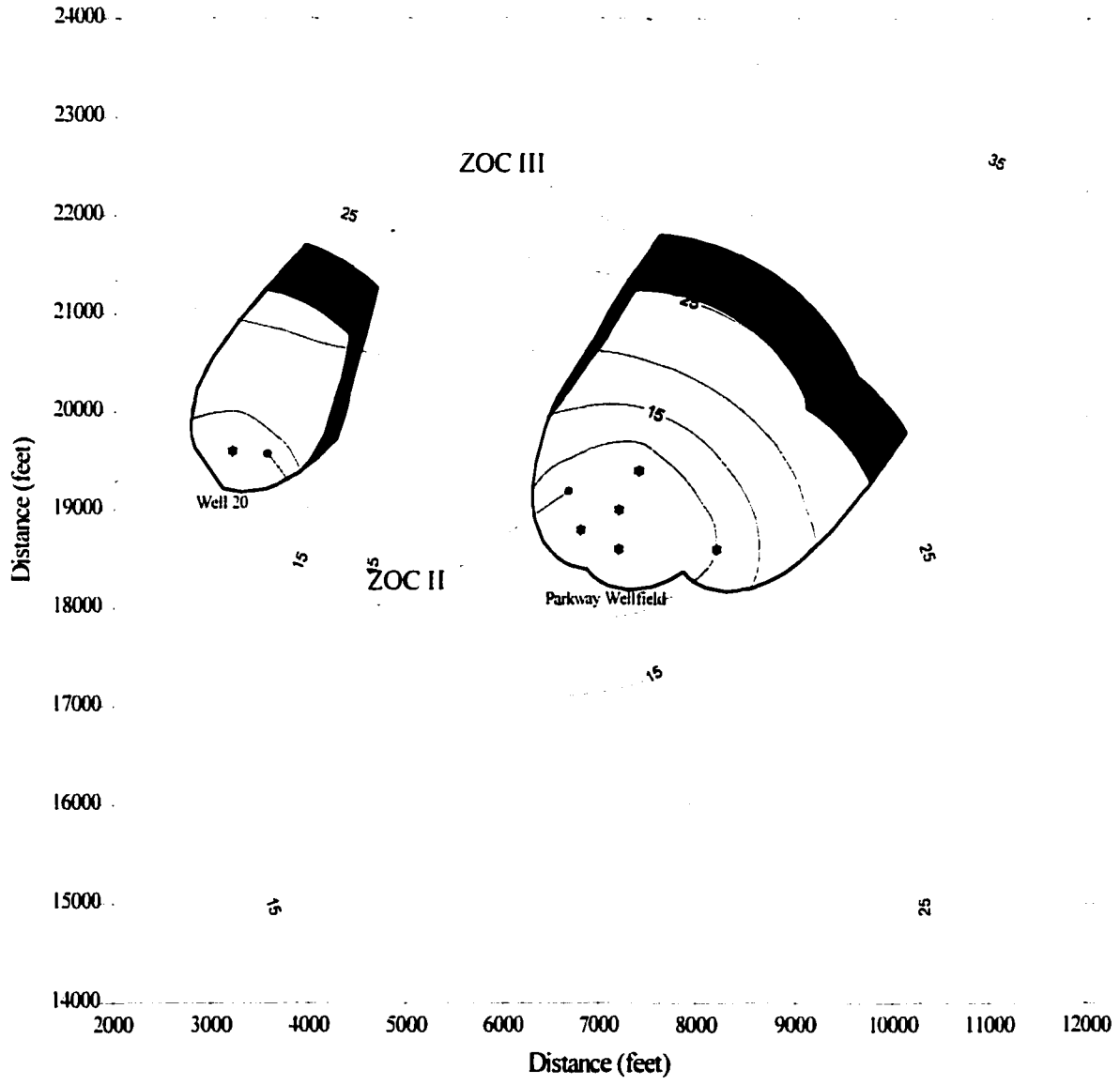


Figure 4.18: The Zone of Confidence (ZOC) for Protection Zones II and III

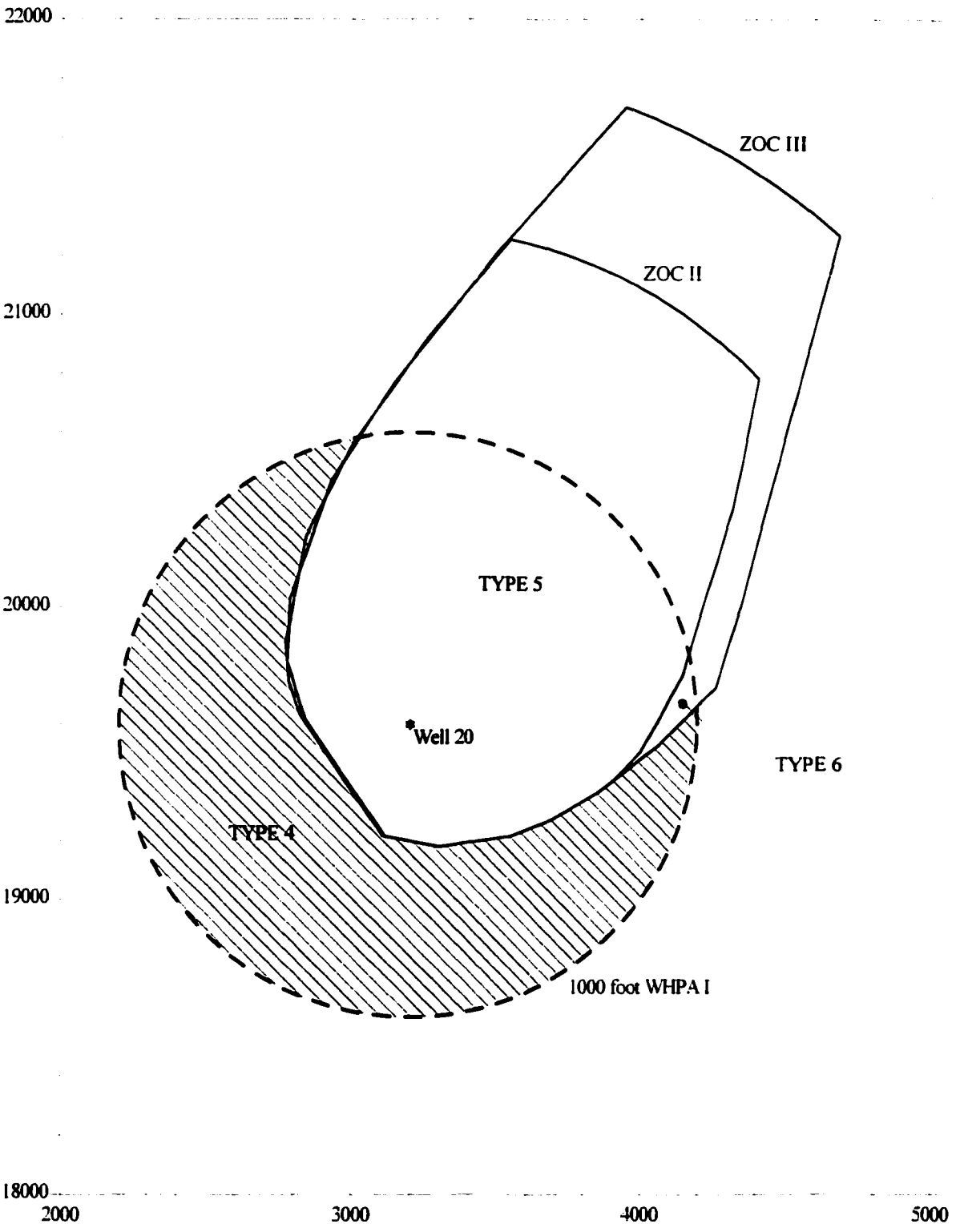


Figure 4.19: The Interaction Between the 1000 foot Zone I Boundary and ZOC II and III

Potential WHPA Boundary	WHPA Boundary Area	
	Well 20 [feet^2]	Parkway Wellfield [feet^2]
250 Foot AFR	196 300	906 900
500 Foot AFR	785 200	2 708 600
1000 Foot AFR	3 140 900	7 011 000
1500 Foot AFR	7 067 100	12 698 200
2000 Foot AFR	12 401 700	19 768 800
½ Mile AFR	18 804 700	29 455 100
3000 Foot AFR	22 059 000	35 554 400
1 Mile AFR	38 698 000	89 831 100
180 Day CFR	772 700	2 766 500
180 Day RWAPT	1 238 800	6 570 700

Table 4.11: The WHPA Boundary Area for Each Potential Zone I Boundary

Potential WHPA Boundary	Failure Type	Failure Area (ZDU)		
		Well 20 [feet^2]	Parkway [feet^2]	Total Area [feet^2]
250 Foot AFR	5	196 300	906 900	1 103 200
500 Foot AFR	4	153 500	208 000	361 500
	5	631 800	2 425 900	3 057 700
1000 Foot AFR	4	1 657 200	2 362 600	4 019 900
	5	1 461 100	4 617 900	6 079 000
	6	22 600	--	22 600
1500 Foot AFR	4	4 843 300	6 228 900	11 072 200
	5	2 117 100	6 326 000	8 443 100
	6	115 700	68 800	184 600
2000 Foot AFR	4	9 597 800	11 604 600	21 202 400
	5	2 330 200	7 325 900	9 656 100
	6	479 000	763 200	1 242 200
½ Mile AFR	4	15 784 500	20 036 700	35 821 200
	5	2 330 200	7 325 900	9 656 100
	6	690 000	2 017 800	2 707 900
3000 Foot AFR	4	19 038 800	26 136 000	45 174 800
	5	2 330 200	7 325 900	9 656 100
	6	690 000	2 017 800	2 707 900
1 Mile AFR	4	35 678 100	73 748 800	109 426 900
	5	2 330 200	7 325 900	9 656 100
	6	690 000	2 017 800	2 707 900
180 Day CFR	4	147 800	195 100	342 900
	5	624 900	2 541 000	3 166 000
180 Day RWAPT	4	125 500	1 475 000	1 600 500
	5	1 113 300	5 065 300	6 178 600

Table 4.12: Failure Areas (ZDUs) for Each Zone I Boundary

Zone I Boundary	P_I	Failure Type	Area of Failure					Sites	Cf	Rf	NPW
			Total [feet^2]	Total [acre]	Developable [acre]	Developed [acre]	Undeveloped [acre]		[$]	[$]	[$]
250 Foot	0.920	5	1 103 200	25.33	12.66	3.17	9.50	2	854 700	786 400	791 400
500 Foot	0.881	4	361 500	8.30	4.15	1.04	3.11	1	1 166 000		
		5	3 057 700	70.19	35.10	8.77	26.32	5	2 274 400	3 031 000	3 036 000
1000 Foot	0.728	4	4 019 800	92.28	46.15	11.54	34.61	6	7 845,700		
		5	6 079 000	139.55	69.78	17.44	52.33	9	4 358 100		
		6	22 600	0.52	0.26	0.06	0.19	1	872 700	9 519 700	9 524 700
1500 Foot	0.498	4	11 072 200	254.18	127.09	31.77	95.32	16	21 083 600		
		5	8 443 100	193.83	96.91	24.23	72.69	13	6 140 000		
		6	184 600	4.24	2.12	0.53	1.59	1	947 100	14 029 000	14 034 000
2000 Foot	0.268	4	21 202 400	486.74	243.37	60.84	182.53	31	40 734 800		
		5	9 656 100	221.67	110.84	27.71	83.13	14	6 871 000		
		6	1 242 200	62.16	14.26	7.77	10.69	2	2 295 100	13 373 400	13 378 400
½ Mile	0.230	4	35 821 200	822.34	411.17	102.79	308.38	52	68 446 800		
		5	9 656 100	221.67	110.84	27.71	83.13	14	6 871 000		
		6	2 707 900	62.16	14.26	7.77	23.31	4	4 692 700	18 402 400	18 407 400
3000 Foot	0.191	4	45 174 800	1037.07	518.54	129.63	388.90	65	85 741 400		
		5	9 656 100	221.67	110.84	27.71	83.13	14	6 871 000		
		6	2 707 900	62.16	14.26	7.77	23.31	4	4 692 700	18 585 300	18 590 300
1 Mile	0.153	4	109 426 900	2512.10	1256.05	314.01	942.04	158	208 241 900		
		5	9 656 100	221.67	110.84	27.71	83.13	14	6 871 000		
		6	2 707 900	62.16	14.26	7.77	23.31	4	4 692 700	33 630 300	33 635 300
180 Day CFR	0.790	4	342 900	7.87	3.94	0.98	2.95	1	1 157 400		
		5	3 166 000	72.68	36.34	9.09	27.26	5	2 324 200	2 750 500	2 758 000
180 Day RWAPT	0.100	4	1 600 500	36.74	18.37	4.59	13.78	3	3 734 800		
		5	6 178 600	141.84	70.92	17.73	53.19	9	4 403 800	813 900	858 900

Table 4.13: The Net Present Worth Costs of Delineating Zone I WHPAs

4.6.2.2 The Zone II and Zone III WHPA Boundaries

WHPA decision making, for Zone II and III, will be based on determining the area that falls within each protection zone which is outside of WHPA I. This will guarantee the avoidance of double counting in the decision making process. Figure 4.20 shows the placement of the WHPA boundaries for the Zone II and III calculated fixed radii (CFR) model around the UWTR wellfields. The area within the Zone I WHPA boundary is 193,600 ft^2 for well 20 and 906,900 ft^2 for the Parkway wellfield. For the Zone II CFR boundary the area of failure was determined by subtracting the area within the CFR boundary from the ZOC for Zone II. This failure area is comprised of three types of failure. Type 7 failure contains an area of 6,530,300 ft^2 for well 20 and 8,227,500 ft^2 for the Parkway wellfield. Type 9 failure contains an area of 147,200 ft^2 for well 20 and 115,000 ft^2 for the Parkway wellfield. Type 10 failure contains an area of 5,292,100 ft^2 for well 20 and 6,603,600 ft^2 for the Parkway wellfield.

Figure 4.21 shows the placement of the WHPA boundaries for the Zone II and III uniform flow equation (UFE) model. Figures 4.22, 4.23 and 4.24 present the placement of the Zone II and Zone III WHPA boundaries for the GPTRAC, MWCAP and RESSQC analytical models, respectively. Figures 4.25 and 4.26 present the placement of the Zone II and Zone III WHPA boundaries for the STLINE and RWAPT numerical models, respectively. Table 4.14 presents the WHPA boundary areas for the seven techniques for delineating Zone II and Zone III boundaries, respectively. Table 4.15 presents the failure areas that are associated with the interaction between each of these potential Zone II and Zone III boundaries and the WHPA I, ZOC II and ZOC III boundaries. The environmental risk that is associated with each Zone II and III delineation technique is presented in Table 4.16. The net present worth of the cost of delineating each WHPA boundary is determined by adding the cost of modeling the final WHPA boundary and the risk that is associated with the WHPA model. For each delineation technique the total environmental risk is a combination of the risk in Zones II and III.

The best alternative for the delineation of the Zone II and Zone III WHPA boundaries is the RWAPT numerical modeling boundary, with the lowest net present cost of $3,980,800. The next best alternative is the STLINE numerical model with a net present cost of $5,716,400. The extra effort put toward the use of advective-dispersive (RWAPT) particle tracking reduces the risk of failure to below that of advective particle tracking. The regret associated with not using the RWAPT numerical model for Zone II and Zone III delineation will be investigated further in Chapter 5.

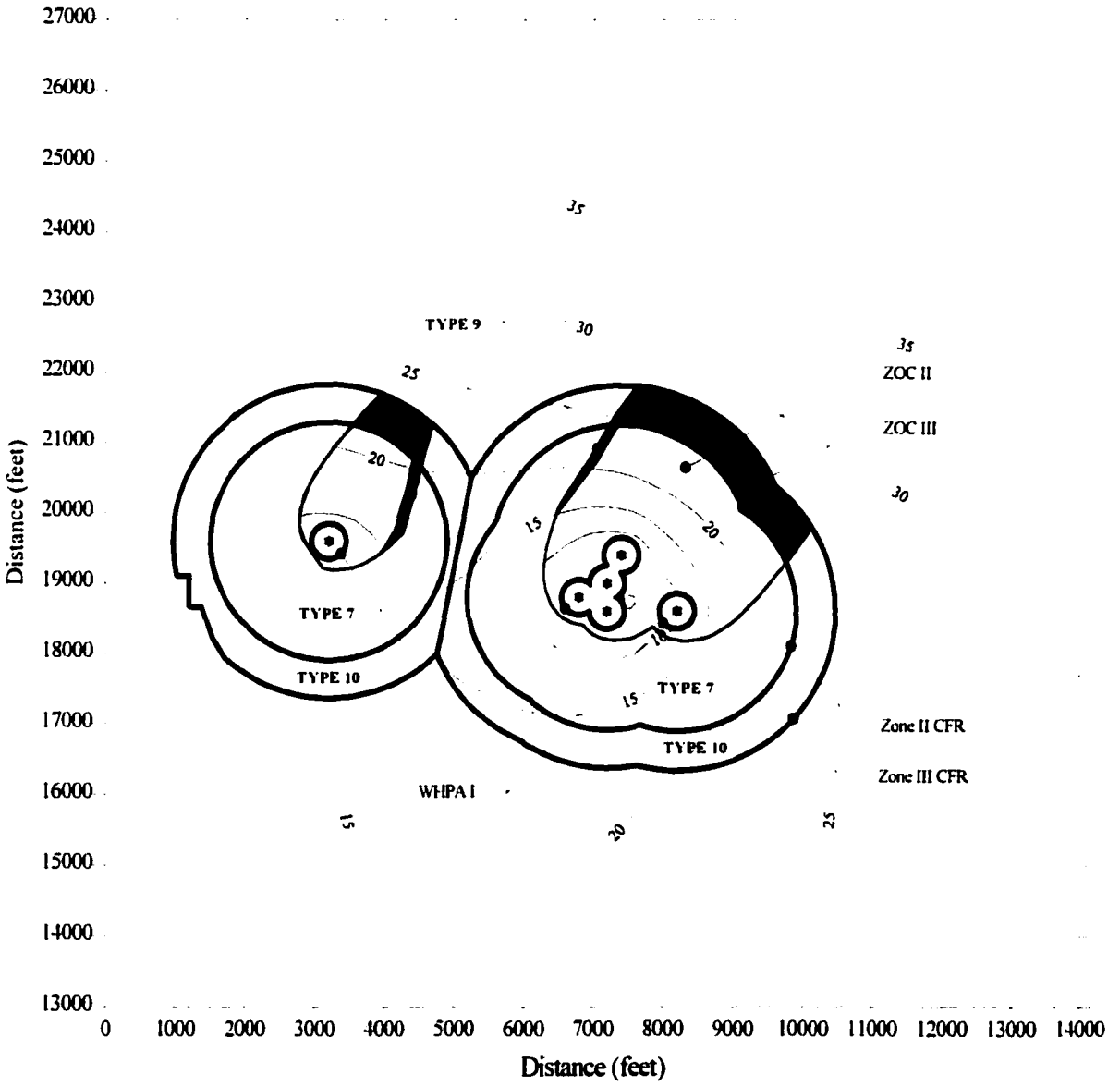


Figure 4.20: Wellhead Protection Area Decision Making for Calculated Fixed Radii

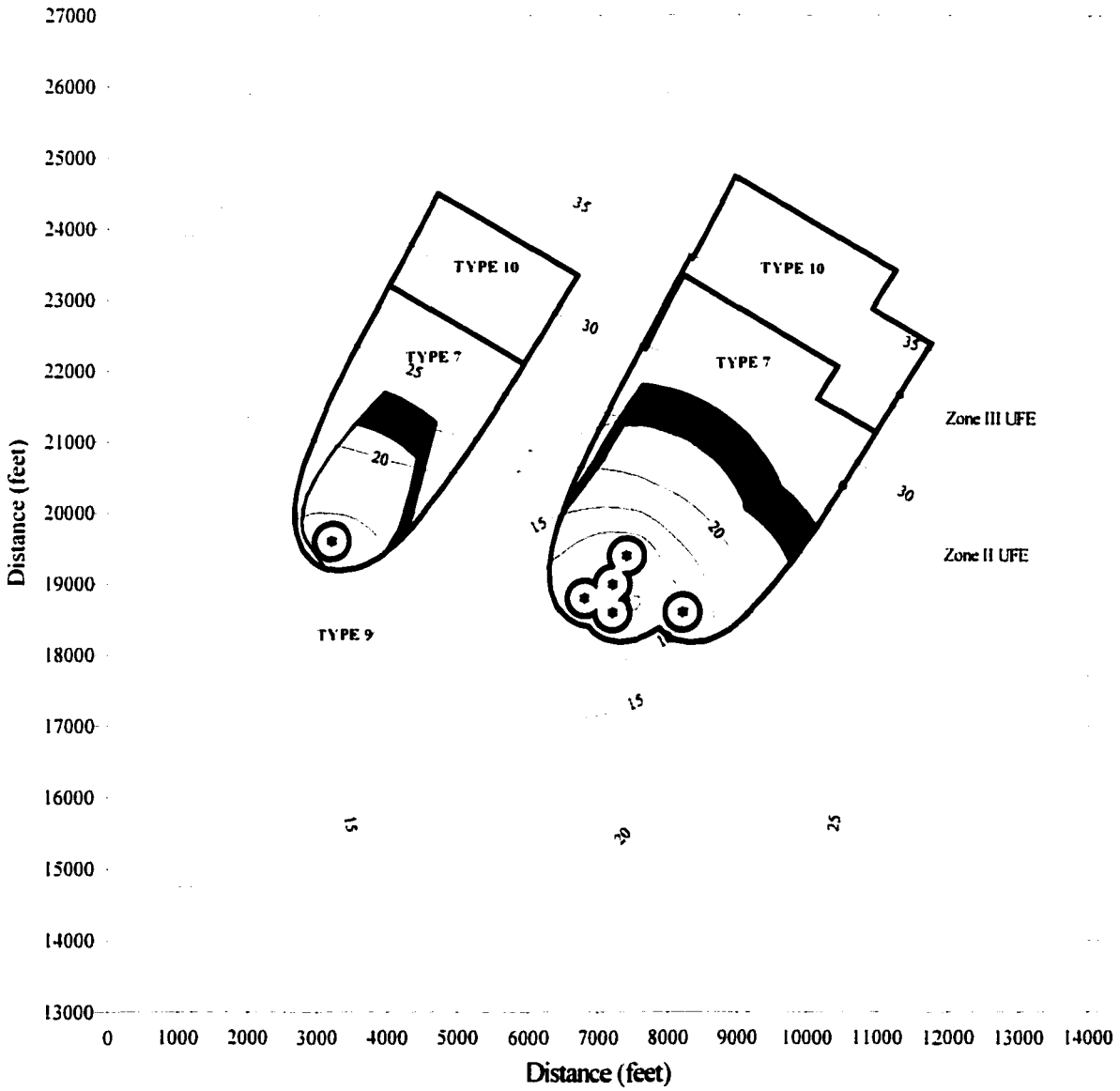


Figure 4.21: Wellhead Protection Area Decision Making for the Uniform Flow Equation

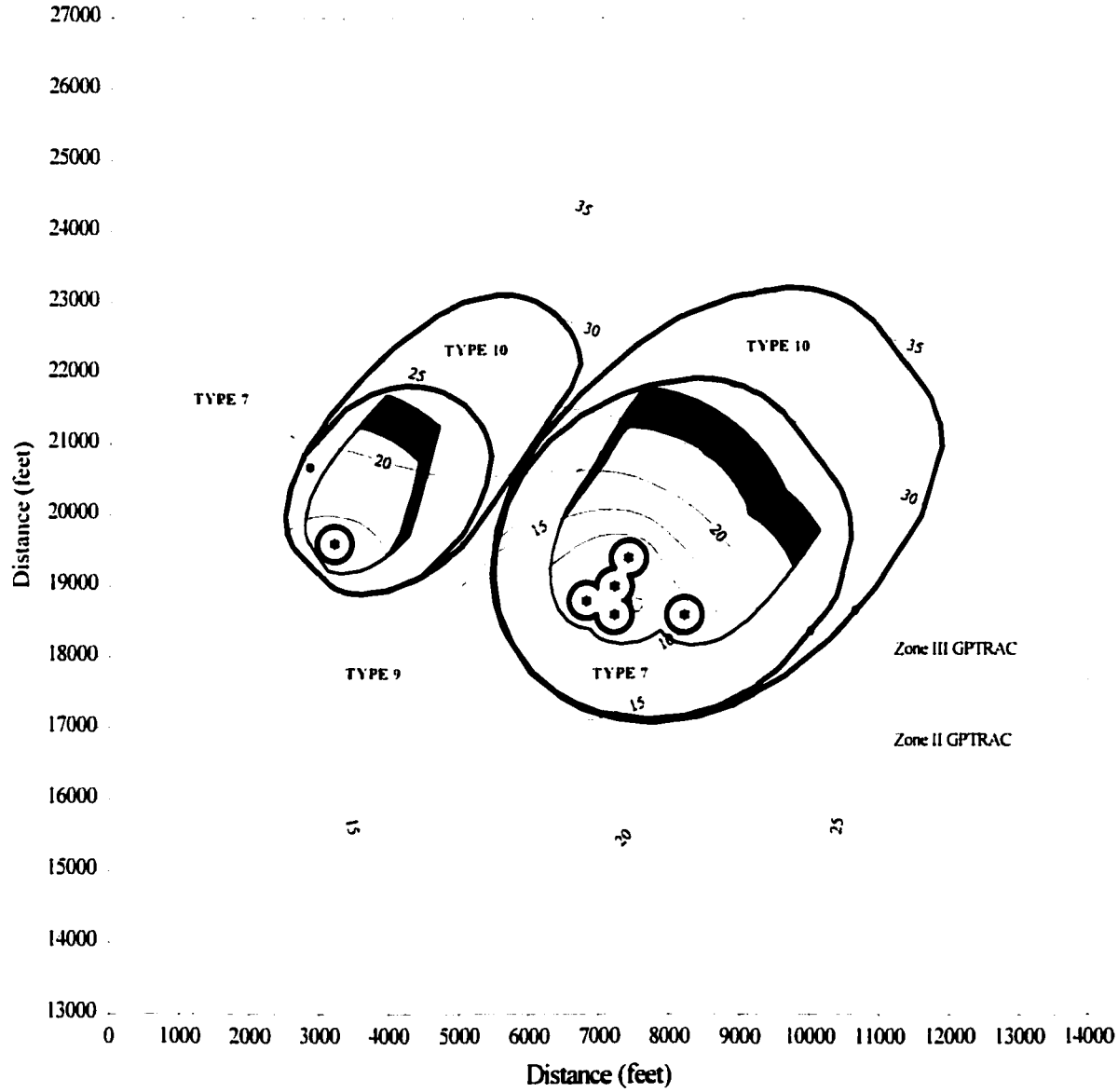


Figure 4.22: Wellhead Protection Area Decision Making for the GPTRAC Model

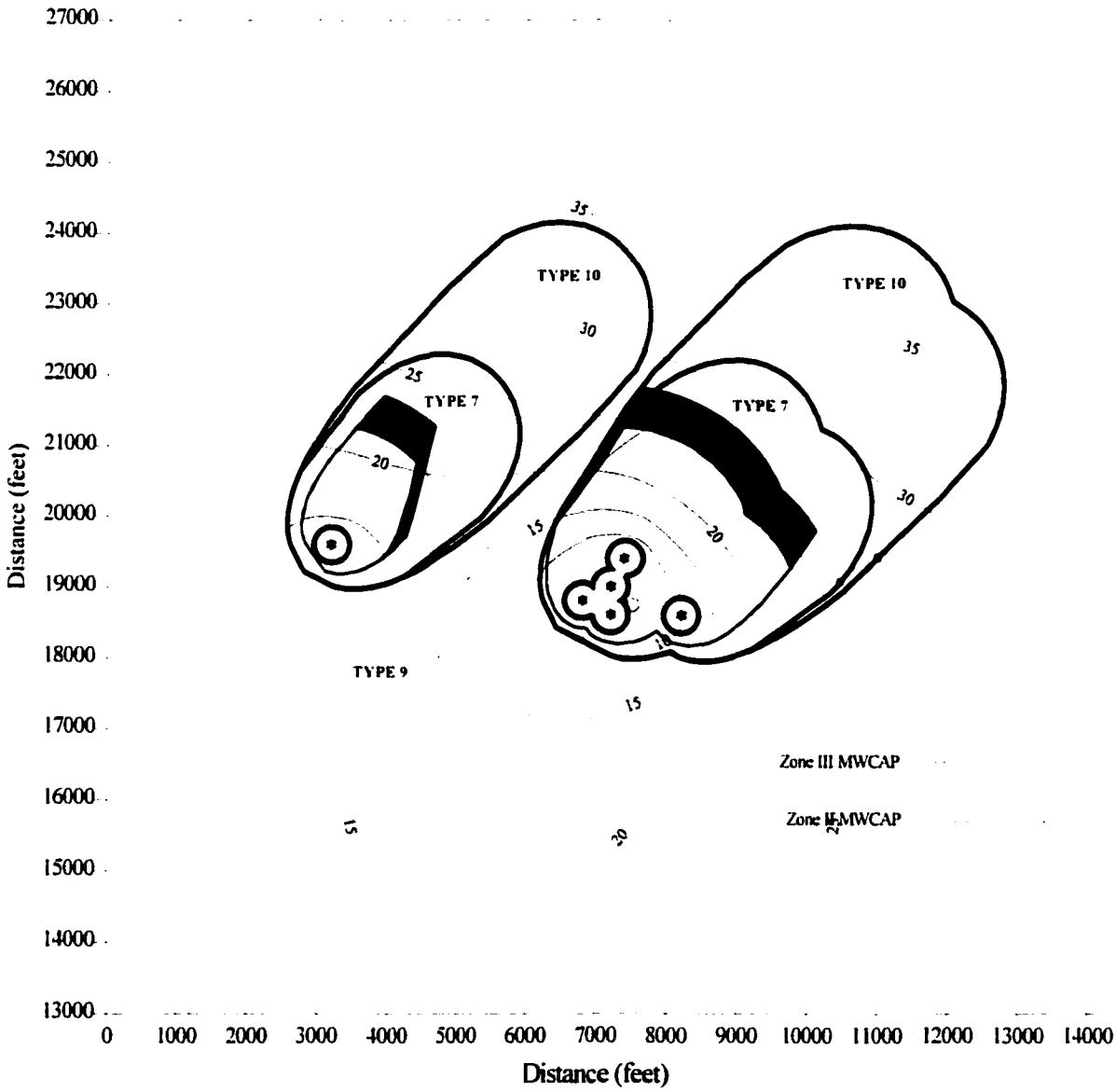


Figure 4.23: Wellhead Protection Area Decision Making for the MWCAP Model

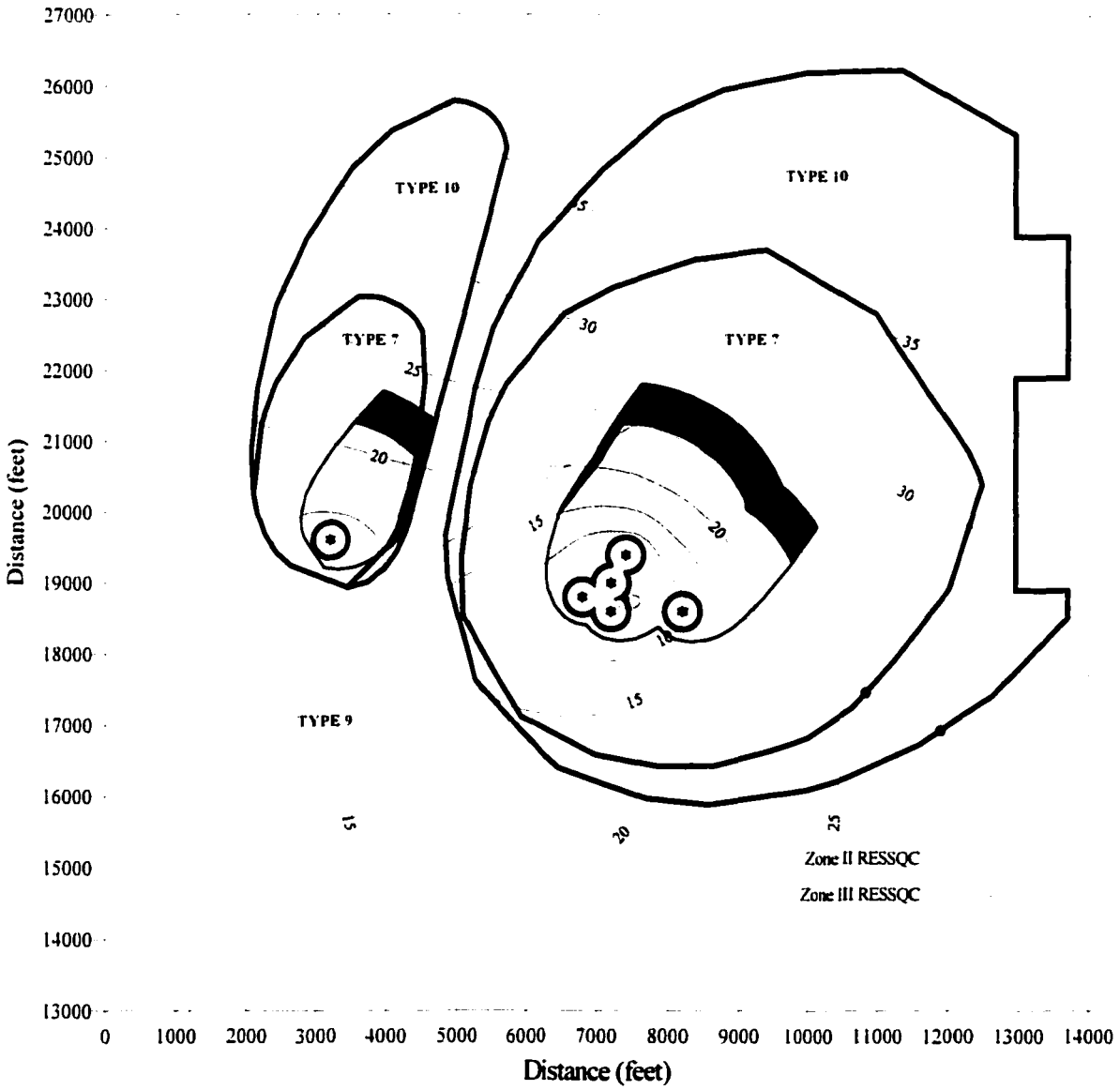


Figure 4.24: Wellhead Protection Area Decision Making for the RESSQC Model

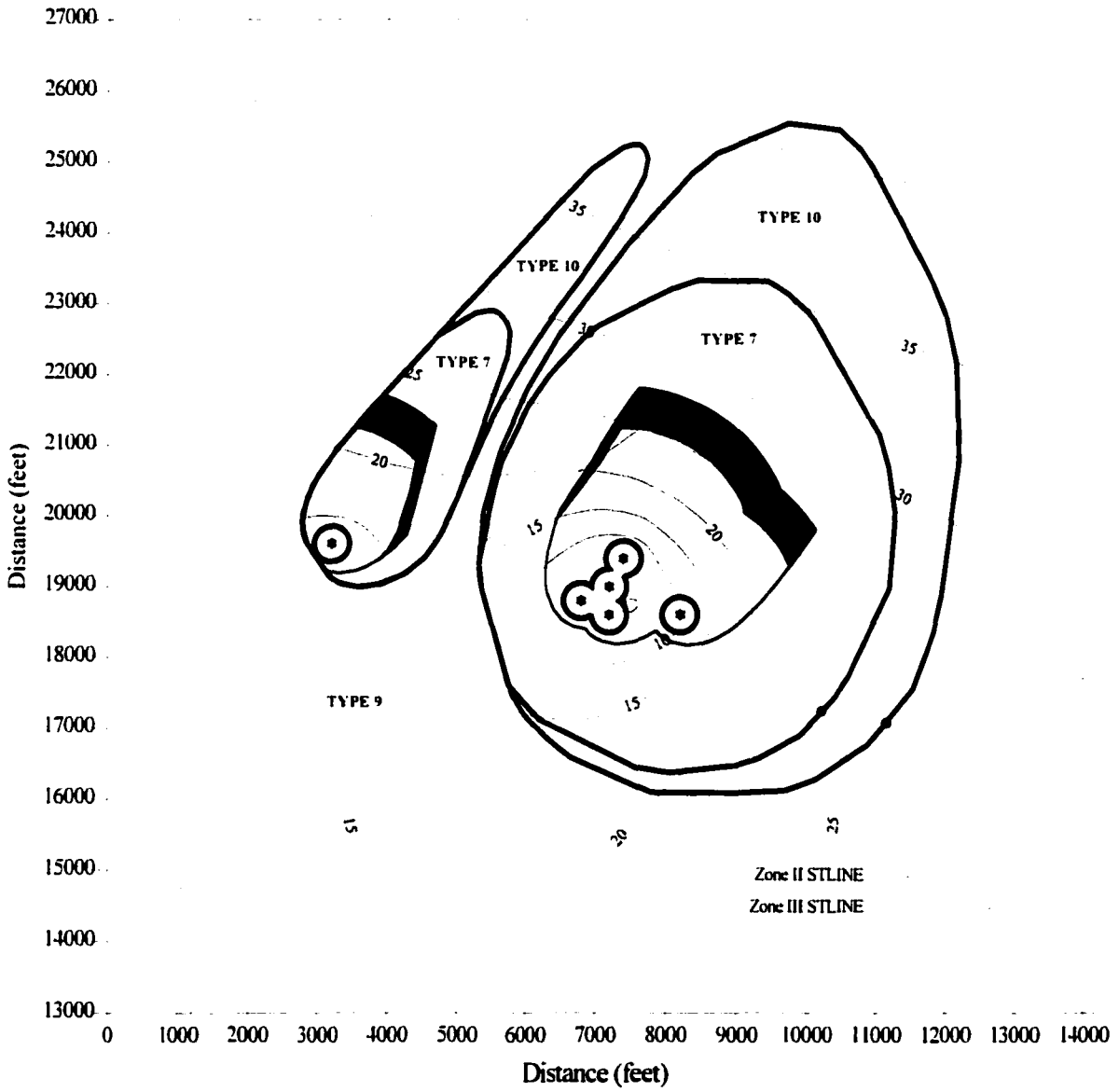


Figure 4.25: Wellhead Protection Areas Decision Making for the STLINE Model

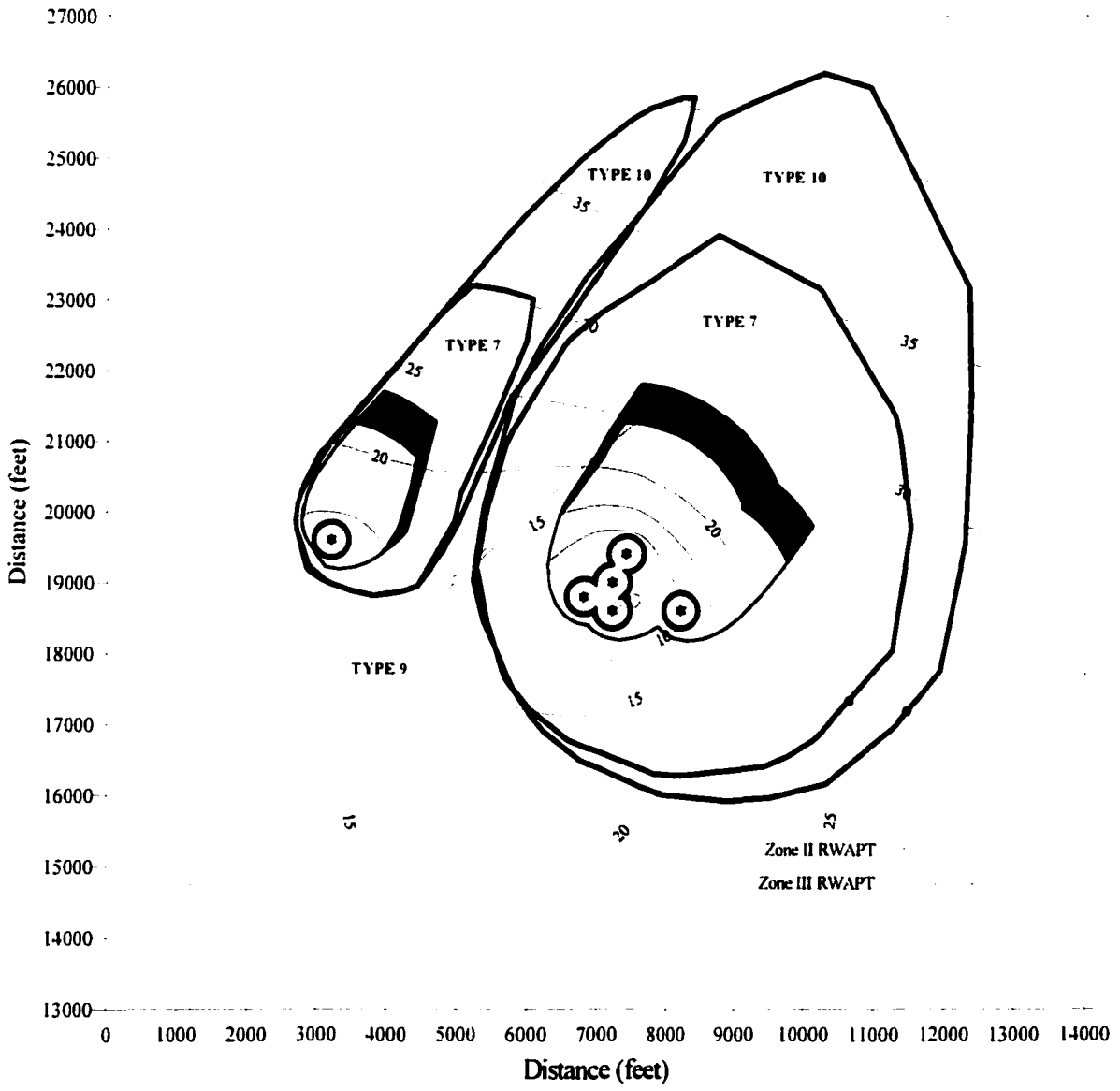


Figure 4.26: Wellhead Protection Area Decision Making for the RWAPT Model

WHPA Delineation Technique	Zone II Area		Zone III Area	
	Well 20 [feet^2]	Parkway [feet^2]	Well 20 [feet^2]	Parkway [feet^2]
Calculated FR	9 001 700	14 842 500	15 743 100	24 245 800
Uniform Flow	7 016 600	13 969 400	10 503 000	20 498 800
RESSQC	7 378 400	40 268 400	15 300 900	71 326 100
GPTRAC	6 116 300	17 687 700	10 807 800	29 962 100
MWCAP	7 461 700	13 459 900	15 180 000	25 700 800
STLINE	6 282 100	31 672 800	9 318 500	49 051 400
RWAPT	7 880 800	35 367 900	12 646 500	54 477 100

Table 4.14: The WHPA Boundary Areas for Potential Zone II and III Boundaries

Potential WHPA Boundary	Failure Type	Failure Area (ZDU)		
		Well 20 [feet^2]	Parkway [feet^2]	Total Area [feet^2]
CFR	7	6 530 300	8 227 500	14 757 800
	9	147 200	115 000	262 300
	10	5 292 100	6 603 600	11 895 700
UFE	7	4 192 700	5 457 900	9 650 600
	9	690 000	2 017 800	2 707 900
	10	3 290 100	5 622 500	8 912 600
RESSQC	7	4 609 000	30 850 000	35 459 000
	9	439 200	1 819 100	2 258 400
	10	7 922 500	31 057 600	38 980 200
GPTRAC	7	3 292 400	9 167 200	12 459 600
	9	690 000	2 017 800	2 707 900
	10	4 495 200	9 367 500	13 862 700
MWCAP	7	4 637 800	5 147 100	9 784 900
	9	690 000	1 819 100	2 509 100
	10	7 522 000	11 135 300	18 657 300
STLINE	7	3 261 900	22 254 400	25 516 200
	9	690 000	2 017 800	2 707 900
	10	3 036 400	17 378 600	20 415 000
RWAPT	7	4 860 600	25 949 400	30 810 000
	9	690 000	2 017 800	2 707 900
	10	4 765 700	19 109 300	23 875 000

Table 4.15: Failure Areas (ZDUs) for Each Zone II and Zone III Boundary

WHPA Method	Zone	P_f	Failure Type	Area of Failure					Sites	Cf	Rf	NPW
				Total [feet^2]	Total [acre]	Developable [acre]	Developed [acre]	Undeveloped [acre]		[$]	[$]	[$]
CFR	II	0.564	7	14 757 800	338.79	169.40	42.35	127.05	22	18 169 600		
			9	262 300	6.02	3.01	0.75	2.26	1	982 800		
	III	0.280	10	11 895 700	273.09	136.54	34.14	102.41	18	2 477 700	11 495 700	11 503 200
UFE	II	0.569	7	9 650 600	221.55	110.77	27.69	83.08	14	11 562 500		
			9	2 707 900	62.16	31.08	7.77	23.31	4	4 692 700		
	III	0.223	10	8 912 600	204.60	102.30	25.58	76.73	13	1 789 400	9 648 200	9 658 200
RESSQC	II	0.442	7	35 459 000	814.03	407.01	101.75	305.26	51	42 120 400		
			9	2 258 400	51.85	25.92	6.48	19.44	4	4 486 300		
	III	0.173	10	38 980 200	894.86	447.43	111.86	335.57	56	7 708 300	21 933 700	21 948 700
GPTRAC	II	0.424	7	12 459 600	286.03	143.02	35.75	107.26	18	14 866 000		
			9	2 707 900	62.16	31.08	7.77	23.31	4	4 692 700		
	III	0.166	10	13 862 700	318.24	159.12	39.78	119.34	20	2 753 000	8 749 900	8 764 900
MWCAP	II	0.461	7	9 784 900	224.63	112.32	28.08	84.24	15	12 388 300		
			9	2 509 100	57.60	28.80	7.20	21.60	4	4 601 400		
	III	0.181	10	18 657 300	428.31	214.16	53.54	160.62	27	3 716 500	8 505 000	8 520 000
STLINE	II	0.154	7	25 516 200	585.77	292.89	73.22	219.66	37	30 557 900		
			9	2 707 900	62.16	31.08	7.77	23.31	4	4 692 700		
	III	0.060	10	20 415 000	468.66	234.33	58.58	175.75	30	4 129 400	5 676 400	5 716 400
RWAPT	II	0.090	7	30 810 000	707.30	353.65	88.41	265.24	45	37 165 000		
			9	2 707 900	62.16	31.08	7.77	23.31	4	4 692 700		
	III	0.035	10	23 875 000	548.09	274.05	68.51	205.54	35	4 817 700	3 935 800	3 980 800

Table 4.16: The Net Present Worth Costs of Delineating Zone II and Zone III WHPAs

4.7 Discussion

Risk-benefit-cost analysis has been shown to be a useful application of environmental decision making for determining the best alternative for delineating wellhead protection areas. Figure 4.27 presents the best alternatives for WHPA boundary delineation that were determined using benefit-cost-risk analysis. These results are specific to the site conditions of the Cohansey aquifer and the Wellhead Protection Plan for the Pleasant Plains community. The best alternative for Zone I delineation is the 250 foot arbitrary fixed radius model. The best alternative for Zone II and Zone III WHPA delineation is the numerical model of SWIFT and RWAPT.

It is also evident from Tables 4.13 and 4.16 that the risk associated with each WHPA delineation technique is between 2 and 3 orders of magnitude greater than the cost of delineation. This shows that the risk of incorrectly delineating the WHPA boundaries has a profound effect on the net present worth of groundwater protection. It also shows that the nominal increase in cost associated with the use of a better groundwater model has a large impact on reducing the risk of failure for delineating the best WHPA boundary.

For the Zone I boundary the arbitrary fixed radius method is very easy to implement from a technical standpoint and involves very little cost. However, the average risk of using arbitrary fixed radii for WHPA boundary delineation is approximately $14,000,000. By spending an extra $2,500 to implement the calculated fixed radius method, this risk may be reduced to $2,750,000 and the results are more technically sound but involve a greater understanding of the scientific basis behind wellhead protection. By spending another $35,000 to invest in a calibrated groundwater flow model the risk of failure may be reduced even further to $810,000. However, the methodology may only be properly implemented by a knowledgeable groundwater modeler with a good understanding of the hydrogeology of the study site and the hydrologic stresses that affect groundwater flow. It may be concluded that the analysis presented herein shows that the added cost of using a numerical model to delineate the WHPA boundaries has a large payback in reducing the risk of failure of these groundwater protection zones.

4.8 Summary

The complicated nature of the groundwater environment and the importance of community development plans make it necessary to utilize multilevel Wellhead Protection Plans to protect the groundwater around municipal wellheads. These plans will be composed of a number of zones of groundwater protection. There are different methods for delineating WHPAs for each protection zone and different criteria for determining failure. The present chapter generated a Wellhead Protection

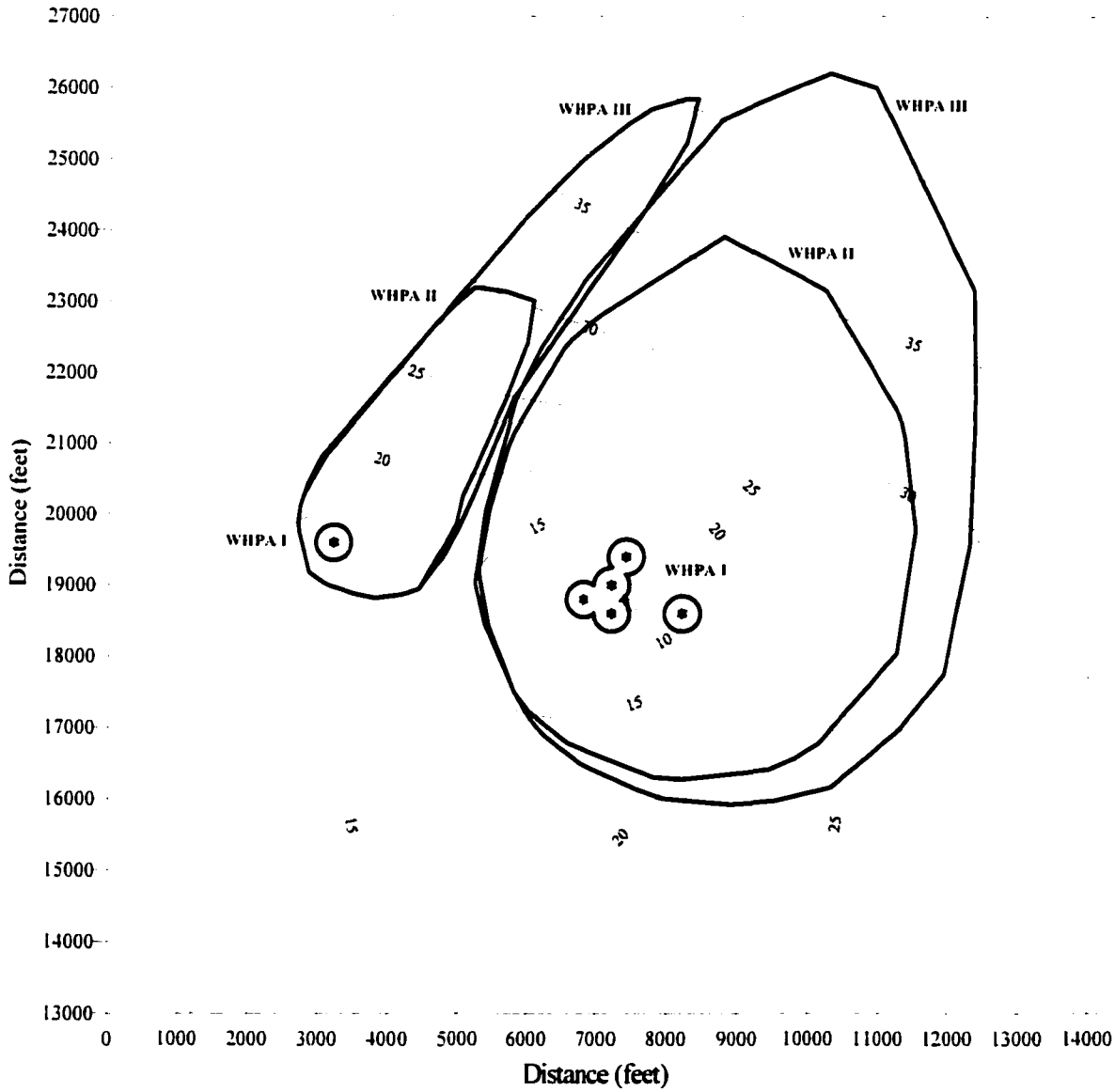


Figure 4.27: The Best Alternative for Zone I, II and III Groundwater Protection Zones

Plan for the United Water Toms River wellfields and compared all of the acceptable methods of WHPA delineation. For delineating Zone I WHPAs the best methodology involves the use of arbitrary fixed radius, and for Zone II and Zone III WHPA delineation the best methodology involves the use of a numerical groundwater model. Environmental engineering endeavours are commonly compared using a benefit-cost approach. However, a cost-benefit analysis that does not take into account the environmental risk if each groundwater protection alternative misses a great deal of information on the real costs of delineation wellhead protection areas. For this reason, the results of the present analysis have shown that WHPA decision making is a useful application of the benefit-cost-risk analysis methodology.

CHAPTER 5
REGRET ANALYSIS FOR WHPA DELINEATION

5.1 Introduction

In Chapter 4, the best alternative for WHPA delineation was determined by comparing a suite of acceptable alternatives using benefit-cost-risk analysis. The best alternative among the time of travel based methods was the RWAPT numerical WHPA model. The RWAPT model is the most scientifically defensible method of WHPA delineation with the lowest probability of failure. The purpose of Chapter 5 is to use regret analysis to determine the regret, or opportunity loss, associated with not choosing the best alternative for WHPA delineation at the municipal wellfields of Pleasant Plains, New Jersey. This will be achieved by setting the RWAPT boundary to be the best alternative for WHPA modeling for all protection zones, and comparing them to the other WHPA model. The same benefit-cost-risk model that was developed in Section 4.3 will be used for regret analysis.

5.2 Regret Analysis of WHPA Delineation

The benefits and costs of groundwater protection that were developed in Chapter 4 remain the same for regret analysis. However, the performance standard was chosen to be the Zone I, II and III RWAPT boundaries, and the probability of failure was assigned a value of 1.0 for all non-optimal WHPA models which, by definition, have failed to delineate the best WHPA boundary.

Regret analysis for WHPA delineation was implemented as follows. The Zone I boundaries, which are principally based on the distance criterion, were delineated on the same figure as the RWAPT boundaries to determine Zone I areas of failure and types of failure. The Zone II and Zone III boundaries, which are based on the time of travel criterion, were delineated on the same figure as the RWAPT boundaries to determine Zone II and III areas of failure and types of failure. Benefit-cost-risk analysis was then used to determine the regret associated with choosing each of the non-optimal WHPA delineation techniques.

5.2.1 The Zone I WHPA Boundary

Figure 5.1 presents the ½ year, 5 year and 10 year RWAPT boundaries, which are the standard for regret analysis. To illustrate regret analysis, Figure 5.2 shows the ½ year calculated fixed radius non-optimal Zone I alternative, in proximity to the RWAPT boundaries around well 20. The CFR boundary intersects the optimal WHPA boundary resulting in three failure areas. The first area is outside of the Zone II RWAPT boundary and inside of the CFR boundary, representing type 4 failure, and encompasses an area of 14,300 feet^2. The second area is outside of the Zone I RWAPT

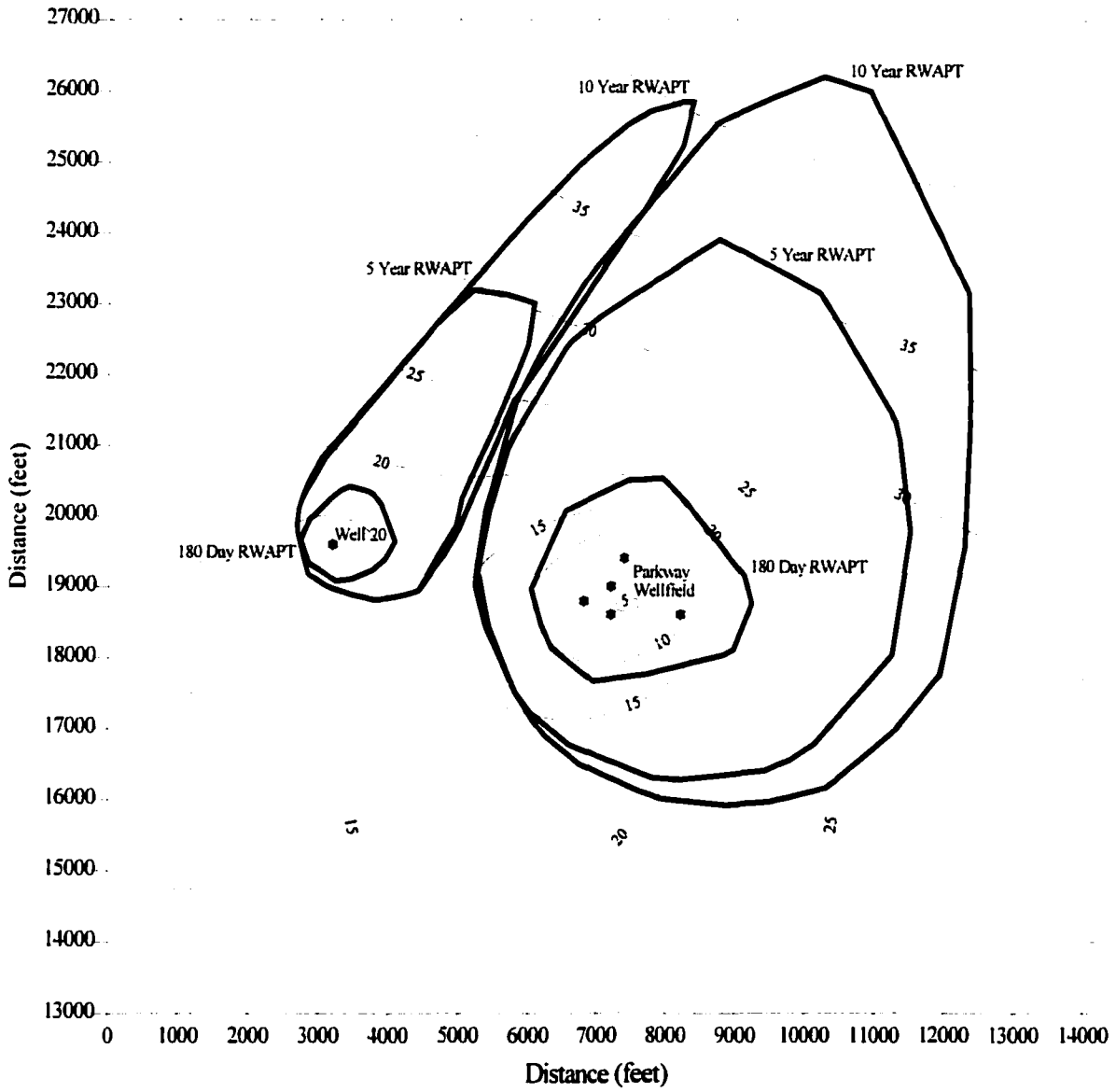


Figure 5.1: The Standard RWAPT WHPA Boundaries for Regret Analysis

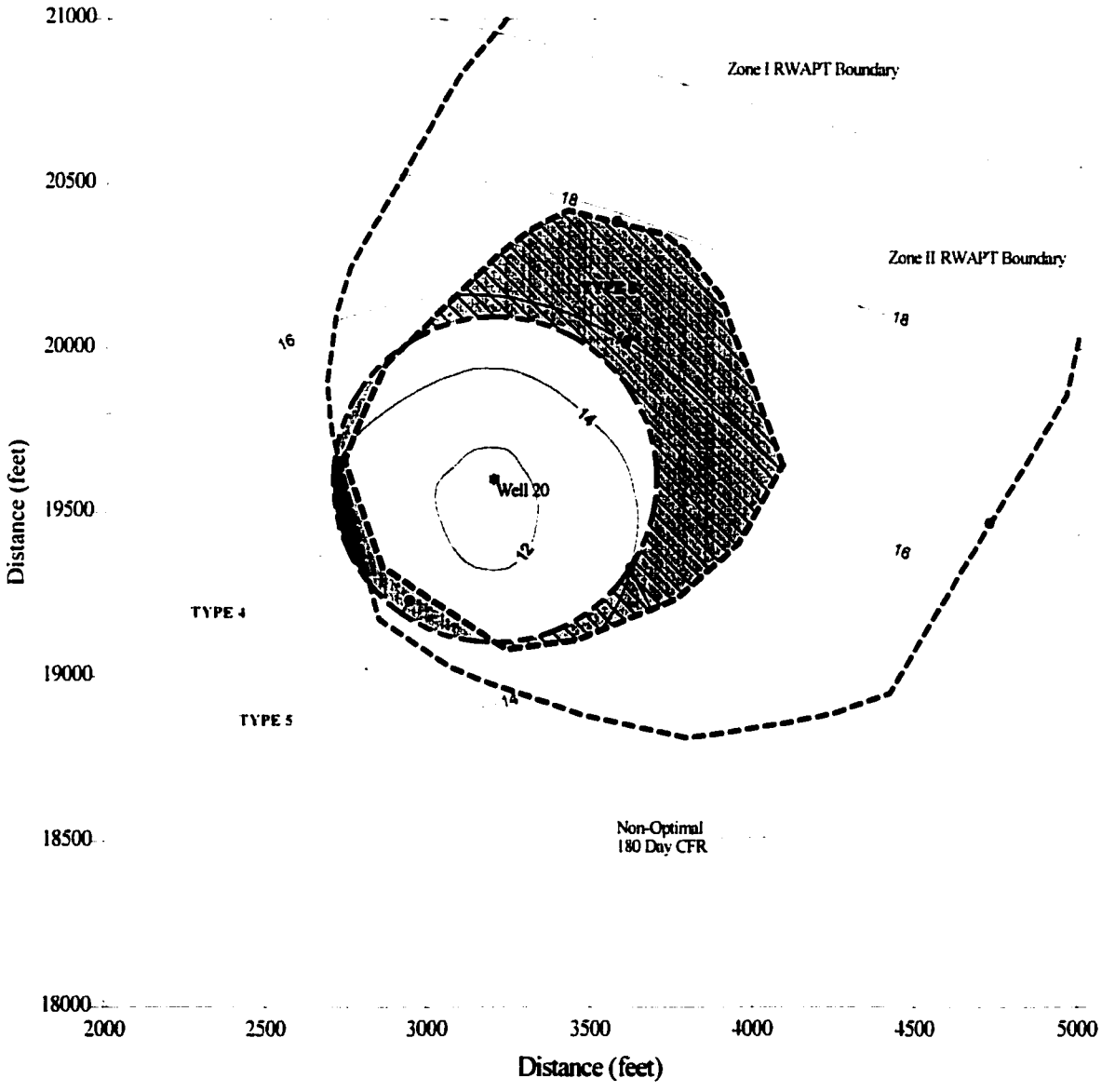


Figure 5.2: Failure Associated with the Zone I Calculated Fixed Radius Boundary

boundary and inside of the CFR boundary, representing type 5 failure, and encompasses an area of 54,000 feet^2. The third area is inside of the Zone I RWAPT boundary and outside of the CFR boundary, representing type 8 failure, and encompasses an area of 534,200 feet^2. The failure areas for all of the 9 non-optimal WHPA boundaries for delineating Zone I WHPA boundaries, for both UWTR wellfields, are presented in Table 5.1.

Regret for each Zone I boundary was determined as follows. The failure areas were calculated for each WHPA boundary. The cost of failure was determined from the size of these failure areas. The probability of failure for each model was assigned a value of 1.0. Economic regret, for each WHPA boundary, was determined by adding the cost of failure to the cost of WHPA delineation. Figures 5.3 and 5.4 show the 9 non-optimal Zone I boundaries for well 20 and the Parkway wellfield, respectively, in proximity to the optimal WHPA boundaries. Table 5.2 presents the opportunity loss associated with choosing each of the non-optimal WHPA boundaries for the Zone I protection area.

5.2.2 The Zone II and Zone III WHPA Boundaries

Figure 5.5 presents the Zone II and Zone III WHPA boundaries around well 20, for the calculated fixed radii method, and their proximity to the optimal RWAPT boundary. For the CFR model around well 20 there are 6 areas of failure. Type 7 failure, which was modeled as Zone II but should not be, has an area of 5,016,300 feet^2. Type 9 failure, which was modeled as Zone II but should be Zone III, has an area of 76,200 feet^2. Type 10 failure, which was modeled as Zone III but should not be, has an area of 4,658,700 feet^2. Type 12 failure, which was modeled as Zone III but should be Zone II, has an area of 1,080,300 feet^2. Type 14 failure, which was not modeled at all but should be Zone II, has an area of 2,914,800 feet^2. Finally, type 15 failure, which was not modeled at all but should be Zone III, has an area of 4,547,100 feet^2.

Figure 5.6 presents the WHPA boundaries for the uniform flow equation method, and their relationship to the optimal RWAPT boundaries. Figures 5.7, 5.8 and 5.9 present the WHPA boundaries for the RESSQC, GPTRAC and MWCAP methods of delineation. Figures 5.10 presents the WHPA boundaries for the STLINE method of delineation. Tables 5.3 and 5.4 present the failure areas, for both wellfields, for the 6 non-optimal methods for delineating Zone II and Zone III WHPA boundaries. Table 5.5 presents the opportunity loss associated with choosing each of the non-optimal methods of delineating the Zone II and Zone III protection areas.

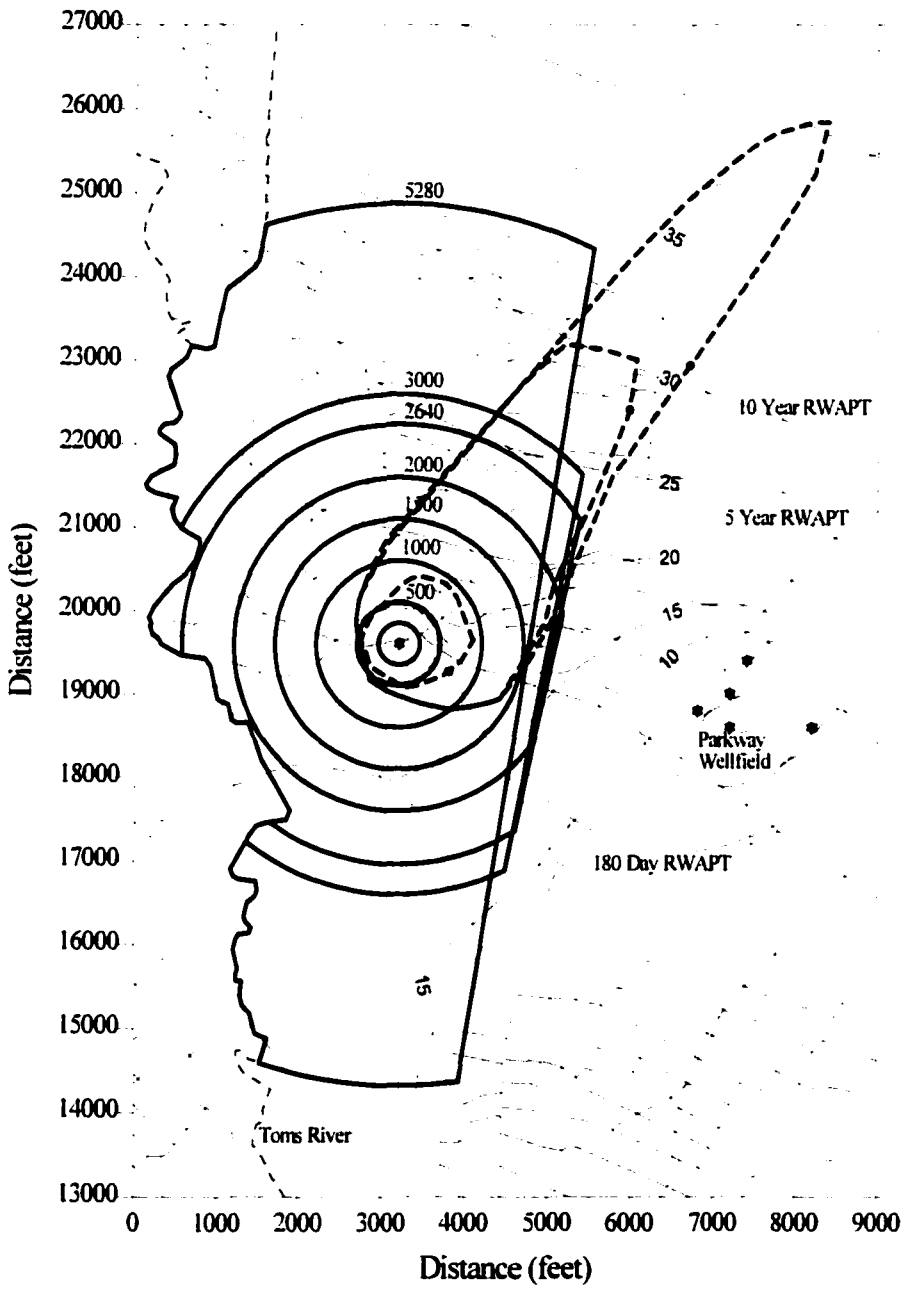


Figure 5.3: The Interaction Between Non-optimal and Optimal Zone I WHPA Boundaries

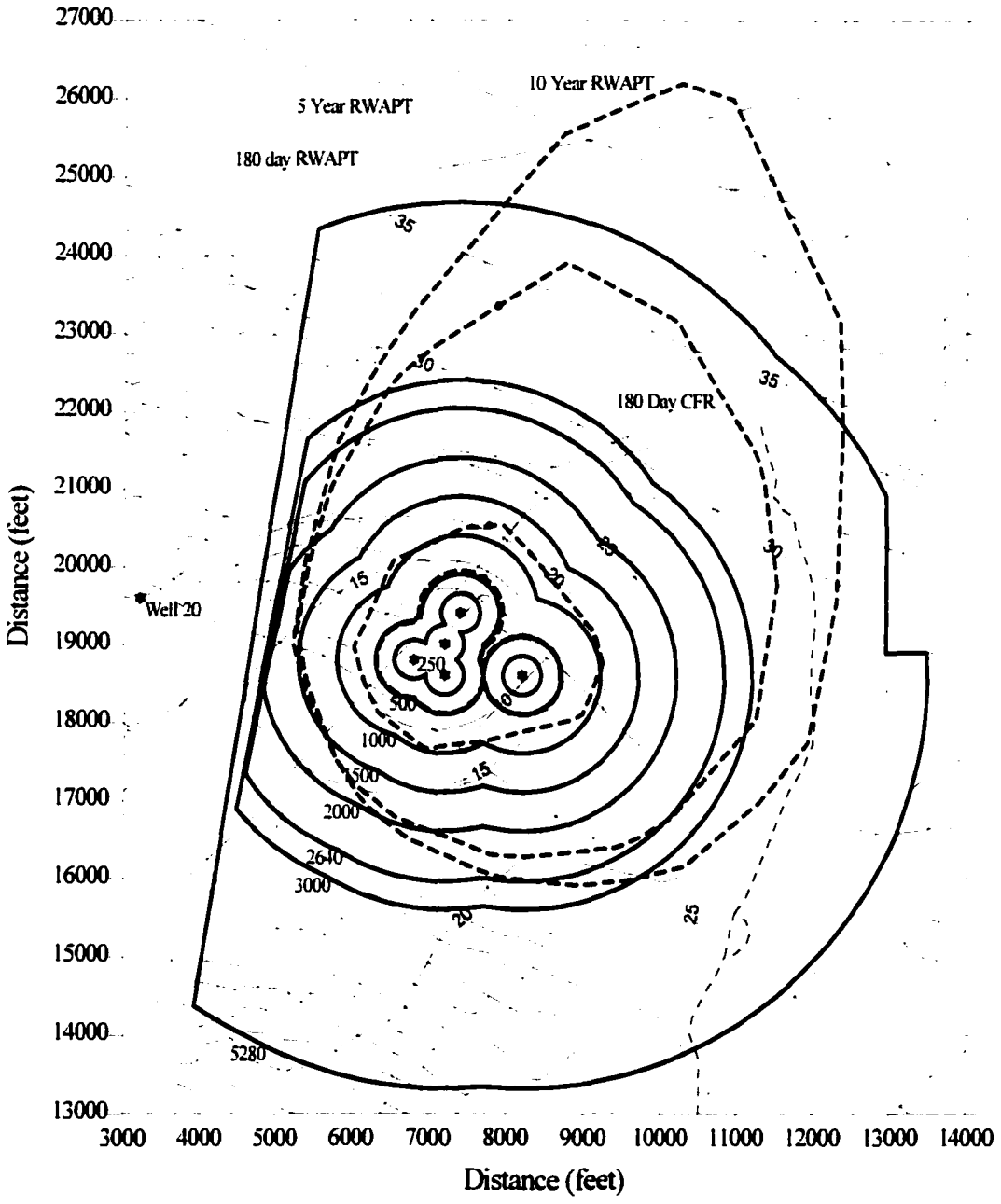


Figure 5.4: The Interaction Between Non-optimal and Optimal Zone I WHPA Boundaries

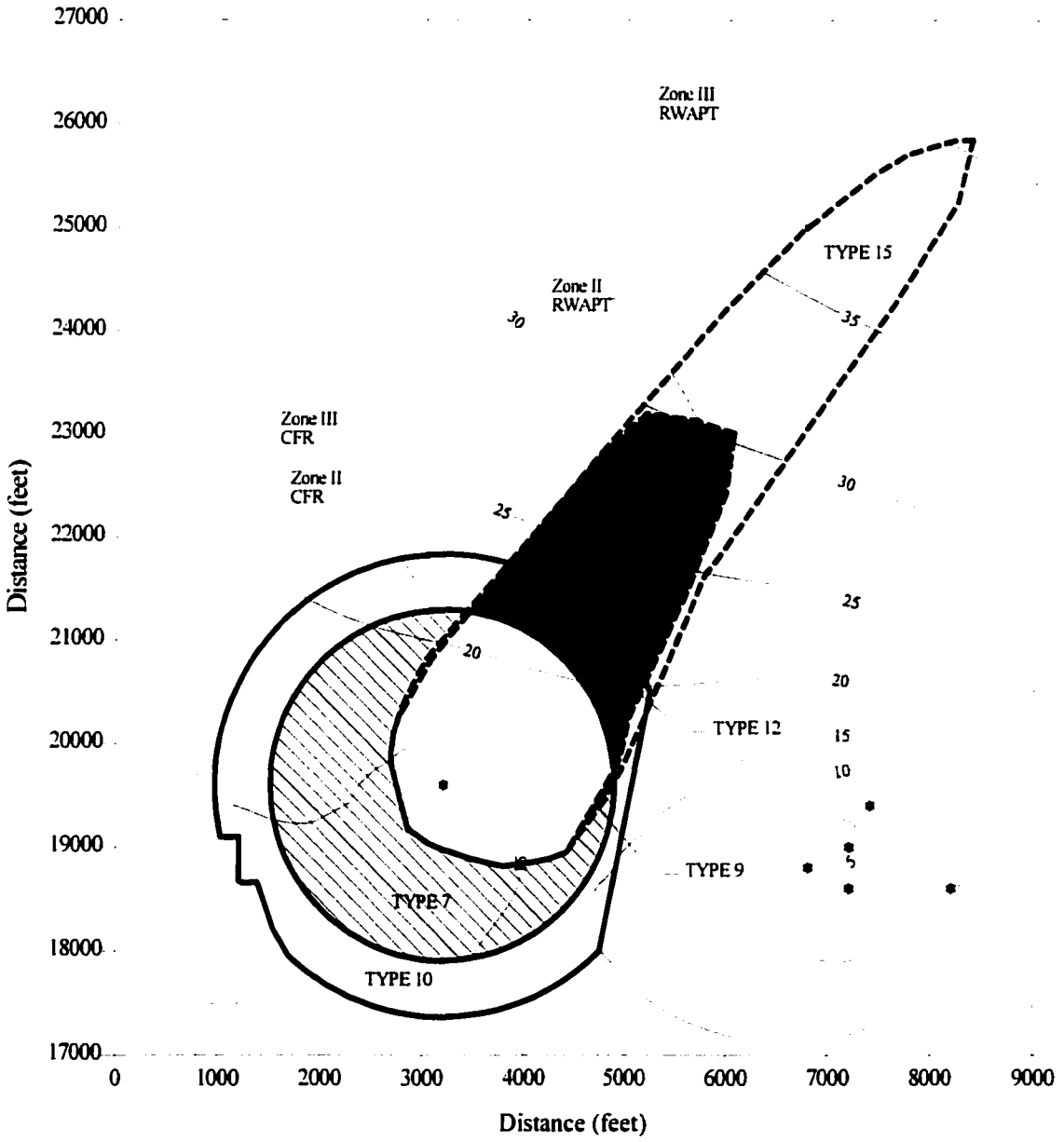


Figure 5.5: Failure Areas for the Zones II and III Calculated Fixed Radii Around Well 20

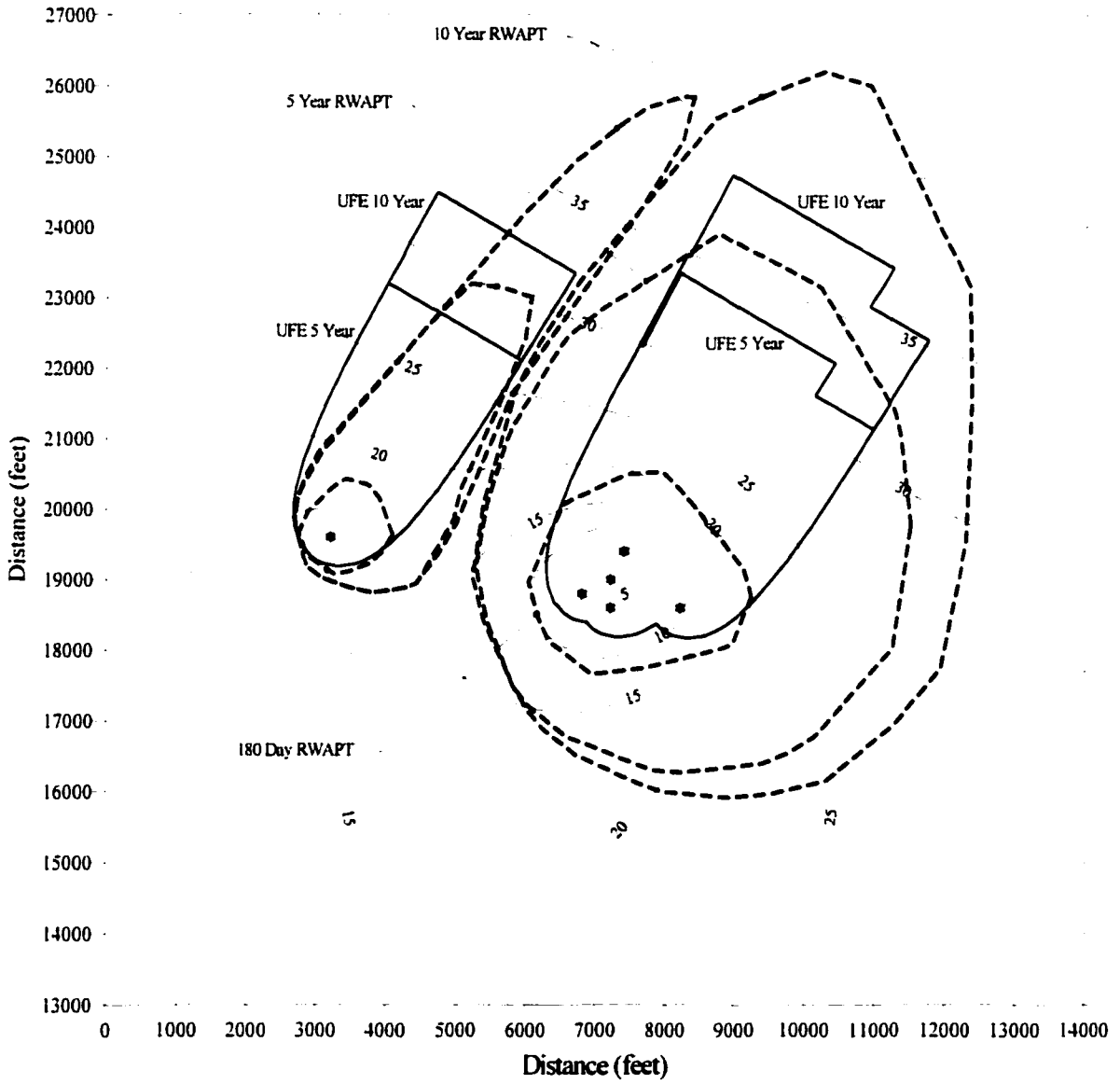


Figure 5.6: Regret Analysis of the WHPA Boundaries Using the Uniform Flow Equation

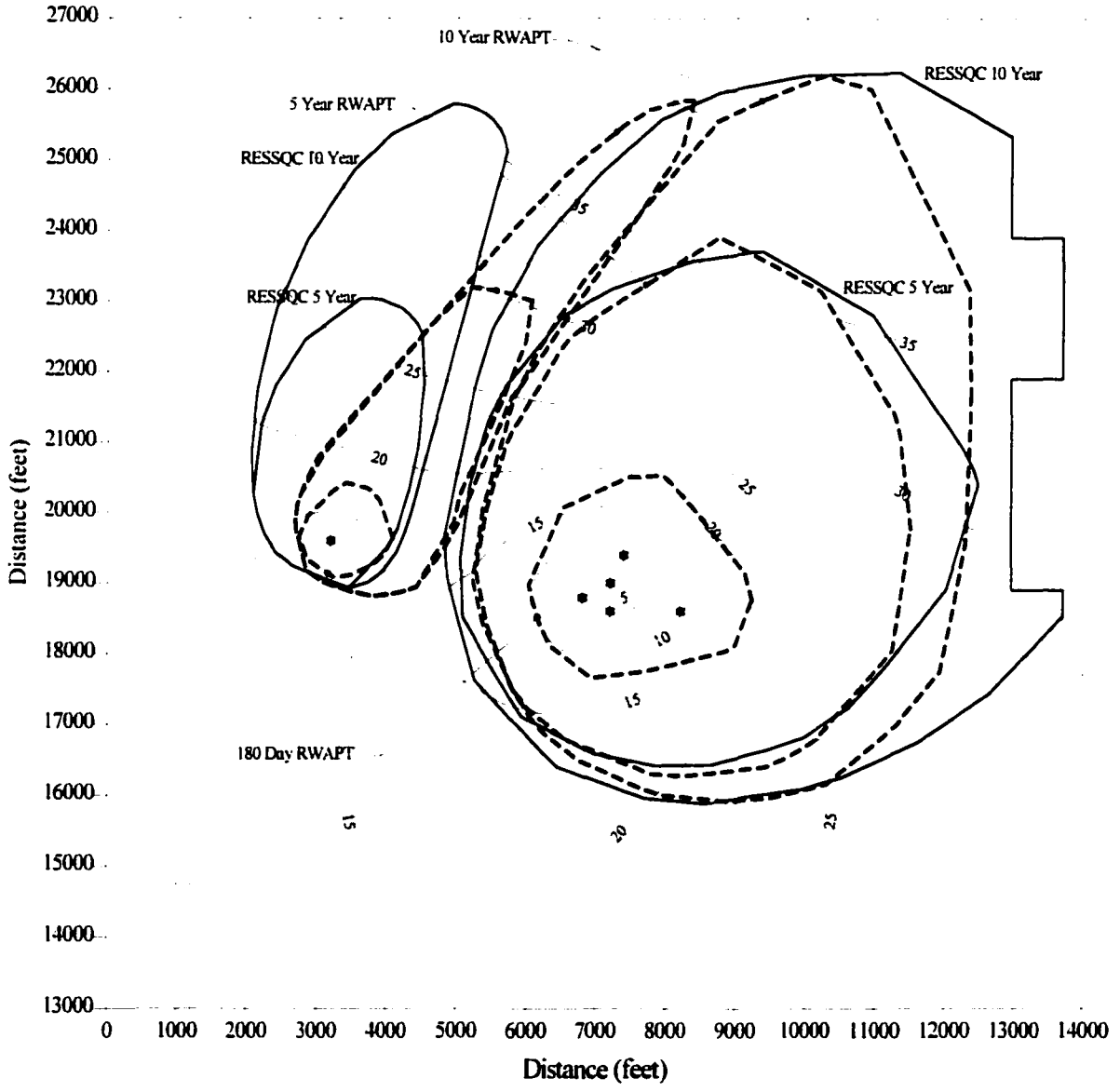


Figure 5.7: Regret Analysis of the WHPA Boundaries Using the RESSQC Model

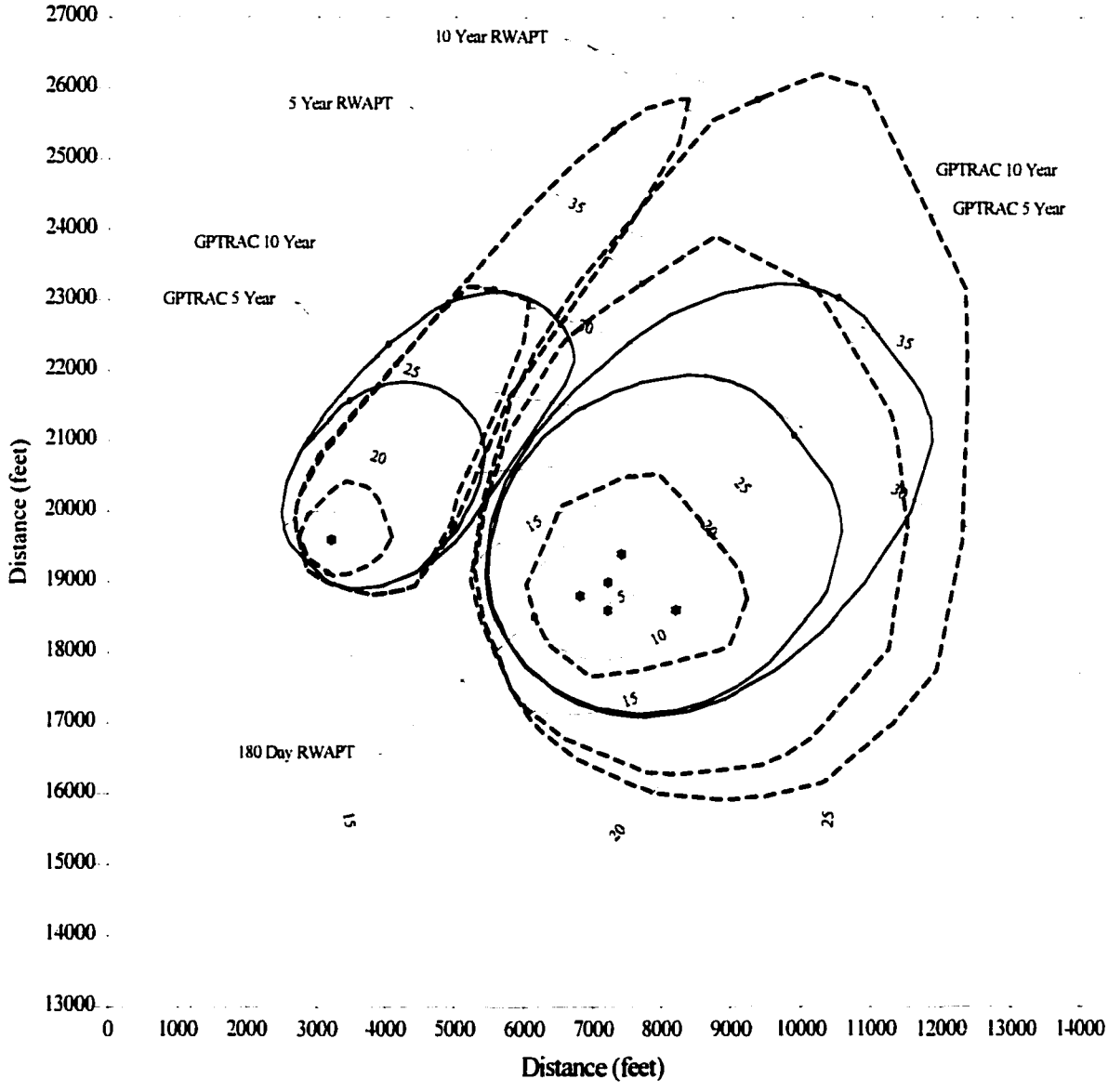


Figure 5.8: Regret Analysis of the WHPA Boundaries Using the GPTRAC Model

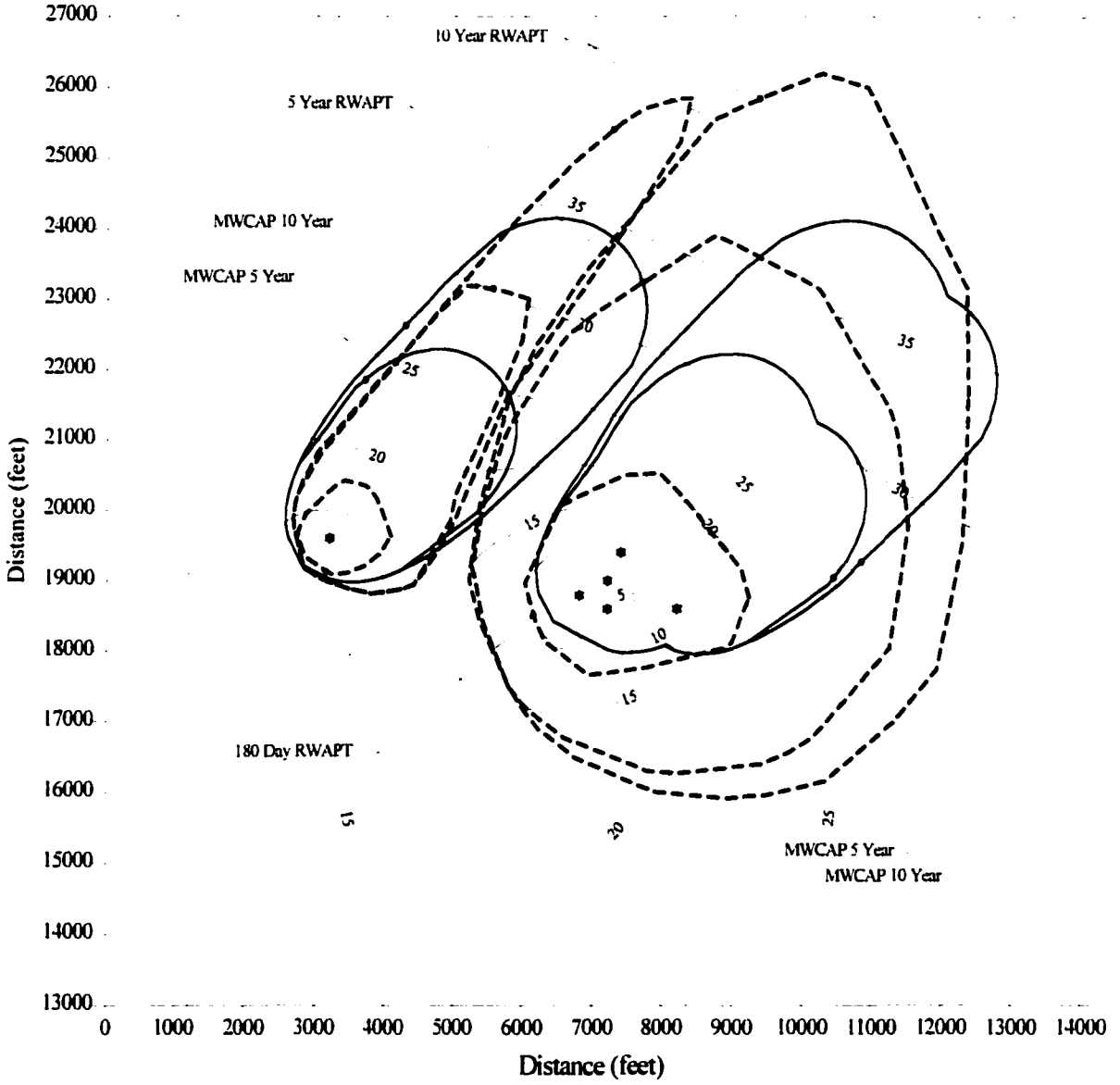


Figure 5.9: Regret Analysis of the WHPA Boundaries Using the MWCAP Model

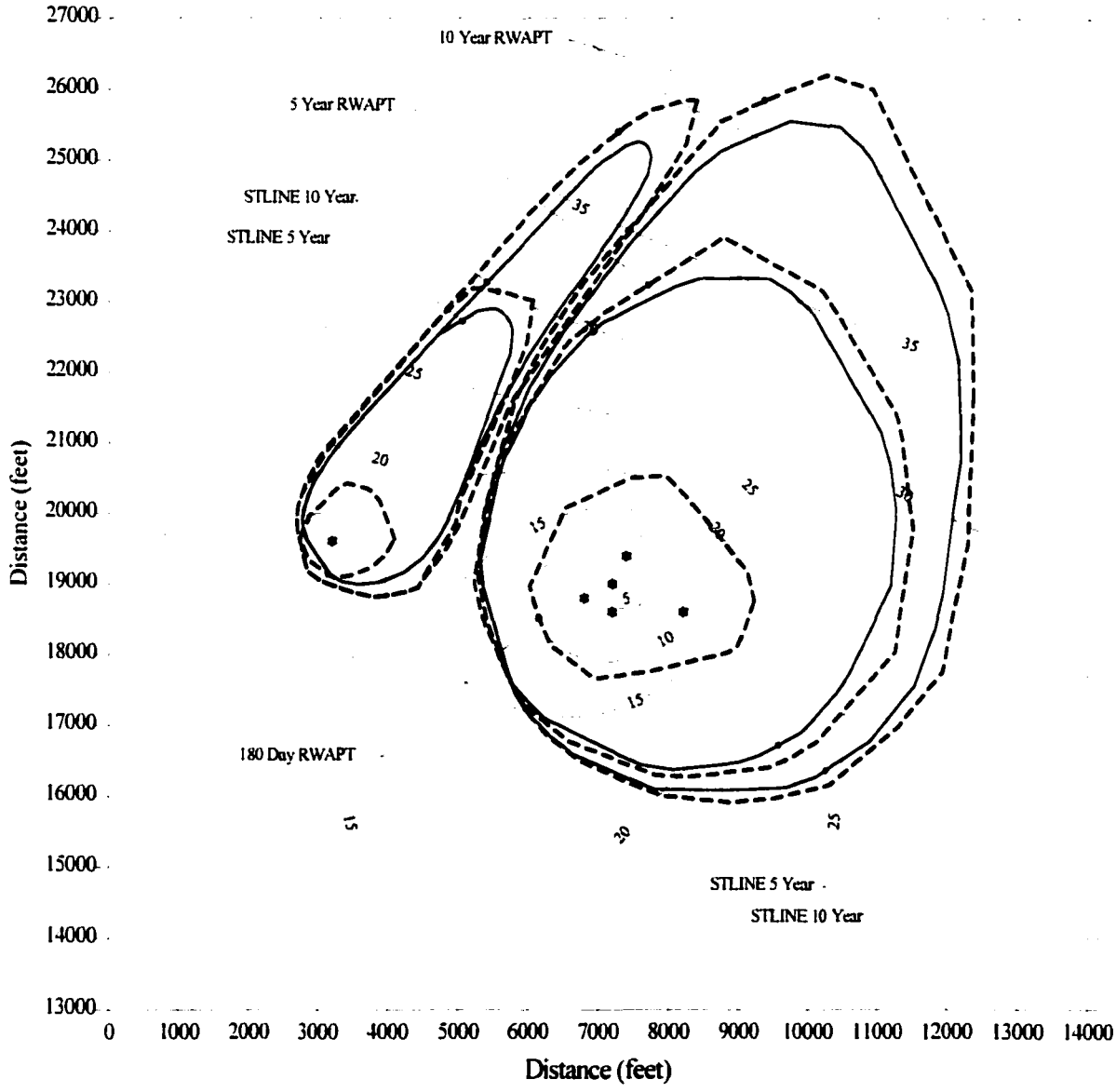


Figure 5.10: Regret Analysis of the WHPA Boundaries Using the STLINE Model

Potential WHPA Boundary	Failure Type	Failure Area (ZDU)		
		Well 20 [feet^2]	Parkway [feet^2]	Total Area [feet^2]
250 Foot AFR	8	1 042 400	5 633 400	6 675 800
500 Foot AFR	4	16 100	0	16 100
	5	57 300	0	57 300
	8	526 900	3 862 100	4 389 000
1000 Foot AFR	4	1 047 600	0	1 047 600
	5	846 600	888 700	1 735 300
	6	8 000	0	8 000
	8	0	454 400	454 400
1500 Foot AFR	4	3 565 800	34 000	3 599 800
	5	2 218 100	6 049 100	8 267 200
	6	44 400	44 400	88 800
2000 Foot AFR	4	7 751 900	1 235 800	8 987 700
	5	3 314 200	11 734 400	15 048 600
	6	132 900	227 900	360 800
½ Mile AFR	4	12 910 800	3 573 600	16 484 400
	5	4 435 100	18 190 900	22 626 000
	6	202 100	1 119 900	1 322 000
3000 Foot AFR	4	15 736 800	5 826 000	21 562 800
	5	4 919 300	21 029 200	25 948 500
	6	164 200	2 128 500	2 292 700
1 Mile AFR	4	32 271 600	36 118 600	68 390 200
	5	5 018 000	11 680 700	16 698 700
	6	160 600	28 797 100	28 957 700
180 Day CFR	4	14 300	0	14 300
	5	54 000	0	54 000
	8	534 200	3 804 400	4 338 600

Table 5.1: Failure Areas for Regret Analysis of the Zone I Boundary

Zone I Boundary	Failure Type	Area of Failure					Sites	Cf	Rf	NPW
		Total [feet^2]	Total [acre]	Developable [acre]	Developed [acre]	Undeveloped [acre]		[$]	[$]	[$]
250 Foot	8	6 675 800	153.26	76.63	19.16	57.47	10	4,806,200	4,806,200	4,811,200
500 Foot	4	16 100	0.37	0.18	0.05	0.14	1	1,007,400		
	5	57 300	1.32	0.66	0.16	0.49	1	200,400		
	8	4 389 000	100.76	50.38	12.59	37.78	7	3,233,900	4,441,800	4,446,800
1000 Foot	4	1 047 600	24.05	12.02	3.01	9.02	2	2,481,000		
	5	1 735 300	39.84	19.92	4.98	14.94	3	1,319,100		
	6	8 000	0.18	0.09	0.02	0.07	1	866,000		
	8	454 400	10.43	5.22	1.30	3.91	1	382,700	4,182,800	4,187,800
1500 Foot	4	3 599 800	82.64	41.32	10.33	30.99	6	7,652,800		
	5	8 267 200	189.79	94.89	23.72	71.17	12	5,885,100		
	6	88 800	2.04	1.02	0.25	0.76	1	903,100	14,441,000	14,446,000
2000 Foot	4	8 987 700	206.33	103.16	25.79	77.37	13	17,126,600		
	5	15 048 600	345.47	172.73	43.18	129.55	22	10,739,800		
	6	360 800	8.28	4.14	1.04	3.11	1	1,028,000	28,894,400	28,899,400
½ Mile	4	16 484 400	378.43	189.22	47.30	141.91	24	31,568,600		
	5	22 626 000	519.42	259.71	64.93	194.78	33	16,134,000		
	6	1 322 000	30.35	15.17	3.79	11.38	2	2,331,700	50,034,300	50,039,300
3000 Foot	4	21 562 800	495.01	247.51	61.88	185.63	31	40,900,300		
	5	25 948 500	595.70	297.85	74.46	223.39	38	18,530,100		
	6	2 292 700	52.63	26.32	6.58	19.74	4	4,502,000	63,932,400	63,937,400
1 Mile	4	68 390 200	1570.02	785.01	196.25	588.76	99	130,400,500		
	5	16 698 700	383.35	191.68	47.92	143.76	24	11,845,700		
	6	28 957 700	664.78	332.39	83.10	249.29	42	49,514,300	191,760,500	191,765,500
180 Day CFR	4	14 300	0.33	0.16	0.04	0.12	1	1,006,600		
	5	54 000	1.24	0.62	0.16	0.47	1	198,900		
	8	4 338 600	99.60	49.80	12.45	37.35	7	3,210,800	4,416,300	4,426,300

Table 5.2: The Regret Associated with Using Non-Optimal Boundaries to Delineate Zone I WHPAs

Potential Zone II/III Boundary	Failure Type	Failure Area (ZDU)		
		Well 20 [feet^2]	Parkway [feet^2]	Total Area [feet^2]
CFR	7	5 016 300	190 600	5 206 900
	9	76 200	70 800	147 000
	10	4 658 700	1 792 200	6 450 900
	12	1 080 300	6 371 900	7 452 200
	14	2 914 800	13 514 400	16 429 200
	15	4 547 100	18 698 600	23 245 700
UFE	7	1 422 900	0	1 422 900
	9	82 500	0	82 500
	10	1 474 500	0	1 474 500
	12	812 200	2 628 900	3 441 100
	13	72 700	1 475 000	1 547 700
	14	1 331 300	16 287 700	17 619 000
	15	3 644 500	16 115 700	19 760 200
RESSQC	7	375 300	1 168 700	1 544 000
	9	68 200	4 328 700	4 396 900
	10	6 913 000	15 727 400	22 640 400
	12	969 900	596 300	1 566 200
	14	3 374 100	0	3 374 100
	15	4 638 500	47 100	4 685 600
GPTRAC	7	615 700	0	615 700
	9	216 400	0	216 400
	10	1 738 200	0	1 738 200
	12	2 226 600	8 073 500	10 300 100
	14	192 800	8 744 800	8 937 600
	15	4 000 800	17 770 200	21 771 000
MWCAP	7	1 041 000	0	1 041 000
	9	311 800	0	311 800
	10	3 962 100	597 000	4 559 100
	12	1 337 100	5 096 500	6 433 600
	13	0	789 800	789 800
	14	264 600	15 120 000	15 384 600
	15	2 203 600	13 463 400	15 667 000
STLINE	12	602 200	3 695 100	4 297 300
	14	966 500	0	966 500
	15	2 297 600	5 425 800	7 723 400

Table 5.3: Failure Areas for the Zone II and Zone III Boundaries

Potential Zone II/III Boundary	Failure Type	Failure Area (ZDU)					Existing Sites
		Total [feet^2]	Total [acres]	Developabl [acres]	Developed [acres]	Undeveloped [acres]	
CFR	7	5 206 900	119.53	59.77	14.94	44.83	8
	9	147 000	3.38	1.69	0.42	1.27	1
	10	6 450 900	148.09	74.05	18.51	55.54	10
	12	7 452 200	171.08	85.54	21.38	64.15	11
	14	16 429 200	377.16	188.58	47.15	141.44	24
	15	23 245 700	533.65	266.82	66.71	200.12	34
UFE	7	1 422 900	32.66	16.33	4.08	12.25	3
	9	82 500	1.89	0.95	0.24	0.71	1
	10	1 474 500	33.85	16.92	4.23	12.69	3
	12	3 441 100	79.00	39.50	9.87	29.62	5
	13	1 547 700	35.53	17.77	4.44	13.32	3
	14	17 619 000	404.47	202.24	50.56	151.68	26
	15	19 760 200	453.63	226.82	56.70	170.11	29
RESSQC	7	1 544 000	35.45	17.72	4.43	13.29	3
	9	4 396 900	100.94	50.47	12.62	37.85	7
	10	22 640 400	519.75	259.88	64.97	194.91	33
	12	1 566 200	35.96	17.98	4.49	13.48	3
	14	3 374 100	77.46	38.73	9.68	29.05	5
	15	4 685 600	107.57	53.78	13.45	40.34	7
GPTRAC	7	615 700	14.13	7.07	1.77	5.30	1
	9	216 400	4.97	2.48	0.62	1.86	1
	10	1 738 200	39.90	19.95	4.99	14.96	3
	12	10 300 100	236.46	118.23	29.56	88.56	15
	14	8 937 600	205.18	102.59	25.65	76.94	13
	15	21 771 000	499.79	249.90	62.47	187.42	32
MWCAP	7	1 041 000	23.90	11.95	2.99	8.96	2
	9	311 800	7.16	3.58	0.89	2.68	1
	10	4 559 100	104.66	52.33	13.08	39.25	7
	12	6 433 600	147.70	73.85	18.46	55.39	10
	13	789 800	18.13	9.07	2.27	6.80	2
	14	15 384 600	353.18	176.59	44.15	132.44	23
	15	15 667 000	359.67	179.83	44.96	134.87	23
STLINE	12	4 297 300	98.65	49.33	12.33	36.99	7
	14	966 500	22.19	11.09	2.77	8.32	2
	15	7 723 400	177.30	88.65	22.16	66.49	12

Table 5.4: Failure Areas for Zone II and Zone III Boundaries

Potential Zone II/III Boundary	Probability of Failure	Failure Type	Cost of Failure [$]	Risk of Failure [$]	NPW Cost [$]
CFR	1.00	7	6,607,118		
		9	929,883		
		10	1,376,483		
		12	12,907,458		
		14	19,821,355		
		15	4,680,042	46,322,300	46,327,300
UFE	1.00	7	2,477,700		
		9	900,200		
		10	412,900		
		12	5,891,700		
		13	3,710,600		
		14	21,473,100		
		15	3,991,800	38,858,100	38,863,100
RESSQC	1.00	7	2,477,700		
		9	8,055,200		
		10	4,542,400		
		12	3,306,200		
		14	4,129,400		
		15	963,500	23,474,500	23,484,500
GPTRAC	1.00	7	825,900		
		9	961,700		
		10	412,900		
		12	17,664,400		
		14	10,736,600		
		15	4,404,700	35,006,300	35,016,300
MWCAP	1.00	7	1,651,800		
		9	1,005,500		
		10	963,500		
		12	11,577,400		
		13	2,362,600		
		14	18,995,500		
		15	3,165,900	39,722,300	39,732,300
STLINE	1.00	12	8,009,500		
		14	1,651,800		
		15	1,651,800	11,313,000	11,343,000

Table 5.5: Regret Analysis of Methods for Zone II and III Boundary Delineation

5.3 Discussion

Regret analysis was used to quantify the economic impact, or expected opportunity loss, associated with not choosing the best alternative for an engineering decision. From an environmental engineering perspective, regret analysis may be used to compare the net present worth of each method of delineating groundwater protection zones to the best alternative. The best alternative for WHPA delineation was chosen to be the RWAPT technique. This model is based on the most relevant hydrogeologic information that is available to the WHPA modeler. The results of the regret analysis shed some light on the modeling process.

The 15 failure types identified in Table 4.4 may be divided into three classes of failure. The first class of failure occurs when the delineation technique determines an area that does not have any hydraulic connection to the wellfield (failure types 4, 7 and 10). The second class of failure occurs when the delineation technique does not determine an area that does have a hydraulic connection to the wellfield (failure types 13, 14 and 15). The third class of failure occurs when the delineation technique determines an area that is hydraulically connected to the wellfield but has been identified as the wrong type of protection zone (failure types 5, 6, 8, 9, 11 and 12). The first two classes of failure represent the inability of the WHPA model to correctly incorporate all of the area that contributes groundwater to the wellfield. The third class of failure represents the inability of the WHPA model to correctly apportion the area within the true WHPA boundary to the true protection zone. Table 5.6 presents the areas encompassed by these three failure classes for each delineation technique. The delineation techniques may be classified as well according to the complexity of modeling in the same manner that was used to determine their probabilities of failure. There is a trend in Table 5.6 that indicates that, as the delineation technique becomes more scientifically complex, the area within Class 1 reduces. This emphasizes the fact that more scientifically defensible the WHPA model the lower the risk of failure.

Delineation Technique	Failure Area	
	Classes 1&2 [acres]	Class 3 [acres]
Calculated Fixed Radius	1178.43	174.46
Uniform Flow Equation	960.14	80.89
Analytical Modeling	786.27	177.73
Numerical Modeling	199.49	98.65

Table 5.6: Failure Areas for the Zone II and Zone III Boundaries

A related issue for a multilevel Wellhead Protection Plan is the amount of land that is zoned as WHPA I because this land is unavailable for development. Zoning land as WHPA I has a serious

impact on the amount of development that is allowed within a community, and therefore, the choice of delineation technique for the Zone I boundary is very important. The arbitrary fixed radius method for delineating the Zone I boundary could significantly limit development in the region depending on the value chosen for the fixed radius. The unfortunate aspect of using this method of WHPA delineation is the arbitrariness in choosing the value of distance for the fixed radius. As a result, the WHPA boundary could encompass potential development areas that have no hydraulic impact on the wellfield, and therefore, pose no risk of contamination to the region's water supply. Type 4 failure represents a Zone I area that has no hydrogeologic impact on the wellfield. For Zone I AFR boundaries these failure areas encompass between 0.2 acres for the 250 foot boundary and 1570 acres for the 1 mile boundary. Taking into account all source of failure, these results indicate that the risk of failure for using the arbitrary fixed radius method is large and, therefore, this WHPA model should not be considered an acceptable technique for WHPA delineation in anything but the simplest of hydrogeologic settings.

5.4 Summary

From the analysis presented herein the results indicate that the choice of WHPA delineation models has a serious impact on the amount of land encompassed by the WHPA boundary. It also has an impact on the size of the failure areas, the type of failure and, as a result, the risk of failure for each delineation technique. There is a direct correlation between the scientific complexity of the WHPA model and its ability to represent the true WHPA boundary. There are also serious implications for using the arbitrary fixed radius technique for delineating the Zone I boundary. The purpose of the WHPA I protection zone is to prevent industrial development in order to reduce the immediate risk of groundwater contamination reaching the wellfield. Therefore, the WHPA delineation technique should be complex enough to determine whether the area within the WHPA boundary is hydraulically connected to the wellfield.

CHAPTER 6
NUMERICAL WHPA MODEL UNCERTAINTY

6.1 Introduction

Uncertainty analysis is a technique that is used to measure the uncertainty in model output based on the uncertainty in model input. Two common models that are used to implement uncertainty analysis are the first order second moment method and the direct parameter sampling method. The first order second moment method is useful for defining regions in the conceptual model that are uncertain. The first order second moment method calculates the output variance of a model by summing, for each input variable, the product of the marginal sensitivity to the input variable and the variance of the input variable. The direct parameter sampling method can be used to measure the distribution of uncertainty in the conceptual model, but it can also be used to measure the value of information on model uncertainty. The direct parameter sampling method is implemented by first assuming a probability density function for each uncertain input parameter. Repetitive random sampling of each input parameter distribution generates the input for sequential model simulation, which provides a probability density function of an output performance measure. The output probability density function can then be used to determine the mean and variance of the output parameter of interest. First order second moment analysis will be used to identify uncertainty in the delineation of groundwater capture zones, and direct parameter sampling will be used to estimate the value of information on unceratainty in numerical WHPA modeling.

6.2 First Order Second Moment Analysis

The first order second moment method (FOSM) was used to estimate the uncertainty in a model performance measure by summing the independent contributions of the uncertainty from each model input parameter. Assuming that input parameters are independent, the relationship between output variance and input variance based on the FOSM is given by the following:

$$\mathrm{var}(P) = \sum_i \left[\left(\frac{\partial P}{\partial \alpha_i} \right)^2 * \mathrm{var}(\alpha_i) \right] \qquad (6.1)$$

where: P = output performance measure

$\left(\frac{\partial P}{\partial \alpha_i} \right)$ = the marginal sensitivity of output P to input α_i

$\mathrm{var}(\alpha_i)$ = the variance of model input parameter α_i

The marginal sensitivities in Equation 6.1 are expressed using a first order approximation of the Taylor Series expansion and thus the centered difference approach implemented in Chapter 3 was used in the FOSM analysis. For a performance measure of hydraulic head, and the input parameters listed in Table 6.1, the FOSM relationship is given as follows:

$$\mathrm{var}(h)=\left(\frac{\partial h}{\partial K}\right)^2 \mathrm{var}(K)+\left(\frac{\partial h}{\partial I}\right)^2 \mathrm{var}(I) + \left(\frac{\partial h}{\partial Q_{20}}\right)^2 \mathrm{var}(Q_{20})+\left(\frac{\partial h}{\partial Q_p}\right)^2 \mathrm{var}(Q_p) \qquad (6.2)$$

The mean input parameter values and standard deviations are presented in Table 6.1. The average head field resulting from the mean input parameter values, detailed in Chapter 3, is presented in Figure 6.1. The variance in the hydraulic head within the Cohansey aquifer is presented in Figure 6.2. Since there is an implicit assumption of independence in the variability of each input parameter, it is possible to calculate the separate contributions of the variance of each input parameter to the total variance in head. This is presented using the two transect lines that were defined in Figure 3.18. Figures 6.3 and 6.4 present the contributions of each input parameter to the total variance at each node in the transect lines through the UWTR wellfields.

A number of points are evident from these variance maps. The variance of infiltration makes up over 98.5% of the total variance of the hydraulic head performance measure. For well 20 the next most important source of variance is the well 20 pumping rate and for the Parkway wellfield the next most important source of variance is the average Parkway wellfield pumping rate. The variance of hydraulic conductivity is the smallest source of total variance in the hydraulic head field.

Parameter	Symbol	Mean Value	Standard Deviation	Correlation Length
Conductivity	K	150 ft/day	10 ft/day	1600 ft
Infiltration	I	0.00434 ft/day	0.00025 ft/day	----
Well w-20	Q_{20}	64,400 ft^3/day	7,500 ft^3/day	----
Well w-22	Q_p	75,500 ft^3/day	7,500 ft^3/day	----
Well w-24		66,200 ft^3/day	7,500 ft^3/day	----
Well w-26		62,400 ft^3/day	6,200 ft^3/day	----
Well w-28		62,500 ft^3/day	6,300 ft^3/day	----
Well w-29		63,800 ft^3/day	6,400 ft^3/day	----

Table 6.1: Statistical Moments for Uncertain Parameter Values at the Study Site

For capture zone modeling the output parameter of concern is the size of the capture zone and this may be represented by the area of the capture zone. The FOSM relationship for capture zone

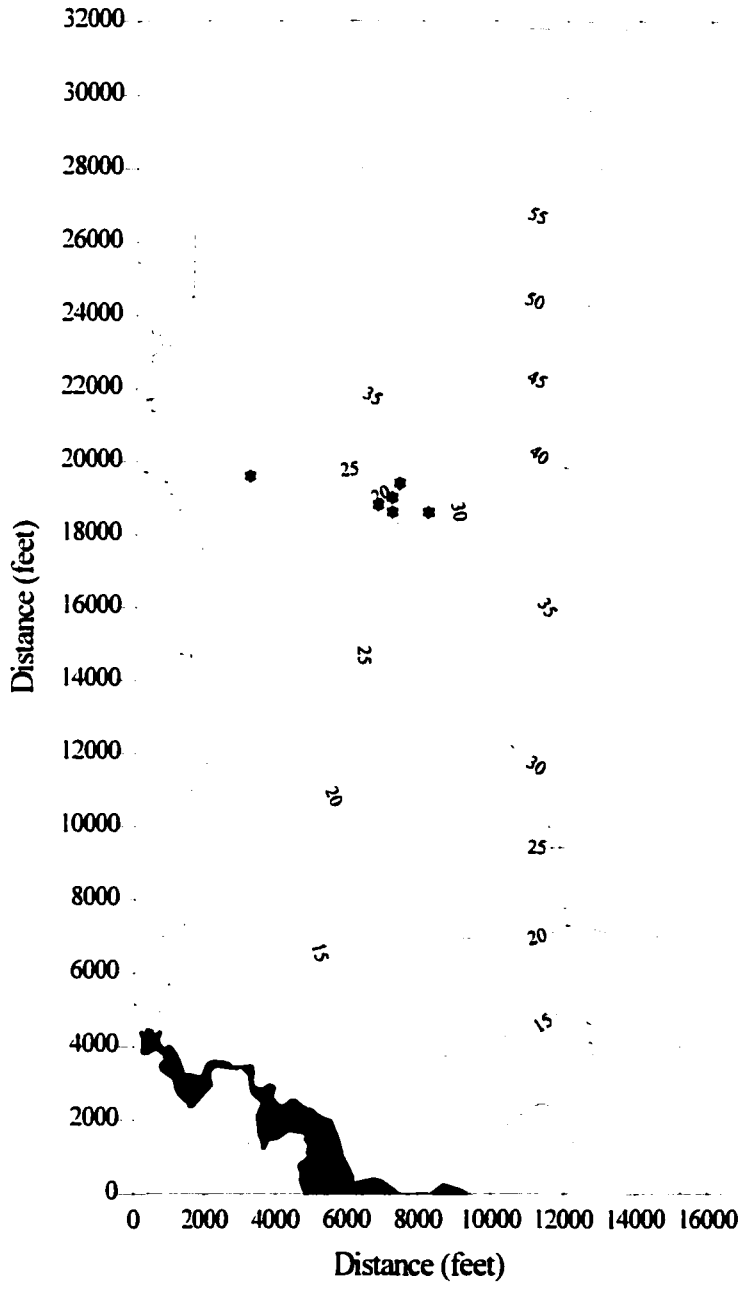


Figure 6.1: The Steady State Hydraulic Head Field in the Cohansey Aquifer

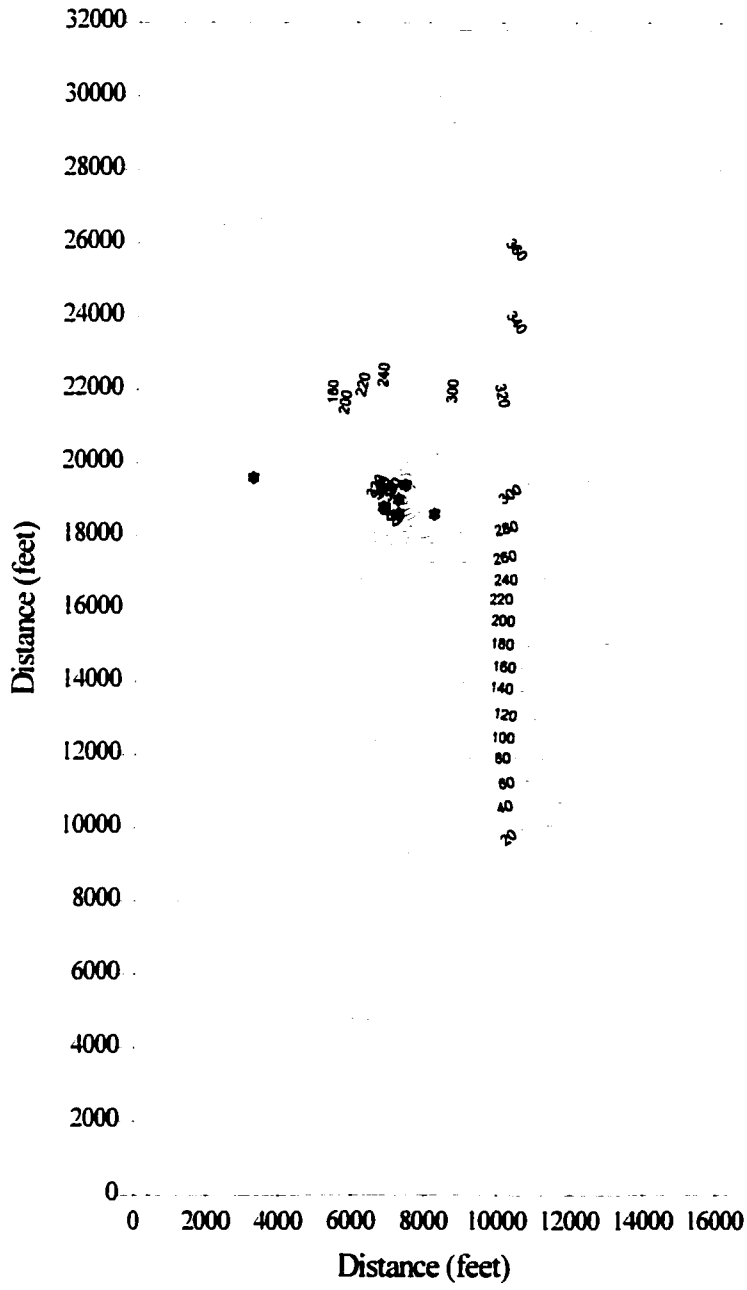


Figure 6.2: The Variance in Head Which Results from the FOSM Method

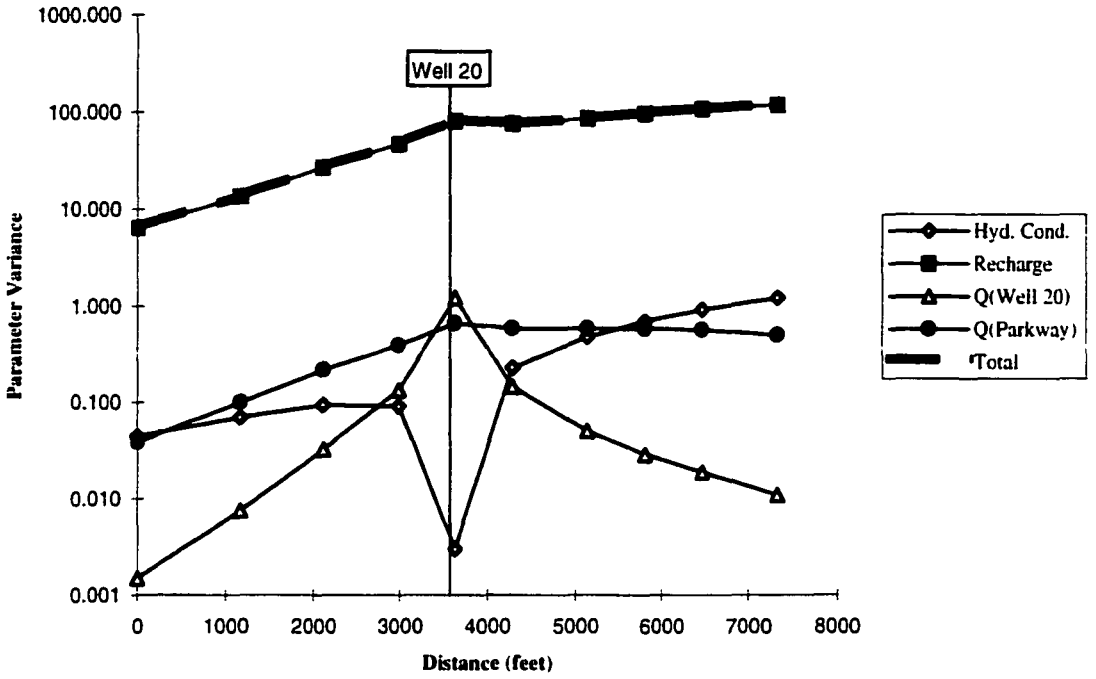


Figure 6.3: The Contribution of Parameter Variance to Total Variance for Transect 1

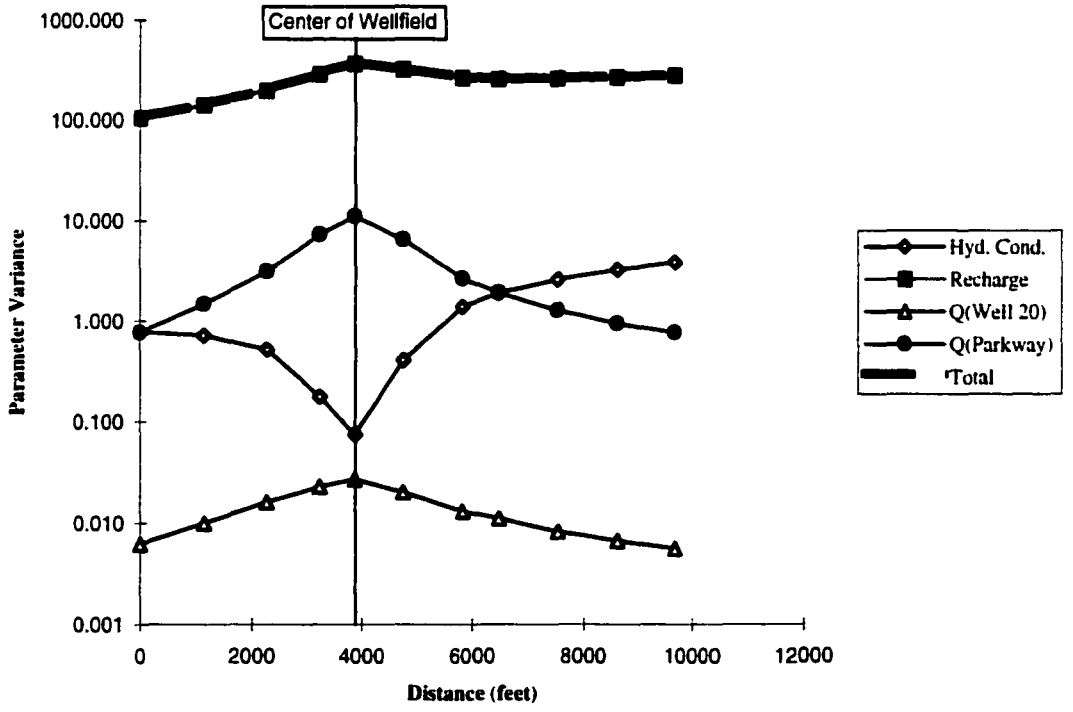


Figure 6.4: The Contribution of Parameter Variance to Total Variance for Transect 2

area (A) is given by the following:

$$\mathrm{var}(A)=\left(\frac{\partial A}{\partial K}\right)^2 \mathrm{var}(K)+\left(\frac{\partial A}{\partial I}\right)^2 \mathrm{var}(I)$$
$$+\left(\frac{\partial A}{\partial Q_{20}}\right)^2 \mathrm{var}(Q_{20})+\left(\frac{\partial A}{\partial Q_p}\right)^2 \mathrm{var}(Q_p) \qquad (6.3)$$

Table 6.2 presents contribution of each input parameter to the total variance of the capture zone areas for the 5 year capture zones around the UWTR wellfields. As was seen in the uncertainty maps for hydraulic head, the greatest source of uncertianty in capture zone modeling comes from the uncertainty in net infiltration to the groundwater system which provides approximately 85% of the total uncertainty. The next most important parameter is well pumping rate.

Wellfield	α_i	$(dA/d\alpha)^2$	$\mathrm{var}(\alpha_i)$	var(A)	% Total
Parkway	K	1.93033 E+09	1.0000 E+02	1.93033 E+11	0.220
	I	1.18489 E+19	6.2500 E-06	7.40558 E+13	84.078
	Q_{20}	3.47413 E+01	5.6250 E+07	1.95420 E+09	0.002
	Q_p	3.00850 E+05	4.5968 E+07	1.38296 E+13	15.700
	Total			8.80804 E+13	100.000
Well 20	K	3.25318 E+07	1.0000 E+02	3.25318 E+09	0.040
	I	1.06213 E+19	6.2500 E-06	6.63828 E+12	87.400
	Q_{20}	1.64806 E+04	5.6250 E+07	9.27040 E+11	12.210
	Q_p	5.79608 E+02	4.5968 E+07	2.65175 E+10	0.350
	Total			7.59509 E+12	100.000

Table 6.2: Contributions of Input Uncertainty to Total Capture Zone Area Variance

6.3 Stochastic Analysis

Direct parameter sampling, as a form of uncertainty analysis, is a method of determining the economic value associated with model uncertainty. For the base case analysis the purpose was to determine the location of the WHPA boundary based on average model input values. Adding model input uncertainty and multiple simulation allows the determination of a probability density function of WHPA boundary location. Each of these WHPA boudary realizations encompasses a different area. To determine the value of information the 50th percentile boundary was used as the standard for determining failure. The reason for choosing this standard is that the 50th percentile boundary is a measure of the average model results from repetitive uncertainty analysis of numerical WHPA modeling. Each simulation is compared to the standard to determine its failure in determining the

best alterantive, where failure is defined as the inability to choose the correct input parameters to determine the average result.

Direct parameter sampling, to estimate the uncertainty in a model performance measure, was implemented using the following steps: input parameter sampling, distribution of the input values within the conceptual model of the site, and repetitive sequential simulation using the groundwater flow and particle tracking numerical models. In order to use direct parameter sampling it was necessary to choose parameter distributions for each of the input variables to the groundwater model and to estimate the moments for each distribution. The lognormal parameter distribution was chosen for rainfall infiltration rate and the wellhead pumping rate for the 6 production wells. The moments for each parameter distribution were presented in Table 6.1. Multiple numerical simulation were performed using random sampling of each of the lognormal parameter distributions. In addition, for hydraulic conductivity, a random field generator was used to produce a single realization of the distribution of hydraulic conductivity for each model simulation run. Figure 6.5 presents the random hydraulic conductivity field generated during one simulation of groundwater flow analysis.

Repetitive model simulation was used to produce an output distribution of the location of the WHPA boundary according to the following sequence. The LATIN model was used to choose the random values of each input parameter. SWIFT was used to generate a hydraulic head field. STLINE and RWAPT were used to generate advective and random walk particle pathlines. CAPZON was used to generate a convex hull of the particle pathlines to produce a single realization of the numerical WHPA boundary. A statistical analysis program was used to analyze the ensemble of WHPA boundaries.

The statistical analysis program, CZSTAT, was written to analyse multiple capture zone boundaries produced by numerical WHPA simulation. The FORTRAN code for this program is presented in Appendix V. CZSTAT generates a statistical record of the ensemble of multiple capture zones generated by CAPZON in the following manner. The model reads n capture zones from a cumulative input file. It determines the center of mass of all capture zone points and generates 180 radial transect lines emanating from this center of mass. For each transect line, the intersection point with all n capture zones are determined, and sorted by distance from the center of mass. The model then determines four statistical capture zones including the zone of certainty (ZOC), the zone of uncertainty (ZOU), the average, or the 50^{th} percentile capture zone and the 95^{th} percentile capture zone.

The CZSTAT model also determines the value of information associated with the uncertainty in the numerical model of WHPA delineation. This is accomplished by comparing each of the n

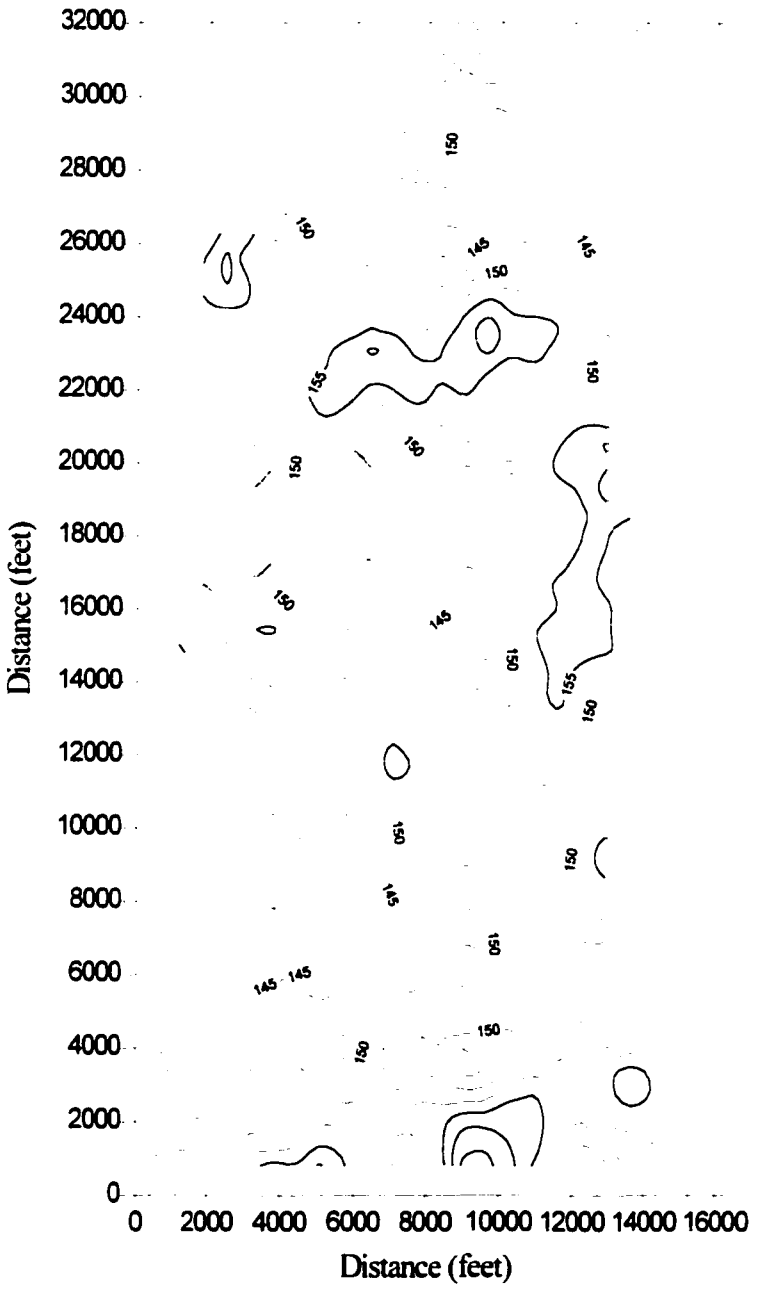


Figure 6.5: A Single Realization of a Random Hydraulic Conductivity Field

realizations of the boundary location to the 50th percentile capture zone location and determining the area between the two boundaries. This area is considered the failure area for each model realization, and this area has an associated cost of failure. The probability of failure is the inverse ($^1/_n$) of the total number of model simulations. The value of information for numerical WHPA delineation was determined according to the following relationship:

$$VOI = \frac{1}{n}\left[\sum_{1}^{n}(A_n - A_{50})\right] * C_f \qquad (6.4)$$

where: n = the number of model simulations

$\frac{1}{n}$ = probability of failure for each simulation

A_n = the area contained within the n^{th} boundary realization

A_{50} = area of the 50^{th} percentile WHPA boundary

C_f = cost of failure for the simulation

Value of information represents an estimate of the maximum field sampling budget that may be spent acquiring new data to provide a better representation of the input probability density functions in order to reduce model uncertainty. The cost of failure is based on the assumption that the numerical model delineates slightly more or less area at the edge of the time related capture zone boundary. For Zone II the failure cost is based on the difference between Zone II and Zone III monitoring, and for Zone III delineation the failure cost is based on the cost of monitoring in Zone III. These costs are calculated according to the same techniques developed in Chapter 4.

To implement Latin Hypercube sampling of the input parameter distributions it was necessary to determine the optimal number of samples to be taken. This was done so that the uncertainty analysis would adequately describe the distribution of output capture zones. An analysis was performed which varied the number of simuations and checked the mean and variance of the numerical WHPA boundary location based on a normal distribution of the output parameter. Figure 6.6 presents the change in the probability density of the distance of the Zone III STLINE WHPA boundary from the center of the Parkway wellfield as a function of the number of model simulations. The difference between the mean of the capture zone area for 200 and 300 simulations is 0.26%. The difference between the variance of the capture zone area is 6.59%. As a result, the following uncertainty analysis was performed using 300 Latin Hypercube samples for SWIFT simulation. For RWAPT simulation, due to constraints on computational time, the uncertainty analysis was performed using 100 model simulations.

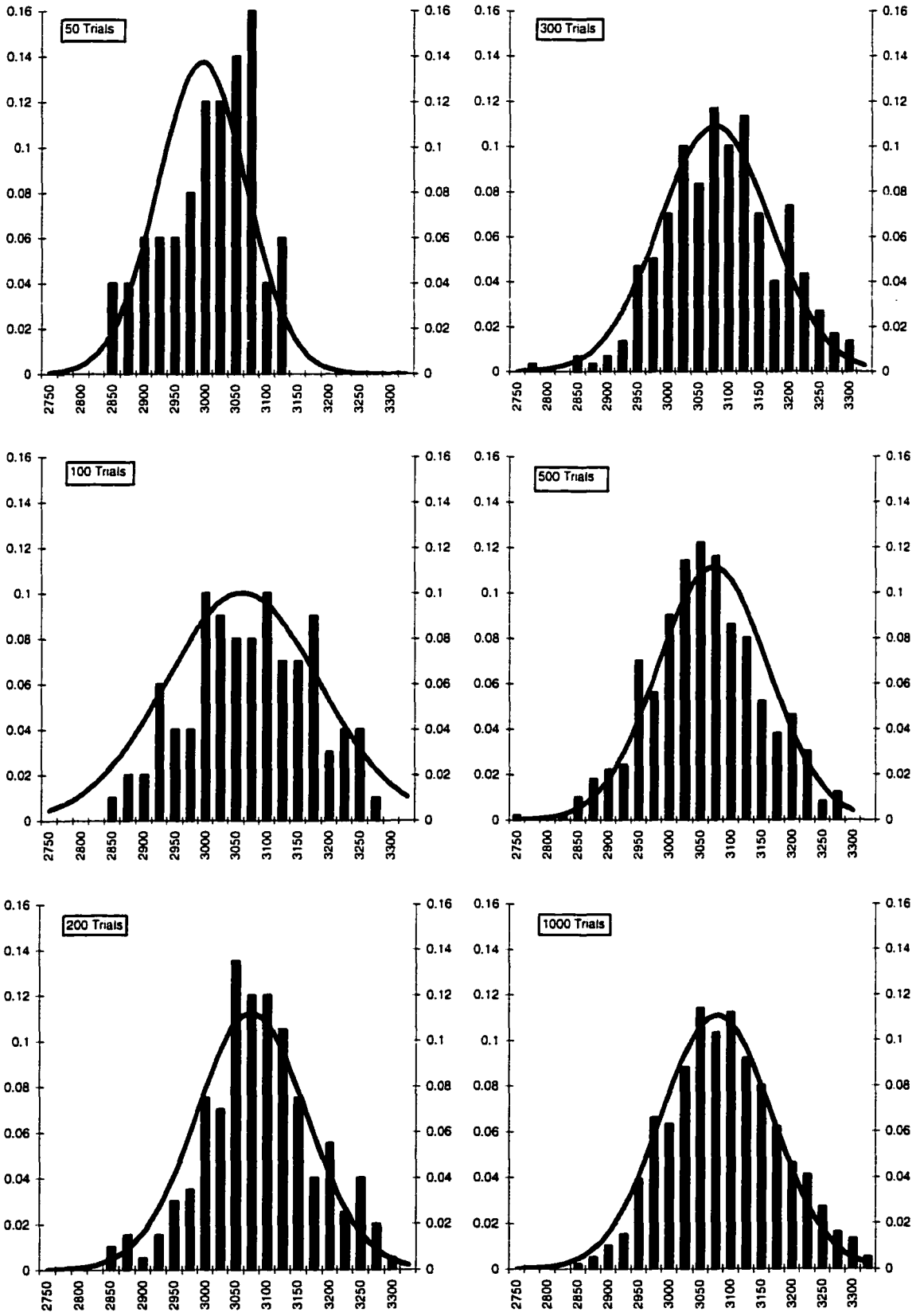


Figure 6.6: Normalized Probability Density of Zone III STLINE Boundary Location

6.3.1 Analysis of STLINE Modeling

The analysis of numerical WHPA modeling using SWIFT and STLINE is presented as follows. Figures 6.7 and 6.8 present the ensemble of 300 capture zone boundaries for the Zone II and Zone III WHPA boundaries, respectively. These figures show that the ensemble of capture zones demonstrates a wide variation in the position of the capture zone boundary. Figures 6.9 and 6.10 present the ZOC and the ZOU for each of these protection zones. Figures 6.11 and 6.12 compare the 50th percentile WHPA boundary from uncertainty analysis with the deterministic STLINE boundary from Chapter 4. Figure 6.13 compares the 50th percentile WHPA boundary with the 95th percentile boundary. A comparison of the statistical parameters of the Zone II and Zone III boundaries is presented in Table 6.3.

Protection Zone	Wellfield	ZOC Area [sq.ft.]	50th Boundary [sq.ft.]	ZOU [sq.ft.]	Risk Cost [$]
II	Well 20	2 937 900	6 069 500	10 581 700	12,138
	Parkway	25 643 300	31 454 600	38 307 300	35,274
				Total =	47,412
III	Well 20	3 944 600	9 900 000	18 176 400	2,753
	Parkway	39 217 500	48 881 400	60 484 400	5,506
				Total =	8,259

Table 6.3: A Summary of the Statistical Parameters from STLINE Uncertainty

Figure 6.6, which presents the distribution of WHPA boundary location, shows that 300 random parameter samples adequately represents a normal probability density function. It also shows that, as the number of parameter samples increases, the fit between the output distribution and the normal probability curve increases. However, in order to optimize two components of the modeling, increased simulations and reduced total simulation time, the results for 300 simulations of STLINE advective particle tracking and 100 simulations of the RWAPT advective dispersive particle tracking appear to be adequate.

Figures 6.11 and 6.12 show that the uncertainty analysis returns a mean WHPA boundary (50th percentile capture zone from 300 model simulations) that is almost identical to the WHPA boundary obtained from deterministic modeling. However, the shape of the 50th percentile boundary is smoother in appearance. This is a result of the fact that each of the 180 points that were used to delineate the 50th percentile capture zone result from an average of 300 boundary points. The deterministic WHPA boundary was produced by a simulation of only one set of input particle pathlines and, as a result, is rough in appearance because of gaps between the pathline data points.

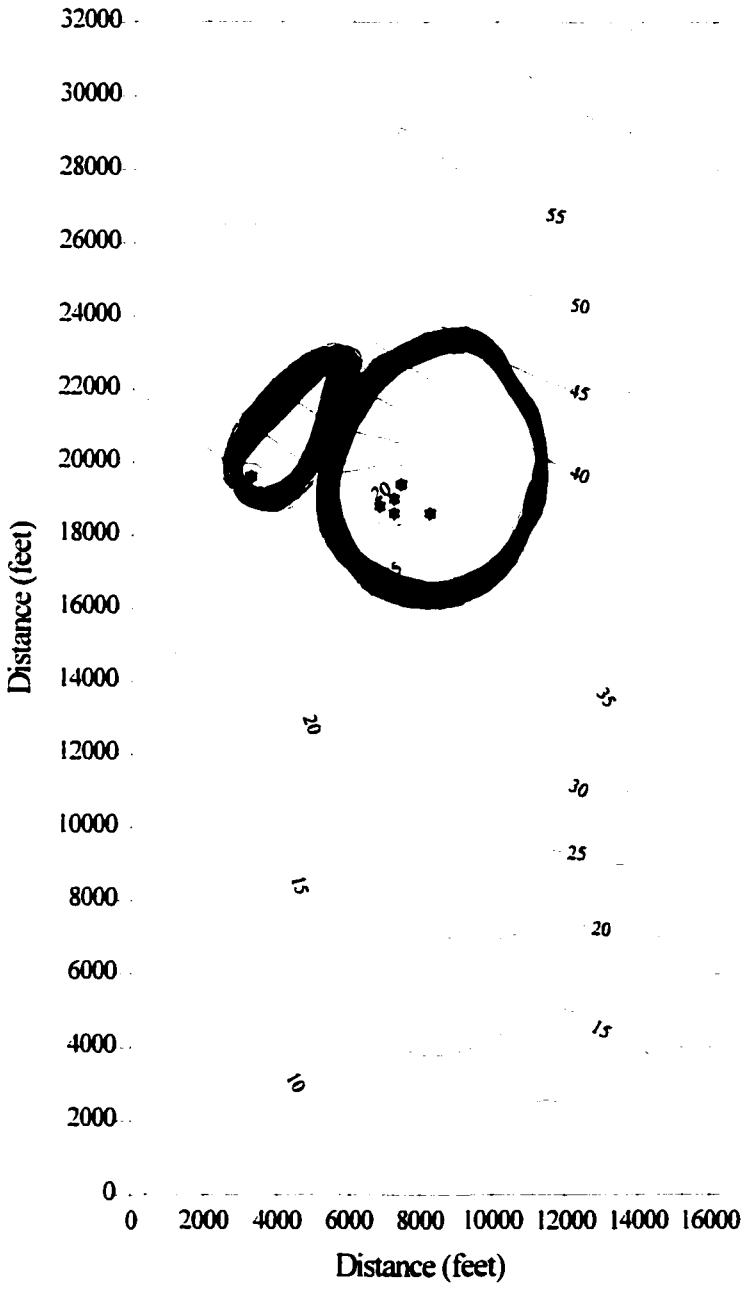


Figure 6.7: Three Hundred Latin Hypercube Simulations of the Zone II STLINE Boundary

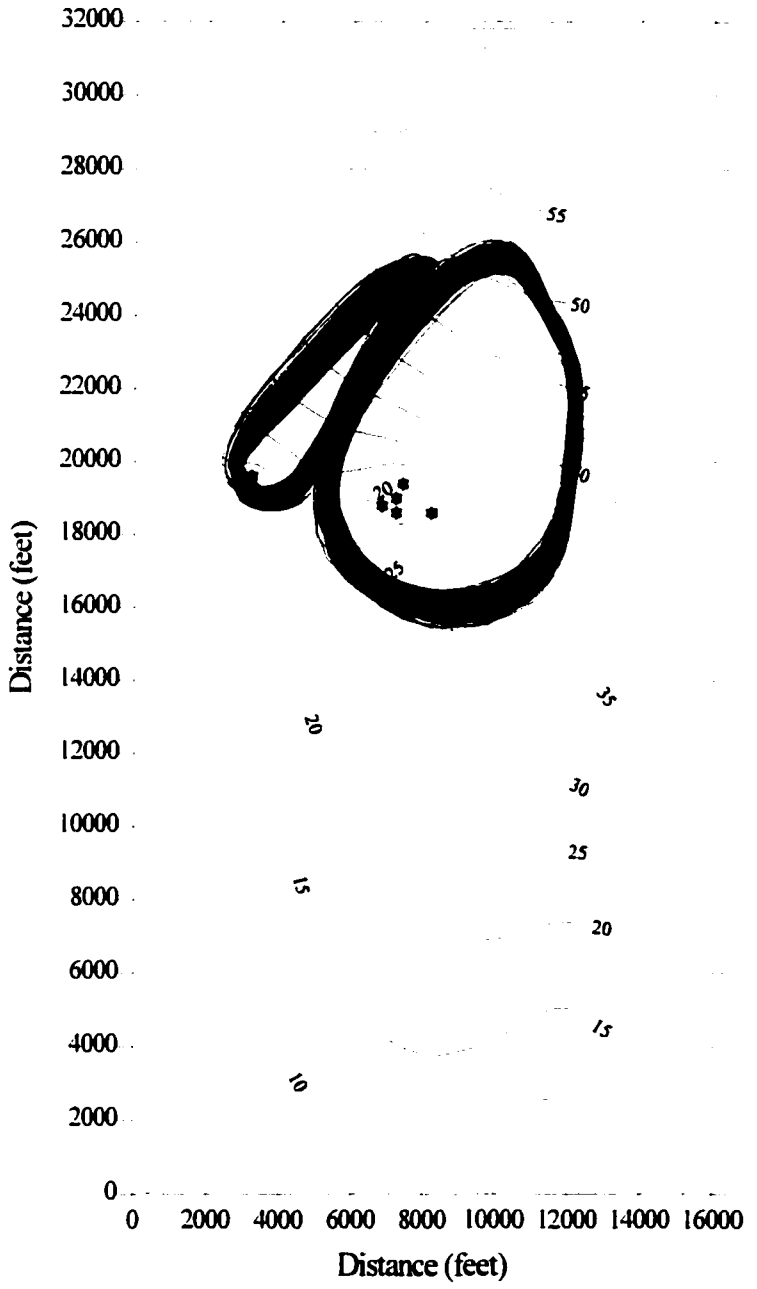


Figure 6.8: Three Hundred Latin Hypercube Simulations of the Zone III STLINE Boundary

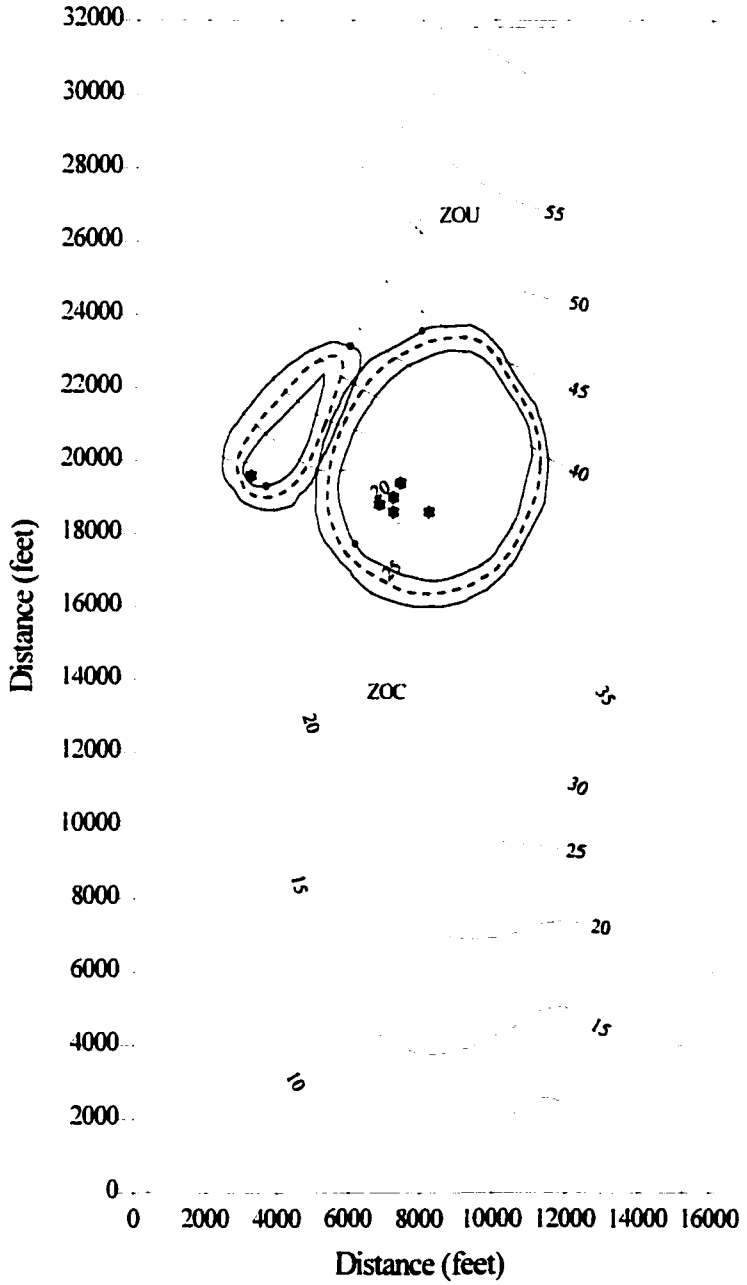


Figure 6.9: The ZOC, ZOU and 50th Percentile Boundaries for 300 Zone II STLINE Simulations

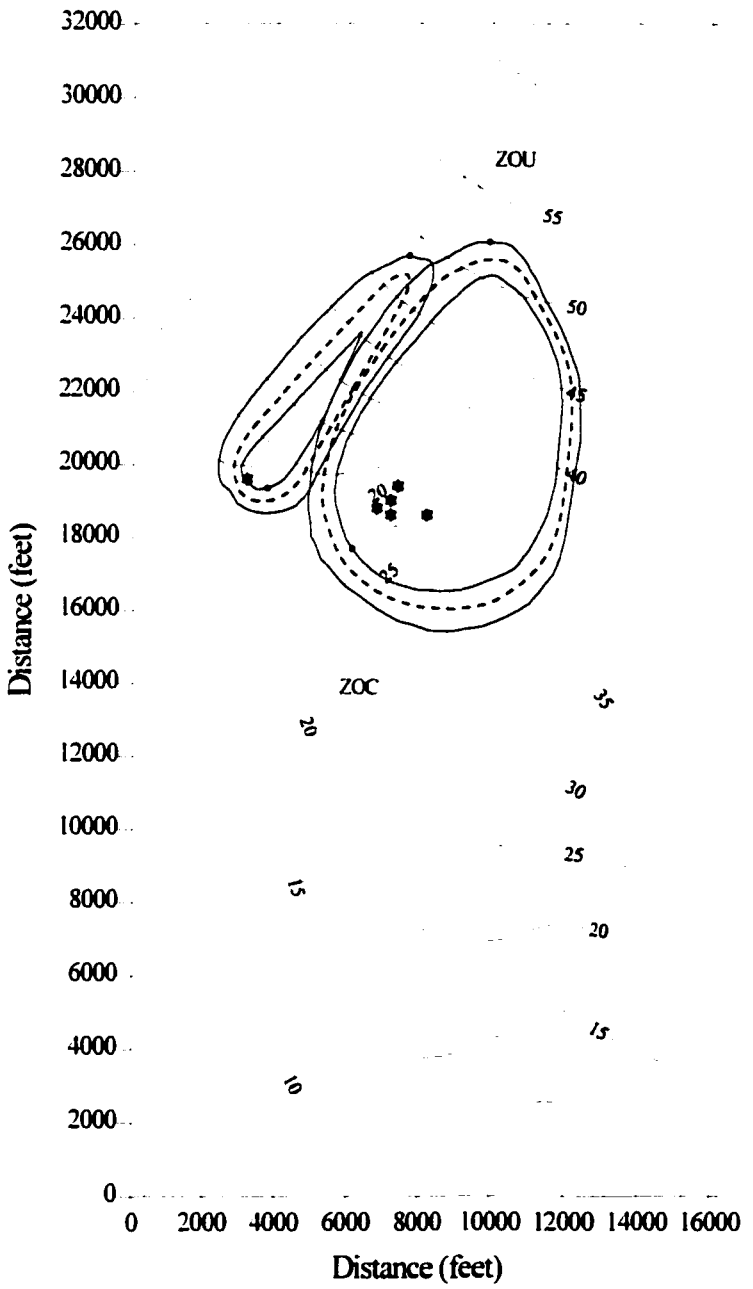


Figure 6.10: The ZOC, ZOU and 50th Percentile Boundaries for 300 Zone III STLINE Simulations

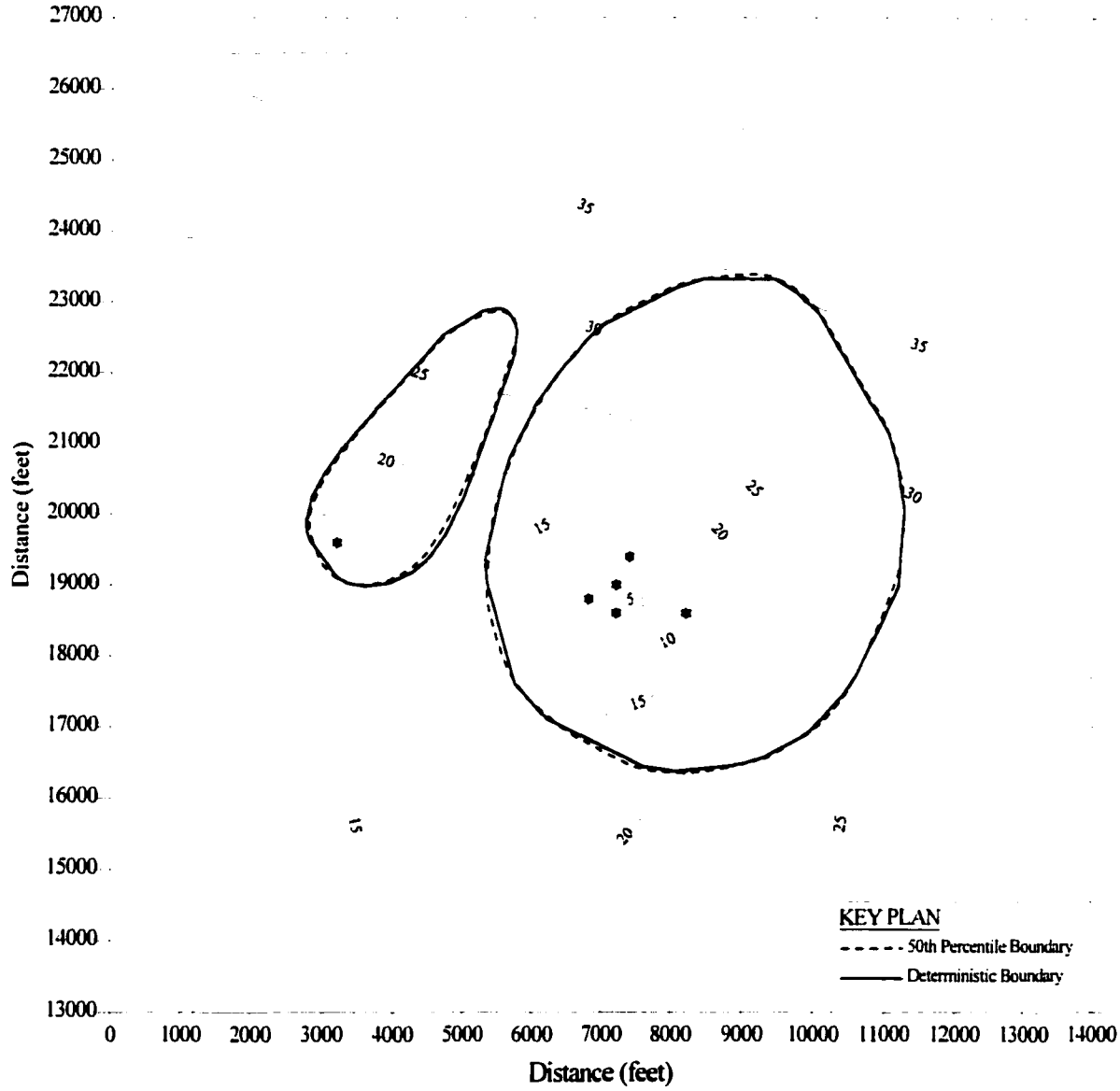


Figure 6.11: A Comparison of the Deterministic and 50th Percentile Zone II STLINE Boundaries

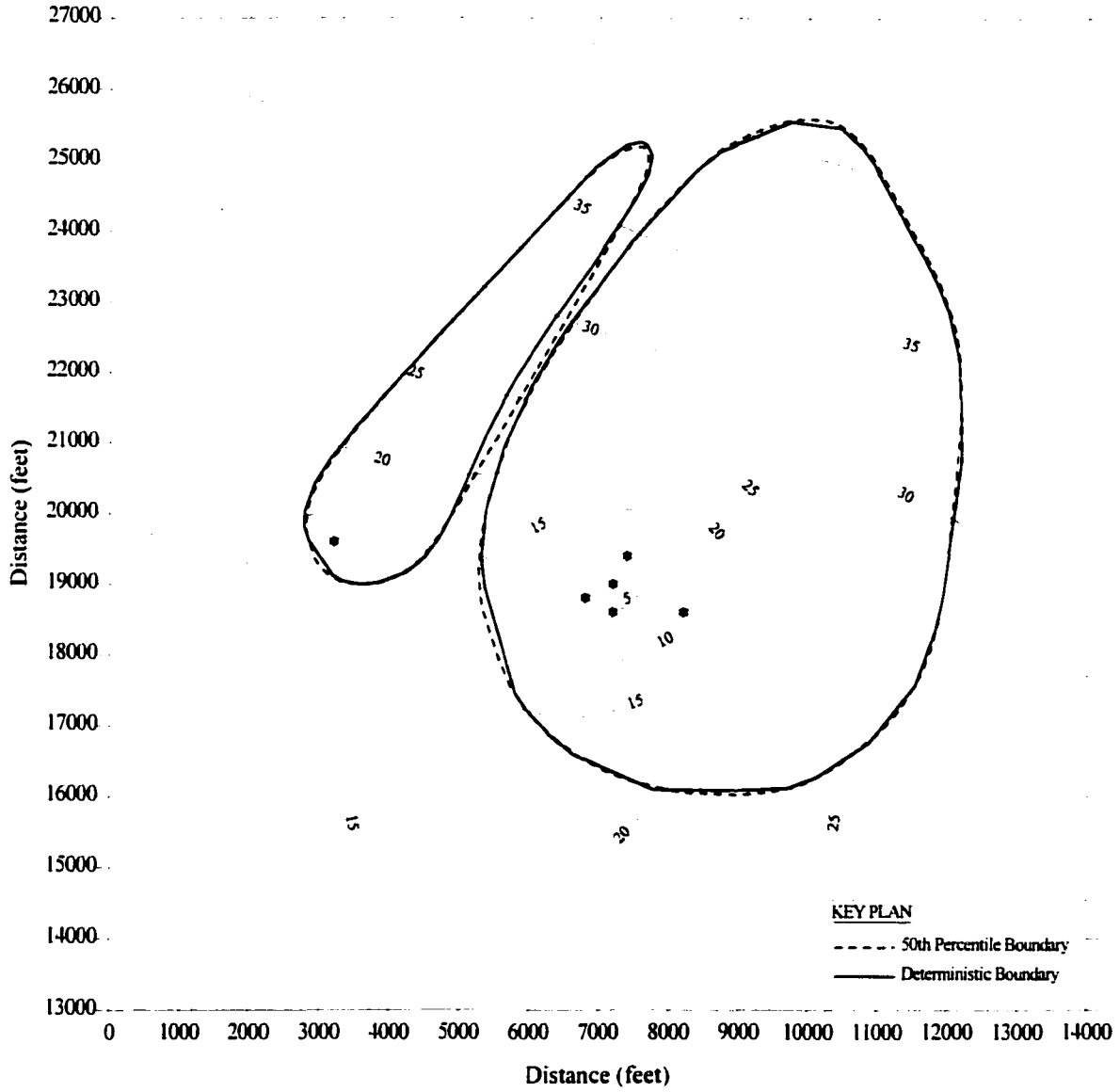


Figure 6.12: A Comparison of the Deterministic and 50th Percentile Zone III STLINE Boundaries

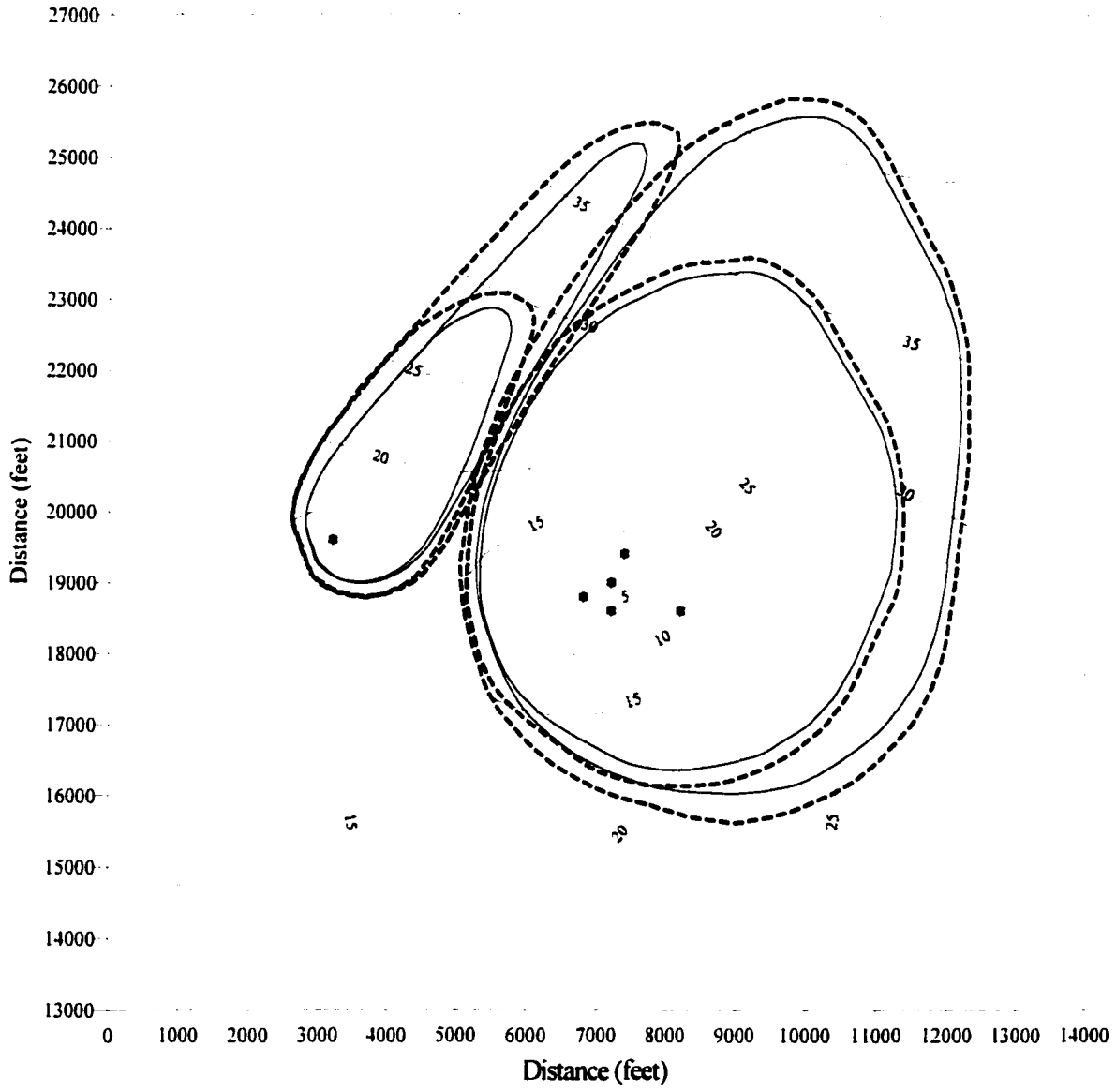


Figure 6.13: A Comparison of the 50th and 95th Percentile STLINE Boundaries

For these reasons the 50th percentile capture zone provides a better representation of the average numerical modeling WHPA boundary.

Figure 6.13 shows the difference between the 50th and 95th percentile WHPA boundary. A number of authors have proposed that the 95th percentile numerical boundary be used for WHPA zoning. When the variance of the input parameter distributions is reduced, by increased field sampling, the difference between these two boundaries will reduce as the 95th percentile boundary approaches the mean of the distribution. For these reasons the 95th percentile boundary provides a better choice for the WHPA boundary for the purpose of zoning than the average numerical time of travel boundary.

The risk cost associated with WHPA simulation around each wellhead represents the value of model uncertainty. For the 5 year numerical WHPA boundary this cost is $47,412 and for the 10 year boundary this cost is $8,259. These costs sum to a total value of information of $55,670. This value represents an estimate of the maximum amount of money that may be spent acquiring new data to better represent the input probability density functions in order to reduce model uncertainty. For STLINE modeling there were 8 model parameters that were sampled during the Latin Hypercube simulation. Of these parameters, the best application of the budget equivalent to the value of information would be for the parameter which has the greatest impact on reducing model uncertainty. This parameter was identified in the FOSM analysis as the uniformly distributed net infiltration. Therefore, to best reduce uncertainty field sampling should be directed toward the understanding of the temporal and spatial distribution of net infiltration.

Reducing the uncertainty in net infiltration involves acquiring updated values for weather data at the study site. This information is available from the National Climatic Data Center in a number of formats that include average monthly values. This information may then be input to an infiltration model to determine the components of the water balance at the study site. The HELP model is one infiltration model that has been calibrated and validated at many sites across North America. Other more site specific methods of obtaining this information might involve setting up a weather station at the wellfields to determine the necessary infiltration parameters.

6.3.2 Analysis of RWAPT Modeling

Figures 6.14 and 6.15 present the ensemble of 100 capture zone boundaries for the Zone II and Zone III RWAPT boundaries, respectively. These figures show that the ensemble of capture zones provides for a wide variation in the position of the capture zone boundary. Figures 6.16 and 6.17 show the distribution of the location of the Zone II and Zone III RWAPT boundaries, respectively. Figures 6.18 and 6.19 present the ZOC, the ZOU and the 50th percentile capture zone

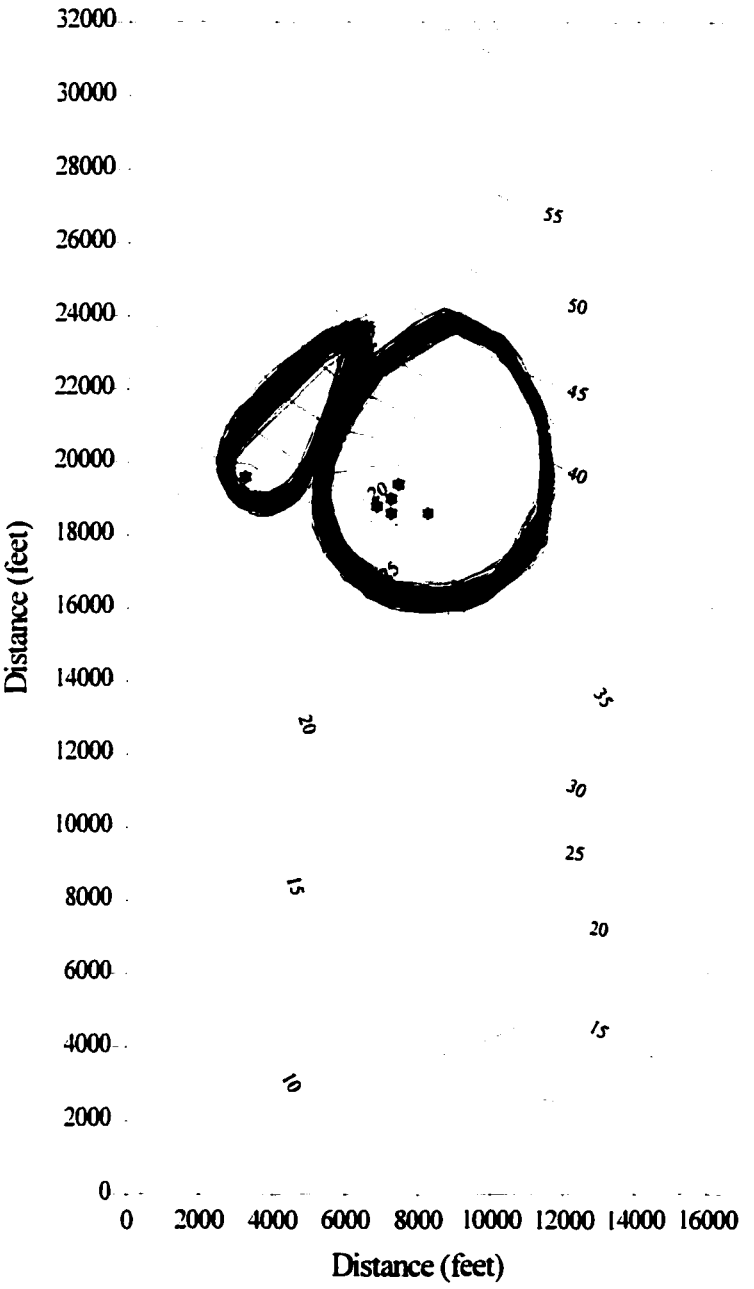


Figure 6.14: One Hundred Latin Hypercube Simulations of the Zone II RWAPT Boundary

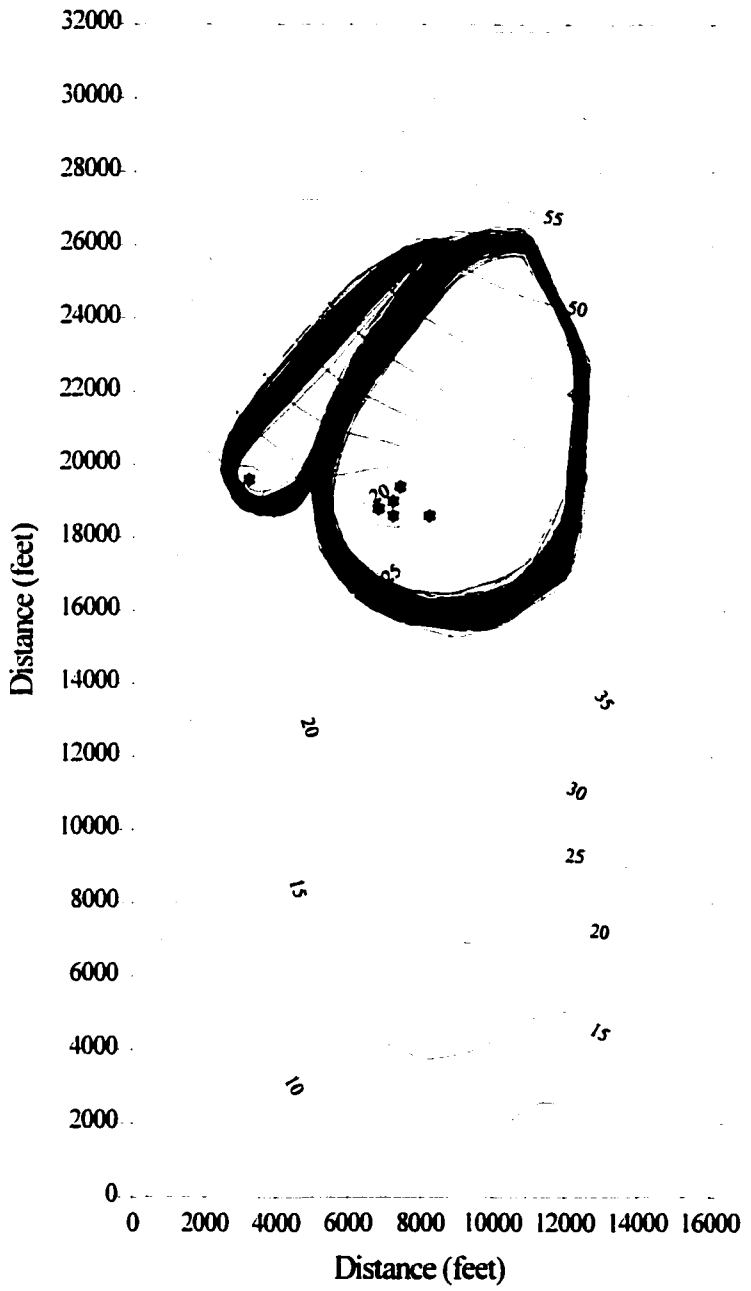


Figure 6.15: One Hundred Latin Hypercube Simulations of the Zone III RWAPT Boundary

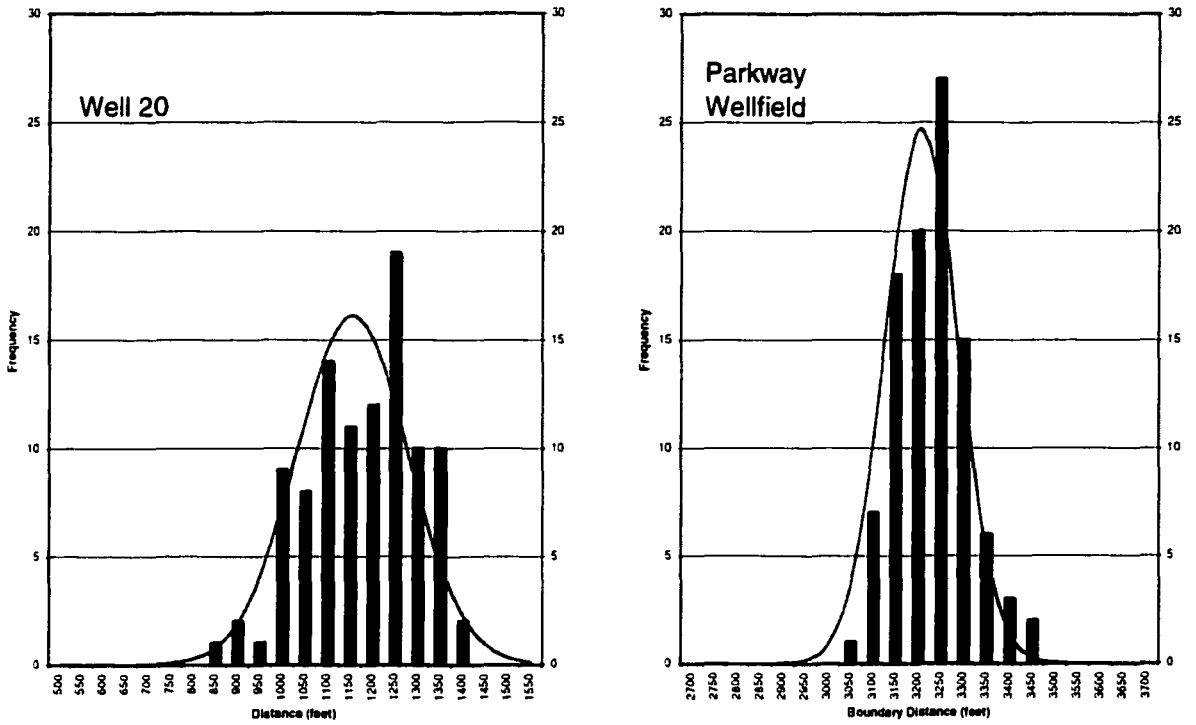


Figure 6.16: Probability Density of the Zone II RWAPT WHPA Boundaries

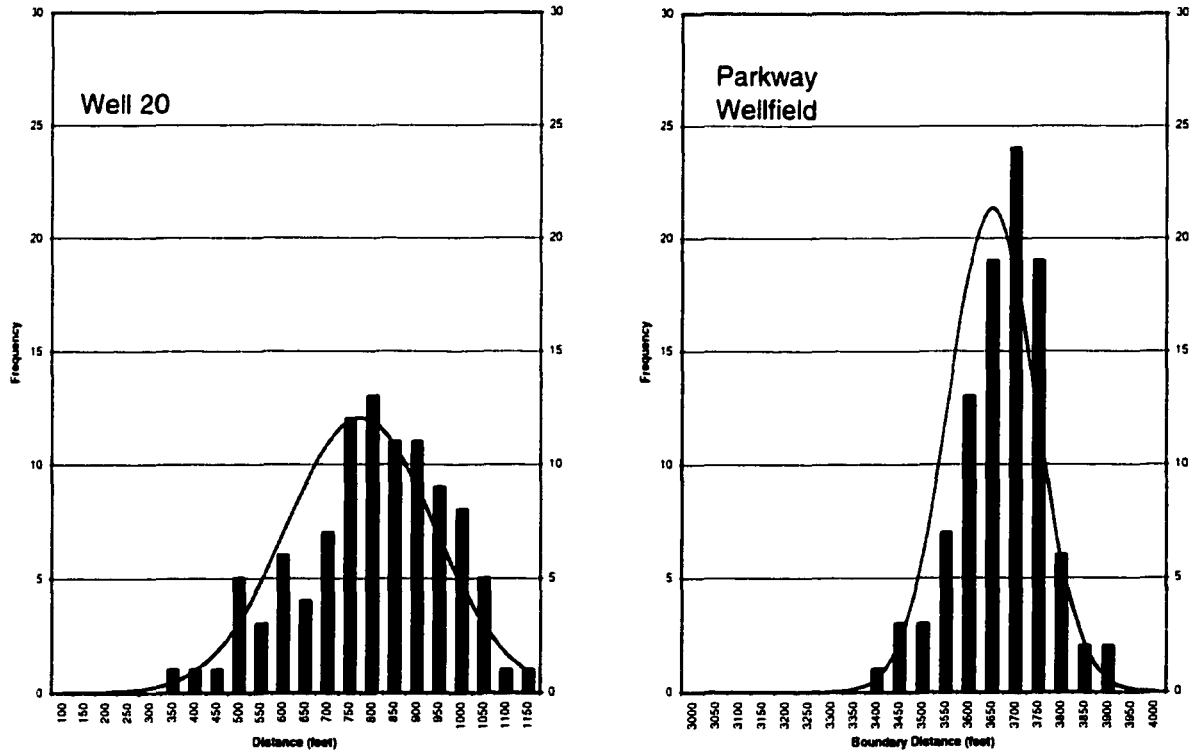


Figure 6.17: Probability Density of the Zone III RWAPT WHPA Boundaries

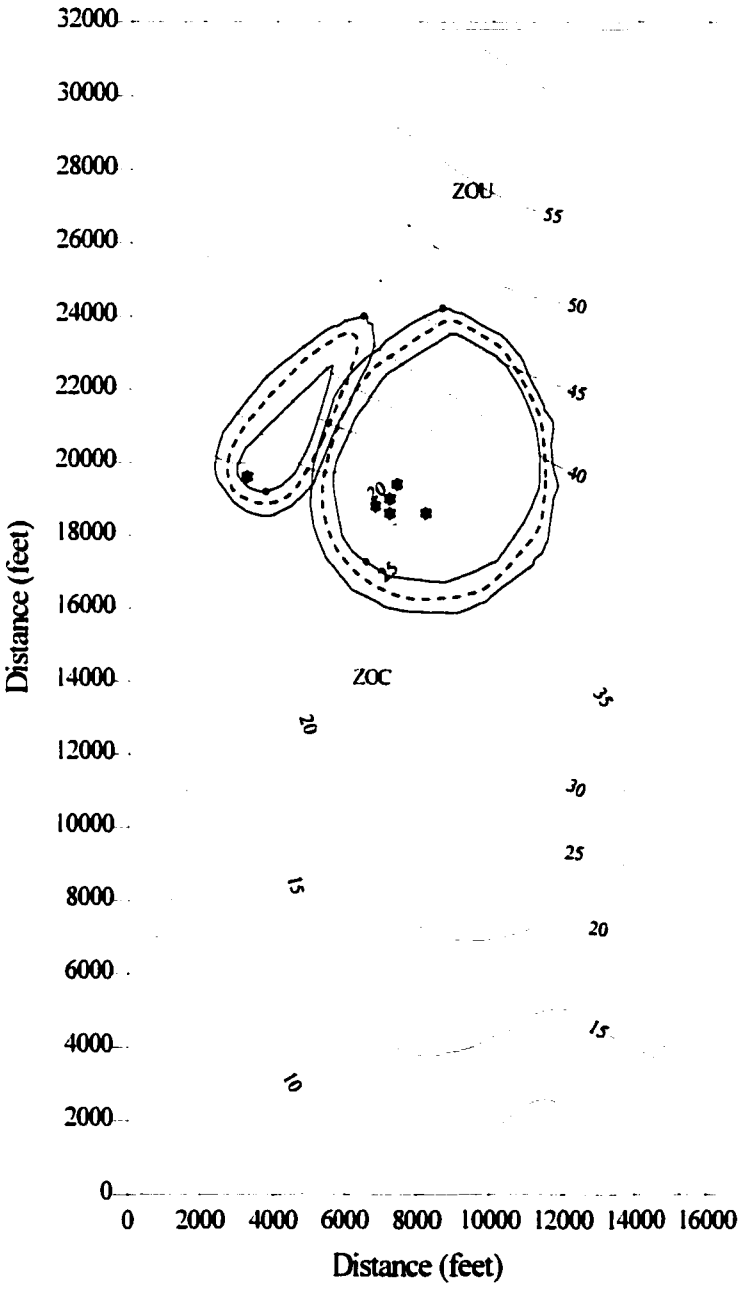


Figure 6.18: The ZOC, ZOU and 50th Percentile Boundaries for 100 Zone II RWAPT Simulations

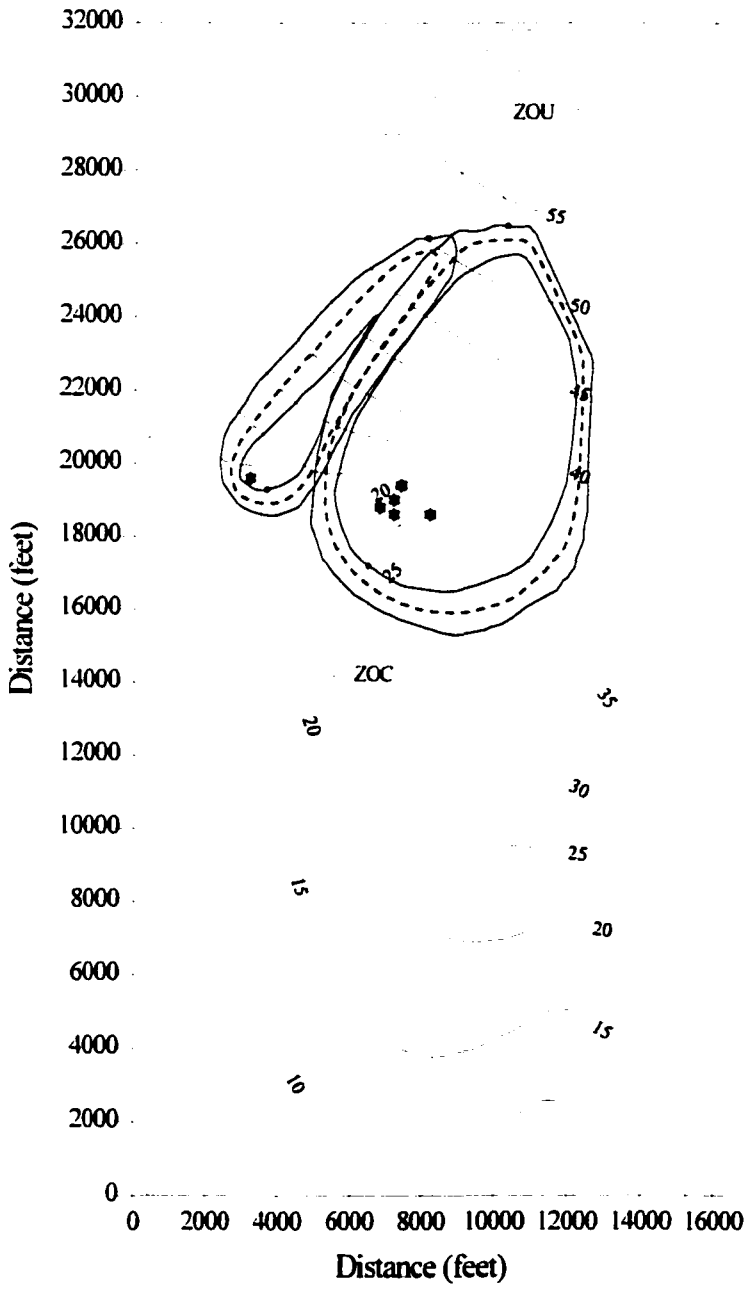


Figure 6.19: The ZOC, ZOU and 50th Percentile Boundaries for 100 Zone III RWAPT Simulations

for each of these protection zones. Figures 6.20 and 6.21 compare the 50th percentile capture zone with the deterministic RWAPT capture zone, based on average values of each input parameter, which was produced during the environmental decision making in Chapter 4. A comparison of the statistical parameters of the Zone II and Zone III WHPA boundaries is presented in Table 6.4.

Protection Zone	Wellfield	ZOC Area [sq.ft.]	50th Boundary [sq.ft.]	ZOU [sq.ft.]	Risk Cost [$]
II	Well 20	3 824 100	8 568 400	13 021 600	21,622
	Parkway	28 808 600	35 150 800	43 325 300	47,419
				Total =	69,041
III	Well 20	4 535 800	12 799 800	20 785 000	23,715
	Parkway	43 981 400	54 163 100	66 423 300	62,672
				Total =	86,387

Table 6.4: A Summary of the Statistical Parameters from RWAPT Uncertainty

Figures 6.16 and 6.17 show that the simulation, based on 100 random parameter samples, provides a good representation of a normal distribution. Therefore, the use of 100 model simulations for random walk particle tracking is adequate for the purposes of this uncertainty analysis. Figures 6.20 and 6.21 show that the uncertainty analysis returns a mean WHPA boundary (50th percentile capture zone from 100 model simulations) that is almost identical to the boundary obtained from deterministic modeling. However, there are places around the WHPA boundary where the 50th percentile line is outside of the deterministic boundary. This is a result of the fact that the smoothing which occurs with numerical averaging of multiple simulations provides more information about the location of the true average boundary locations. Thus, the 50th percentile boundary is a better representation of average RWAPT simulation. Figure 6.22 shows the difference between the 50th and 95th percentile boundary. For the same reasons presented in the STLINE modeling, the 95th percentile boundary provides a better choice for the WHPA boundary for zoning purposes than the average numerical time of travel boundary.

The risk cost associated with RWAPT WHPA simulation around each wellhead represents the value of model uncertainty. For the 5 year numerical RWAPT boundary this cost is $69,041 and for the 10 year boundary this cost is $86,387. These values sum to a total value of information of $155,428. This value represents an estimate of the maximum sampling budget for reducing parameter uncertainty in the RWAPT modeling. The risk cost for RWAPT simulation is greater than this value for STLINE modeling. This is a result of the fact that the hydrodynamic dispersion, which is modeled using random particle movement, provides for a greater spread in the location of the WHPA

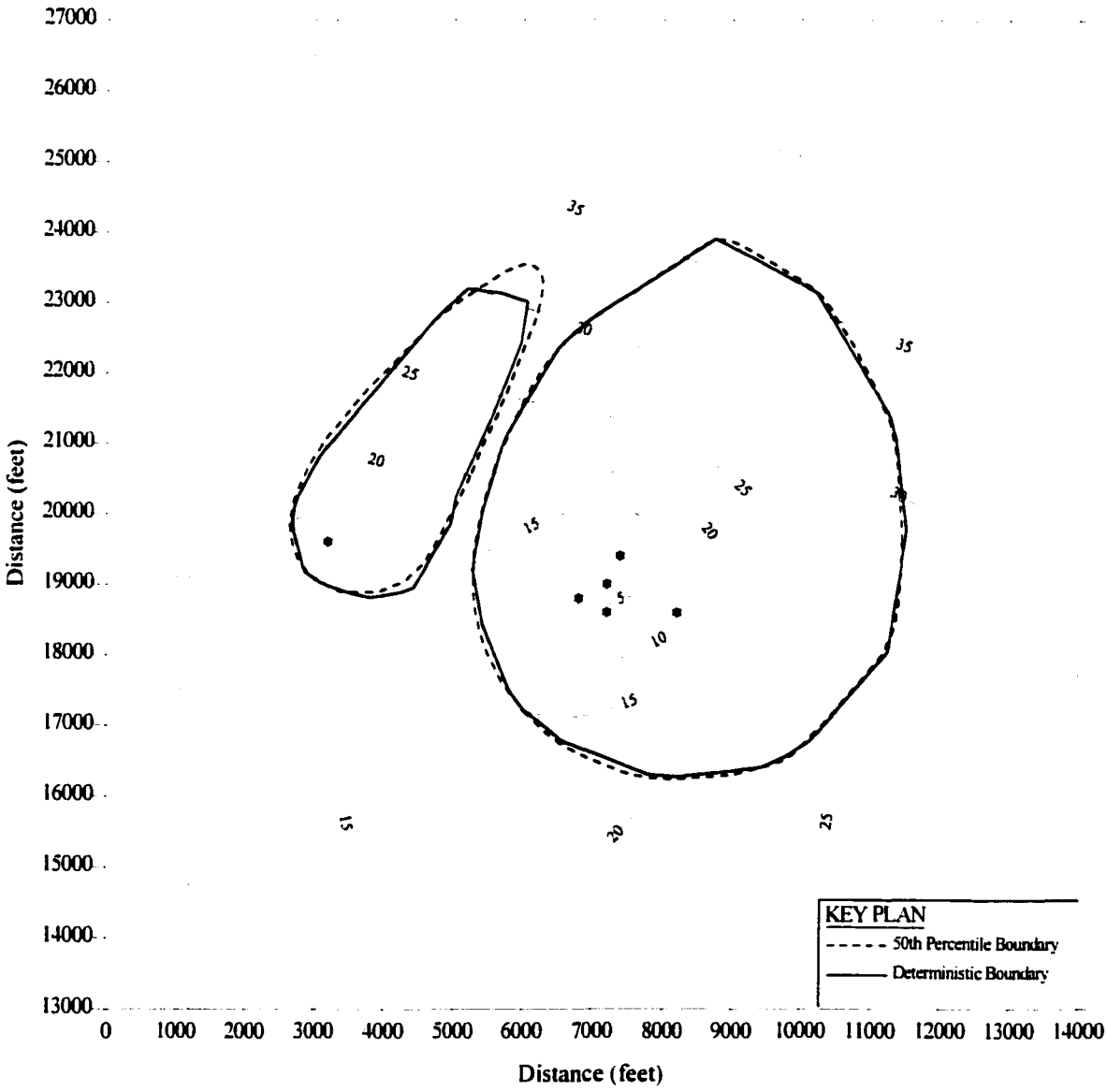


Figure 6.20: A Comparison of the Deterministic and 50th Percentile Zone II RWAPT Boundaries

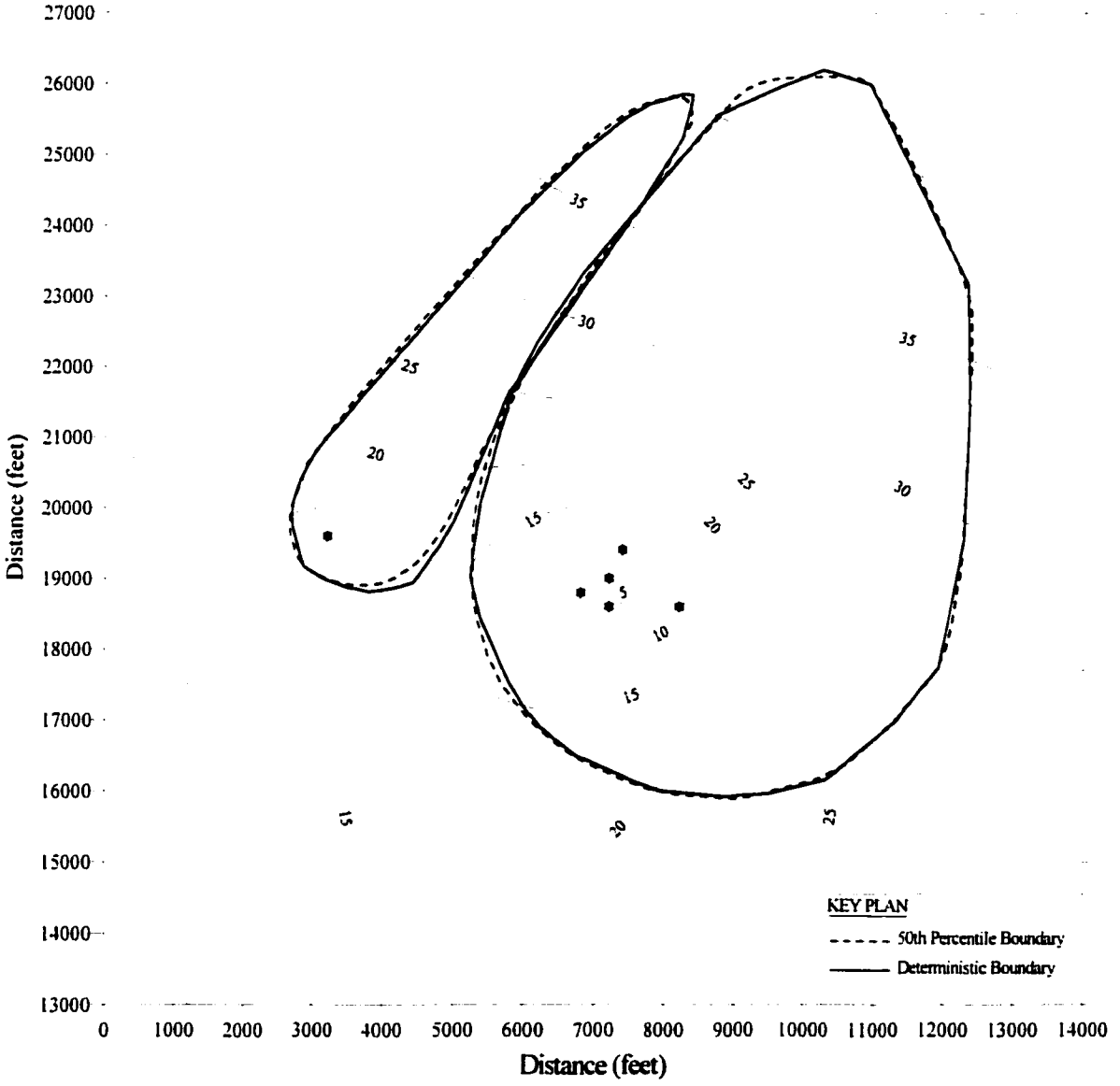


Figure 6.21: A Comparison of the Deterministic and 50th Percentile Zone III RWAPT Boundaries

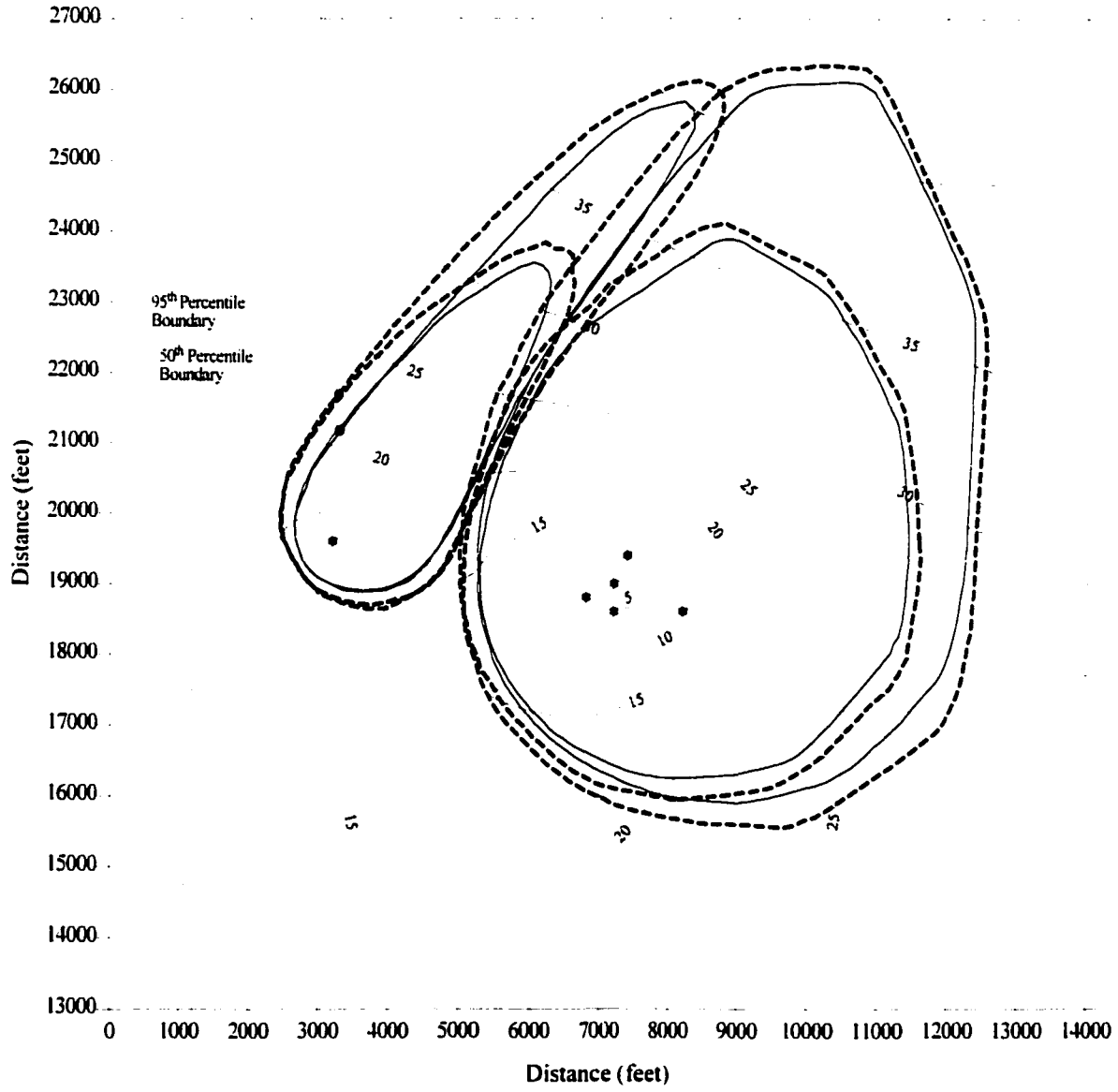


Figure 6.22: A Comparison of the 50th and 95th Percentile RWAPT WHPA Boundaries

boundary. This indicates that hydrodynamic dispersion should be investigated using uncertainty analysis to determine its affect on the WHPA delineation process.

6.4 Summary

There is uncertainty associated with many aspects of numerical groundwater modeling. Two common techniques that are used to analyze model uncertainty are the first order second moment method and the direct parameter sampling method. The first order second moment method has shown that net infiltration provides for approximately 85% of the total uncertainty in the size of the numerical STLINE capture zone. Well pumping rates provide for most of the remaining uncertainty in capture zone size. This information is useful for apportioning the field sampling budget in order to reduce model uncertainty in the final application of WHPA delineation.

Direct parameter sampling was used to provide multiple realizations of the output WHPA boundary for both STLINE and RWAPT modeling. The locations of the Zone II and Zone III boundaries were found to be normally distributed, and the 50^{th} percentile WHPA boundary was found to be in almost the exact location of the deterministic WHPA boundary. However, the 50^{th} percentile boundary was smoother in appearance and was, in general, on the outside of the deterministic boundary in places where the deterministic boundary was jagged in appearance. This is a result of the fact that numerical averaging of multiple realizations of the WHPA boundary uses more information about boundary location to determine the "average" boundary than the deterministic boundary. Thus, the 50^{th} percentile boundary provides a better representation of the average numerical WHPA boundary.

Direct parameter sampling was also used to determine the 95^{th} percentile boundary location. This boundary was found to be approximately 35% larger for the Well 20 WHPA boundaries and approximately 15% larger for the Parkway WHPA boundaries. However, as uncertainty in the input parameters is reduced this difference will also be reduced. The 95^{th} percentile boundary contains 95% of the capture zones that result from multiple model simulation and therefore is a more conservative representation of a WHPA boundary than the 50^{th} percentile WHPA boundary. For these reasons, the 95^{th} percentile boundary was recommended as a the best representation of a numerical WHPA boundary.

The value of information on uncertainty was also determined using uncertainty analysis. This value represents the maximum exploration and sampling budget that should be put toward obtaining new sample points to reduce input uncertainty. Based on the first order second moment analysis, the best use of this budget would be for reducing uncertainty in the

knowledge of net infiltration to the groundwater flow model because a reduction in the variance of the infiltration will have the greatest impact on reducing the variance in WHPA boundary location.

CHAPTER 7
TRANSIENT ANALYSIS OF WHPA DELINEATION

7.1 Introduction

All of the travel time related techniques, which are recommended by the USEPA for delineating wellhead protection areas, are based on steady state groundwater flow analysis. A steady state value for each model parameter is determined from a statistical average of the sample data that are available. For example, pump operating records are used to generate a steady state value for the pump rate for each of the municipal wellheads. However, as presented in Chapter 3, pumping at most public supply wells is transient in nature and, therefore, a steady state value may not be appropriate for representing this parameter in decision making for WHPA delineation. The purpose of Chapter 7 is to analyse the transient nature of groundwater flowfields through an analysis of changes to well pumping rates to determine the effect that this has on the size and shape of numerical WHPA boundaries

7.2 The Transient Nature of Groundwater Capture Zones

Time-averaged values of well pumping rates are commonly used for steady state analysis of numerical groundwater capture zones. These time-averaged parameter values are determined from the wellhead pumping rates that are available from each pump station. The more data that are available the better the estimate of long-term steady state values. However, it is difficult to estimate the long-term steady state value for new wells during the initial period of pump operation because of insufficient data. It is also difficult to estimate long-term rates for older pumping stations where historical pumping rates may not have been recorded. As a result, an important aspect of steady state capture zone analysis is the point in time when the analysis was performed and the data on hydrogeologic stresses that were available at that time. To illustrate the effect that time varying pumping rates have on the size and shape of groundwater capture zones at the UWTR wellfields, a year-by-year investigation of numerical time of travel capture zones was performed. For each year, from 1971 to 1995, a 10 year time of travel numerical STLINE capture zone was generated based on the values of well pumping rate that were averaged over that year.

Figure 7.1 presents the 10 year capture zone for well 20 for 1971. Figure 7.2 presents the 10 year capture zones for well 20 and the Parkway wellfield (including wells 22 and 26) for 1972. Figure 7.3 and 7.4 present the 10 year capture zones for well 20 and the Parkway wellfield (including wells 22, 24 and 26) for 1973 and 1974, respectively. Figure 7.5, 7.6 and 7.7 present the 10 year

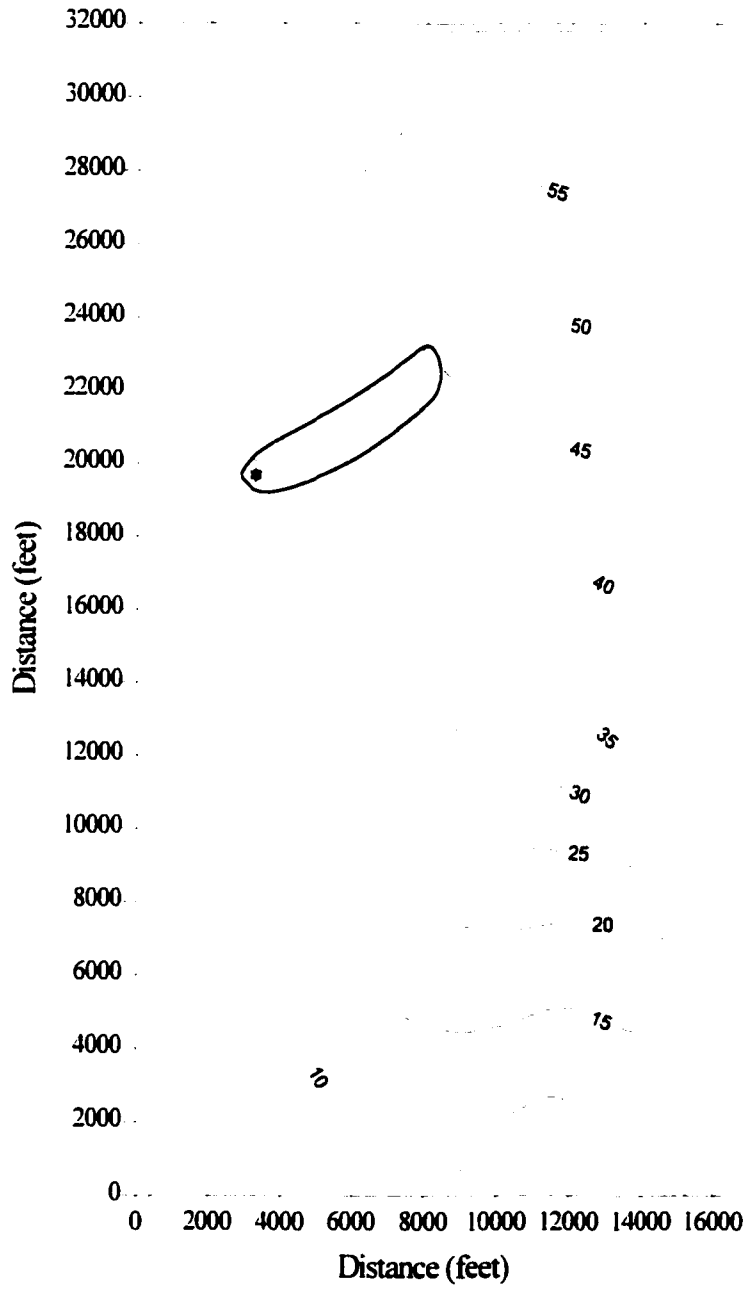


Figure 7.1: The Zone III WHPA Boundary for Well 20 Based on the 1971 Pumping Rate

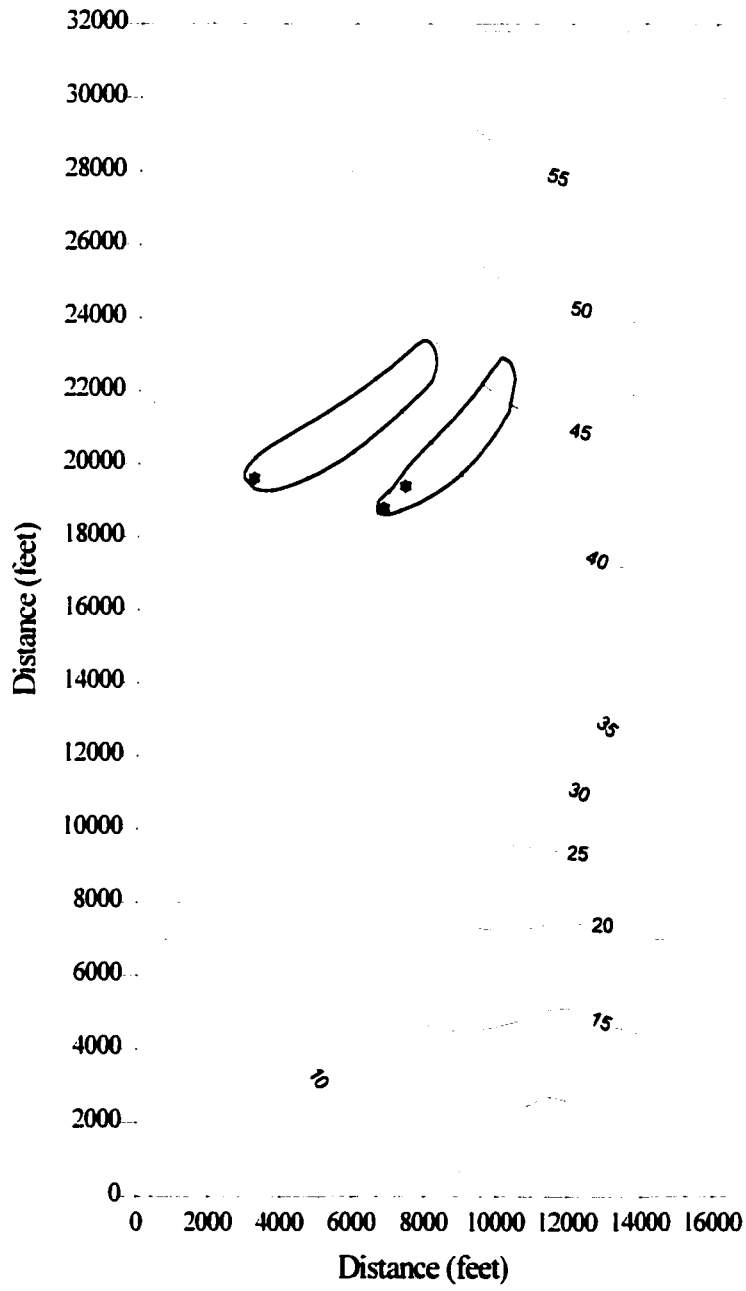


Figure 7.2: The Zone III WHPA Boundaries Based on 1972 Pumping Rates

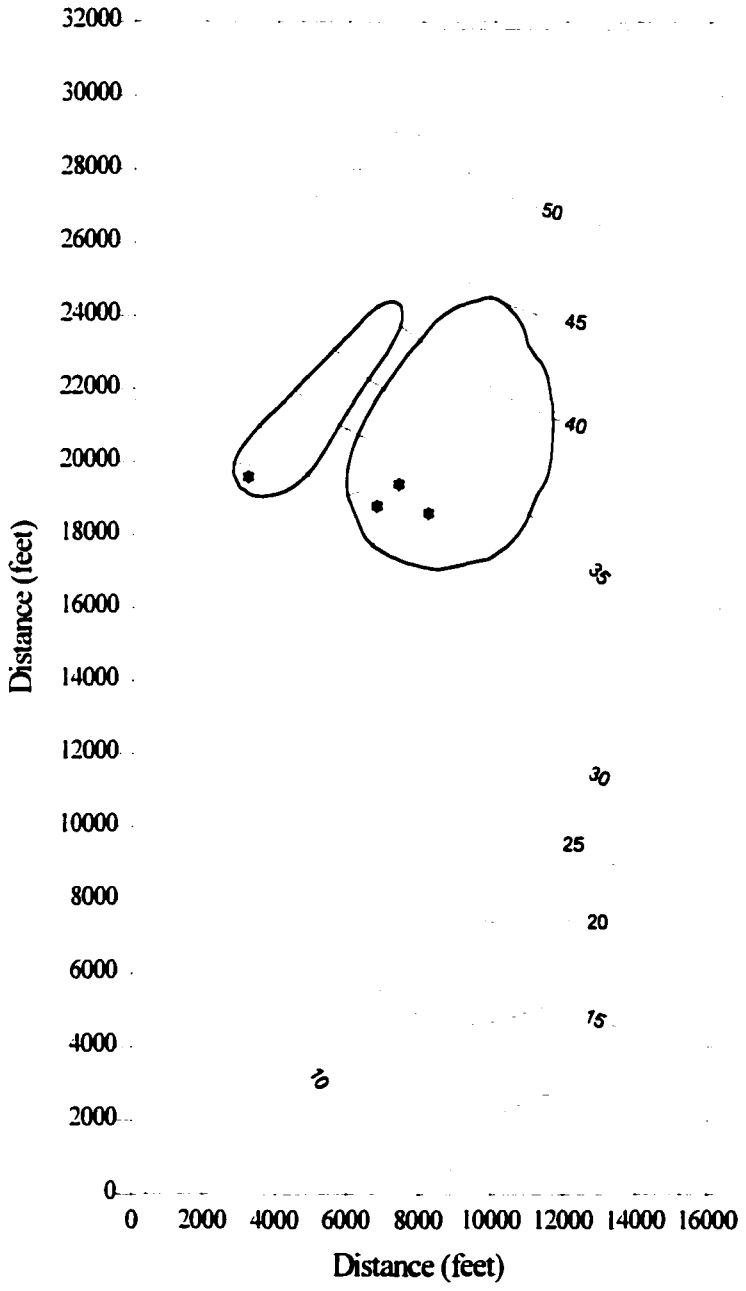


Figure 7.3: The Zone III WHPA Boundaries Based on 1973 Pumping Rates

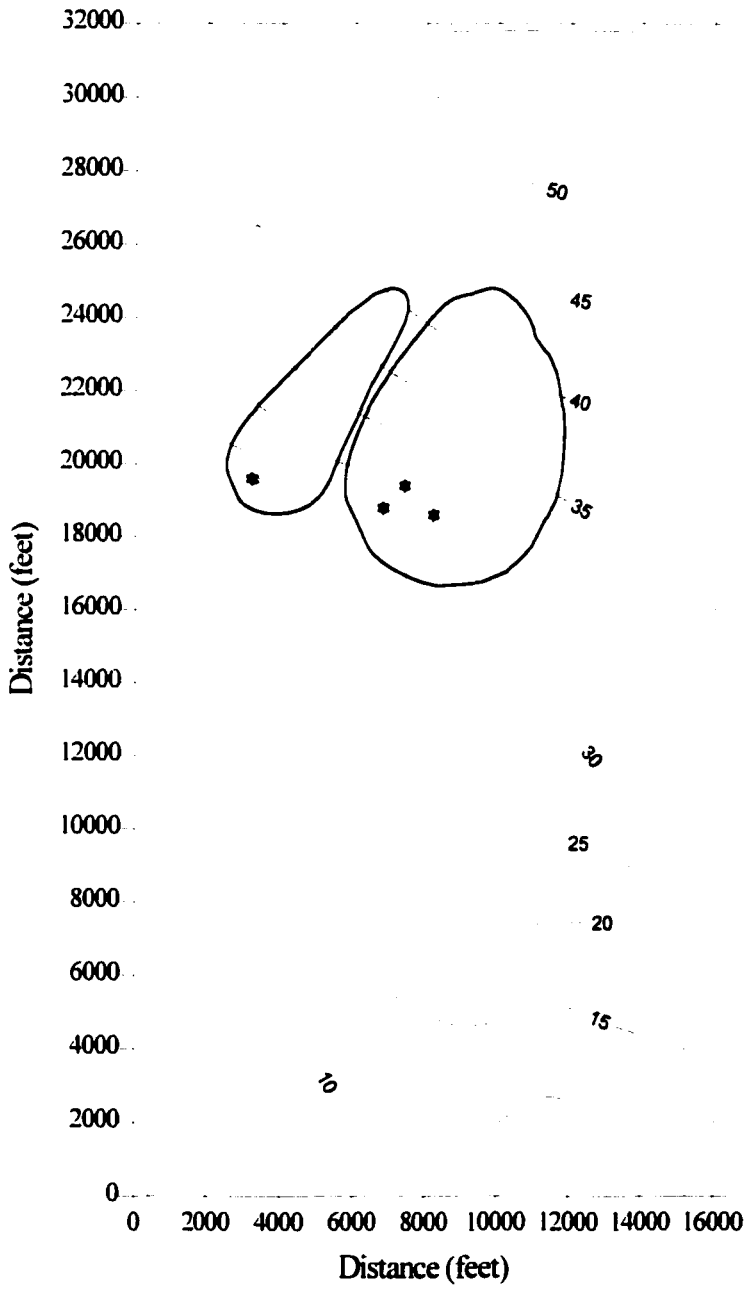


Figure 7.4: The Zone III WHPA Boundaries Based on the 1974 Pumping Rates

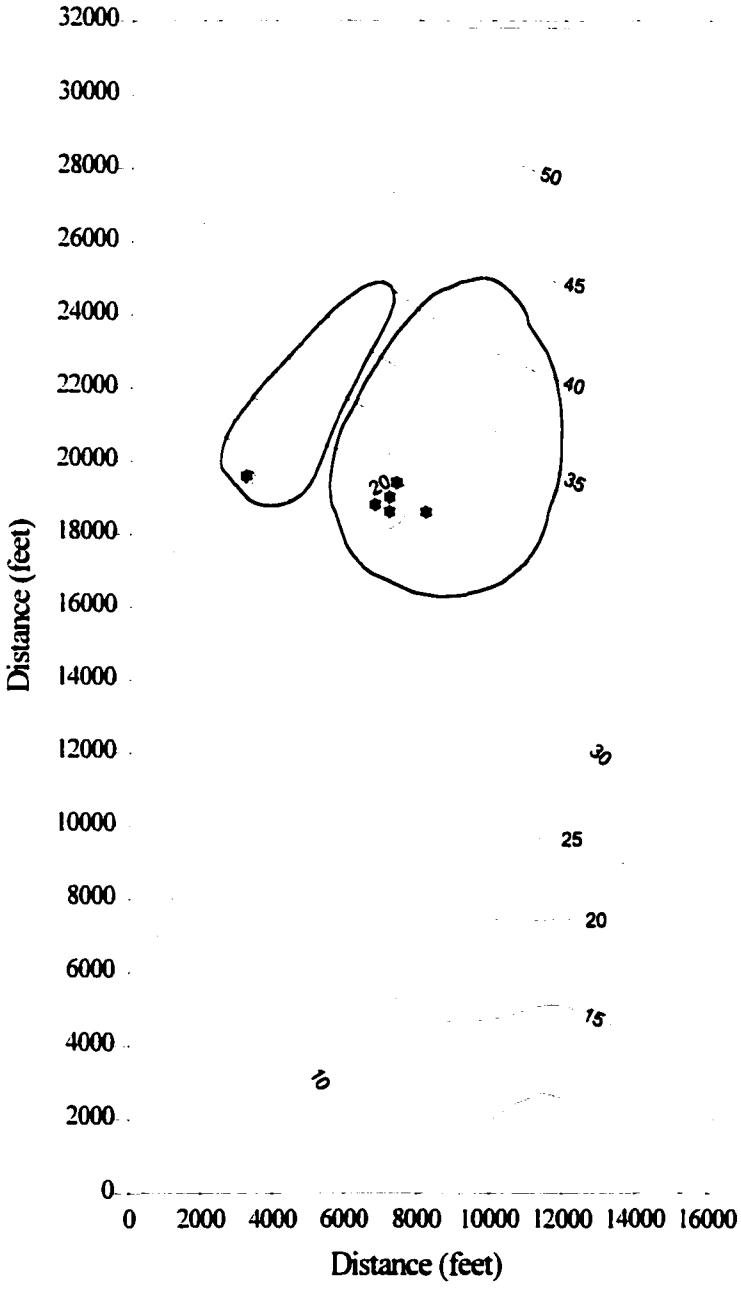


Figure 7.5: The Zone III WHPA Boundaries Based on the 1975 Pumping Rates

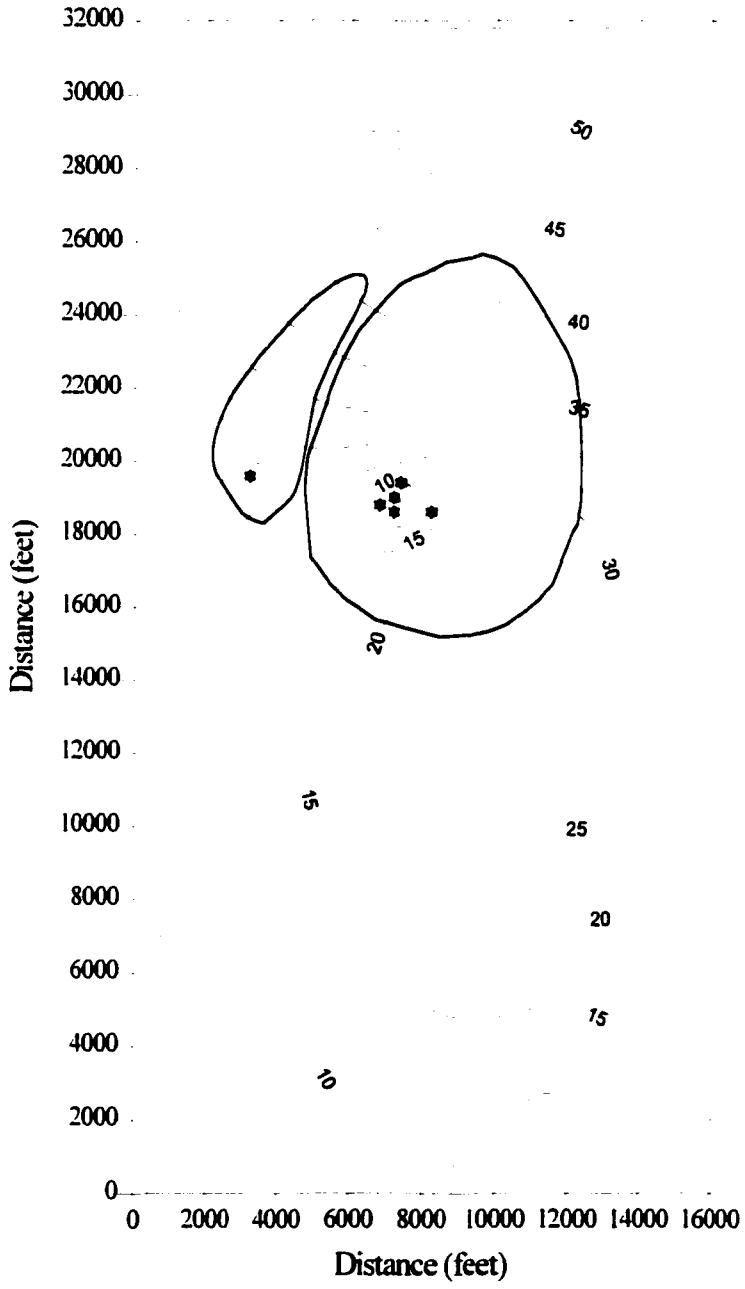


Figure 7.6: The Zone III WHPA Boundaries Based on the 1985 Pumping Rates

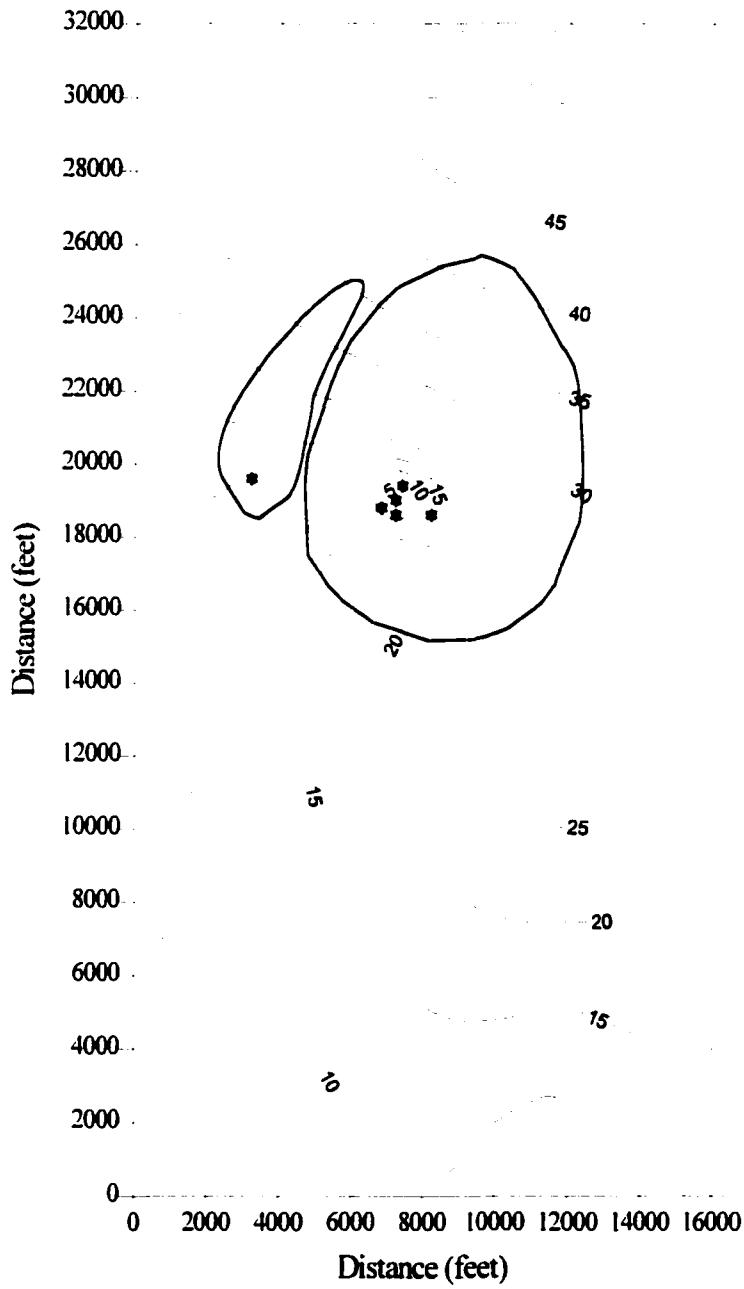


Figure 7.7: The Zone III WHPA Boundaries Based on the 1995 Pumping Rates

capture zones for well 20 and the Parkway Wellfield (including wells 22, 24, 26, 28 and 29) for years 1975, 1985 and 1995, respectively. Table 7.1 presents the areas encompassed by the 10 year numerical boundaries for the UWTR wellfields, and shows that capture zone area changes as a result of the transient nature of wellhead pumping.

Zone III	WHPA Boundary Area						
WHPA	1971	1972	1973	1974	1975	1985	1995
Boundary	[Ac]	[Ac]	[Ac]	[Ac]	[Ac]	[Ac]	[Ac]
Well 20	191.0	167.1	212.2	331.1	309.6	301.6	257.1
Parkway Wellfield	0.0	123.7	708.5	841.6	961.0	1,421.4	1,456.4

Table 7.1: Capture Zone Areas Based on Yearly Values of Well Pumping Rates

From this analysis it is evident that the nature of the groundwater flowfield and the resulting numerical capture zones are affected by temporal changes to the hydrogeologic stresses imposed on the Cohansey aquifer. The size and shape of the capture zones for Well 20 and the Parkway wellfield change significantly from 1971 to 1995. These capture zones grow in size as more water is pumped from each wellfield. Capture zone size, however, can not grow indefinitely because there is a limit to the volumetric flowrate that the aquifer can support. Between 1985 and 1995 the area encompassed by the 10 year capture zones reached a plateau because the amount of groundwater withdrawn from the wells leveled off as they approached the maximum pumping rates that each wellhead could sustain. It is important, therefore, to develop a method of incorporating the transient nature of groundwater flowfields into capture zone analysis in order to determine whether these changes to numerical capture zones will have an effect on the choice of which alternative is the best for WHPA delineation.

7.3 Transient Capture Zone Analysis

By definition a time related capture zone is the area on the ground surface which contains all of the groundwater that exits the wellhead within a specified period of time. The groundwater that exits the wellhead is pumped in a time varying manner based on changes in groundwater availability and consumer demand. A transient groundwater analysis was performed to determine more accurately the source of water that exits each well over the time period specified in the STLINE capture zone analysis.

To perform the transient analysis the complete timeline of wellhead pumping, from 1971 to 1995, was discretized into 25 annual increments. The transient solution to groundwater flow within the Cohansey aquifer was determined using 25 yearly-averaged daily pumping rates for each well and the SWIFT groundwater model. This transient solution provided a velocity field within the Cohansey aquifer for each year of simulation. Capture zone modeling was then performed, in one year time

increments, using advective particle tracking and the 25 groundwater velocity fields. The 25 sequential velocity fields were used in reverse order starting with the velocity field for 1995. The endpoints of reverse particle tracking for a specific year provided the start points for reverse particle tracking in the previous year. The position of the particles at the end of the particle tracking simulation represents the boundary of the volume of groundwater that was pumped from the wellheads within the time of travel prior to 1995.

Figure 7.8 presents the 5 year time of travel capture zones based on transient particle tracking analysis of the Parkway wellfield. This transient capture zone boundary is compared to the 50th percentile steady state STLINE boundary. Figure 7.9 presents the 10 year transient STLINE boundary and compares it to the 50th percentile steady state STLINE boundary. The areas encompassed by the 5 year and 10 year transient boundaries are presented in Table 7.2. They provide a better representation of the actual volume of water that was withdrawn from the wellhead, for a specific travel time, than the steady state STLINE boundary. However, pumping rates will change in the future just as they have changed over the past 25 years. Therefore, these capture zones, which are based on reverse particle tracking from 1995, will not accurately represent the area from which water is withdrawn under future pumping scenarios. It is, therefore, important to develop a standard method of capture zone analysis, which minimizes the effects of the transient nature of hydrogeologic stresses on the aquifer system.

Wellhead	WHPA Boundary	Average Well Rate [sq.ft.]	Transient Capture Zones [sq.ft.]	Percentage Difference [%]
Well 20	5 Year	6 568 900	5 649 000	- 14.00
	10 Year	9 931 300	10 153 900	+ 2.24
Parkway Field	5 Year	31 737 300	37 204 100	+ 17.23
	10 Year	49 402 000	59 455 700	+ 20.35

Table 7.2: A Comparison of WHPA Areas Based on Transient Analysis

7.4 Sustainable Well Yield Analysis

In order to remove analytical errors that are associated with the transient nature of well pumping rates from the delineation of numerical capture zones, it was necessary to develop a standard well pumping rate that is independent of the time period over which the analysis was performed. This standard pumping rate was chosen to be the maximum sustainable yield for each wellhead. Sustainable yield is defined as the "maximum rate at which water can be withdrawn on a continuing basis" from an aquifer without causing the ultimate depletion of the aquifer (Viessman and Hammer, 1993). There are a number of methods that have been proposed for determining the

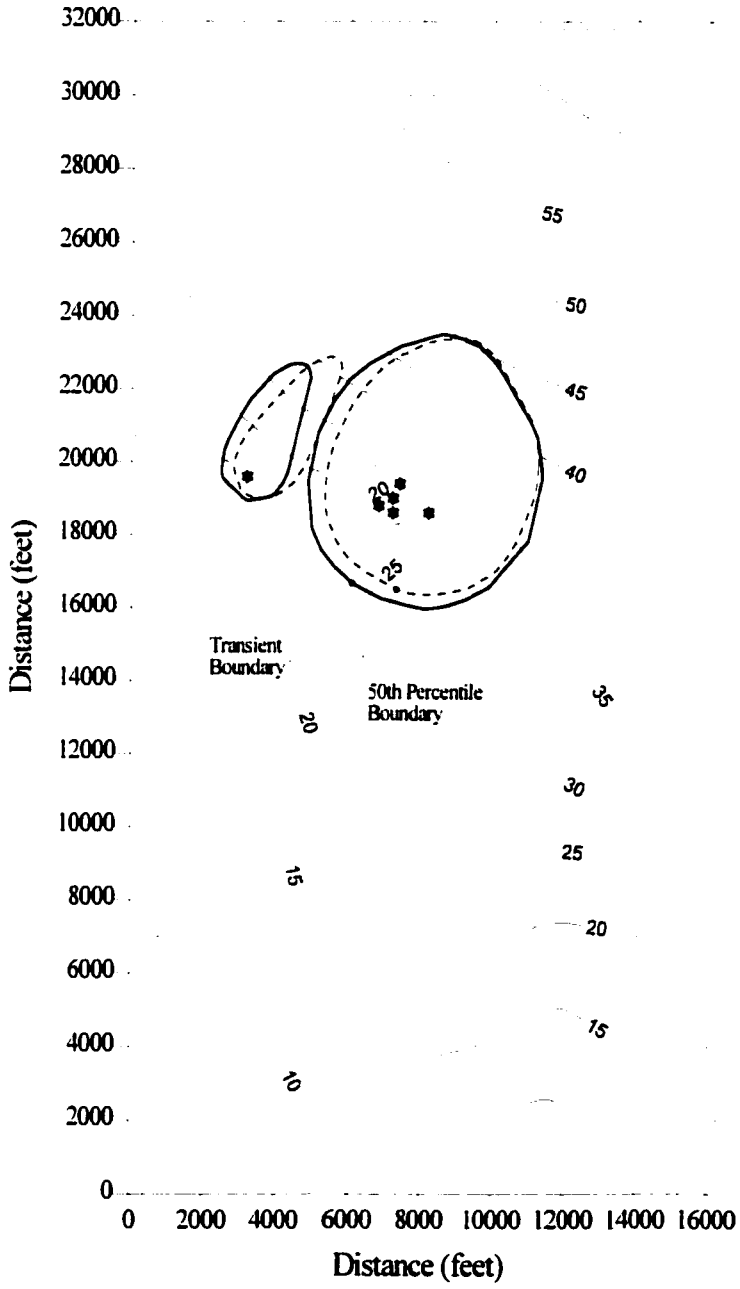


Figure 7.8: The Zone II STLINE Boundaries using Transient Particle Tracking Analysis

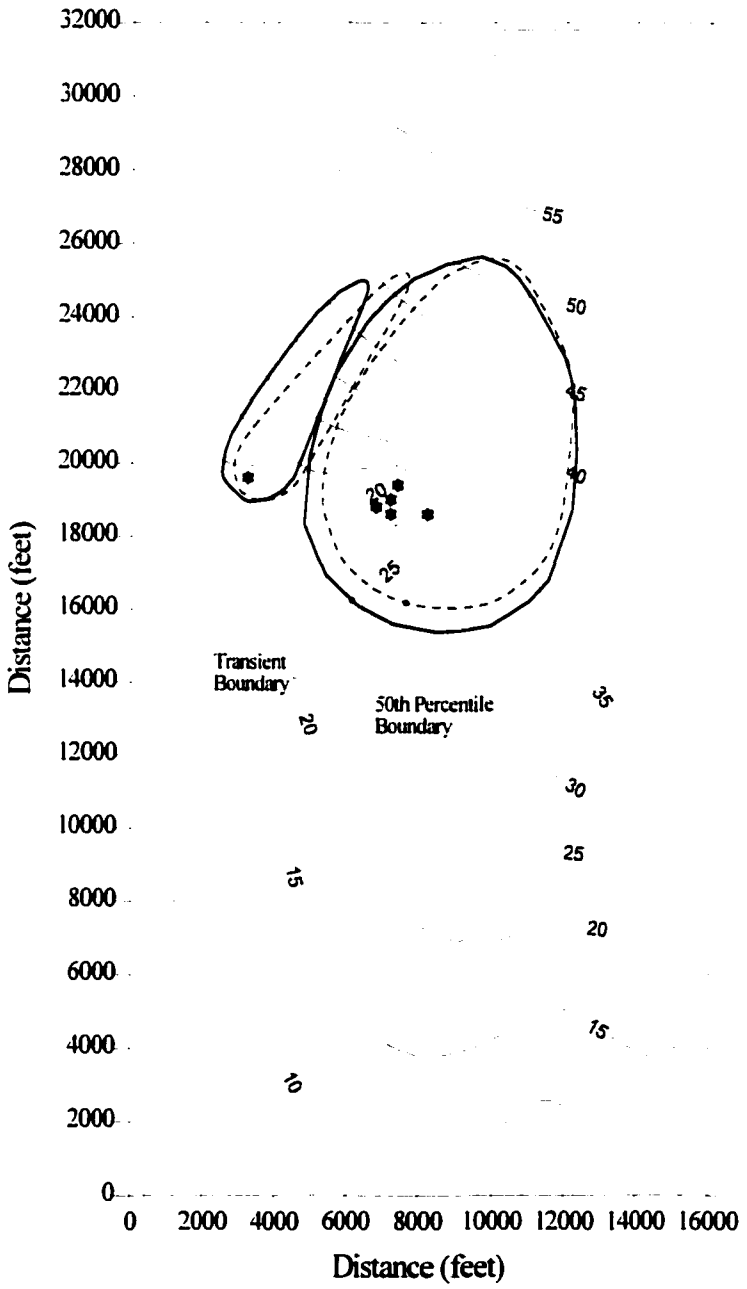


Figure 7.9: The Zone III STLINE Boundaries using Transient Particle Tracking Analysis

sustainable yield of an aquifer that are based on field observations of groundwater levels and annual wellfield production. For the purposes of the present research the maximum sustainable yield of the UWTR wellfields was analyzed using the numerical model of the Cohansey aquifer. For the UWTR wells these pumping rates were obtained by optimizing the value of each well rate under the constraint of maximizing the total flowrate from the wellfield as a whole. This was obtained by pumping the water table down to just above the bottom of the aquifer at each wellhead. The sustainable yield for the 6 UWTR wells were determined to be 115000 ft^3/day, 81000 ft^3/day, 120000 ft^3/day, 68000 ft^3/day, 68000 ft^3/day and 68000 ft^3/day, respectively. The maximum flowrate from this wellfield was determined to be 520000 ft^3/day.

Figures 7.10 and 7.11 present the 5 year and 10 year capture zones based on these well rates. These capture zones are the largest that can be generated for a specific time of travel under the existing configuration of wellheads. They can not be any larger because each pumping rate is at its maximum value based on the conceptual model of the Cohansey aquifer. Therefore, these capture zones provide a conservative estimate of the location of the STLINE WHPA boundary.

The areas encompassed by these WHPA boundaries and their difference to the WHPA boundaries based on average well pumping rate are presented in Table 7.3. If these capture zones were used to delineate WHPAs for each wellfield there would not be any errors associated with too little land in the groundwater protection area. From this table it is evident that there is a large effect to using well pumping rates that are less than the maximum rates that the aquifer can sustain in a long-term sense based on the hydrogeology of the area. The trend at the UWTR wellfields is for the slow increase in the pump rates as consumer demand increases. Thus over time the WHPA boundary that would result from an average steady state well pumping rate analysis would also increase. At some point in the future the maximum sustainable well rate would be encountered. The effect of using average pump rates for WHPA analysis is to delineate the Zone II and Zone III which are 55% and 80% of the size that might be expected in the future for well 20 and the Parkway wellfield, respectively.

Wellhead	WHPA Boundary	Average Well Rate [sq.ft.]	Sustainable Well Rate [sq.ft.]	Percentage Difference [%]
Well 20	Zone II	6 568 900	11 896 800	+81.11
	Zone III	9 931 300	17 965 400	+80.90
Parkway Field	Zone II	31 737 300	39 211 500	+23.55
	Zone III	49 402 000	61 482 800	+24.45

Table 7.3: A Comparison of WHPA Areas Based on Sustainable Well Yield

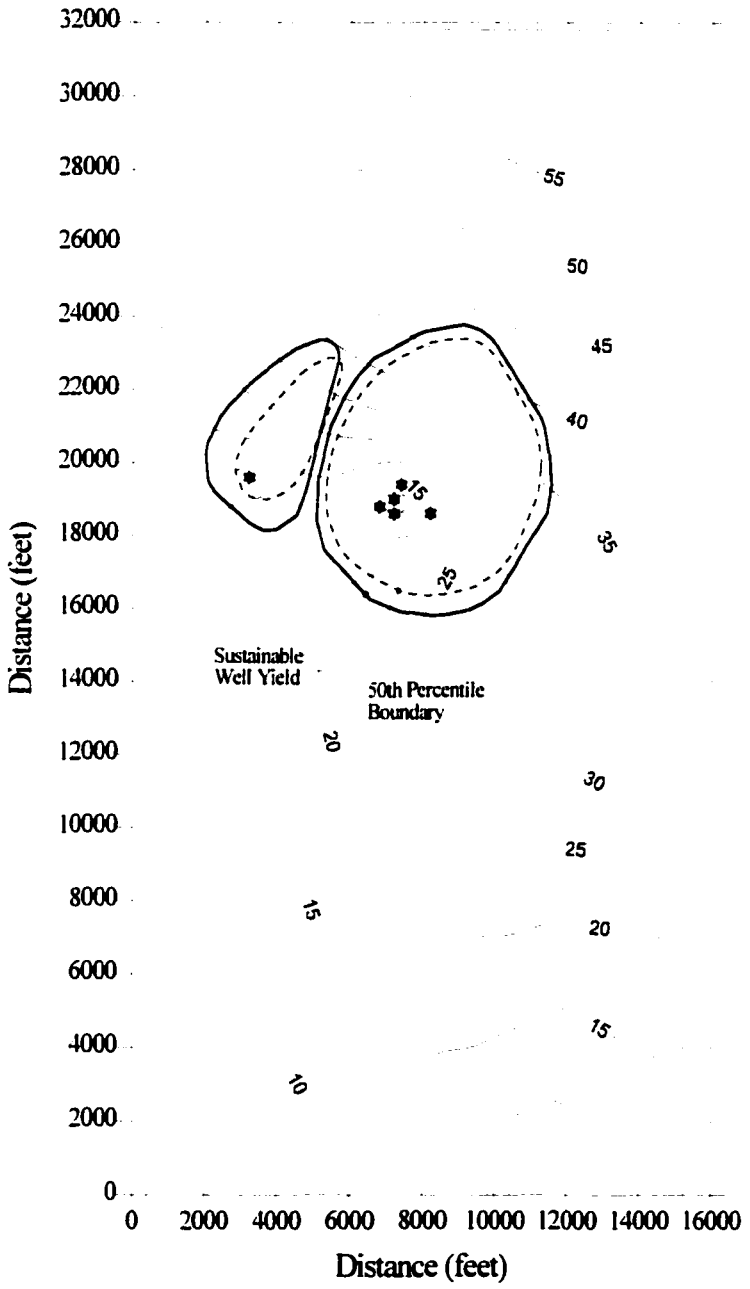


Figure 7.10: The Zone II STLINE Boundaries Based on Sustainable Well Yield Analysis

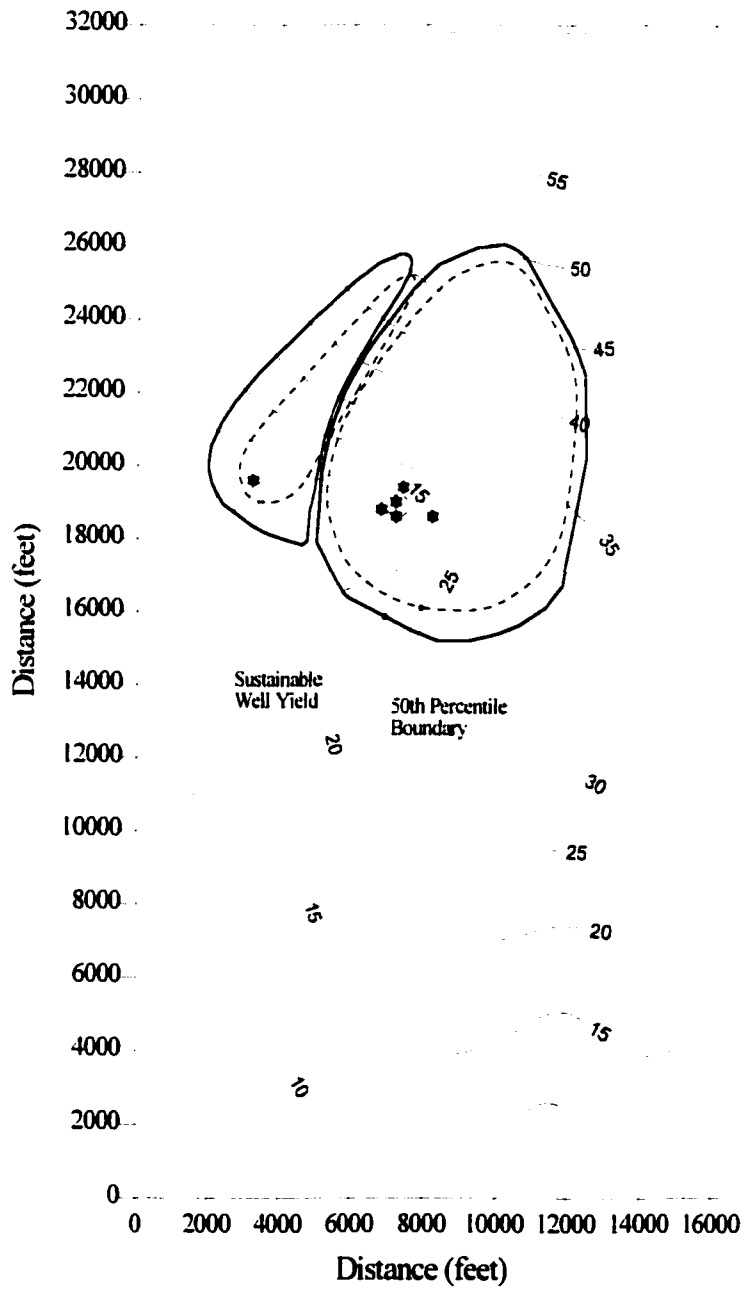


Figure 7.11: The Zone III STLINE Boundaries Based on Sustainable Well Yield Analysis

7.5 Addition of New Wells to the Wellfield

The addition of a new well within a watershed will have an effect on the direction and magnitude of groundwater flow within the aquifer. With respect to WHPA delineation there are two possible scenarios for the location of a new well in proximity to an existing wellfield. The new well may be far enough away so that it has no effect on the location of existing WHPA boundaries, or near enough to an existing boundary to effect its size and shape. If the new well is far away from the existing wells and does not have an effect on the flowfield created by the existing wells, then the WHPA delineation process will be based on the same procedure that has been developed in this research. The result be a new WHPA boundary that will be zoned within the region. However, if the new well is close enough to an existing set of WHPA boundaries to have an effect on the groundwater flowfield, then the new well will change the area from which each well withdraws its groundwater.

At the UWTR wellfields one new well has recently been added to the Parkway wellfield. Figure 7.12 shows the placement of the new well 44 and its proximity to the cluster of wells at the Parkway wellfield. A steady state analysis was performed to determine the maximum long term well rate for well 44 in combination with the pumping rates for the existing 6 wells in the UWTR wellfields. The purpose of this analysis was to maximize the flowrate from all of the wells in the UWTR wellfield. The addition of well 44 had an effect on the magnitude of groundwater velocity around the UWTR wellfields and thus affected the size and shape of both the well 20 and Parkway WHPA boundaries. The updated well rates for the 7 wells in UWTR wellfields are 107000 ft^3/day, 73000 ft^3/day, 110000 ft^3/day, 62000 ft^3/day, 61000 ft^3/day, 61000 ft^3/day and 81000 ft^3/day, respectively. Thus the maximum flowrate from this wellfield increased to 555000 ft^3/day, which represents an increase of 6.7%.

Figures 7.13 and 7.14 present the Zone II and Zone III numerical WHPA boundaries based on these wellrates. The areas encompassed by these WHPA boundaries and the difference in the WHPA boundaries based on average well pumping rate are presented in Table 7.4.

Wellhead	WHPA Boundary	Sustainable 6 Wells [sq.ft.]	Sustainable 7 Wells [sq.ft.]	Percentage Difference [%]
Well 20	Zone II	11 896 800	10 994 500	- 7.58
	Zone III	17 965 400	16 498 700	- 8.17
Parkway Field	Zone II	39 211 500	44 060 400	+ 12.36
	Zone III	61 482 800	68 812 900	+ 11.92

Table 7.4: A Comparison of WHPA Areas Based on the Addition of Well 44

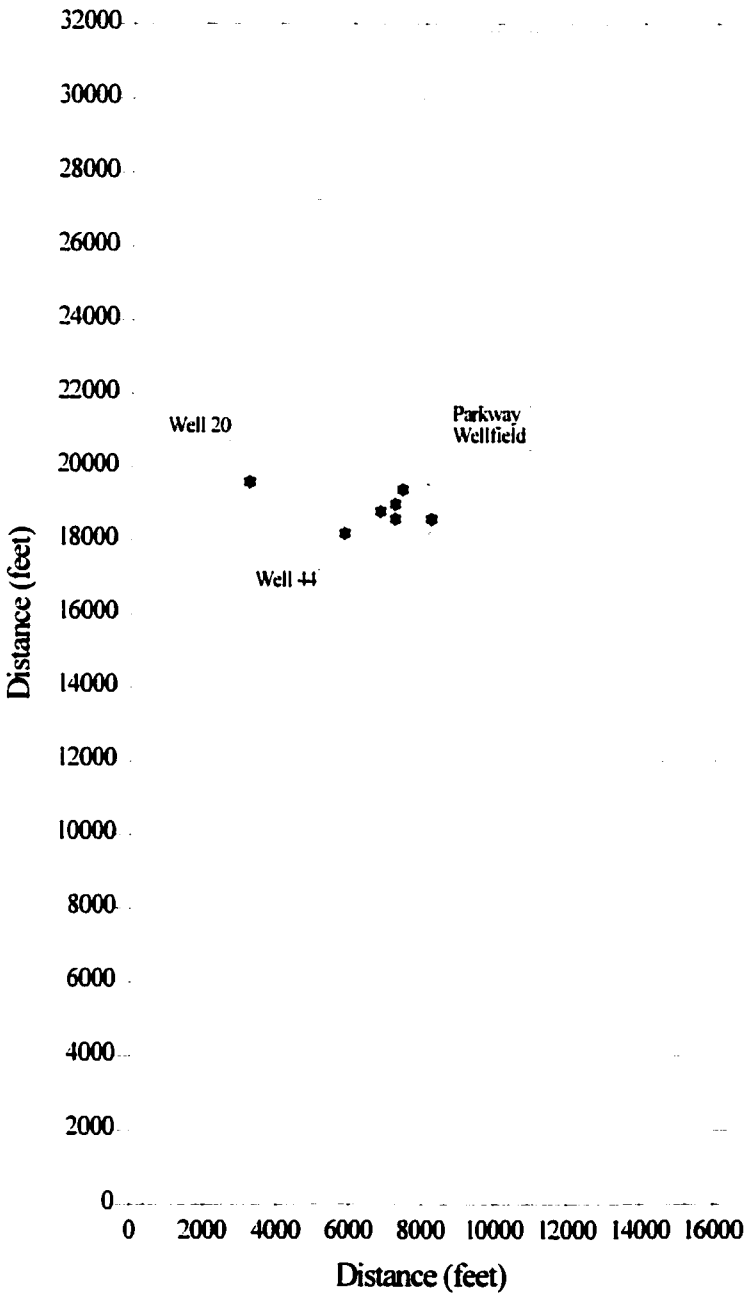


Figure 7.12: The Location of Additional Well 44 in Proximity to the UWTR Wellfields

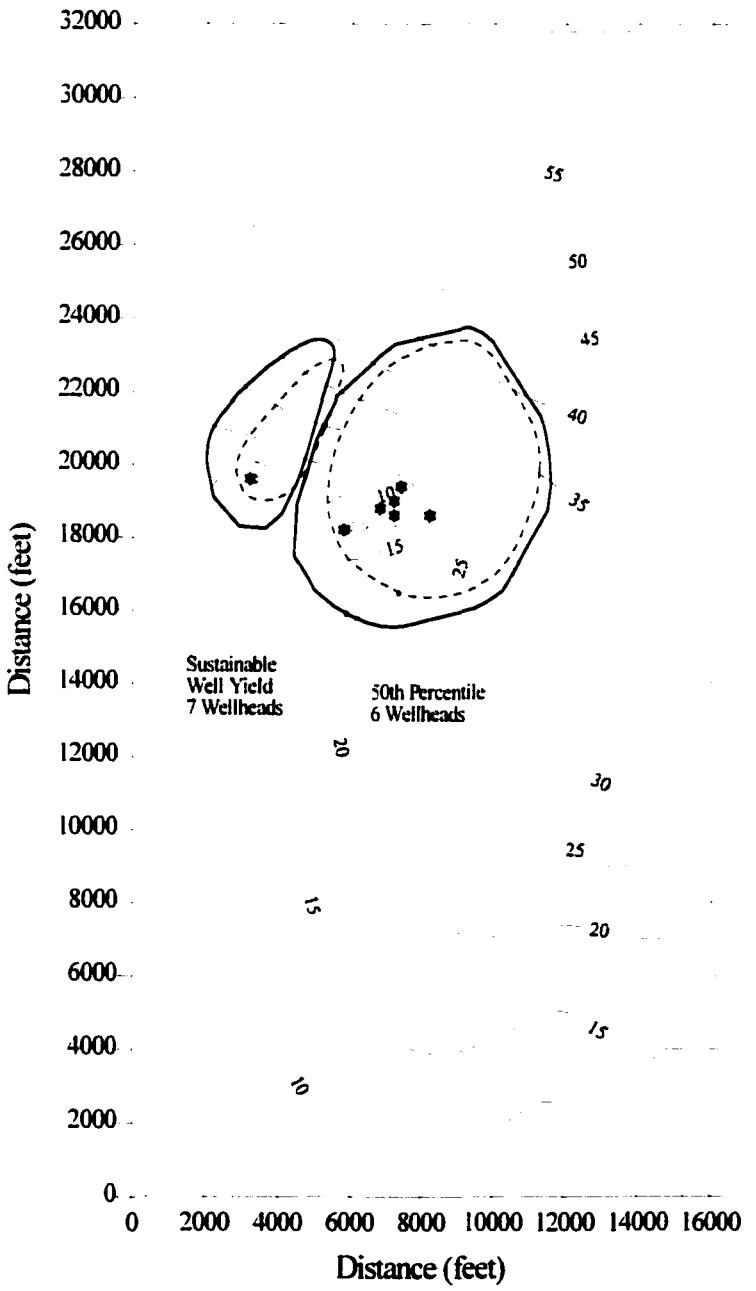


Figure 7.13: The Zone II STLINE Boundary Based on Sustainable Well Yields for 7 Wellheads

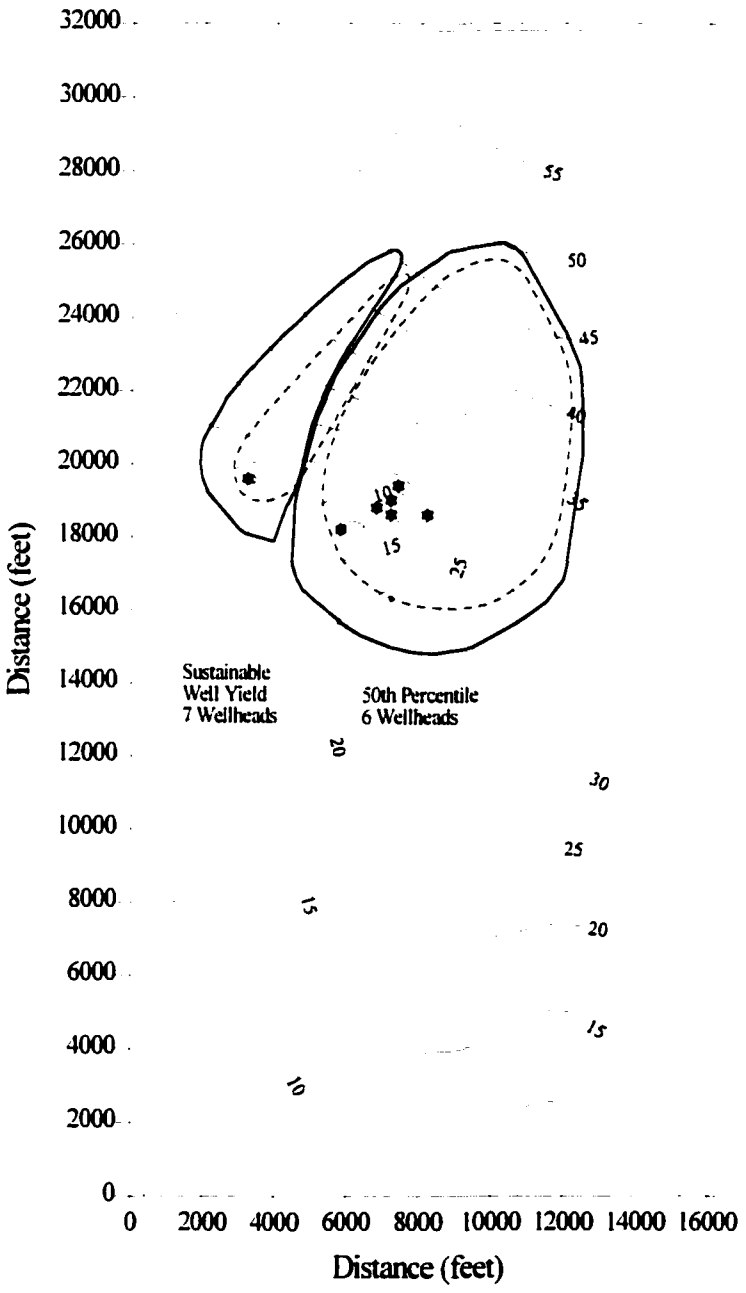


Figure 7.14: The Zone III STLINE Boundaries Based on Sustainable Well Yields for 7 Wellheads

It is standard practice in many municipalities, as a part of the Wellhead Protection Report, to prohibit the development of new wells within previously delineated WHPAs without first modeling the protection areas of all wells to ascertain the resulting WHPA boundaries. If a new well is located within the WHPA boundary delineated under a previous modeling exercise, its effect will be to expand this boundary to some extent. This is presented in Figure 7.15, which shows the expansion of the area encompassed by the WHPAs when well 44 is added to the conceptual model. The expanded WHPA boundary encompasses an area of 7,042,700 ft^2, which is an increase in the size from the original WHPA boundaries of 8.9%.

7.6 Decommissioning of an Existing Well at the Wellfield

The decommissioning of an existing well in a wellfield will also have an effect on the direction and magnitude of groundwater flow in the aquifer. The loss of a wellhead will reduce the total pumping rate for the wellfield, which will reduce the hydraulic stress imposed on the groundwater flowfield. This will result in a reduction in the groundwater velocities in the vicinity of the wellfield. At the UWTR wellfields the plume of TCE and PCE was detected in one of the Parkway wellheads in 1985. As a result of this wellhead contamination the owner has been under pressure to decommission the affected well until such time as the existing contaminant plume is reduced to below drinking water guidelines for TCE and PCE. For the present research, analysis of well decommissioning was accomplished by removing well 26 from the active wells in the Parkway wellfield and determining the effect that this had on the existing WHPA boundaries generated using steady state groundwater flow analysis.

After the removal of well 26, the well rates for the 5 remaining wells are 64400 ft^3/day, 75500 ft^3/day, 66200 ft^3/day, 62500 ft^3/day, and 63800 ft^3/day, respectively. A steady state analysis was performed using SWIFT. Figures 7.16 shows the effect of well decommissioning on the head in the upper Cohansey aquifer and the change in the location of the WHPA boundaries for the remaining wellheads. The effect of removing well 20 is that the drawdown of groundwater head in the vicinity of the Parkway wellfield is not as pronounced and, therefore, the magnitude of groundwater velocity is reduced in the vicinity of the wellheads. As a result, the length of time related particle pathlines are reduced, and the STLINE WHPA boundaries are smaller. It is also evident that the Parkway wellfield does not have as great an effect on the drawdown cone for well 20 because of the reduced magnitude of groundwater velocity at the Parkway wellfield. As a result, the WHPA boundaries for well 20 are closer to the Parkway wellfield and the area contained within each boundary is smaller.

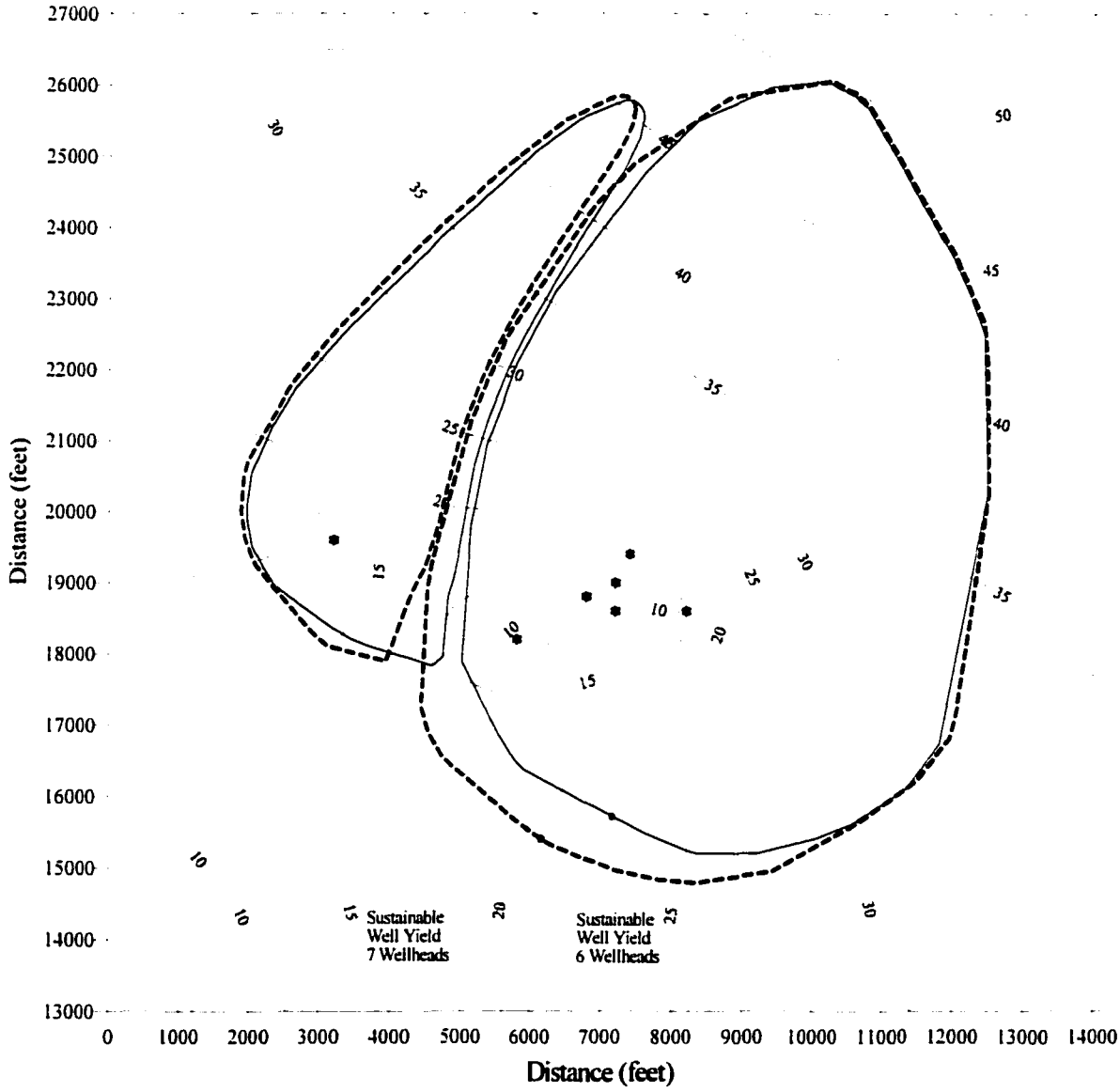


Figure 7.15: The Change in the Zone III WHPA Boundary With the Addition of Well 44

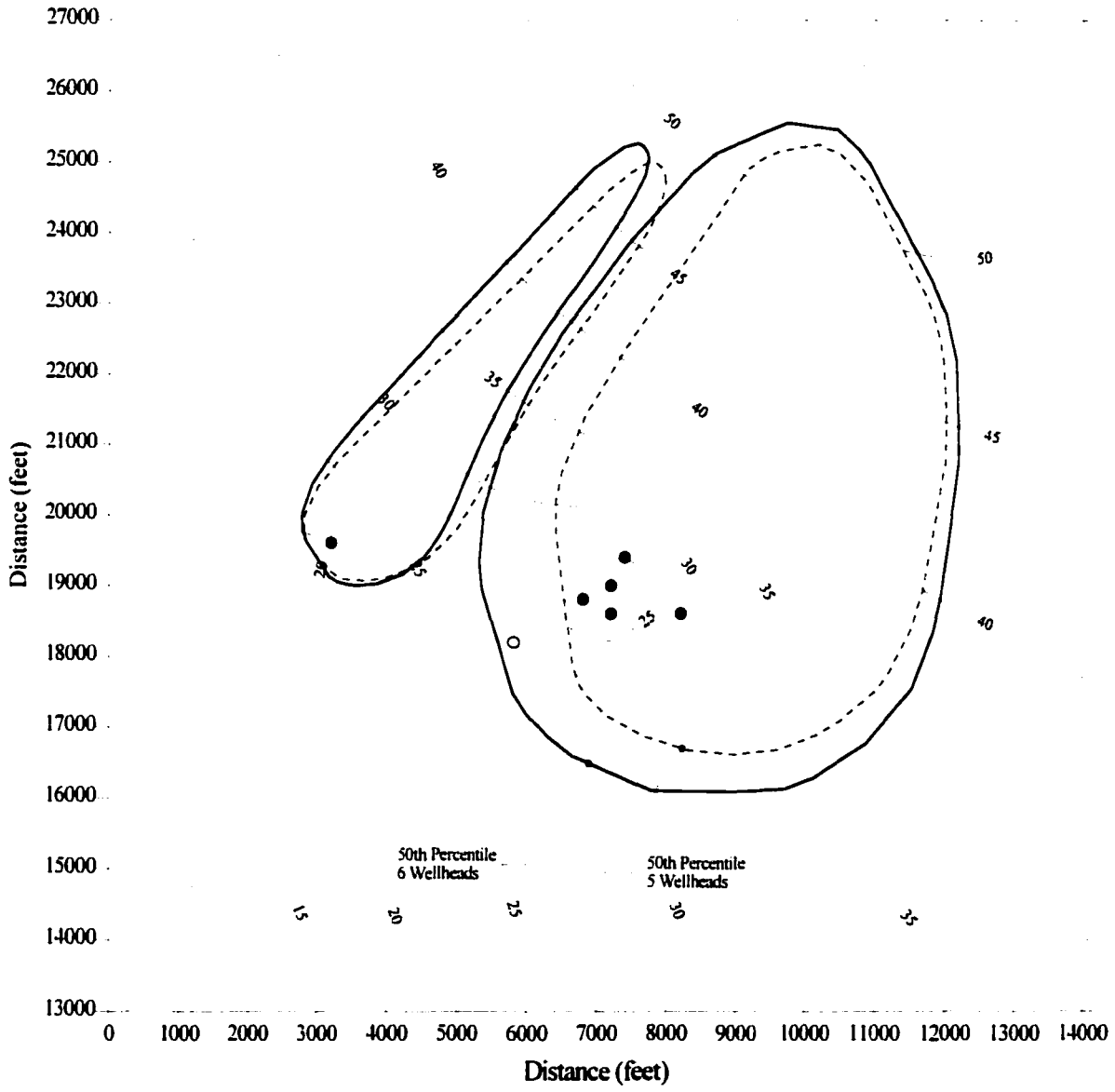


Figure 7.16: A Comparison of the WHPA Boundaries with the Decommissioning of Well 26

However, the decommissioning of this wellhead may only be temporary. For the UWTR wellfields, the transient nature of the contaminant plume within the aquifer makes it such that the wellhead may be turned back on at some point in the future. As a result, even though the decommissioning of the wellhead has a measurable effect on the size of the WHPA boundaries, this effect may be temporary. Therefore, there is no reason to change the location of the original Zone II and Zone III boundaries that were based on the hydrogeologic stresses from both well 20 and the Parkway wellfield operating under normal constraints. This decision is again conservative but, given the pressure to find new sources of potable water, there is a lot of pressure to find ways of keeping all municipal wellheads pumping to some degree.

7.7 Discussion

From the above analysis a number of points are evident. The first is that, in order to reduce the errors associated with numerical WHPA modeling, sustainable well pumping rates should be used to generate the WHPA boundaries. This methodology will result in the delineation of a conservative estimate of WHPA boundary location, but this conservatism will reduce the error that is associated with too little area being zoned for groundwater protection under a given set of Wellhead Protection Plan constraints. It is also evident that, if sustainable well rates are used for generating the WHPA boundaries, there is no need to take into account the transient nature of well pumping rates. This is a result of the fact that the sustainable well pumping rate will always be greater that any transient changes to well operating rates.

7.8 Summary

The most important point that emanates from Chapter 7 is that the zoning of groundwater protection areas must take into account both the existing stress conditions within a wellfield, and any potential future development conditions that may effect groundwater pumping. This requires some foresight in the estimation of the potential well development that may arise due to increased demand for potable water. This is best summarized by stating that the delineation of WHPAs should be based on all potential wellheads under their maximum long term well pumping rates. If any future wellhead development occurs in the vicinity of existing WHPAs, then the decision making process for future WHPAs must take into account the added area encompassed by new groundwater protection zones.

CHAPTER 8
DISCUSSION

8.1 Introduction

A methodology was developed for determining the best alternative for delineating wellhead protection areas (WHPAs) around municipal wells in order to protect the supply of potable water for the public. This methodology used benefit-cost-risk analysis as an environmental decision making tool to compare alternative methods for delineating the zoning boundary around a groundwater protection area. The benefits of groundwater protection are the continued supply of clean drinking water to the water distribution network. The costs of each alternative include the costs of delineating the WHPA boundaries and the costs of producing a Wellhead Protection Report, which is a document that shows the best location for the groundwater protection zone boundaries. The risk associated with each decision alternative is a function of its probability of failure and its cost of failure. The probability of failure for each alternative is the probability that the WHPA boundary encompasses land that is not necessary for groundwater protection. The cost of failure for each alternative is the cost of this failure area as it relates to industrial development within the community. The criteria and constraints that provide the basis for delineating each WHPA boundary, and the control over groundwater protection, are summarized in the Wellhead Protection Plan.

This form of environmental decision making has been used to choose the best alternative for implementing design solutions in a number of other areas of environmental engineering. Some of these areas of engineering include the design of the leachate collection system at a waste management site, the design of dams based on the historical frequencies of dam failure, the remediation of groundwater contamination sites, the design of a groundwater control system at an open pit mine, and the remediation of a contaminated aquifer that is affecting water quality in a river. There are a number of factors that make the use of benefit-cost-risk analysis unique in its application to WHPA delineation. The purpose of this section is to discuss some of these factors and how they affect the application of this methodology to groundwater protection planning.

8.2 The Flexibility of the Decision Making Paradigm

It is important that the decision making paradigm that has been developed herein is flexible enough to be applied to all existing and future methods of WHPA delineation. Benefit-cost-risk assessment has been shown in this research to be very flexible because it allows the comparison of any WHPA boundaries, regardless of the methods that were used to produce them, as long as they

abide by the criteria and constraints that are set out in the WHP Plan. This aspect of benefit-cost-risk assessment is both beneficial and detrimental. It is beneficial because it allows expert groundwater modelers to use professional judgement to choose a finite number of reasonable representations of the modeled WHPA boundary for comparison in the risk assessment process. This might include choosing several reasonable numerical models to delineate the WHPA boundaries, or a single numerical model using several equally likely calibrations of the groundwater flow field to produce model predictions. This is somewhat similar to the design process whereby the contributions of a number of experts are compared to come up with the best solution to an engineering problem. It is detrimental because a non-expert modeler may misuse the methodology to choose an alternative that is not the best alternative. This could be achieved by adding of a number of spurious alternatives to the set of WHPA boundary alternatives under comparison and as a result cause the choice of the best alternative to be changed. This has been shown to be a problem in determining the location a new landfill site, and therefore, is not unique to decision making for zoning groundwater protection areas. In spite of its potential drawbacks, benefit-cost-risk assessment is a flexible method for determining the best alternative for the delineation of WHPA boundaries.

8.3 The Robustness of the Decision Making Paradigm

The decision making paradigm must also be robust in order to make the best decision under all of the conditions to which the analysis may be exposed. In order to delineate the best WHPA boundary, benefit-cost-risk assessment must take into account all conditions that affect the criteria and constraints set out in the Wellhead Protection Plan. These conditions include the hydrogeology of the site, the current development characteristics of the community surrounding the wellheads, and any future industrial development that may be expected within the community. Benefit-cost-risk assessment has been shown to be very robust for making decisions in many other areas of economics and engineering. In order to be considered robust for making decisions on delineating groundwater protection zones it must take into account all components of risk that affect environmental design.

The risk component that applies specifically to environmental engineering design consists of the probability of failure and the cost of failure. Both of these components involve the concept of failure. In many environmental settings failure can be analy zed deterministically by calculating the extent to which a specific environmental standard has been exceeded. There is no standard of failure for the case of delineating groundwater protection areas. This is a result of the fact that there are no measurable standards for determining the size or shape of specific land classes as part of the zoning process. To determine the extent of failure for delineating WHPA boundaries it was necessary to

develop a standard that could be used to measure failure. Since there may be different models used to delineate potential WHPA boundaries in different protection zones this design standard must be applicable to delineating WHPA boundaries in all protection zones.

The approach that was taken to developing a WHPA failure standard was to make sure that it could be applied to the complete set of boundaries that are being compared for a specific protection zone. This set of boundaries represents all of the possible realizations of the actual WHPA boundary. The total area of intersection for the set of WHPA boundaries is called the zone of confidence, and represents the common area that is contained by all of the boundaries. The zone of confidence represents the area that must be within the true WHPA boundary because it is based on all of the possible realizations of the actual boundary. Therefore, the zone of confidence was chosen to be the standard for comparing WHPA delineation alternatives. The area contained within a specific boundary alternative, which is outside of the zone of confidence, is called the zone of delineation uncertainty. From a probabilistic perspective, the ZDU may, or may not, be within the actual WHPA boundary. Therefore, the ZDU represents the failure of the modeling technique to delineate the true WHPA boundary.

For environmental decision making the probability of failure is the probability that a specific delineation technique fails to generate the true WHPA boundary. The probability of failure may be determined from failure predictions based on environmental modeling or based on historical failure frequencies. There is no mathematical model that can be used to predict the type of methodology that will be used to generate WHPA boundary alternatives. Therefore, historical frequencies of WHPA delineation techniques, from actual groundwater protection efforts in the Unites States, were used to predict the probability of failure.

The cost of failure is a function of the constraints in the Wellhead Protection Report that relate to the amount of development that is allowed within each groundwater protection zone. The purpose of municipal planning is the division of a jurisdiction into districts to enable the regulation of land to promote the orderly development of the area and the protection of public health, safety and welfare. The need to provide land for industrial development has resulted from the need to promote business development within a community. If an area of potentially developable land were zoned as a groundwater protection area there would be a restriction placed on industrial development within the community. The restrictions on development within a wellhead protection area may range from a complete ban on development to increased groundwater monitoring to minimize the probability of contamination release to the groundwater environment. For each protection zone there are different development restrictions and, as a result, different costs of failure.

For a protection zone in which there is a complete restriction on industrial development the cost of failure is the cost of purchasing land. There are two perspectives from which to look at a complete ban on development. For companies located within the proposed protection zone, the property would have to be purchased so that they could relocate, which is contingent on the community being able to apply the groundwater protection ordinances to existing facilities. For companies wanting to locate on undeveloped land, the community would no longer be able to sell the land for development and therefore loose it as a source of revenue. For a protection zone in which restricted development is allowed the cost of failure is dependent on the type of restrictions that are in place. For example, if development is limited to industries that pose a low risk of contamination and the restriction on development involves increased groundwater monitoring then the cost of failure is the extra cost associated with monitoring the quality of the groundwater at a predetermined number of monitoring wells.

From the above discussion it is evident that the benefit-cost-risk function provides a robust methodology to determine the best alternative for delineating groundwater protection area boundaries. This methodology has been applied in other environmental settings to make equally difficult decisions and has become an accepted standard for these applications. The application to groundwater protection is unique, however, because of the lack of a concrete standard for determining failure. A standard was developed, that is based on the analysis of the acceptable techniques for WHPA delineation. This creates a robust application for this environmental decision making paradigm.

8.4 Application to Three-Dimensional Groundwater Flow Analysis

The decision making paradigm developed herein can also be applied in any type of hydrogeologic setting. For the present research, benefit-cost-risk assessment was applied to a study site for which the specific field conditions of the aquifer are two-dimensional in nature. However, this analysis could also be applied to a study site that is three-dimensional in nature. For groundwater protection, three-dimensional application of WHPA delineation is important in regions where multiple confined and unconfined aquifers below the community are being used for water supply. The difference in the assessment process is that a vertical component must be added to the conceptual model of the aquifer. The resulting groundwater velocity field is three-dimensional and, therefore, the WHPA boundaries are delineated on the ground surface as the locus of points where the particle pathline endpoints intersect the upper surface of the groundwater flow regime. The analysis may, therefore, become very complex because of the increase in uncertainty associated with

the structure of aquifers and aquitards that make up the conceptual model of a three-dimensional study site. The purpose of WHPA zoning is to protect the surface and subsurface environment that is contained by the WHPA boundary from contamination. A boundary produced using three-dimensional analysis has the same effect as a boundary produced using two-dimensional analysis, except that the numerical model used to generate the three-dimensional capture zone may be much more complex.

8.5 Application of WHPA Boundaries to Other Environmental Decisions

The delineation of WHPA boundaries, and the zoning regulations associated with each protection zone, reduces the land that is available for the location of high risk industries within specific areas of a community. This presents difficulties to municipal planners for determining the location of, for example, a new solid waste landfill site for the community. Landfills have been shown to pose a significant risk of contamination to the groundwater environment. It is important that they are located in areas in close proximity to the community and that they pose little risk for contaminating the potable water supply. The problem associated with finding a location for a new landfill site is exacerbated when WHPA boundaries are delineated.

Determining the location of a new landfill is often accomplished using negative constraint mapping. All the land classes that are inappropriate for siting a landfill are identified around the community and excluded from the planning process. This includes land that is zoned for groundwater protection. The remaining land, which is not deemed inappropriate, is then available for the purposes of developing potential waste management sites. Even though it makes the siting of a solid waste landfill more difficult, it makes the planning process easier to implement because it clearly identifies areas of the community that are at a higher risk to wellhead contamination.

8.6 Accounting for Contaminants in the Decision Making Process

One of the principle objectives of the Wellhead Protection Program is the identification of potential contaminant sources that could have an effect on water quality at the wellfield. Most hazardous waste sites, which might have an impact on the quality of wellwater, contain a number of different pollutant chemicals (Watts, 1997). Within the region around the wellhead there are numerous industries that could be considered as potential contaminant sources. As a result, there might be hundreds of chemicals that could affect water quality at the wellhead. The delineation of wellhead protection areas should take into account the nature of these potential contaminants in the

WHPA analysis in order to provide better protection to the public water supply from chemical contamination.

The main transport phenomena that influence contaminant movement in the groundwater environment are advection, dispersion, diffusion and reaction. In order to ensure that wellhead protection boundaries reflect the nature of the contaminants, for which they were zoned to protect, these contaminant transport processes should be represented in WHPA modeling. Advection is the only one of these processes that is accounted for under current guidelines for delineating WHPA boundaries. The random walk model, which was proposed herein as a method for WHPA delineation, uses both advection and dispersion to generate time related capture zones. However, dispersion is solely a function of the porous media through which the contaminants travel. To introduce information into the analysis that accounts for contaminant properties, it is necessary to account for chemical reaction in WHPA modeling. This may be achieved using a retardation factor, which is a parameter that relates the velocity of a contaminant species to the groundwater velocity. It could be added to WHPA delineation by applying the retardation factor to the velocity field that results from the groundwater flow analysis.

The dilemma associated with adding contaminant transport information to the delineation of WHPAs is the fact that there are many chemicals that could potentially affect the quality of the water exiting the wellhead. These chemicals might already be used by industries in the region, and therefore, pose an immediate threat to the wellfields. They might also be chemicals that are used by industries that propose to locate to the region in the future. All of these chemicals have different values associated with each of the contaminant transport parameters. It is important to take into account the affect that this range of contaminant parameter values has on the modeling process. This could be achieved by developing a surrogate chemical, which has the statistical properties of the range of chemicals that are important within the region.

Choosing which chemicals to include in the surrogate chemical parameter analysis is further complicated because each groundwater contaminant poses a different risk to the human population and to the natural environment. The most hazardous chemicals, which pose the greatest risk to humans, can be found on the EPA's priority pollutants list. Therefore, to account for the greatest environmental risk, the surrogate chemical should be developed as a probability density function of the chemicals in the region that are found on the EPA's priority pollutants list. This will ensure that the WHPA boundary is based on the contaminant properties that are important to potential contaminant sources in the region.

The contaminant transport parameter that was integrated into the RWAPT model is dispersion. The affect of uncertainty in the dispersion parameter on model output was not investigated in the RWAPT analysis of the wellheads at the study site. This remains as an avenue of future research that might help to standardize the contaminant transport aspects of WHPA delineation. Uncertainty analysis could be implemented by first choosing a mean and standard deviation for longitudinal and transverse dispersivity for the surrogate chemical. Multiple simulation of the RWAPT boundaries generates a statistical distribution of the boundary location that includes the 95^{th} percentile boundary. The 95^{th} percentile boundary contains 95 percent of the possible pathline endpoints that were generated using both advection and dispersion, and therefore, represents a conservative approximation of the location of the true WHPA boundary that is based on both advection and dispersion.

8.7 Accounting for Non-Point Source Pollutants

One of the important sources of groundwater contamination results from non-point source pollution. Some of the major activities that contribute to non-point source pollution include pesticide and fertilizer application to agricultural fields, land application of waste sludge, leaching of landfills and septic beds, chemical storage in surface impoundments, and de-icing salt application to roadways. The affect that non-point source pollution has on the groundwater environment is to add a small amount of chemicals to the unsaturated zone over a wide area. Of the activities listed above, fertilizer application to farm fields is an agricultural management activity that provides a major source of elevated nutrient levels to the subsurface environment.

Fertilizers are materials that contain appreciable amounts of plant nutrients. They are produced in both natural (manure, bonemeal, rock phosphate) and synthetic (dry granular, slow release, soluble) formulations. Synthetic fertilizers consist almost entirely of nitrogen, potassium and phosphorus because these three compounds are most likely to be in short enough supply to limit plant growth. Nitrogen is the likeliest one of these chemicals to leach into groundwater. This is a result of the fact that it is the most common component of fertilizers and it is extremely soluble in soil water making it the most mobile of these species in the subsurface environment. As a result, nitrogen represents the most frequently reported contaminant that is considered a major threat to groundwater quality (USEPA, 1990).

Plants can not use nitrogen in its gaseous form directly. It must be in a mineral form as either ammonia (NH_4^+) or nitrate (NO_3^-). In order to generate this mineral formulation, industrial fertilizer producers use the process of atmospheric nitrogen fixation. In the unsaturated zone nitrate leachs

directly to the water table with percolating rain water. Excess ammonia that is not taken up by plants is oxidized to nitrate and leached to the water table. Thus, the real problem with fertilizer application to agricultural land is the contamination of the groundwater environment with nitrate-N.

The maximum permissible drinking water concentration for nitrate-N in the United States is 10 mg/l (Wilhelm *et al.*, 1994). This standard is often exceeded by the leaching of fertilizers into drinking water aquifers in agricultural areas. Because nitrate-N poses a significant risk of contamination to municipal wellheads, WHPA delineation should account for areas of the watershed that are zoned for agricultural management. Farming usually precedes urban development in the orderly planning of an area. As a result, any efforts to institute changes to farming practices in order to accommodate the protection of drinking water aquifers would have to be imposed after the WHPA boundaries had been zoned. This may best be achieved by instituting a soil sampling program to identify nitrate concentrations at all farms contained within each WHPA boundary, and providing agricultural extension information to educate farm operators on the health hazards of increased nitrates in drinking water. However, the cost of such a sampling and education program would likely have to be paid for by the municipality since these procedures are not a generally accepted part of current agricultural management practices.

8.8 The Use of Geographic Information Systems for Decision Making

A Geographic Information System database, in ArchInfo format, has just recently become available for the region of Dover Township, New Jersey. This database contains information on the development characteristics around the UWTR wellfields, which includes existing industrial land, and areas that could potentially be developed as industrial land. This database has the potential to be used for determining the exact amount of each type of development within each wellhead protection area. This would have the effect of providing a very accurate method of determining the cost of failure associated with each zone of delineation uncertainty. This remains as an area of potential research.

8.9 Summary

A number of issues arose out of the application of environmental decision making to the determination of the best methodology for delineating WHPA boundaries around municipal wellfields. From the research it is evident that the decision making paradigm developed herein is both flexible and robust. It has been successfully applied to determining the best alternative for WHPA delineation under all of the criteria and constraints currently detailed out by the USEPA. It

may also be applied to WHPA delineation under circumstances that were not specifically analyzed in the present research study. This includes the use of three-dimensional groundwater analysis for delineating WHPA boundaries, the addition of contaminant transport phenomena to the WHPA delineation process, and the accounting for non-point source pollution protection in the process. With additional research, this decision making paradigm has the potential to be a more powerful tool for solving groundwater protection issues that are faced by communities in the preservation of the water quality of drinking water aquifers.

CHAPTER 9
CONCLUSIONS AND RECOMMENDATIONS

The goal of this research study was to develop a decision making methodology that could be used to determine the best alternative for delineating wellhead protection areas around municipal wellheads, and to apply this methodology to the municipal wells at a field site. The first step that was taken to achieve this goal was to choose a suitable study site for the application of the decision making model. The next steps for achieving this goal were to develop the concept of the risk of failure of wellhead protection areas as the basis of decision making, to develop a Wellhead Protection Plan for the study site, to apply all potential WHPA delineation techniques to the wells at the site, and to use the decision making model to choose the best alternative for groundwater protection. Regret analysis was used to determine the regret, or opportunity loss, associated with choosing non-optimal delineation techniques. Uncertainty analysis was applied to the best alternative to determine the uncertainty associated with the location of the WHPA boundary from numerical WHPA modeling. Finally, this research study analyzed the transient nature of wellfield operation and investigated sustainable well rates to select a more appropriate well rate for implementing WHPA delineation.

The municipal wellfields for the community of Pleasant Plains, New Jersey were chosen to be the study site as presented in Chapter 3. These wellfields are owned by United Water Toms River and are located directly downgradient of the Reich Farm Superfund site. The fact that a Superfund site is hydraulically linked to the water supply aquifer for the community indicates that groundwater protection is needed. A conceptual model was developed for the groundwater flow system in the Pleasant Plains area of Dover Township, Ocean County, New Jersey. From a hydrogeologic perspective Dover Township is underlain by the Cohansey-Kirkwood aquifer system. The Cohansey Formation is the upper phreatic aquifer that is the principle source of water for Dover Township. A steady state groundwater flow analysis was performed for the Cohansey aquifer beneath the United Water Toms River wellfields. This analysis revealed that prior to the operation of the wells, contaminants from the Superfund site migrated toward the Toms River. The imposition of the pumping wells on the aquifer changed the flow of groundwater and directed contaminants toward the municipal wells. The addition of dispersive transport to the forward particle tracking analysis resulted in a greater number of the wellheads in the Parkway wellfield becoming contaminated. A sensitivity analysis revealed that the most sensitive parameter for the performance measure of groundwater head is net infiltration and that the most sensitive parameter for the performance measure of capture zone area is wellhead pumping rate.

The fact that the Superfund site is a source of contamination to the municipal wellheads indicated that the delineation of wellhead protection areas should include information on contaminant movement in the subsurface environment. As a first step, a random walk (RWAPT) model was developed to include dispersive transport to the analysis of particle movement in the groundwater flow field. A convex hull capture zone model was developed to generate a WHPA boundary from the resulting numerical model particle pathlines. The RWAPT model was added to the suite of acceptable techniques that would be used for delineating WHPA boundaries around the wellheads at the study site.

A WHPA boundary decision making model, based on the benefit-cost-risk model, was developed in Chapter 4. Benefit-cost-risk analysis was originally developed for comparing engineering designs that pose a risk of failure to the natural environment. The benefits of wellhead protection areas are the communal benefits of a clean source of potable water. The costs of WHPA delineation are the costs of modeling the WHPA boundary and the cost of producing the Wellhead Protection Report that accompanies the WHPA boundary. The risks associated with WHPA delineation are entrenched in the cost of failure and probability of failure for the modeled boundary. The standard for determining failure for WHPA modeling was chosen to be the zone of confidence for the complete set of boundaries under comparison. The zone of delineation uncertainty for each boundary represents the failure of the model to delineate the true WHPA boundary. The cost of failure is a function of the amount of land within the failure area and the economic value attributed to groundwater protection in each WHPA boundary. The probability of failure is the probability that WHPA model has failed to generate the true WHPA boundary.

The next step to determining the best alternative for groundwater protection was to apply the complete set of WHPA modeling techniques to the UWTR wellheads as presented in Chapter 4. Benefit-cost-risk analysis was then used to compare the set of boundaries that were produced for each protection zone. The best alternative for Zone I was the 250 foot arbitrary fixed radius boundary and for Zones II and III was the RWAPT numerical modeling boundary. The results of the present analysis have shown that WHPA decision making is a useful application for the benefit-cost-risk analysis methodology. This research study shows that the added cost of using a numerical model to delineate the WHPA boundaries has a large return in reducing the risk of failure.

Regret analysis was applied to the best alternative for WHPA delineation in Chapter 5. The Zone I, Zone II and Zone III RWAPT boundaries were subsequently compared to the other WHPA boundaries in order to determine the regret associated with choosing a non-optimal WHPA boundary. From the analysis, the results indicate that the choice of WHPA delineation technique has serious

implications on the amount of land encompassed within each WHPA boundary. There is a direct correlation between the scientific complexity of the delineation model and its ability to represent the true WHPA boundary. There are also serious implications for using the arbitrary fixed radius technique for delineating the Zone I boundary. The purpose of the WHPA I protection zone is to prevent industrial development in order to reduce the immediate risk of groundwater contamination reaching the wellfield. Therefore, the WHPA delineation technique should be complex enough to determine whether an area is hydraulically connected to the wellfield.

Uncertainty analysis was applied to the numerical modeling WHPA boundaries in Chapter 6. Two techniques were used to analyze the uncertainty associated with model input parameters. The first technique was first order second moment analysis and the results indicate that net infiltration to the upper boundary of the conceptual model contributes approximately 85% to the total uncertainty in the size of the numerical capture zone. Well pumping rates contribute to almost all of the rest of the uncertainty in capture zone size. The second technique was direct parameter sampling. This technique was used to provide multiple realizations of both STLINE and RWAPT numerical models of the WHPA boundary. The probability distribution of WHPA boundary was found to be normal and the 50^{th} percentile WHPA boundary was found to be in almost the exact location of the deterministic WHPA boundary. It was concluded that the 50^{th} percentile boundary provides a better representation of the average numerical WHPA boundary. It was also concluded that the 95^{th} percentile boundary approaches the 50^{th} percentile boundary as the uncertainty in the input parameters is reduced, and therefore, the 95^{th} percentile boundary was recommended as the boundary that best represents the numerical modeling WHPA boundary for WHPA decision making.

The value of information on uncertainty was also determined using uncertainty analysis. This value represents the maximum exploration and sampling budget that should be put toward obtaining new sample points to reduce input uncertainty. Based on the first order second moment analysis, the best use of this budget is to put it toward reducing uncertainty in the knowledge of net infiltration to the groundwater flow model. A reduction in the variance of the infiltration will have the greatest impact on reducing the variance in WHPA boundary location.

Transient analysis was applied to the delineation of wellhead protection areas in Chapter 7. From the transient analysis of wellfield operation, the zoning of groundwater protection areas must take into account both the existing conditions within a wellfield and any potential future development conditions that may effect groundwater pumping. This requires some foresight into the potential well development that may arise due to an increased demand for potable water. The transient analysis provided information that is best summarized by stating that the delineation of WHPAs should be

based on all potential wellheads under their maximum sustainable well pumping rates. If any future wellhead development occurs in the vicinity of existing WHPAs, the decision making process for future WHPAs must take into account the added area encompassed by new groundwater protection zones. The decommissioning of an existing well within a wellfield will also have an effect on the direction and magnitude of groundwater velocity in the aquifer. However, the decommissioning of a wellhead may only be temporary depending on the water quality and water quantity conditions of the aquifer around the wellhead. As a result, even though the decommissioning of the wellhead has a measurable effect on the size of the WHPA boundaries, there is no reason to change the location of the original WHPA boundaries until the fate of the decommissioned wellhead has been finalized.

Finally, in Chapter 8, a number of factors that make the use of benefit-cost-risk analysis for groundwater protection planning unique were discussed in order to look at the implications of environmental decision making on the delineation of WHPA boundaries. It is evident that the decision making paradigm developed in this research study is both flexible and robust. It has been successfully applied to determining the best WHPA boundary under all of the criteria and constraints currently suggested out by the USEPA. It may also be applied to WHPA delineation under circumstances that were not specifically analyzed in the present research study. This includes the use of three-dimensional groundwater analysis for delineating WHPA boundaries, the addition of contaminant transport phenomena to the WHPA delineation process, and the accounting for non-point source pollution protection in the process. With additional research, this decision making paradigm has the potential to be a powerful tool for solving groundwater protection problems faced by communities in the preservation of the water quality of drinking water aquifers.

In conclusion, the author feels that the present study provides a comprehensive analysis of the decision making process for delineating wellhead protection area boundaries. However, as presented in this summary, there are a number of areas of research that have not yet been addressed. These include the application of environmental decision making to three-dimensional WHPA boundaries, the affect of uncertainty in dispersion, the development of a surrogate chemical for introducing contaminant transport into WHPA delineation and the use of a GIS database of development at the study site to better determine the cost of failure. Continued research into these areas will provide better validation of the potential of this technique to help municipal planners make more knowledgeable decision about groundwater protection.

CHAPTER 10

REFERENCES

Adams, B. and Foster, S.D. (1992) "Land-surface zoning for groundwater protection". **Journal of the Institute of Water and Environmental Management** 6: 312-319.

Akindunni, F.F., Gillham, R.W., Conant, B.Jr. and Franz, T. (1995) "Modeling of contaminant movement near pumping wells: saturated-unsaturated flow with particle tracking". **Ground Water** 31(2): 264-274.

Baecher, G.B., Pate, M.E. and De Neufville, R. (1980) "Risk of dam failure in benefit-cost approach". **Water Resource Research** 16(3): 449-456.

Bair, E.S., Sheets, R.A. and Eberts, S.M. (1990) "Particle-tracking analysis of flowpaths and travel times from hypothetical spill sites within the capture area of a wellfield". **Ground Water** 28(6): 884-892.

Bair, E.S., Safreed, C.M. and Stasny, E.A. (1991) "A Monte Carlo-based approach for determining traveltime-related capture zones of wells using convex hulls as confidence regions". **Ground Water** 29(6): 849-855.

Bair, E.S. and Roadcap, G.S. (1992) "Comparison of flow models used to delineate capture zones of wells: 1. Leaky confined fractured-carbonate aquifer". **Ground Water** 30(2): 199-211.

Baker, C.P., Bradley, M.D. and Kaczor-Bobiak, S.M. (1993) "Wellhead protection area delineation: linking flow model with GIS". **Journal of Water Resources Planning and Management** 119(2): 275-287.

Bakker, M. and Strack, O.D.L. (1996) "Capture zone delineation in two-dimensional groundwater flow models". **Water Resources Research** 32(5): 1309-1315.

Barlow, P.M. (1994) "Two- and three-dimensional pathline analysis of contributing areas to public-supply wells of Cape Cod, Massachusetts". **Ground Water** 32(3): 399-410.

Bates, J.K. and Evans, J.E. (1996) "Evaluation of wellhead protection area delineation methods, applied to the municipal well field at Elmore, Ottawa County, Ohio". **Ohio Journal of Science** 96(1): 13-22.

Blandford, T.N. and Huyakorn, P.S. (1990) "WHPA: a modular semi-analytical model for the delineation of wellhead protection areas". USEPA. Office of Ground-Water Protection.

Buxton, H.T., Reilly, T.E., Pollock, D.W. and Smolensky, D.A. (1991) "Particle tracking analysis of recharge areas on Long Island, New York". **Ground Water** 29(1): 63-71.

Carrera, J. (1993) "An overview of uncertainties in modelling groundwater solute transport". **Journal of Contaminant Hydrology** 13: 23-48.

Cleary, C.B.F. and Cleary, R.W. (1991) "Delineation of wellhead protection areas: theory and practice". **Water Science and Technology** 24(11): 239-250.

Coe, C.J., Jenkins, T. and Bhatt, H. (1989) "Developing a wellfield protection, development and management plan in a glacial valley-till aquifer - a case study". **Proceedings of the Fourth Annual Hazardous Waste & Hazardous Material Management Conference**. September 12-14, 1989, Cincinnati, Ohio. p 243-260.

Cordes, C. and Kinzelbach, W. (1992) "Continuous groundwater velocity fields and path lines in linear, bilinear and trilinear finite elements". **Water Resources Research** 28(11): 2903-2911.

Costanza, R. and Sklar, F.H. (1985) "Articulation, accuracy and effectiveness of mathematical models: a review of freshwater wetland applications". **Ecological Modelling** 27: 45-68.

Coughanowr, C.A., Witten, J.D. and Horsley, S.W. (1989) "Cumulative impacts of land development within wellhead protection areas: assessment and control". **Proceedings of the FOCUS**

Conference on Eastern Regional Ground Water Issues. October 17 - 19, 1989, Kitchener, Ontario. National Water Well Association, Dublin, Ohio. 1989. p 407-421.

Dagan, G. (1986) "Spatial theory of groundwater flow and transport: pore to laboratory, laboratory to formation, and formation to regional scale". **Water Resources Research** 22(9): 120S-134S.

Davis, D.R., Kisiel, C.C. and Duckstein, L. (1972) "Bayesian decision theory applied to design in hydrology". **Water Resources Research** 8(1): 33-41.

DeHan, R.S. (1986) "New approach to protection of sensitive aquifers in Florida". **Proceedings of the FOCUS Conference on Southeastern Ground Water Issues**. October 6-8, 1986, Tampa, Fla. National Water Well Association, Dublin, Ohio. p. 59-69.

DelVecchio, G.M. and Haith, D.A. (1993) "Probabilistic screening of ground-water contaminants". **Journal of Environmental Engineering** 119(2): 287-299.

EBASCO Services Inc. (1988) "Final draft supplemental RI report Reich Farm site, Dover Township, Ocean County, New Jersey". **EPA Contract No. 68-01-7250**.

Eberts, S.M. and Bair, E.S. (1990) "Simulated effects of quarry dewatering near a municipal well field". **Ground Water** 28(1): 37-47.

Evers, S. and Lerner, D.N. (1998) "How uncertain is our estimate of a wellhead protection zone?" **Ground Water** 36(1): 49-57.

Freeze, R.A. (1975) "A stochastic-conceptual analysis of one-dimensional groundwater flow in nonuniform homogeneous media". **Water Resources Research** 11(5): 725-741.

Freeze, R.A. and Cherry, J.A. (1979) "Groundwater". Prentice- Hall, Englewood Cliffs, N.J., 07632. 604 p.

Freeze, R.A., Massmann, J. Smith, L., Sperling, T. and James, B. (1990) "Hydrogeologic decision analysis: 1. A framework". **Ground Water** 28(5): 738-766.

Freeze, R.A., James, B., Massmann, J., Sperling, T. and Smith, L. (1992) "Hydrogeologic decision analysis: 4. The concept of data worth and its use in the development of site investigation strategies". **Ground Water** 30(4): 574-588.

Gelhar, L.W. (1986) "Stochastic subsurface hydrology from theory to applications". **Water Resources Research** 22(9): 135S-145S.

GeoTrans, Inc. (1987) "User's manual: STLINE version 1.9". GeoTrans Inc., 250 Exchange Place, Suite A, Herndon, VA, 22070. 29 p.

GeoTrans Inc. (1989) "Data input guide for SWIFT III the Sandia Waste-Isolation Flow and Transport model for fractured media, release 2.29" GeoTrans Inc., 250 Exchange Place, Suite A, Herndon, VA, 22070.

Gorelick, S.M. (1983) "A review of distributed parameter groundwater management modeling methods". **Water Resources Research** 19(2): 305-319.

Griswold, W.J. and Donohue, J.J. (1989) "Determining the area of contribution to a well field: a case study and methodology for wellhead protection". **Proceedings of the FOCUS Conference on Eastern Regional Ground Water Issues**. October 17 - 19, 1989, Kitchener, Ontario. National Water Well Association, Dublin, Ohio. 1989. p 345-357.

Guiguer, N. and Franz, T. (1991) "Development and applications of a wellhead protection area delineation computer program" **Water Science and Technology** 24(11): 51-62.

Hamed, M.M., Conte, J.P. and Bedient, P.B. (1995) "Probabilistic screening tool for ground water contamination assessment". **Journal of Environmental Engineering** 121(11): 767-775.

Harmsen, E.W., Converse, J.C., Anderson, M.P. and Hoopes, J.A. (1991a) "A model for evaluating the three-dimensional groundwater dividing pathline between a contaminant source and a partially penetrating water-supply well". **Journal of Contaminant Hydrology** 8: 71-90.

Harmsen, E.W., Converse, J.C. and Anderson, M.P. (1991b) "Application of the Monte Carlo simulation procedure to estimate water-supply well/septic tank-drainfield separation distance in the Central Wisconsin sand plain". **Journal of Contaminant Hydrology** 8: 91-109.

Hoeksema, R.J. and Kitanidis, P.K. (1985) "Analysis of the spatial structure of properties of selected aquifers". **Water Resources Research** 21(4): 563-572.

Iman. R.L. and Conover, W.J. (1979) "The use of rank transform in regression". **Technometrics** 21(4): 499-509.

James, B.R. and Freeze, R.A. (1993) "The worth of data in predicting aquitard continuity in hydrogeological design". **Water Resources Research** 29(7): 2049-2065.

James, B.R. and Gorelick, S.M. (1994) "When enough is enough: the worth of monitoring data in aquifer remediation design". **Water Resources Research** 30(12): 3499-3513.

James, B.R., Huff, D.D., Trabalka, J.R., Ketelle, R.H. and Rightmire, C.T. (1996a) "Allocation of environmental remediation funds using economic risk-cost-benefit analysis: a case study". **Ground Water Monitoring and Remediation** 16(4): 95-105.

James, B.R., Gwo, J.-P. and Toran, L. (1996b) "Risk-cost decision framework for aquifer remediation design". **Journal of Water Resources Planning and Management** 122(6): 414-420.

Jardine, K. Smith, L. and Clemo, T. (1996) "Monitoring networks in fractured rocks: a decision analysis approach". **Ground Water** 34(3): 504-518.

Jennings, A.A. and Suresh, P. (1986) "Risk penalty functions for hazardous waste management". **Journal of Environmental Engineering** 112(1): 105-122.

Jennings, A.A., Mehta, N. and Mohan, S. (1994) "Superfund decision analysis in presence of uncertainty". **Journal of Environmental Engineering** 120(5): 1132-1150.

Job, C. (1997) "A summary of state wellhead protection programs". **Groundwater Monitoring and Remediation** 17(2): 61.63.

Keely, J.F. and Tsang, C.F. (1983) "Velocity plots and capture zones of pumping centers for ground-water investigations". **Ground Water** 21(6): 701-714.

La Venue, M., Andrews, R.W. and RamaRao, B.S. (1989) "Groundwater travel time uncertainty analysis using sensitivity derivatives". **Water Resources Research** 25(7): 1551-1566.

LeGrand, H.E. and Rosen, L. (1992) "Common sense in ground-water protection and management in the United States". **Ground Water** 30(6): 867-872.

Linquiti, P. and Harvey, R. (1989) "Wellhead protection: local and state roles". **Proceedings of the 4th Annual Conference on Hazardous Waste and Hazardous Materials Management.** September 12-14, 1989, Cincinatti, Ohio. p. 261-270.

Mantoglou, A. and Wilson, J.L. (1982) "The turning bands method for simulation of random fields using line generation by a spectral method". **Water Resources Research** 18(5): 1379-1394.

Marin, C.M., Medina, Jr., M.A. and Butcher, J.B. (1989) "Monte Carlo analysis and bayesian decision theory for assessing the effects of waste sites on groundwater, I: theory". **Journal of Contaminant Hydrology** 5: 1-13.

Massmann, J. and Freeze, R.A. (1987a) "Groundwater Contamination from waste management sites: The interaction between risk-based engineering design and regulatory policy 1. Methodology". **Water Resources Research** 23(2): 351-367.

Massmann, J. and Freeze, R.A. (1987b) "Groundwater Contamination from waste management sites: The interaction between risk-based engineering design and regulatory policy 1. Results". **Water Resources Research** 23(2): 368-380.

Massmann, J., Freeze, R.A., Smith, L., Sperling, T. and James, B. (1991) "Hydrogeologic decision analysis: 2. Application to ground-water contamination". **Ground Water** 29(4): 536-548.

Medina, Jr., M.A., Butcher, J.B. and Marin, C.M. (1989) "Monte Carlo analysis and bayesian decision theory for assessing the effects of waste sites on groundwater, II: applications". **Journal of Contaminant Hydrology** 5: 15-31.

Mejia, J.M. and Rodriquez-Iturbe, I. (1974) "On the synthesis of random field sampling from the spectrum: an application to the generation of hydrologic spatial processes". **Water Resources Research** 10(4): 705-711.

Mercer, J.W., Silka, L.R. and Faust, C.R. (1983) "Modeling ground-water flow at Love Canal, New York". **Journal of Environmental Engineering** 109(4): 924-942.

Mull, R., Harig, F. and Pielke, M. (1992) "Groundwater management in the urban area of Hanover, Germany". **Journal of the Institute of Water and Environmental Management** 6: 199-205.

National Research Council (1990) "Ground water models: scientific and regulatory applications". Water Science and Technology Board, Committee on Ground Water Modeling Assessment, National Research Council. National Academy Press, Washington, D.C. 303 p.

Neufeld, P. and Mulamootil, G.G. (1991) "Groundwater protection in Canada: a preliminary inquiry". **Ontario Geographer** 37: 15-22.

Neuman, S.P. (1980) "A statistical approach to the inverse problem of aquifer hydrology 3. improved solution method and added perspective" **Water Resources Research** 16(2): 331-346.

Olivieri, A.W., Eisenburg, D.M. and Cooper, R.C. (1986) "Groundwater contamination site ranking methodology". **Journal of Environmental Engineering** 112(4): 757-769.

Pollock, D.W. (1988) "Semianalytic computations of pathlines for finite-difference models" **Ground Water** 26: 743-750.

Press, W.H., Flannery, B.P., Teukolsky, S.A. and W.T. Vetterling (1992) "Numerical recipes: the are of scientific computing". Cambridge University Press, New York, NY, 10011, USA. 702 pp.

Ramanarayanan, T.S., Storm, D.E. and Smolen, M.D. (1995) "Seasonal pumping variation effects on wellhead protection area delineation". **Water Resources Bulletin** 31(3): 421-430.

Raucher, R.L. (1983) "A conceptual framework for measuring the benefits of groundwater protection". **Water Resource Research** 19(2): 320-326.

Reeves, M., Ward, D.S., Johns, N.D., Harlan, C. and Cranwell, R.M. (1985) "Data input guide for SWIFT II the sandia waste-isolation flow and transport model for fractured media". Sandia National Laboratories, Albuquerque, New Mexico 87185. 201 p.

Reichard, E.G. and Evans, J.S. (1989) "Assessing the value of hydrogeologic information for risk-based remedial action decisions". **Water Resources Research** 25(7): 1451-1460.

Reichard, E.G., Cranor, C., Raucher, R. and Zapponi, G. (1990) "Groundwater contamination risk assessment: A guide to understanding and managing uncertainties". **IAHS Publication No. 196**. IAHS Press, Institute of Hydrology, Wallingford, Oxfordshire, U.K. 204 p.

Rifai, H.S., Hendricks, L.A., Kilborn, K. and Bedient, P.B. (1993) "A geographic information system (GIS) user interface for delineating wellhead protection areas". **Ground Water** 31(3): 480-488.

Robin, M.J.L., Gutjahr, A.L., Sudicky, E.A. and Wilson, J.L. (1993) "Cross-correlated random field generation with the direct fourier transform method". **Water Resources Research** 29(7): 2385-2397.

Rudolph, D.L. (1991) "Assessing contamination potential in urban groundwater supply systems through wellhead protection strategies". **AWWA/OWWA Joint Meeting**, Hamilton, Ontario, April 28 - May 1, 1991. 25 p.

Schafer-Perini, A.L. and Wilson, J.L. (1991) "Efficient and accurate front tracking for two-dimensional groundwater flow models". **Water Resources Research** 27(7): 1471-1485.

Schleyer, R., Milde, G. and Milde, K. (1992) "Wellhead protection zones in Germany: delineation, research and management". **Journal of the Institute of Water and Environmental Management** 6: 302-311.

Shafer, J.M. (1987) "Reverse pathline calculation of time-related capture zones in nonuniform flow". **Ground Water** 25(3): 283-289.

Shook, G. and Grantham, C. (1993) "A decision analysis technique for ranking sources of groundwater pollution". **Journal of Environmental Management** 37: 201-206.

Skaggs, T.H. and Barry, D.A. (1996) "Sensitivity methods for time-continuous, spatially discrete groundwater contaminant transport models". **Water Resources Research** 32(8): 2409-2420.

Smith, L. and Freeze, R.A. (1979) "Stochastic analysis of steady state groundwater flow in a bounded domain. 2: Two dimensional simulation". **Water Resources Research** 15(6): 1543-1559.

Smith, L. and Schwartz, F.W. (1981) "Mass transport 2. Analysis of uncertainty in prediction". **Water Resources Research** 17(2): 351-369.

Sperling, T., Freeze, R.A., Massmann, J., Smith, L. and James, B. (1992) "Hydrogeologic decision analysis: 3. Application to design of a ground-water control system at an open pit mine". **Ground Water** 30(3): 376-389.

Springer, A.E. and Bair, E.S. (1992) "Comparison of methods used to delineate capture zones of wells: 2. Stratified-drift buried-valley aquifer". **Ground Water** 30(6): 908-917.

Sykes, J.F., Wilson, J.L. and Andrews, R.W. (1985) "Sensitivity analysis for steady state groundwater flow using adjoint operators". **Water Resources Research** 21(3): 359-371.

Sykes, J.F. (1990) "GWPGM3 Documentation and users guide - statistical version for flow". Department of Civil Engineering, University of Waterloo, Waterloo, Ontario, Canada.

Sykes, J.F. (1995) "Final groundwater modeling supplement to the phase II pre-design report - evaluation of groundwater remedial design scenarios". Report prepared for Union Carbide Corporation, South Charleston, West Virginia. 27 p.

Sykes, J.F. and Harvey, D.J.M. (1996) "The risk associated with aquifer remediation: the influence of parameter uncertainty" **ModelCARE '96** International Conference on Calibration and Reliability in Groundwater Modeling, Golden, Colorado, 24-26 September 1996.

Tiedeman, C. and Gorelick, S. (1993) "Analysis of uncertainty in optimal groundwater containment capture design". **Water Resources Research** 29(7): 2139-2153.

Townley, L.R. and Davidson, M.R. (1988) "Definition of a capture zone for shallow water table lakes". **Journal of Hydrology** 104: 53-76.

Tschannerl, G. (1971) "Designing reservoirs with short streamflow records". **Water Resources Research** 7(4): 827-833.

U.S. Environmental Protection Agency (1987) "Guidelines for delineation of wellhead protection areas". **EPA 440/6-87-010** U.S. EPA, Office of Groundwater Protection, Washington, D.C.

U.S. Environmental Protection Agency (1990) "The national water quality inventory - 1988 report to congress". U.S. EPA, Office of Water, Washington DC 20460.

U.S. Environmental Protection Agency (1991) "Managing groundwater contamination sources in wellhead protection areas: a priority setting approach". U.S. EPA, Office of Water, Washington, DC 20460.

U.S. Environmental Protection Agency (1993) "WHPA: a modular semi-analytical model for the delineation of wellhead protection areas". U.S. EPA, Office of Drinking Water and Ground Water, Washington, DC 20460.

Varljen, M.D. and Shafer, J.M. (1991) "Assessment of uncertainty in time-related capture zones using conditional simulation of hydraulic conductivity". **Ground Water** 29(5): 737-748.

Viessman, Jr. W. and Hammer, M.J. (1993) "Water Supply and Pollution Control". Harper Collins College Publishers, New York, NY, 10022.

Vemuri, V. and Karplus, W.J. (1969) "Identification of nonlinear parameters of ground water basins by hybrid computation" **Water Resources Research** 5(1): 172-185.

Walton, W.C. (1991) "Principles of groundwater engineering". Lewis Publishers Inc., Chelsea, MI. pp. 546.

Watts, R.J. (1997) "Hazardous wastes: sources, pathways, receptors". JohnWiley & Sons, Toronto.

Whittemore, D.O., Merchant, J.W., Whistler, J., McElwee, C.D., and Woods, J.J. (1987) "Ground water protection planning using the ERDAS geographic information system: automation of DRASTIC and time-related capture zones". **Proceedings of the FOCUS Conference on Midwestern Ground Water Issues**. National Water Well Association, Dublin, Ohio. 1987. p. 359-374.

Wijedasa, H.A. and Kemblowski, M.W. (1993) "Bayesian decision analysis for plume interception wells". **Ground Water** 31(6): 948-952.

Wilhelm, S.R., Schiff, S.L. and Cherry, J.A. (1994) "Biogeochemical evolution of domestic waste water in septic systems: 1. conceptual model". **Ground Water** 32(6): 905-916.

Williams, S.A. and El-Kadi A.I. (1986) "COVAR - A computer program for generating two-dimensional fields of autocorrelated parameters by matrix decomposition". International Ground Water Modeling Center, Butler University, Indianapolis, Indiana 46208. 8 p.

Wolka, K.K. and Austin, T.A. (1988) "Groundwater contamination benefit-cost analysis methodology". **Journal of Water Resources Planning and Management** 114(2): 210-221.

Wuolo, R.W., Dahlstrom, D.J. and Fairbrother, M.D. (1995) "Wellhead protection area delineation using the analytic element method of ground-water modeling". **Ground Water** 33(1): 71-83.

Wu, J.S. and Hilger, H. (1984) "Evaluation of EPA's hazard ranking system". **Journal of Environmental Engineering** 110(4): 797-807.

Zaporozec, A. editor (1985) "Groundwater protection principles and alternatives for Rock County, Wisconsin". Wisconsin Geological and Natural History Survey, Madison, WI 53705. 71p.

Zheng, C. (1989) "PATH3D". S.S. Papadopulos & Assoc., Rockville, MD.

APPENDIX I

FORTRAN CODE

CAPZON.FOR

```
*CAPZON.FOR*
C
C   This is a post STLINE filter written to check to see if the
C   capture zone based on the endpoints of the particle tracks
C   contains all of the outer most points in the CZ
C
C                                          Milo Harvey, April 1998
C
C   NP      = number of pathlines generated by G/W flow model
C   NPIP    = number of points in pathline I
C   CPX,CPY = capture zone points (x,y)
C
      IMPLICIT REAL*8 (A-H,O-Z)
      DIMENSION CPX(35),CPY(35),PTX(200,120),PTY(200,120),
     1          CPXOUT(35),CPYOUT(35)
      INTEGER NPIP(200)
C
C   read in pathline information from LINES.BLN
C
      OPEN(UNIT=20,FILE='lines.bln',STATUS='OLD')
      OPEN(UNIT=21,FILE='capzon.bln',STATUS='UNKNOWN')
C
C   echo information to the screen
C
      WRITE(*,*)
      WRITE(*,*)
      WRITE(*,*) '     ***********************************'
      WRITE(*,*) '     *          PROGRAM CAPZON         *'
      WRITE(*,*) '     ***********************************'
      WRITE(*,*)
      WRITE(*,*) '     generate a convex hull capture zone'
      WRITE(*,*)
C
C   initial all interim capture zone points to 0.0
C
      DO 7000 I0=1,33
        CPX(I0)=0.0
        CPY(I0)=0.0
 7000 CONTINUE
C
C   read in pathline points and determine the four extreme
C   points for analysis
C                              (9) <= ymax
C     xmin => (17)
C                                     (1) <= xmax
C               ymin => (25)
C
      READ(20,*) NP
      DO 7001 I1=1,NP
        READ(20,*) NPIP(I1)
        DO 7002 I2=1,NPIP(I1)
          READ(20,*) PTX(I1,I2),PTY(I1,I2)
C
C   initialize extreme points
C
          IF(I1.EQ.1.AND.I2.EQ.1) THEN
            CPX(1)=PTX(I1,I2)
            CPY(1)=PTY(I1,I2)
            CPX(9)=PTX(I1,I2)
            CPY(9)=PTY(I1,I2)
            CPX(17)=PTX(I1,I2)
            CPY(17)=PTY(I1,I2)
            CPX(25)=PTX(I1,I2)
            CPY(25)=PTY(I1,I2)
          ENDIF
C
C   determine extreme points
C
          IF(PTX(I1,I2).GT.CPX(1)) THEN
            CPX(1)=PTX(I1,I2)
            CPY(1)=PTY(I1,I2)
          ENDIF
          IF(PTY(I1,I2).GT.CPY(9)) THEN
            CPX(9)=PTX(I1,I2)
            CPY(9)=PTY(I1,I2)
          ENDIF
          IF(PTX(I1,I2).LT.CPX(17)) THEN
            CPX(17)=PTX(I1,I2)
            CPY(17)=PTY(I1,I2)
          ENDIF
          IF(PTY(I1,I2).LT.CPY(25)) THEN
            CPX(25)=PTX(I1,I2)
            CPY(25)=PTY(I1,I2)
          ENDIF
 7002   CONTINUE
 7001 CONTINUE
C
C   add one capture zone point on the end for closure
C
      CPX(33)=CPX(1)
      CPY(33)=CPY(1)
C
C   set a tolerance for determining if a point is an
C   extra capture zone point or just (0.0,0.0)
C
      TOLER=0.000001
C
C   for each of the 4 quadrants which are defined by
C   these 4 points determine a convex hull
C
C   1. QUADRANT I - pt(9)
C
C                                .
C                                  .
C                                    .
C                                      pt(1)
C
C   determine algebraic parameters needed for analysis
C
      IF(CPX(1).EQ.CPX(9).OR.CPY(1).EQ.CPY(9)) GOTO 7020
      DX=CPX(9)-CPX(1)
      DY=CPY(9)-CPY(1)
      SLOPE1=DY/DX
      SLOPE2=-DX/DY
C
C   for all of the points in each pathline
C   find the one that is the farthest away from the line
C   between CP(1) and CP(9), and call it CP(5)
C
      DISTMX=0.0
      DO 7004 I4=1,NP
        DO 7005 I5=1,NPIP(I4)
          IF(PTX(I4,I5).GT.CPX(9).AND.
     1       PTY(I4,I5).GT.CPY(1)) THEN
            DSLOPE=(SLOPE2-SLOPE1)
            XINT=((CPY(9)-PTY(I4,I5))-(SLOPE1*CPX(9))+
     1            (SLOPE2*PTX(I4,I5)))/DSLOPE
            YINT=(CPY(9)-(SLOPE1*(CPX(9)-XINT)))
            IF(PTX(I4,I5).GT.XINT) THEN
              DIST=((ABS(PTX(I4,I5)-XINT)**2.0)+
     1              (ABS(PTY(I4,I5)-YINT)**2.0))**0.50
              IF(DIST.GT.DISTMX) THEN
                CPX(5)=PTX(I4,I5)
                CPY(5)=PTY(I4,I5)
                DISTMX=DIST
              ENDIF
            ENDIF
          ENDIF
 7005   CONTINUE
 7004 CONTINUE
C
C   if we do not find a value for CP(5) there are no
C   extra points outside of the line from CP(1) to CP(9)
C   and we can end our analysis in Quadrant I
C
      IF(CPX(5).LT.TOLER.AND.CPY(5).LT.TOLER) GOTO 7020
C
C   now find one between CP(1) and CP(5), and call it CP(3)
C
      DX=CPX(5)-CPX(1)
      DY=CPY(5)-CPY(1)
      SLOPE1=DY/DX
      SLOPE2=-DX/DY
      DISTMX=0.0
      DO 7006 I6=1,NP
        DO 7007 I7=1,NPIP(I6)
          IF(PTX(I6,I7).GT.CPX(5).AND.
     1       PTY(I6,I7).GT.CPY(1)) THEN
            DSLOPE=(SLOPE2-SLOPE1)
            XINT=((CPY(5)-PTY(I6,I7))-(SLOPE1*CPX(5))+
     1            (SLOPE2*PTX(I6,I7)))/DSLOPE
            YINT=(CPY(5)-(SLOPE1*(CPX(5)-XINT)))
            IF(PTX(I6,I7).GT.XINT) THEN
              DIST=((ABS(PTX(I6,I7)-XINT)**2.0)+
     1              (ABS(PTY(I6,I7)-YINT)**2.0))**0.50
              IF(DIST.GT.DISTMX) THEN
                CPX(3)=PTX(I6,I7)
                CPY(3)=PTY(I6,I7)
                DISTMX=DIST
              ENDIF
            ENDIF
          ENDIF
 7007   CONTINUE
 7006 CONTINUE
C
C   now find one between CP(5) and CP(9), and call it CP(7)
C
      DX=CPX(9)-CPX(5)
      DY=CPY(9)-CPY(5)
      SLOPE1=DY/DX
      SLOPE2=-DX/DY
      DISTMX=0.0
      DO 7008 I8=1,NP
        DO 7009 I9=1,NPIP(I8)
          IF(PTX(I8,I9).GT.CPX(9).AND.
     1       PTY(I8,I9).GT.CPY(5)) THEN
            DSLOPE=(SLOPE2-SLOPE1)
            XINT=((CPY(9)-PTY(I8,I9))-(SLOPE1*CPX(9))+
     1            (SLOPE2*PTX(I8,I9)))/DSLOPE
            YINT=(CPY(9)-(SLOPE1*(CPX(9)-XINT)))
            IF(PTX(I8,I9).GT.XINT) THEN
              DIST=((ABS(PTX(I8,I9)-XINT)**2.0)+
     1              (ABS(PTY(I8,I9)-YINT)**2.0))**0.50
              IF(DIST.GT.DISTMX) THEN
                CPX(7)=PTX(I8,I9)
                CPY(7)=PTY(I8,I9)
                DISTMX=DIST
              ENDIF
            ENDIF
          ENDIF
 7009   CONTINUE
 7008 CONTINUE
C
C   if we do not find a value for CP(3) there are no
C   extra points outside of the line from CP(1) to CP(5)
C   so we can skip up and look between CP(5) and CP(9)
C
      IF(CPX(3).LT.TOLER.AND.CPY(3).LT.TOLER) GOTO 7019
C
C   now find one between CP(1) and CP(3), and call it CP(2)
C
      DX=CPX(3)-CPX(1)
      DY=CPY(3)-CPY(1)
      SLOPE1=DY/DX
      SLOPE2=-DX/DY
      DISTMX=0.0
      DO 7010 I10=1,NP
        DO 7011 I11=1,NPIP(I10)
          IF(PTX(I10,I11).GT.CPX(3).AND.
     1       PTY(I10,I11).GT.CPY(1)) THEN
            DSLOPE=(SLOPE2-SLOPE1)
            XINT=((CPY(3)-PTY(I10,I11))-(SLOPE1*CPX(3))+
     1            (SLOPE2*PTX(I10,I11)))/DSLOPE
            YINT=(CPY(3)-(SLOPE1*(CPX(3)-XINT)))
            IF(PTX(I10,I11).GT.XINT) THEN
              DIST=((ABS(PTX(I10,I11)-XINT)**2.0)+
     1              (ABS(PTY(I10,I11)-YINT)**2.0))**0.50
              IF(DIST.GT.DISTMX) THEN
                CPX(2)=PTX(I10,I11)
                CPY(2)=PTY(I10,I11)
                DISTMX=DIST
              ENDIF
            ENDIF
          ENDIF
 7011   CONTINUE
 7010 CONTINUE
C
C   now find one between CP(3) and CP(5), and call it CP(4)
```

```
C
      DX=CPX(5)-CPX(3)
      DY=CPY(5)-CPY(3)
      SLOPE1=DY/DX
      SLOPE2=-DX/DY
      DISTMX=0.0
      DO 7012 I12=1,NP
        DO 7013 I13=1,NPIP(I12)
          IF(PTX(I12,I13).GT.CPX(5).AND.
     1       PTY(I12,I13).GT.CPY(3)) THEN
            DSLOPE=(SLOPE2-SLOPE1)
            XINT=((CPY(5)-PTY(I12,I13))-(SLOPE1*CPX(5))+
     1            (SLOPE2*PTX(I12,I13)))/DSLOPE
            YINT=(CPY(5)-(SLOPE1*(CPX(5)-XINT)))
            IF(PTX(I12,I13).GT.XINT) THEN
              DIST=((ABS(PTX(I12,I13)-XINT)**2.0)+
     1              (ABS(PTY(I12,I13)-YINT)**2.0))**0.50
              IF(DIST.GT.DISTMX) THEN
                CPX(4)=PTX(I12,I13)
                CPY(4)=PTY(I12,I13)
                DISTMX=DIST
              ENDIF
            ENDIF
          ENDIF
 7013   CONTINUE
 7012 CONTINUE
C
C   if we do not find a value for CP(7) there are no
C   extra points outside of the line from CP(5) to CP(9)
C   and we can skip to the end
C
 7019 CONTINUE
      IF(CPX(7).LT.TOLER.AND.CPY(7).LT.TOLER) GOTO 7020
C
C   now find one between CP(5) and CP(7), and call it CP(6)
C
      DX=CPX(7)-CPX(5)
      DY=CPY(7)-CPY(5)
      SLOPE1=DY/DX
      SLOPE2=-DX/DY
      DISTMX=0.0
      DO 7014 I14=1,NP
        DO 7015 I15=1,NPIP(I14)
          IF(PTX(I14,I15).GT.CPX(7).AND.
     1       PTY(I14,I15).GT.CPY(5)) THEN
            DSLOPE=(SLOPE2-SLOPE1)
            XINT=((CPY(7)-PTY(I14,I15))-(SLOPE1*CPX(7))+
     1            (SLOPE2*PTX(I14,I15)))/DSLOPE
            YINT=(CPY(7)-(SLOPE1*(CPX(7)-XINT)))
            IF(PTX(I14,I15).GT.XINT) THEN
              DIST=((ABS(PTX(I14,I15)-XINT)**2.0)+
     1              (ABS(PTY(I14,I15)-YINT)**2.0))**0.50
              IF(DIST.GT.DISTMX) THEN
                CPX(6)=PTX(I14,I15)
                CPY(6)=PTY(I14,I15)
                DISTMX=DIST
              ENDIF
            ENDIF
          ENDIF
 7015   CONTINUE
 7014 CONTINUE
C
C   now find one between CP(7) and CP(9), and call it CP(8)
C
      DX=CPX(9)-CPX(7)
      DY=CPY(9)-CPY(7)
      SLOPE1=DY/DX
      SLOPE2=-DX/DY
      DISTMX=0.0
      DO 7016 I16=1,NP
        DO 7017 I17=1,NPIP(I16)
          IF(PTX(I16,I17).GT.CPX(9).AND.
     1       PTY(I16,I17).GT.CPY(7)) THEN
            DSLOPE=(SLOPE2-SLOPE1)
            XINT=((CPY(9)-PTY(I16,I17))-(SLOPE1*CPX(9))+
     1            (SLOPE2*PTX(I16,I17)))/DSLOPE
            YINT=(CPY(9)-(SLOPE1*(CPX(9)-XINT)))
            IF(PTX(I16,I17).GT.XINT) THEN
              DIST=((ABS(PTX(I16,I17)-XINT)**2.0)+
     1              (ABS(PTY(I16,I17)-YINT)**2.0))**0.50
              IF(DIST.GT.DISTMX) THEN
                CPX(8)=PTX(I16,I17)
                CPY(8)=PTY(I16,I17)
                DISTMX=DIST
              ENDIF
            ENDIF
          ENDIF
 7017   CONTINUE
 7016 CONTINUE
C
C   if any of the simulations don't produce extra points
C   jump out of the simulation loop
C
 7020 CONTINUE
C
C   2. QUADRANT II -              pt(9)
C
C
C
C
C                   pt(17)
C
C   determine algebraic parameters needed for analysis
C
      IF(CPX(9).EQ.CPX(17).OR.CPY(9).EQ.CPY(17)) GOTO 7040
      DX=CPX(17)-CPX(9)
      DY=CPY(17)-CPY(9)
      SLOPE1=DY/DX
      SLOPE2=-DX/DY
C
C   for all of the points in each pathline
C   find the one that is the farthest away from the line
C   between CP(9) and CP(17), and call it CP(13)
C
      DISTMX=0.0
      DO 7021 I21=1,NP
        DO 7022 I22=1,NPIP(I21)
          IF(PTX(I21,I22).LT.CPX(9).AND.
     1       PTY(I21,I22).GT.CPY(17)) THEN
            DSLOPE=(SLOPE2-SLOPE1)
            XINT=((CPY(17)-PTY(I21,I22))-(SLOPE1*CPX(17))
     1           +(SLOPE2*PTX(I21,I22)))/DSLOPE
            YINT=(CPY(17)-(SLOPE1*(CPX(17)-XINT)))
            IF(PTX(I21,I22).LT.XINT) THEN
              DIST=((ABS(PTX(I21,I22)-XINT)**2.0)+
     1              (ABS(PTY(I21,I22)-YINT)**2.0))**0.50
              IF(DIST.GT.DISTMX) THEN
                CPX(13)=PTX(I21,I22)
                CPY(13)=PTY(I21,I22)
                DISTMX=DIST
              ENDIF
            ENDIF
          ENDIF
 7022   CONTINUE
 7021 CONTINUE
C
C   if we do not find a value for CP(13) there are no
C   extra points outside of the line from CP(9) to CP(17)
C   and we can end our analysis in Quadrant II
C
      IF(CPX(13).LT.TOLER.AND.CPY(13).LT.TOLER) GOTO 7040
C
C   now find one between CP(9) and CP(13), and call it CP(11)
C
      DX=CPX(13)-CPX(9)
      DY=CPY(13)-CPY(9)
      SLOPE1=DY/DX
      SLOPE2=-DX/DY
      DISTMX=0.0
      DO 7023 I23=1,NP
        DO 7024 I24=1,NPIP(I23)
          IF(PTX(I23,I24).LT.CPX(9).AND.
     1       PTY(I23,I24).GT.CPY(13)) THEN
            DSLOPE=(SLOPE2-SLOPE1)
            XINT=((CPY(13)-PTY(I23,I24))-(SLOPE1*CPX(13)))+
     1           (SLOPE2*PTX(I23,I24)))/DSLOPE
            YINT=(CPY(13)-(SLOPE1*(CPX(13)-XINT)))
            IF(PTX(I23,I24).LT.XINT) THEN
              DIST=((ABS(PTX(I23,I24)-XINT)**2.0)+
     1              (ABS(PTY(I23,I24)-YINT)**2.0))**0.50
              IF(DIST.GT.DISTMX) THEN
                CPX(11)=PTX(I23,I24)
                CPY(11)=PTY(I23,I24)
                DISTMX=DIST
              ENDIF
            ENDIF
          ENDIF
 7024   CONTINUE
 7023 CONTINUE
C
C   now find one between CP(13) and CP(17), and call it CP(15)
C
      DX=CPX(17)-CPX(13)
      DY=CPY(17)-CPY(13)
      SLOPE1=DY/DX
      SLOPE2=-DX/DY
      DISTMX=0.0
      DO 7025 I25=1,NP
        DO 7026 I26=1,NPIP(I25)
          IF(PTX(I25,I26).LT.CPX(13).AND
     1       PTY(I25,I26).GT.CPY(17)) THEN
            DSLOPE=(SLOPE2-SLOPE1)
            XINT=((CPY(17)-PTY(I25,I26))-(SLOPE1*CPX(17))+
     1            (SLOPE2*PTX(I25,I26)))/DSLOPE
            YINT=(CPY(17)-(SLOPE1*(CPX(17)-XINT)))
            IF(PTX(I25,I26).LT.XINT) THEN
              DIST=((ABS(PTX(I25,I26)-XINT)**2.0)+
     1              (ABS(PTY(I25,I26)-YINT)**2.0))**0.50
              IF(DIST.GT.DISTMX) THEN
                CPX(15)=PTX(I25,I26)
                CPY(15)=PTY(I25,I26)
                DISTMX=DIST
              ENDIF
            ENDIF
          ENDIF
 7026   CONTINUE
 7025 CONTINUE
C
C   if we do not find a value for CP(11) there are no
C   extra points outside of the line from CP(9) to CP(13)
C   so we can skip up and look between CP(13) and CP(17)
C
      IF(CPX(11).LT.TOLER.AND.CPY(11).LT.TOLER) GOTO 7039
C
C   now find one between CP(9) and CP(11), and call it CP(10)
C
      DX=CPX(11)-CPX(9)
      DY=CPY(11)-CPY(9)
      SLOPE1=DY/DX
      SLOPE2=-DX/DY
      DISTMX=0.0
      DO 7027 I27=1,NP
        DO 7028 I28=1,NPIP(I27)
          IF(PTX(I27,I28).LT.CPX(9).AND.
     1       PTY(I27,I28).GT.CPY(11)) THEN
            DSLOPE=(SLOPE2-SLOPE1)
            XINT=((CPY(11)-PTY(I27,I28))-(SLOPE1*CPX(11))+
     1            (SLOPE2*PTX(I27,I28)))/DSLOPE
            YINT=(CPY(11)-(SLOPE1*(CPX(11)-XINT)))
            IF(PTX(I27,I28).LT.XINT) THEN
              DIST=((ABS(PTX(I27,I28)-XINT)**2.0)+
     1              (ABS(PTY(I27,I28)-YINT)**2.0))**0.50
              IF(DIST.GT.DISTMX) THEN
                CPX(10)=PTX(I27,I28)
                CPY(10)=PTY(I27,I28)
                DISTMX=DIST
              ENDIF
            ENDIF
          ENDIF
 7028   CONTINUE
 7027 CONTINUE
C
C   now find one between CP(11) and CP(13), and call it CP(12)
C
      DX=CPX(13)-CPX(11)
      DY=CPY(13)-CPY(11)
      SLOPE1=DY/DX
      SLOPE2=-DX/DY
      DISTMX=0.0
      DO 7029 I29=1,NP
```

```
      DO 7030 I30=1,NPIP(I29)
        IF(PTX(I29,I30).LT.CPX(11).AND.
     1     PTY(I29,I30).GT.CPY(13)) THEN
          DSLOPE=(SLOPE2-SLOPE1)
          XINT=((CPY(13)-PTY(I29,I30))-(SLOPE1*CPX(13))+
     1          (SLOPE2*PTX(I29,I30)))/DSLOPE
          YINT=(CPY(13)-(SLOPE1*(CPX(13)-XINT)))
          IF(PTX(I29,I30).LT.XINT) THEN
            DIST=((ABS(PTX(I29,I30)-XINT)**2.0)+
     1            (ABS(PTY(I29,I30)-YINT)**2.0))**0.50
            IF(DIST.GT.DISTMX) THEN
              CPX(12)=PTX(I29,I30)
              CPY(12)=PTY(I29,I30)
              DISTMX=DIST
            ENDIF
          ENDIF
        ENDIF
 7030   CONTINUE
 7029 CONTINUE
C
C   if we do not find a value for CP(15) there are no
C   extra points outside of the line from CP(13) to CP(17)
C   and we can skip to the end
C
 7039 CONTINUE
      IF(CPX(15).LT.TOLER.AND.CPY(15).LT.TOLER) GOTO 7040
C
C   now find one between CP(13) and CP(15), and call it CP(14)
C
      DX=CPX(15)-CPX(13)
      DY=CPY(15)-CPY(13)
      SLOPE1=DY/DX
      SLOPE2=-DX/DY
      DISTMX=0.0
      DO 7031 I31=1,NP
        DO 7032 I32=1,NPIP(I31)
          IF(PTX(I31,I32).LT.CPX(13).AND.
     1       PTY(I31,I32).GT.CPY(15)) THEN
            DSLOPE=(SLOPE2-SLOPE1)
            XINT=((CPY(15)-PTY(I31,I32))-(SLOPE1*CPX(15))+
     1            (SLOPE2*PTX(I31,I32)))/DSLOPE
            YINT=(CPY(15)-(SLOPE1*(CPX(15)-XINT)))
            IF(PTX(I31,I32).LT.XINT) THEN
              DIST=((ABS(PTX(I31,I32)-XINT)**2.0)+
     1              (ABS(PTY(I31,I32)-YINT)**2.0))**0.50
              IF(DIST.GT.DISTMX) THEN
                CPX(14)=PTX(I31,I32)
                CPY(14)=PTY(I31,I32)
                DISTMX=DIST
              ENDIF
            ENDIF
          ENDIF
 7032   CONTINUE
 7031 CONTINUE
C
C   now find one between CP(15) and CP(17), and call it CP(16)
C
      DX=CPX(17)-CPX(15)
      DY=CPY(17)-CPY(15)
      SLOPE1=DY/DX
      SLOPE2=-DX/DY
      DISTMX=0.0
      DO 7033 I33=1,NP
        DO 7034 I34=1,NPIP(I33)
          IF(PTX(I33,I34).LT.CPX(15).AND.
     1       PTY(I33,I34).GT.CPY(17)) THEN
            DSLOPE=(SLOPE2-SLOPE1)
            XINT=((CPY(17)-PTY(I33,I34))-(SLOPE1*CPX(17))+
     1            (SLOPE2*PTX(I33,I34)))/DSLOPE
            YINT=(CPY(17)-(SLOPE1*(CPX(17)-XINT)))
            IF(PTX(I33,I34).LT.XINT) THEN
              DIST=((ABS(PTX(I33,I34)-XINT)**2.0)+
     1              (ABS(PTY(I33,I34)-YINT)**2.0))**0.50
              IF(DIST.GT.DISTMX) THEN
                CPX(16)=PTX(I33,I34)
                CPY(16)=PTY(I33,I34)
                DISTMX=DIST
              ENDIF
            ENDIF
          ENDIF
 7034   CONTINUE
 7033 CONTINUE
C
C   if any of the simulations don't produce extra points
C   jump out of the simulation loop
C
 7040 CONTINUE
C
C   3. QUADRANT III -  pt(17)
C
C
C
C
C                                      pt(25)
C
C   determine algebraic parameters needed for analysis
C
      IF(CPX(17).EQ.CPX(25).OR.CPY(17).EQ.CPY(25)) GOTO 7060
      DX=CPX(25)-CPX(17)
      DY=CPY(25)-CPY(17)
      SLOPE1=DY/DX
      SLOPE2=-DX/DY
C
C   for all of the points in each pathline
C   find the one that is the farthest away from the line
C   between CP(17) and CP(25), and call it CP(21)
C
      DISTMX=0.0
      DO 7041 I41=1,NP
        DO 7042 I42=1,NPIP(I41)
          IF(PTX(I41,I42).LT.CPX(25).AND.
     1       PTY(I41,I42).LT.CPY(17)) THEN
            DSLOPE=(SLOPE2-SLOPE1)
            XINT=((CPY(25)-PTY(I41,I42))-(SLOPE1*CPX(25))
     1            +(SLOPE2*PTX(I41,I42)))/DSLOPE
            YINT=(CPY(25)-(SLOPE1*(CPX(25)-XINT)))
            IF(PTX(I41,I42).LT.XINT) THEN
              DIST=((ABS(PTX(I41,I42)-XINT)**2.0)+
     1              (ABS(PTY(I41,I42)-YINT)**2.0))**0.50
              IF(DIST.GT.DISTMX) THEN
                CPX(21)=PTX(I41,I42)
                CPY(21)=PTY(I41,I42)
                DISTMX=DIST
              ENDIF
            ENDIF
          ENDIF
 7042   CONTINUE
 7041 CONTINUE
C
C   if we do not find a value for CP(5) there are no
C   extra points outside of the line from CP(1) to CP(9)
C   and we can end our analysis in Quadrant I
C
      IF(CPX(21).LT.TOLER.AND.CPY(21).LT.TOLER) GOTO 7060
C
C   now find one between CP(17) and CP(21), and call it CP(19)
C
      DX=CPX(21)-CPX(17)
      DY=CPY(21)-CPY(17)
      SLOPE1=DY/DX
      SLOPE2=-DX/DY
      DISTMX=0.0
      DO 7043 I43=1,NP
        DO 7044 I44=1,NPIP(I43)
          IF(PTX(I43,I44).LT.CPX(21).AND.
     1       PTY(I43,I44).LT.CPY(17)) THEN
            DSLOPE=(SLOPE2-SLOPE1)
            XINT=((CPY(21)-PTY(I43,I44))-(SLOPE1*CPX(21))+
     1            (SLOPE2*PTX(I43,I44)))/DSLOPE
            YINT=(CPY(21)-(SLOPE1*(CPX(21)-XINT)))
            IF(PTX(I43,I44).LT.XINT) THEN
              DIST=((ABS(PTX(I43,I44)-XINT)**2.0)+
     1              (ABS(PTY(I43,I44)-YINT)**2.0))**0.50
              IF(DIST.GT.DISTMX) THEN
                CPX(19)=PTX(I43,I44)
                CPY(19)=PTY(I43,I44)
                DISTMX=DIST
              ENDIF
            ENDIF
          ENDIF
 7044   CONTINUE
 7043 CONTINUE
C
C   now find one between CP(21) and CP(25), and call it CP(23)
C
      DX=CPX(25)-CPX(21)
      DY=CPY(25)-CPY(21)
      SLOPE1=DY/DX
      SLOPE2=-DX/DY
      DISTMX=0.0
      DO 7045 I45=1,NP
        DO 7046 I46=1,NPIP(I45)
          IF(PTX(I45,I46).LT.CPX(25).AND.
     1       PTY(I45,I46).LT.CPY(21)) THEN
            DSLOPE=(SLOPE2-SLOPE1)
            XINT=((CPY(25)-PTY(I45,I46))-(SLOPE1*CPX(25))+
     1            (SLOPE2*PTX(I45,I46)))/DSLOPE
            YINT=(CPY(25)-(SLOPE1*(CPX(25)-XINT)))
            IF(PTX(I45,I46).LT.XINT) THEN
              DIST=((ABS(PTX(I45,I46)-XINT)**2.0)+
     1              (ABS(PTY(I45,I46)-YINT)**2.0))**0.50
              IF(DIST.GT.DISTMX) THEN
                CPX(23)=PTX(I45,I46)
                CPY(23)=PTY(I45,I46)
                DISTMX=DIST
              ENDIF
            ENDIF
          ENDIF
 7046   CONTINUE
 7045 CONTINUE
C
C   if we do not find a value for CP(19) there are no
C   extra points outside of the line from CP(17) to CP(21)
C   so we can skip up and look between CP(21) and CP(25)
C
      IF(CPX(19).LT.TOLER.AND.CPY(19).LT.TOLER) GOTO 7059
C
C   now find one between CP(17) and CP(19), and call it CP(18)
C
      DX=CPX(19)-CPX(17)
      DY=CPY(19)-CPY(17)
      SLOPE1=DY/DX
      SLOPE2=-DX/DY
      DISTMX=0.0
      DO 7047 I47=1,NP
        DO 7048 I48=1,NPIP(I47)
          IF(PTX(I47,I48).LT.CPX(19).AND.
     1       PTY(I47,I48).LT.CPY(17)) THEN
            DSLOPE=(SLOPE2-SLOPE1)
            XINT=((CPY(19)-PTY(I47,I48))-(SLOPE1*CPX(19))+
     1            (SLOPE2*PTX(I47,I48)))/DSLOPE
            YINT=(CPY(19)-(SLOPE1*(CPX(19)-XINT)))
            IF(PTX(I47,I48).LT.XINT) THEN
              DIST=((ABS(PTX(I47,I48)-XINT)**2.0)+
     1              (ABS(PTY(I47,I48)-YINT)**2.0))**0.50
              IF(DIST.GT.DISTMX) THEN
                CPX(18)=PTX(I47,I48)
                CPY(18)=PTY(I47,I48)
                DISTMX=DIST
              ENDIF
            ENDIF
          ENDIF
 7048   CONTINUE
 7047 CONTINUE
C
C   now find one between CP(19) and CP(21), and call it CP(20)
C
      DX=CPX(21)-CPX(19)
      DY=CPY(21)-CPY(19)
      SLOPE1=DY/DX
      SLOPE2=-DX/DY
      DISTMX=0.0
      DO 7049 I49=1,NP
        DO 7050 I50=1,NPIP(I49)
          IF(PTX(I49,I50).LT.CPX(21).AND.
     1       PTY(I49,I50).LT.CPY(19)) THEN
            DSLOPE=(SLOPE2-SLOPE1)
            XINT=((CPY(21)-PTY(I49,I50))-(SLOPE1*CPX(21))+
     1            (SLOPE2*PTX(I49,I50)))/DSLOPE
            YINT=(CPY(21)-(SLOPE1*(CPX(21)-XINT)))
```

```
            IF(PTX(I49,I50).LT.XINT) THEN
              DIST=((ABS(PTX(I49,I50)-XINT)**2.0)+
     1              (ABS(PTY(I49,I50)-YINT)**2.0))**0.50
              IF(DIST.GT.DISTMX) THEN
                CPX(20)=PTX(I49,I50)
                CPY(20)=PTY(I49,I50)
                DISTMX=DIST
              ENDIF
            ENDIF
          ENDIF
 7050   CONTINUE
 7049 CONTINUE
C
C   if we do not find a value for CP(23) there are no
C   extra points outside of the line from CP(21) to CP(25)
C   and we can skip to the end
C
 7059 CONTINUE
      IF(CPX(23).LT.TOLER.AND.CPY(23).LT.TOLER) GOTO 7060
C
C   now find one between CP(21) and CP(23), and call it CP(22)
C
      DX=CPX(23)-CPX(21)
      DY=CPY(23)-CPY(21)
      SLOPE1=DY/DX
      SLOPE2=-DX/DY
      DISTMX=0.0
      DO 7051 I51=1,NP
        DO 7052 I52=1,NPIP(I51)
          IF(PTX(I51,I52).LT.CPX(23).AND.
     1       PTY(I51,I52).LT.CPY(21)) THEN
            DSLOPE=(SLOPE2-SLOPE1)
            XINT=((CPY(23)-PTY(I51,I52))-(SLOPE1*CPX(23))+
     1            (SLOPE2*PTX(I51,I52)))/DSLOPE
            YINT=(CPY(23)-(SLOPE1*(CPX(23)-XINT)))
            IF(PTX(I51,I52).LT.XINT) THEN
              DIST=((ABS(PTX(I51,I52)-XINT)**2.0)+
     1              (ABS(PTY(I51,I52)-YINT)**2.0))**0.50
              IF(DIST.GT.DISTMX) THEN
                CPX(22)=PTX(I51,I52)
                CPY(22)=PTY(I51,I52)
                DISTMX=DIST
              ENDIF
            ENDIF
          ENDIF
 7052   CONTINUE
 7051 CONTINUE
C
C   now find one between CP(23) and CP(25), and call it CP(24)
C
      DX=CPX(25)-CPX(23)
      DY=CPY(25)-CPY(23)
      SLOPE1=DY/DX
      SLOPE2=-DX/DY
      DISTMX=0.0
      DO 7053 I53=1,NP
        DO 7054 I54=1,NPIP(I53)
          IF(PTX(I53,I54).LT.CPX(25).AND.
     1       PTY(I53,I54).LT.CPY(23)) THEN
            DSLOPE=(SLOPE2-SLOPE1)
            XINT=((CPY(25)-PTY(I53,I54))-(SLOPE1*CPX(25))+
     1            (SLOPE2*PTX(I53,I54)))/DSLOPE
            YINT=(CPY(25)-(SLOPE1*(CPX(25)-XINT)))
            IF(PTX(I53,I54).LT.XINT) THEN
              DIST=((ABS(PTX(I53,I54)-XINT)**2.0)+
     1              (ABS(PTY(I53,I54)-YINT)**2.0))**0.50
              IF(DIST.GT.DISTMX) THEN
                CPX(24)=PTX(I53,I54)
                CPY(24)=PTY(I53,I54)
                DISTMX=DIST
              ENDIF
            ENDIF
          ENDIF
 7054   CONTINUE
 7053 CONTINUE
C
C   if any of the simulations don't produce extra points
C   jump out of the simulation loop
C
 7060 CONTINUE
C
C   4. QUADRANT IV -              pt(33)
C
C
C
C
C                  pt(25)
C
C
C   determine algebraic parameters needed for analysis
C
      IF(CPX(25).EQ.CPX(33).OR.CPY(25).EQ.CPY(33)) GOTO 7080
      DX=CPX(33)-CPX(25)
      DY=CPY(33)-CPY(25)
      SLOPE1=DY/DX
      SLOPE2=-DX/DY
C
C   for all of the points in each pathline
C   find the one that is the farthest away from the line
C   between CP(25) and CP(33), and call it CP(29)
C
      DISTMX=0.0
      DO 7061 I61=1,NP
        DO 7062 I62=1,NPIP(I61)
          IF(PTX(I61,I62).GT.CPX(25).AND.
     1       PTY(I61,I62).LT.CPY(33)) THEN
            DSLOPE=(SLOPE2-SLOPE1)
            XINT=((CPY(33)-PTY(I61,I62))-(SLOPE1*CPX(33))
     1            +(SLOPE2*PTX(I61,I62)))/DSLOPE
            YINT=(CPY(33)-(SLOPE1*(CPX(33)-XINT)))
            IF(PTX(I61,I62).GT.XINT) THEN
              DIST=((ABS(PTX(I61,I62)-XINT)**2.0)+
     1              (ABS(PTY(I61,I62)-YINT)**2.0))**0.50
              IF(DIST.GT.DISTMX) THEN
                CPX(29)=PTX(I61,I62)
                CPY(29)=PTY(I61,I62)
                DISTMX=DIST
              ENDIF
            ENDIF
          ENDIF
 7062   CONTINUE
 7061 CONTINUE
C
C   if we do not find a value for CP(29) there are no
C   extra points outside of the line from CP(25) to CP(33)
C   and we can end our analysis in Quadrant IV
C
      IF(CPX(29).LT.TOLER.AND.CPY(29).LT.TOLER) GOTO 7080
C
C   now find one between CP(25) and CP(29), and call it CP(27)
C
      DX=CPX(29)-CPX(25)
      DY=CPY(29)-CPY(25)
      SLOPE1=DY/DX
      SLOPE2=-DX/DY
      DISTMX=0.0
      DO 7063 I63=1,NP
        DO 7064 I64=1,NPIP(I63)
          IF(PTX(I63,I64).GT.CPX(25).AND.
     1       PTY(I63,I64).LT.CPY(29)) THEN
            DSLOPE=(SLOPE2-SLOPE1)
            XINT=((CPY(29)-PTY(I63,I64))-(SLOPE1*CPX(29))+
     1            (SLOPE2*PTX(I63,I64)))/DSLOPE
            YINT=(CPY(29)-(SLOPE1*(CPX(29)-XINT)))
            IF(PTX(I63,I64).GT.XINT) THEN
              DIST=((ABS(PTX(I63,I64)-XINT)**2.0)+
     1              (ABS(PTY(I63,I64)-YINT)**2.0))**0.50
              IF(DIST.GT.DISTMX) THEN
                CPX(27)=PTX(I63,I64)
                CPY(27)=PTY(I63,I64)
                DISTMX=DIST
              ENDIF
            ENDIF
          ENDIF
 7064   CONTINUE
 7063 CONTINUE
C
C   now find one between CP(29) and CP(33), and call it CP(31)
C
      DX=CPX(33)-CPX(29)
      DY=CPY(33)-CPY(29)
      SLOPE1=DY/DX
      SLOPE2=-DX/DY
      DISTMX=0.0
      DO 7065 I65=1,NP
        DO 7066 I66=1,NPIP(I65)
          IF(PTX(I65,I66).GT.CPX(29).AND.
     1       PTY(I65,I66).LT.CPY(33)) THEN
            DSLOPE=(SLOPE2-SLOPE1)
            XINT=((CPY(33)-PTY(I65,I66))-(SLOPE1*CPX(33))+
     1            (SLOPE2*PTX(I65,I66)))/DSLOPE
            YINT=(CPY(33)-(SLOPE1*(CPX(33)-XINT)))
            IF(PTX(I65,I66).GT.XINT) THEN
              DIST=((ABS(PTX(I65,I66)-XINT)**2.0)+
     1              (ABS(PTY(I65,I66)-YINT)**2.0))**0.50
              IF(DIST.GT.DISTMX) THEN
                CPX(31)=PTX(I65,I66)
                CPY(31)=PTY(I65,I66)
                DISTMX=DIST
              ENDIF
            ENDIF
          ENDIF
 7066   CONTINUE
 7065 CONTINUE
C
C   if we do not find a value for CP(27) there are no
C   extra points outside of the line from CP(25) to CP(29)
C   so we can skip up and look between CP(29) and CP(33)
C
      IF(CPX(27).EQ.0.0.AND.CPY(27).EQ.0.0) GOTO 7070
C
C   now find one between CP(25) and CP(27), and call it CP(26)
C
      DX=CPX(27)-CPX(25)
      DY=CPY(27)-CPY(25)
      SLOPE1=DY/DX
      SLOPE2=-DX/DY
      DISTMX=0.0
      DO 7067 I67=1,NP
        DO 7068 I68=1,NPIP(I67)
          IF(PTX(I67,I68).GT.CPX(25).AND.
     1       PTY(I67,I68).LT.CPY(27)) THEN
            DSLOPE=(SLOPE2-SLOPE1)
            XINT=((CPY(27)-PTY(I67,I68))-(SLOPE1*CPX(27))+
     1            (SLOPE2*PTX(I67,I68)))/DSLOPE
            YINT=(CPY(27)-(SLOPE1*(CPX(27)-XINT)))
            IF(PTX(I67,I68).GT.XINT) THEN
              DIST=((ABS(PTX(I67,I68)-XINT)**2.0)+
     1              (ABS(PTY(I67,I68)-YINT)**2.0))**0.50
              IF(DIST.GT.DISTMX) THEN
                CPX(26)=PTX(I67,I68)
                CPY(26)=PTY(I67,I68)
                DISTMX=DIST
              ENDIF
            ENDIF
          ENDIF
 7068   CONTINUE
 7067 CONTINUE
C
C   now find one between CP(27) and CP(29), and call it CP(28)
C
      DX=CPX(29)-CPX(27)
      DY=CPY(29)-CPY(27)
      SLOPE1=DY/DX
      SLOPE2=-DX/DY
      DISTMX=0.0
      DO 7069 I69=1,NP
        DO 7070 I70=1,NPIP(I69)
          IF(PTX(I69,I70).GT.CPX(27).AND.
     1       PTY(I69,I70).LT.CPY(29)) THEN
            DSLOPE=(SLOPE2-SLOPE1)
            XINT=((CPY(29)-PTY(I69,I70))-(SLOPE1*CPX(29))+
     1            (SLOPE2*PTX(I69,I70)))/DSLOPE
            YINT=(CPY(29)-(SLOPE1*(CPX(29)-XINT)))
            IF(PTX(I69,I70).GT.XINT) THEN
              DIST=((ABS(PTX(I69,I70)-XINT)**2.0)+
     1              (ABS(PTY(I69,I70)-YINT)**2.0))**0.50
              IF(DIST.GT.DISTMX) THEN
                CPX(28)=PTX(I69,I70)
                CPY(28)=PTY(I69,I70)
                DISTMX=DIST
```

```
            ENDIF
          ENDIF
        ENDIF
 7070   CONTINUE
 7069 CONTINUE
C
C   if we do not find a value for CP(31) there are no
C   extra points outside of the line from CP(29) to CP(33)
C   and we can skip to the end
C
 7079 CONTINUE
      IF(CPX(31).LT.TOLER.AND.CPY(31).LT.TOLER) GOTO 7080
C
C   now find one between CP(29) and CP(31), and call it CP(30)
C
      DX=CPX(31)-CPX(29)
      DY=CPY(31)-CPY(29)
      SLOPE1=DY/DX
      SLOPE2=-DX/DY
      DISTMX=0.0
      DO 7071 I71=1,NP
        DO 7072 I72=1,NPIP(I71)
          IF(PTX(I71,I72).GT.CPX(29).AND.
     1       PTY(I71,I72).LT.CPY(31)) THEN
            DSLOPE=(SLOPE2-SLOPE1)
            XINT=((CPY(31)-PTY(I71,I72))-(SLOPE1*CPX(31))+
     1            (SLOPE2*PTX(I71,I72)))/DSLOPE
            YINT=(CPY(31)-(SLOPE1*(CPX(31)-XINT)))
            IF(PTX(I71,I72).GT.XINT) THEN
              DIST=((ABS(PTX(I71,I72)-XINT)**2.0)+
     1              (ABS(PTY(I71,I72)-YINT)**2.0))**0.50
              IF(DIST.GT.DISTMX) THEN
                CPX(30)=PTX(I71,I72)
                CPY(30)=PTY(I71,I72)
                DISTMX=DIST
              ENDIF
            ENDIF
          ENDIF
 7072   CONTINUE
 7071 CONTINUE
C
C   now find one between CP(31) and CP(33), and call it CP(32)
C
      DX=CPX(33)-CPX(31)
      DY=CPY(33)-CPY(31)
      SLOPE1=DY/DX
      SLOPE2=-DX/DY
      DISTMX=0.0
      DO 7073 I73=1,NP
        DO 7074 I74=1,NPIP(I73)
          IF(PTX(I73,I74).LT.CPX(31).AND.
     1       PTY(I73,I74).GT.CPY(33)) THEN
            DSLOPE=(SLOPE2-SLOPE1)
            XINT=((CPY(33)-PTY(I73,I74))-(SLOPE1*CPX(33))+
     1            (SLOPE2*PTX(I73,I74)))/DSLOPE
            YINT=(CPY(33)-(SLOPE1*(CPX(33)-XINT)))
            IF(PTX(I73,I74).GT.XINT) THEN
              DIST=((ABS(PTX(I73,I74)-XINT)**2.0)+
     1              (ABS(PTY(I73,I74)-YINT)**2.0))**0.50
              IF(DIST.GT.DISTMX) THEN
                CPX(32)=PTX(I73,I74)
                CPY(32)=PTY(I73,I74)
                DISTMX=DIST
              ENDIF
            ENDIF
          ENDIF
 7074   CONTINUE
 7073 CONTINUE
C
C   if any of the simulations don't produce extra points
C   jump out of the simulation loop
C
 7080 CONTINUE
C
C   sort the final capture zone to remove null values (0.0,0.0)
C
      IEX=0
      IOUT=0
      DO 7100 I100=1,33
        IF(CPX(I100).LT.TOLER.AND.CPY(I100).LT.TOLER) THEN
          IEX=IEX+1
        ELSE
          IOUT=IOUT+1
          CPXOUT(I100-IEX)=CPX(I100)
          CPYOUT(I100-IEX)=CPY(I100)
        ENDIF
 7100 CONTINUE
C
C   now write the points to an output file
C
      WRITE (21,7500) IOUT
      DO 7101 I101=1,IOUT
        WRITE(21,7502) CPXOUT(I101),CPYOUT(I101)
 7101 CONTINUE
C
      WRITE(*,*)
      WRITE(*,*) '     **** end of CAPZON simulation ****'
      WRITE(*,*)
C
C   formatting information
C
 7500 FORMAT(I6)
 7502 FORMAT(2X,F9.2,2X,F9.2)
      END
```

APPENDIX II

FORTRAN CODE

RWAPT.FOR

"RWAPT.FOR"

```
C
C     ******************************************************
C     *                                                    *
C     *    RWALK is a particle tracking program which      *
C     *    performs both advective and random walk         *
C     *    particle tracking and capture zone modeling     *
C     *                                                    *
C     *                                D.J. Miln Harvey    *
C     *                                     July 1997      *
C     *                                                    *
C     ******************************************************
C
C
C        variables list
C
      IMPLICIT REAL*8(A-H,O-Z)
      COMMON /FDGRID/ XSTEP,YSTEP,XDIST,YDIST,XFACE,YFACE
      COMMON /HEADS/ HX,HY,HEAD
      COMMON /PARAM/ RK,ALONG,ATRAN,XPORO
      COMMON /BNDRY/ RHI,RVI,LIDI,RHJ,RVJ,LIDJ
      COMMON /VELDIS/ VXPOSX,VXPOSY,VYPOSX,VYPOSY,VX,VY,DX,DY
      COMMON /WELLOC/ NWELS,XWEL,YWEL,WRAD
      COMMON /CRITS/ WCRIT,ILBB,JLBB,ITBB,JTBB,IBBB,JBBB,IRBB,JRBB
      DIMENSION XSTEP(100),YSTEP(100),XDIST(101),YDIST(101),
     2          XFACE(101),YFACE(101),
     3  HX(100,100),HY(100,100),HEAD(100,100),
     4  RK(100,100),DX(100,101),DY(101,100),
     5  RHI(100,2),RVI(100,2),RHJ(2,100),RVJ(2,100),
     6          LIDI(100,2),LIDJ(2,100),
     7  VXPOSX(101,100),VXPOSY(101,100),VYPOSX(100,101),
     8          VYPOSY(100,101),VX(101,100),VY(100,101),
     9  XP(200),YP(200),XPO(200,201),YPO(200,201),NPO(200),
     A  XWEL(50),YWEL(50),WRAD(50),
     B  WCRIT(50),ILBB(150),JLBB(150),ITBB(150),JTBB(150),
     C            IBBB(150),JBBB(150),IRBB(150),JRBB(150)
C
C        open input data file
C
      OPEN(20,FILE='rwaptin.dat',STATUS='OLD')
C
C        input grid spacing from external file and determine
C        the center of each grid block (xdist,ydist) and the
C        position of each grid block face (xface,yface)
C
      CALL INGRID(NX,NY,NX1,NY1,XSMIN,YSMIN,IRWFL,IFORM)
C
C        input head field from SWIFT III output (which has
C        been post processed to have block centered values
C        of head HEADIN.DAT) and the hydraulic conductivity
C        field from an external file
C
      CALL INPUT(NX,NY)
C
C        determine the boundary conditions for the system
C
      CALL BOUNDS(NX,NY)
C
C        determine the (x,y) position of the center of each block
C        face within the grid system, and the value of velocity at
C        at each face position (i.e. the velocity field)
C
      CALL VELFLD(NX,NY,NX1,NY1,VXMAX,VYMAX,IFORM)
C
C        determine the value of dispersion at each face position
C        (i.e. the dispersion field)
C
      IF (IRWFL.EQ.1) THEN
            WRITE(*,*)
            WRITE(*,*)'************************************************'
            WRITE(*,*)
            WRITE(*,*) '     The Random Walk Method is being          '
            WRITE(*,*) '     used to track particle movement !        '
            WRITE(*,*)
            WRITE(*,*)'************************************************'
            WRITE(*,*)
            CALL DISPLD(NX,NY,NX1,NY1)
      ELSE
            WRITE(*,*)
            WRITE(*,*)'************************************************'
            WRITE(*,*)
            WRITE(*,*) '     Particle tracking is being performed     '
            WRITE(*,*) '     using advective velocities only !        '
            WRITE(*,*)
            WRITE(*,*)'************************************************'
            WRITE(*,*)
      ENDIF
C
C        input starting particle positions
C
      CALL INPART(NPART,NOUT,DT,NITS,XP,YP,IDUM)
C
C        check that integer values for particle tracking are ok
C
      IF (NPART.GT.200.OR.NITS.GT.100.OR.NOUT.GT.500) THEN
            WRITE(*,*)
            WRITE(*,*)'************************************************'
            WRITE(*,*)
            WRITE(*,*) ' The following integer limits are in effect: '
            WRITE(*,*) '       NOUT  <= 500                          '
            WRITE(*,*) '       NITS  <= 100                          '
            WRITE(*,*) '       NPART <= 200                          '
            WRITE(*,*) ' Choose new integer values and start again!  '
            WRITE(*,*)
            WRITE(*,*)'************************************************'
            STOP
      ENDIF
C
C        check that the maximum particle movement in any one
C        time step (VMAX*DT) is less than 1/5th of the
C        smallest grid block discretization
C
      DXMAX=VXMAX*DT
      DYMAX=VYMAX*DT
      XMIN=0.2*XSMIN
      YMIN=0.2*YSMIN
      IF (DXMAX.GT.XMIN.OR.DYMAX.GT.YMIN) THEN
            WRITE(*,*)
            WRITE(*,*)'************************************************'
            WRITE(*,*)
            WRITE(*,*) ' The time step (DT) that you have chosen     '
            WRITE(*,*) ' is too large for the grid block spacing in  '
            WRITE(*,*) ' your conceptual model.  Reduce DT in the    '
            WRITE(*,*) ' PARTIN.DAT file and restart the simulation! '
            WRITE(*,*)
            WRITE(*,*)'************************************************'
            STOP
      ENDIF
C
C        determine the number and location of production wells
C        within the conceptual model, which could capture any
C        particles released within the flowfield
C
      CALL WELLS
C
C        determine stopping criteria for particle tracks
C
      CALL CRITER(NX,NY,NLBB,NTBB,NBBB,NRBB)
C
C        for each particle determine the particle pathlines
C
      DO 100 I=1,NPART
            IFLAG=0
            XPI=XP(I)
            YPI=YP(I)
            XPO(I,1)=XPI
            YPO(I,1)=YPI
            NPO(I)=1
            WRITE(*,500) I
            DO 101 J=1,NOUT
              WRITE(*,501) J
              DO 102 K=1,NITS
C
C        find the 4 closest values of velocity and dispersion,
C        interpolate velocity at the particle position, and
C        determine new particle position
C
                CALL VDINT(NX1,NY1,XPI,YPI,IDUM,IFLAG,DT,
     1                NLBB,NTBB,NBBB,NRBB,IRWFL)
C
C        stop particle tracking if STOP criterion is reached
C
                IF (IFLAG.EQ.1) THEN
                  XPO(I,J+1)=XPI
                  YPO(I,J+1)=YPI
                  NPO(I)=J+1
                  GOTO 100
                ENDIF
  102         CONTINUE
C
C        save new particle position in output array
C
              XPO(I,J+1)=XPI
              YPO(I,J+1)=YPI
              NPO(I)=J+1
  101       CONTINUE
  100 CONTINUE
  500 FORMAT(5X,'Tracking Particle #',I5)
  501 FORMAT(10X,'Output Time Step ',I5)
C
C        output particle track to a surfer * bln file
C
      CALL OUTPUT(NPART,XPO,YPO,NPO)
      WRITE(*,*)
      WRITE(*,*) '  ************************************** '
      WRITE(*,*) '  *                                    * '
      WRITE(*,*) '  *       Normal Termination of RWAPT  * '
      WRITE(*,*) '  *                                    * '
      WRITE(*,*) '  *       Output located in RWAPT.BLN  * '
      WRITE(*,*) '  *                                    * '
      WRITE(*,*) '  ************************************** '
      WRITE(*,*)
      STOP
      END
C
C     ******************************************************
C     *                                                    *
C     *                                                    *
C     *           *****  subroutines  *****                *
C     *                                                    *
C     *                                                    *
C     ******************************************************
C
C        subroutine INGRID gets input grid information
C        from an external file (DATAIN.DAT)
C
      SUBROUTINE INGRID(IBLKX,IBLKY,NX1,NY1,XSMIN,YSMIN,IRWFL,
     1                  IFORM)
      IMPLICIT REAL*8(A-H,O-Z)
      CHARACTER*80 HEADER1
      COMMON /FDGRID/ XSTEP,YSTEP,XDIST,YDIST,XFACE,YFACE
      COMMON /PARAM/ RK,ALONG,ATRAN,XPORO
      DIMENSION XSTEP(100),YSTEP(100),XFACE(101),YFACE(101),
     1          XDIST(101),YDIST(101),
     2 RK(100,100)
C
C        read block spacing in the x-direction
C
C        XSTEP(I) = block discretization in the x direction
C        YSTEP(J) = block discretization in the y direction
C        XDIST(I) = distance to block center from x-axis
C        YDIST(J) = distance to block center from y-axis
C        XFACE(I) = distance to block face from x-axis
C        YFACE(J) = distance to block face from y-axis
C        XSMIN = minimum grid block spacing in the x-direction
C        YSMIN = minimum grid block spacing in the y-direction
C
      READ(20,1505) HEADER1
      READ(20,1500) IBLKX,NROWX
C
C        determine number of block faces in each dir
C
      NX1=IBLKX+1
```

```
      LROWX=MOD(IBLKX,10)
      IF (LROWX.EQ.0) LROWX=10
      DO 1000 J1=1,NROWX-1
            K1=10*J1
            L1=K1-9
            READ(20,1501) (XSTEP(M1),M1=L1,K1)
 1000 CONTINUE
      L1=10*(NROWX-1)+1
      K1=L1+LROWX-1
      READ(20,1501) (XSTEP(M1),M1=L1,K1)
C
C        read block spacing in the y-direction
C
      READ(20,1500) IBLKY,NROWY
      NY1=IBLKY+1
      LROWY=MOD(IBLKY,10)
      IF (LROWY.EQ.0) LROWY=10
      DO 1010 J2=1,NROWY-1
            K2=10*J2
            L2=K2-9
            READ(20,1501) (YSTEP(M2),M2=L2,K2)
 1010 CONTINUE
      L2=10*(NROWY-1)+1
      K2=L2+LROWY-1
      READ(20,1501) (YSTEP(M2),M2=L2,K2)
C
C        read in alpha(L), alpha(T) and porosity
C
      READ(20,1502) ALONG,ATRAN
      READ(20,1503) XPORO
C
C       read random walk flag where:
C            IRWFL = 1  - indicates random walk tracking
C            IRWFL = -1 - indicates advective particle tracking
C
      READ (20,1504) IRWFL
C
C       read forward/reverse direction flag
C            IFORW = 1  - indicated forward tracking
C            IFORW = -1 - indicated reverse tracking
C
      READ (20,1504) IFORW
C
C        determine the distance of the grid block
C        face and center from the x and y-axes, and
C        the minimum block spacing (xsmin,ysmin)
C
C        x-direction
C
      SUMX=0.0
      TEMPX=0.0
      XSMIN=XSTEP(1)
      XDIST(1)=0.0
      XFACE(1)=0.0
      DO 1020 I=1,IBLKX
            TEMPX=XSTEP(I)/2.0
            XDIST(I+1)=SUMX+TEMPX
            XFACE(I+1)=XFACE(I)+XSTEP(I)
            SUMX=SUMX+XSTEP(I)
            IF (XSTEP(I).LT.XSMIN) XSMIN=XSTEP(I)
 1020 CONTINUE
C
C        y-direction
C
      SUMY=0.0
      TEMPY=0.0
      YSMIN=YSTEP(1)
      YDIST(1)=0.0
      YFACE(1)=0.0
      DO 1030 J=1,IBLKY
            TEMPY=YSTEP(J)/2.0
            YDIST(J+1)=SUMY+TEMPY
            YFACE(J+1)=YFACE(J)+YSTEP(J)
            SUMY=SUMY+YSTEP(J)
            IF (YSTEP(J).LT.YSMIN) YSMIN=YSTEP(J)
 1030 CONTINUE
 1500 FORMAT (2I5)
 1501 FORMAT (10F10.1)
 1502 FORMAT (2F10.2)
 1503 FORMAT (F10.2)
 1504 FORMAT (I5)
 1505 FORMAT (A80)
      RETURN
      END
C
C       subroutine INPUT gets input head values from
C       an external file (HEADIN.DAT) and hydraulic
C       conductivity values from another file (KFLDIN.DAT)
C
      SUBROUTINE INPUT(NX,NY)
      IMPLICIT REAL*8(A-H,O-Z)
      CHARACTER*80 HEADER2, HEADER3
      COMMON /HEADS/ HX,HY,HEAD
      COMMON /PARAM/ RK,ALONG,ATRAN,XPORO
      DIMENSION HX(100,100),HY(100,100),HEAD(100,100),
     1  RK(100,100)
C
C       read hydraulic head field from input file
C
      READ(20,2502) HEADER2
      DO 2000 I1=1,NX
            DO 2001 J1=1,NY
              READ(20,2500) HX(I1,J1),HY(I1,J1),HEAD(I1,J1)
 2001   CONTINUE
 2000 CONTINUE
C
C       read hydraulic conductivity field from input file
C
      READ(20,2502) HEADER3
      DO 2020 J3=1,NY
            DO 2021 I3=1,NX
              READ(20,2501) RK(I3,J3)
 2021   CONTINUE
 2020 CONTINUE
 2500 FORMAT(2F10.1,F10.4)
 2501 FORMAT(25X,F10.5)
 2502 FORMAT(A80)
      RETURN
      END
C
C       subroutine BOUNDS gets input boundary conditions
C
      SUBROUTINE BOUNDS(NX,NY)
      IMPLICIT REAL*8(A-H,O-Z)
      CHARACTER*80 HEADER4
      COMMON /BNDRY/ RHI,RVI,LIDI,RHJ,RVJ,LIDJ
      DIMENSION RHI(100,2),RVI(100,2),LIDI(100,2),
     1          RHJ(2,100),RVJ(2,100),LIDJ(2,100)
C
C       LIDI(I,J) = 1 (head), 2(flux) on I boundary
C       RHI(I,J) = prescribed head on I boundary (top/bottom)
C       RVI(I,J) = prescribed flux on I boundary
C       LIDJ(I,J) = 1 (head), 2(flux) on J boundary
C       RHJ(I,J) = prescribed head on J boundary (left/right)
C       RVJ(I,J) = prescribed flux on J boundary
C
C       zero the boundary arrays
C
      DO 3000 J1=1,2
            DO 3001 I1=1,NX
              RHI(I1,J1)=0.0
              RVI(I1,J1)=0.0
 3001   CONTINUE
 3000 CONTINUE
      DO 3005 I2=1,2
            DO 3006 J2=1,NY
              RHJ(I2,J2)=0.0
              RVJ(I2,J2)=0.0
 3006   CONTINUE
 3005 CONTINUE
C
C       read input from external file
C
      READ(20,3501) HEADER4
C
C       read bottom and top boundary conditions
C
      DO 3010 J3=1,2
            DO 3011 I3=1,NX
              READ (20,3500) LIDI(I3,J3),RNUM
              IF (LIDI(I3,J3).EQ.1) THEN
                RHI(I3,J3)=RNUM
              ELSE
                RVI(I3,J3)=RNUM
              ENDIF
 3011   CONTINUE
 3010 CONTINUE
C
C       read left and right boundary conditions
C
      DO 3020 I4=1,2
            DO 3021 J4=1,NY
              READ (20,3500) LIDJ(I4,J4),RNUM
              IF (LIDJ(I4,J4).EQ.1) THEN
                RHJ(I4,J4)=RNUM
              ELSE
                RVJ(I4,J4)=RNUM
              ENDIF
 3021   CONTINUE
 3020 CONTINUE
 3500 FORMAT(I4,F6.2)
 3501 FORMAT(A80)
      RETURN
      END
C
C       subroutine VELFLD determines the x and y position
C       of the location of each grid block face and the
C       velocities at these face locations
C
      SUBROUTINE VELFLD(NX,NY,NX1,NY1,VXMAX,VYMAX,IFORW)
      IMPLICIT REAL*8(A-H,O-Z)
      COMMON /FDGRID/ XSTEP,YSTEP,XDIST,YDIST,XFACE,YFACE
      COMMON /HEADS/ HX,HY,HEAD
      COMMON /PARAM/ RK,ALONG,ATRAN,XPORO
      COMMON /BNDRY/ RHI,RVI,LIDI,RHJ,RVJ,LIDJ
      COMMON /VELDIS/ VXPOSX,VXPOSY,VYPOSX,VYPOSY,VX,VY,DX,DY
      DIMENSION XSTEP(100),YSTEP(100),XDIST(101),YDIST(101),
     1          XFACE(101),YFACE(101),
     2  HX(100,100),HY(100,100),HEAD(100,100),
     3  RK(100,100),DX(100,101),DY(101,100),
     4  VXPOSX(101,100),VXPOSY(101,100),VYPOSX(100,101),
     5          VYPOSY(100,101),VX(101,100),VY(100,101),
     6  RHI(100,2),RVI(100,2),RHJ(2,100),RVJ(2,100),
     7             LIDI(100,2),LIDJ(2,100)
C
C       do VX(I,J) and VY(I,J) separately
C
C       VX(I,J) = velocity in the x-direction
C       VY(I,J) = velocity in the y-direction
C       VXMAX = maximum value of velocity in the x-dir
C       VYMAX = maximum value of velocity in the y-dir
C
      VXMAX=0.0
      VYMAX=0.0
      DO 4000 J=1,NY
            DO 4001 I=1,NX1
              VXPOSX(I,J)=XFACE(I)
              VXPOSY(I,J)=YDIST(J+1)
              IF (I.EQ.1) THEN
C
C       left side of system boundary condition
C
                IF (LIDJ(1,J).EQ.1) THEN
                  IF (HEAD(I,J).EQ.-99.0) THEN
C
```

```
C       assign VX=0.0 to face of no flow blocks
C
                        VX(I,J)=0.0
                        GOTO 4001
                      ELSE
                        VX(I,J)=2.0*RK(I,J)*(HEAD(I,J)-RHJ(I,J))/
     1                  XSTEP(I)/XPORO
                        IF (VX(I,J).GT.VXMAX) VXMAX=VX(I,J)
                      ENDIF
                    ELSE
                      VX(I,J)=RVJ(I,J)
                      IF (VX(I,J).GT.VXMAX) VXMAX=VX(I,J)
                    ENDIF
                    GOTO 4001
                  ENDIF
C
C       right side of system boundary condition
C
                IF (I.EQ.NX1) THEN
                  IF (LIDJ(2,J).EQ.1) THEN
                    IF (HEAD(NX,J).EQ.-99.0) THEN
C
C       assign VX=0.0 to face of no flow blocks
C
                        VX(NX1,J)=0.0
                        GOTO 4001
                      ELSE
                        VX(NX1,J)=2.0*RK(NX,J)*(RHJ(2,J)-HEAD(NX,J))/
     1                    XSTEP(NX)/XPORO
                        IF (VX(NX1,J).GT.VXMAX) VXMAX=VX(NX1,J)
                      ENDIF
                    ELSE
                      VX(NX1,J)=RVJ(2,J)
                      IF (VX(NX1,J).GT.VXMAX) VXMAX=VX(NX1,J)
                    ENDIF
                    GOTO 4001
                  ENDIF
C
C       determine the velocity at each block face by taking
C       the harmonic mean between two nodal values of head
C
                IF (HEAD(I-1,J).EQ.-99.0.OR.HEAD(I,J).EQ.-99.0) THEN
C
C       assign VX=0.0 to face of no flow blocks
C
                  VX(I,J)=0.0
                  GOTO 4001
                ELSE
                  VX(I,J)=2.0*(HEAD(I,J)-HEAD(I-1,J))/
     1            ((XSTEP(I)/RK(I,J))+(XSTEP(I-1)/RK(I-1,J)))/XPORO
                  IF (VX(I,J).GT.VXMAX) VXMAX=VX(I,J)
                ENDIF
 4001   CONTINUE
 4000 CONTINUE
C
C       for each VY determine location and velocity
C
      DO 4010 I=1,NX
            DO 4011 J=1,NY1
              VYPOSX(I,J)=XDIST(I+1)
              VYPOSY(I,J)=YFACE(J)
              IF (J.EQ.1) THEN
C
C       bottom of system boundary condition
C
                IF (LIDI(I,1).EQ.1) THEN
                  IF (HEAD(I,1).EQ.-99.0) THEN
C
C       assign VY=0.0 to face of no flow blocks
C
                        VY(I,1)=0.0
                        GOTO 4011
                      ELSE
                        VY(I,1)=2.0*RK(I,1)*(HEAD(I,1)-RHI(I,1))/
     1                  YSTEP(1)/XPORO
                        IF (VY(I,1).GT.VYMAX) VYMAX=VY(I,1)
                      ENDIF
                    ELSE
                      VY(I,1)=RVI(I,1)
                      IF (VY(I,1).GT.VYMAX) VYMAX=VY(I,1)
                    ENDIF
                    GOTO 4011
                  ENDIF
C
C       top of system boundary condition
C
                IF (J.EQ.NY1) THEN
                  IF (LIDI(I,2).EQ.1) THEN
                    IF (HEAD(I,NY).EQ.-99.0) THEN
C
C       assign VY=0.0 to face of no flow blocks
C
                        VY(I,NY1)=0.0
                        GOTO 4011
                      ELSE
                        VY(I,NY1)=2.0*RK(I,NY)*(RHI(I,2)-HEAD(I,NY))/
     1                    YSTEP(NY)/XPORO
                        IF (VY(I,NY1).GT.VYMAX) VYMAX=VY(I,NY1)
                      ENDIF
                    ELSE
                      VY(I,NY1)=RVI(I,2)
                      IF (VY(I,NY1).GT.VYMAX) VYMAX=VY(I,NY1)
                    ENDIF
                    GOTO 4011
                  ENDIF
C
C       determine the velocity at each block face by taking
C       the harmonic mean between two nodal values of head
C
                IF (HEAD(I,J-1).EQ.-99.0.OR.HEAD(I,J).EQ.-99.0) THEN
C
C       assign VY=0.0 to face of no flow blocks
C
                  VY(I,J)=0.0
                  GOTO 4011
                ELSE
                  VY(I,J)=2.0*(HEAD(I,J)-HEAD(I,J-1))/
     1            ((YSTEP(J)/RK(I,J))+(YSTEP(J-1)/RK(I,J-1)))/XPORO
                  IF (VY(I,J).GT.VYMAX) VYMAX=VY(I,J)
                ENDIF
 4011   CONTINUE
 4010 CONTINUE
C
C   if IPORW=1, forward particle tracking is needed so,
C   reverse the velocities set up for reverse tracking
C
      IF (IPORW.EQ.1) THEN
        DO 4050 I5=1,NX
          DO 4051 J5=1,NY
            VX(I5,J5)=-VX(I5,J5)
            VY(I5,J5)=-VY(I5,J5)
 4051     CONTINUE
 4050   CONTINUE
      ENDIF
      RETURN
      END
C
C
C       subroutine DISFLD determines the dispersion values
C       the face locations (defined by the velocity field)
C
      SUBROUTINE DISFLD(NX,NY,NX1,NY1)
      IMPLICIT REAL*8(A-H,O-Z)
      COMMON /PDGRID/ XSTEP,YSTEP,XDIST,YDIST,XFACE,YFACE
      COMMON /PARAM/ RK,ALONG,ATRAN,XPORO
      COMMON /VELDIS/ VXPOSX,VXPOSY,VYPOSX,VYPOSY,VX,VY,DX,DY
      DIMENSION XSTEP(100),YSTEP(100),XDIST(101),YDIST(101),
     1          XFACE(101),YFACE(101),
     2  RK(100,100),DX(100,101),DY(101,100),
     3  VXPOSX(101,100),VXPOSY(101,100),VYPOSX(100,101),
     4          VYPOSY(100,101),VX(101,100),VY(100,101)
C
C       VX(I,J) = velocity in the x-direction
C       VY(I,J) = velocity in the y-direction
C       DX(I,J) = dispersion on an x-face
C       DY(I,J) = dispersion on a y-face
C
      TAU=0.70
      DSTAR=1.0E-10
      DO 5000 J=1,NY
C
C       set left and right side system boundary condition
C
          DO 5001 I=1,NX1
            IF (I.EQ.1.OR.I.EQ.NX1) THEN
              DY(I,J)=0.0
              GOTO 5001
            ENDIF
C
C       for internal faces, if Vx=0 then DY=0
C
            IF (VX(I,J).EQ.0.0) THEN
              DY(I,J)=0.0
            ELSE
C
C       interpolate a value of DY, first by finding Vy at
C       DY, determining Vxy, then using the equation.
C
C           DY = aL*(Vx^2)/Vxy + aT*(Vy^2)/Vxy + T*D
C
              A1=XSTEP(I)/2.0
              B1=XSTEP(I-1)/2.0
              C1=A1+B1
              VYTMP2=(VY(I,J)+VY(I,J+1))/2.0
              VYTMP1=(VY(I-1,J)+VY(I-1,J+1))/2.0
              VYTMP=((A1/C1)*VYTMP1)+((B1/C1)*VYTMP2)
              VXY=((ABS(VYTMP)**2.0)+(ABS(VX(I,J))**2.0))**0.5
              DY(I,J)=(ALONG*(ABS(VX(I,J))**2.0)/VXY)+
     1                (ATRAN*(ABS(VYTMP)**2.0)/VXY)+(TAU*DSTAR)
            ENDIF
 5001   CONTINUE
 5000 CONTINUE
C
C       determine DX
C
      DO 5010 I=1,NX
            DO 5011 J=1,NY1
C
C       set bottom and top system boundary condition
C
              IF (J.EQ.1.OR.J.EQ.NY1) THEN
                DX(I,J)=0.0
                GOTO 5011
              ENDIF
C
C       for internal faces, if Vy=0 then DX=0
C
              IF (VY(I,J).EQ.0.0) THEN
                DX(I,J)=0.0
              ELSE
C
C       interpolated a value of DX, first finding Vx at DX,
C       then determining Vxy, then using the equation:
C
C           DX = aL*(Vy^2)/Vxy + aT*(Vx^2)/Vxy + T*D
C
                A2=YSTEP(J)/2.0
                B2=YSTEP(J-1)/2.0
                C2=A2+B2
                VXTMP3=(VX(I,J-1)+VX(I+1,J-1))/2.0
                VXTMP4=(VX(I,J)+VX(I+1,J))/2.0
                VXTMP=((A2/C2)*VXTMP3)+((B2/C2)*VXTMP4)
                VXY=((ABS(VXTMP)**2.0)+(ABS(VY(I,J))**2.0))**0.5
                DX(I,J)=(ALONG*(ABS(VY(I,J))**2.0)/VXY)+
     1                  (ATRAN*(ABS(VXTMP)**2.0)/VXY)+(TAU*DSTAR)
              ENDIF
 5011   CONTINUE
 5010 CONTINUE
      RETURN
      END
```

```
C
C       subroutine INPART gets starting particle positions
C
      SUBROUTINE INPART(NPART,NOUT,DT,NITS,XP,YP,IDUM)
      IMPLICIT REAL*8(A-H,O-Z)
      CHARACTER*80 HEADER5
      DIMENSION XP(200),YP(200)
C
C       NPART = number of particles to be tracked
C       NOUT = number of output time steps
C       DT = time step (depends on units of RK)
C       NITS = number of internal time steps per NOUT
C
      READ (20,6502) HEADER5
      READ (20,6500) NPART,NOUT,DT,NITS
      READ (20,6500) IDUM
      DO 6000 I=1,NPART
            READ (20,6501) XP(I),YP(I)
 6000 CONTINUE
 6500 FORMAT(I5,I7,F10.2,I7)
 6501 FORMAT(2F10.1)
 6502 FORMAT(A80)
      RETURN
      END




C       subroutine WELLS gets the location of any extraction
C       wells from an external file
C
      SUBROUTINE WELLS
      IMPLICIT REAL*8(A-H,O-Z)
      CHARACTER*80 HEADER6
      COMMON /FDGRID/ XSTEP,YSTEP,XDIST,YDIST,XFACE,YFACE
      COMMON /WELLOC/ NWELS,XWEL,YWEL,WRAD
      DIMENSION XWEL(50),YWEL(50),WRAD(50),
     1  XSTEP(100),YSTEP(100),XDIST(101),YDIST(101),
     2            XFACE(101),YFACE(101)
      DATA PI /3.141592654/
C
C       XWEL(I) = location of the well in the x-direction
C       YWEL(I) = location of the well in the y-direction
C       WRAD(I) = well radius for well I
C
      READ (20,7502) HEADER6
      READ (20,7500) NWELS
      IF (NWELS.GT.50) THEN
            WRITE(*,*)
            WRITE(*,*)'************************************************'
            WRITE(*,*)
            WRITE(*,*) ' The number of wells (NWELS) in the system   '
            WRITE(*,*) ' must be less than 50. Choose new integer    '
            WRITE(*,*) ' values and start the simulation again '     '
            WRITE(*,*)
            WRITE(*,*)'************************************************'
            STOP
      ENDIF
      DO 7000 I1=1,NWELS
            READ (20,7501) IW,JW
            XWEL(I1)=XDIST(IW+1)
            WSTPX=XSTEP(IW)
            YWEL(I1)=YDIST(JW+1)
            WSTPY=YSTEP(JW)
C
C       determine the well radius, using the SWIFT definition
C       of radius of influence,    r(bar)=(dx*dy/pi)^0.5
C
            WRAD(I1)=SQRT(WSTPX*WSTPY/PI)
 7000 CONTINUE
 7500 FORMAT(I5)
 7501 FORMAT(2I5)
 7502 FORMAT(A80)
      RETURN
      END




C
C       subroutine CRITER determines the stopping criteria
C       for particle tracking, based on the location of wells
C       and external system boundaries
C
      SUBROUTINE CRITER(NX,NY,NLBB,NTBB,NBBB,NRBB)
      IMPLICIT REAL*8(A-H,O-Z)
      CHARACTER*80 HEADER7
      COMMON /FDGRID/ XSTEP,YSTEP,XDIST,YDIST,XFACE,YFACE
      COMMON /WELLOC/ NWELS,XWEL,YWEL,WRAD
      COMMON /CRITS/ WCRIT,ILBB,JLBB,ITBB,JTBB,IBBB,JBBB,IRBB,JRBB
      DIMENSION XSTEP(100),YSTEP(100),XDIST(101),YDIST(101),
     2          XFACE(101),YFACE(101),
     3  XWEL(50),YWEL(50),WRAD(50),
     4  WCRIT(50),ILBB(150),JLBB(150),ITBB(150),JTBB(150),
     5            IBBB(150),JBBB(150),IRBB(150),JRBB(150)
C
C       a particle stops if it gets within 1/5th of the
C       radius of influence of a pumping well
C
      DO 8000 I=1,NWELS
            WCRIT(I)=0.2*WRAD(I)
 8000 CONTINUE
C
C       or, 1/5th of the edge of the outer most grid blocks
C       in the conceptual model of the system
C
      READ (20,8502) HEADER7
      READ (20,8500) NLBB
      DO 8010 I1=1,NLBB
            READ (20,8501) ILBB(I1),JLBB(I1)
 8010 CONTINUE
      READ (20,8500) NTBB
      DO 8020 I2=1,NTBB
            READ (20,8501) ITBB(I2),JTBB(I2)
 8020 CONTINUE
      READ (20,8500) NBBB
      DO 8030 I3=1,NBBB
            READ (20,8501) IBBB(I3),JBBB(I3)
 8030 CONTINUE
      READ (20,8500) NRBB
      DO 8040 I4=1,NRBB
            READ (20,8501) IRBB(I4),JRBB(I4)
 8040 CONTINUE
 8500 FORMAT(I5)
 8501 FORMAT(2I5)
 8502 FORMAT(A80)
      RETURN
      END




C
C       subroutine VDINT determines the x and y values
C       of velocity using a bilinear velocity interpolator
C       explained in Walton (1987) pp. 349-355 (Chapter 11)
C
      SUBROUTINE VDINT(NX1,NY1,XPI,YPI,IDUM,IFLAG,DT,
     1                 NLBB,NTBB,NBBB,NRBB,IRWFL)
      IMPLICIT REAL*8(A-H,O-Z)
      COMMON /FDGRID/ XSTEP,YSTEP,XDIST,YDIST,XFACE,YFACE
      COMMON /HEADS/ HX,HY,HEAD
      COMMON /PARAM/ RK,ALONG,ATRAN,XPORO
      COMMON /VELDIS/ VXPOSX,VXPOSY,VYPOSX,VYPOSY,VX,VY,DX,DY
      COMMON /WELLOC/ NWELS,XWEL,YWEL,WRAD
      COMMON /CRITS/ WCRIT,ILBB,JLBB,ITBB,JTBB,IBBB,JBBB,IRBB,JRBB
      DIMENSION XSTEP(100),YSTEP(100),XDIST(101),YDIST(101),
     1          XFACE(101),YFACE(101),
     2  HX(100,100),HY(100,100),HEAD(100,100),
     3  VX(101,100),VY(100,101),DX(100,101),DY(101,100),
     4          VXPOSX(101,100),VXPOSY(101,100),
     5          VYPOSX(100,101),VYPOSY(100,101),
     6  RK(100,100),
     7  XWEL(50),YWEL(50),WRAD(50),
     8  WCRIT(50),ILBB(150),JLBB(150),ITBB(150),JTBB(150),
     9            IBBB(150),JBBB(150),IRBB(150),JRBB(150)
C
C       find the nearest grid block center to (XPI,YPI)
C       represented by the integer value (IX,IY)
C
      NX=NX1-1
      NY=NY1-1
      DISTT=1.0E12
      DO 9000 J1=1,NY
            DO 9001 I1=1,NX
              TEMPD=SQRT((ABS(XPI-HX(I1,J1))**2.0)+
     1                   (ABS(YPI-HY(I1,J1))**2.0))
              IF (TEMPD.LE.DISTT) THEN
                DISTT=TEMPD
                IX=I1
                IY=J1
              ENDIF
 9001   CONTINUE
 9000 CONTINUE
C                                                  |                |
C       the 2 nearest values of VX & DY are        |PTZ1---(I,J)---PTZ2|
C                                                  |                |
      PTX1=VXPOSX(IX,IY)
      PTY1=VXPOSY(IX,IY)
      PTZ1=VX(IX,IY)
      PTX2=VXPOSX(IX+1,IY)
      PTY2=VXPOSY(IX+1,IY)
      PTZ2=VX(IX+1,IY)
C                                                  |     PTZ4     |
C                                                  |      |       |
C       the 2 nearest values of VY & DX are        |    (I,J)     |
C                                                  |      |       |
C                                                  |     PTZ3     |
      PTX3=VYPOSX(IX,IY)
      PTY3=VYPOSY(IX,IY)
      PTZ3=VY(IX,IY)
      PTX4=VYPOSX(IX,IY+1)
      PTY4=VYPOSY(IX,IY+1)
      PTZ4=VY(IX,IY+1)
C
C       interpolate velocity at (XPI,YPI) to be (VXP,VYP)
C
      A1=XPI-PTX1
      B1=PTX2-XPI
      C1=A1+B1
      VXP=((A1/C1)*PTZ2)+((B1/C1)*PTZ1)
      A2=YPI-PTY3
      B2=PTY4-YPI
      C2=A2+B2
      VYP=((A2/C2)*PTZ4)+((B2/C2)*PTZ3)
C
C       if particle movement is by random walk
C
      IF (IRWFL.EQ.1) THEN
            PTD1=DY(IX,IY)
            PTD2=DY(IX+1,IY)
            PTD3=DX(IX,IY)
            PTD4=DX(IX,IY+1)
C
C       find the derivative of dispersion in the
C       x-direction and the y-direction to be:
C
C       DDX = dDxx/dx     and     DDY = dDyy/dy
C
            DELX=XSTEP(IX)
            DELY=YSTEP(IY)
            DDX=(PTD2-PTD1)/DELX
            DDY=(PTD4-PTD3)/DELY
C
C       determine particle velocity   Vx' = Vx + dDxx/dx
C                                     Vy' = Vy + dDyy/dy
C                                     Vxy = (Vx^2+Vy^2)^0.5
C
            VXPP=VXP+DDX
            VYPP=VYP+DDY
            VXY=SQRT((ABS(VXP)**2.0)+(ABS(VYP)**2.0))
C
C       choose random numbers - R1 & R2 which are normally
C       distributed random number with moments of N(0,1)
C
            RSUM=0.0
```

```
      DO 9060 IR1=1,12
        RR1=RAN3(IDUM)
        RSUM=RSUM+RR1
 9060 CONTINUE
      R1=RSUM-6.0
C
      RSUM=0.0
      DO 9061 IR2=1,12
        RR2=RAN3(IDUM)
        RSUM=RSUM+RR2
 9061 CONTINUE
      R2=RSUM-6.0
C
C     move XPI and YPI using the random walk equation
C
C     x(t+dt)=x(t)+(Ux'*dT)+(R1*sqrt(2*aL*Uxy*dT)*Ux/Uxy)
C                          +(R2*sqrt(2*aT*Uxy*dT)*Uy/Uxy)
C
          XPIN=XPI+(VXPP*DT)+
     1       (R1*SQRT(2.0*ALONG*ABS(VXY)*DT)*(VXP/VXY))+
     2       (R2*SQRT(2.0*ATRAN*ABS(VXY)*DT)*(VYP/VXY))
          YPIN=YPI+(VYPP*DT)+
     1       (R1*SQRT(2.0*ALONG*ABS(VXY)*DT)*(VYP/VXY))-
     2       (R2*SQRT(2.0*ATRAN*ABS(VXY)*DT)*(VXP/VXY))
C
C     particle movement is by advection only
C
      ELSE
          XPIN=XPI+(VXP*DT)
          YPIN=YPI+(VYP*DT)
      ENDIF
C
C     check criterion for ending particle movement:
C
C       1. if the distance from the particle endpoint to
C          the well center is less than 1/5th of the grid
C          block radius (as defined by MODFLOW)
C       2. if the particle gets within the distal 1/5th of
C          the outermost grid block in the system
C
      DO 9010 I2=1,NWELS
          WDIST=SQRT((ABS(XPIN-XWEL(I2))**2.0)+
     1          (ABS(YPIN-YWEL(I2))**2.0))
          IF (WDIST.LE.WCRIT(I2)) THEN
            IFLAG=1
          ENDIF
 9010 CONTINUE
C
C     first check the left boundary
C
      DO 9020 I3=1,NLBB
C
C       is the particle in a boundary block
C
          IF (IX.EQ.ILBB(I3).AND.IY.EQ.JLBB(I3)) THEN
C
C       the numbering system below applies to the left boundary
C
C        9- [x]
C           [x]   7
C           [x]  /
C        8- [x][x][x] -6
C                 [x]
C                 [x]
C                 [x]
C        3- [x][x][x] -5
C           [x]  \
C        2- [x]   4
C        1- [x]
C
C         boundary block type 1
C
            IF (I3.EQ.1) THEN
              OCRIT1=XFACE(IX)+(0.2*XSTEP(IX))
              IF (XPIN.LE.OCRIT1) IFLAG=1
              OCRIT2=YFACE(IY)+(0.2*YSTEP(IY))
              IF (YPIN.LE.OCRIT2) IFLAG=1
C
C         boundary block type 2
C
            ELSEIF (ILBB(I3).EQ.ILBB(I3-1).AND.
     1          ILBB(I3).EQ.ILBB(I3+1)) THEN
              OCRIT1=XFACE(IX)+(0.2*XSTEP(IX))
              IF (XPIN.LE.OCRIT1) IFLAG=1
C
C         boundary block type 3
C
            ELSEIF (ILBB(I3).EQ.ILBB(I3-1).AND.
     1          ILBB(I3).EQ.(ILBB(I3+1)-1)) THEN
              OCRIT1=XFACE(IX)+(0.2*XSTEP(IX))
              IF (XPIN.LE.OCRIT1) IFLAG=1
              OCRIT2=YFACE(IY)+(0.8*YSTEP(IY))
              IF (YPIN.GE.OCRIT2) IFLAG=1
C
C         boundary block type 4
C
            ELSEIF (ILBB(I3).EQ.(ILBB(I3-1)+1).AND.
     1          ILBB(I3).EQ.(ILBB(I3+1)-1)) THEN
              OCRIT1=YFACE(IY)+(0.8*YSTEP(IY))
              IF (YPIN.GE.OCRIT1) IFLAG=1
C
C         boundary block type 5
C
            ELSEIF (ILBB(I3).EQ.(ILBB(I3-1)+1).AND.
     1          ILBB(I3).EQ.ILBB(I3+1)) THEN
              OCRIT1=XFACE(IX)+(0.2*XSTEP(IX))
              OCRIT2=YFACE(IY)+(0.8*YSTEP(IY))
              IF (XPIN.LE.OCRIT1.AND.YPIN.GE.OCRIT2) IFLAG=1
C
C         boundary block type 6
C
            ELSEIF (ILBB(I3).EQ.ILBB(I3-1).AND.
     1          ILBB(I3).EQ.(ILBB(I3+1)+1)) THEN
              OCRIT1=XFACE(IX)+(0.2*XSTEP(IX))
              OCRIT2=YFACE(IY)+(0.2*YSTEP(IY))
              IF (XPIN.LE.OCRIT1.AND.YPIN.LE.OCRIT2) IFLAG=1
C
C         boundary block type 7
C
            ELSEIF (ILBB(I3).EQ.(ILBB(I3-1)-1).AND.
     1          ILBB(I3).EQ.(ILBB(I3+1)+1)) THEN
              OCRIT1=YFACE(IY)+(0.2*YSTEP(IY))
              IF (YPIN.LE.OCRIT1) IFLAG=1
C
C         boundary block type 8
C
            ELSEIF (ILBB(I3).EQ.(ILBB(I3-1)-1).AND.
     1          ILBB(I3).EQ.ILBB(I3+1)) THEN
              OCRIT1=XFACE(IX)+(0.2*XSTEP(IX))
              IF (XPIN.LE.OCRIT1) IFLAG=1
              OCRIT2=YFACE(IY)+(0.2*YSTEP(IY))
              IF (YPIN.LE.OCRIT2) IFLAG=1
C
C         boundary block type 9
C
            ELSEIF (I3.EQ.NLBB) THEN
              OCRIT1=XFACE(IX)+(0.2*XSTEP(IX))
              IF (XPIN.LE.OCRIT1) IFLAG=1
              OCRIT2=YFACE(IY)+(0.8*YSTEP(IY))
              IF (YPIN.GE.OCRIT2) IFLAG=1
            ENDIF
          ENDIF
 9020 CONTINUE
C
C     next, check the top boundary
C
      DO 9030 I4=1,NTBB
C
C       is the particle in a boundary block
C
          IF (IX.EQ.ITBB(I4).AND.IY.EQ.JTBB(I4)) THEN
C
C       the numbering system below applies to the top boundary
C
C                2  3              8
C                |  |              |
C         1- [x][x][x][x]          [x][x][x][x] -9
C                     [x]         [x]
C                   / [x][x][x][x][x]  \
C                  4  |              |   7
C                     5              6
C
C         boundary block type 1
C
            IF (I4.EQ.1) THEN
              OCRIT1=XFACE(IX)+(0.2*XSTEP(IX))
              IF (XPIN.LE.OCRIT1) IFLAG=1
              OCRIT2=YFACE(IY)+(0.8*YSTEP(IY))
              IF (YPIN.GE.OCRIT2) IFLAG=1
C
C         boundary block type 2
C
            ELSEIF (JTBB(I4).EQ.JTBB(I4-1).AND.
     1          JTBB(I4).EQ.JTBB(I4+1)) THEN
              OCRIT1=YFACE(IY)+(0.8*YSTEP(IY))
              IF (YPIN.GE.OCRIT1) IFLAG=1
C
C         boundary block type 3
C
            ELSEIF (JTBB(I4).EQ.JTBB(I4-1).AND.
     1          JTBB(I4).EQ.(JTBB(I4+1)+1)) THEN
              OCRIT1=XFACE(IX)+(0.8*XSTEP(IX))
              IF (XPIN.GE.OCRIT1) IFLAG=1
              OCRIT2=YFACE(IY)+(0.8*YSTEP(IY))
              IF (YPIN.GE.OCRIT2) IFLAG=1
C
C         boundary block type 4
C
            ELSEIF (JTBB(I4).EQ.(JTBB(I4-1)-1).AND.
     1          JTBB(I4).EQ.(JTBB(I4+1)+1)) THEN
              OCRIT1=XFACE(IX)+(0.8*XSTEP(IX))
              IF (XPIN.GE.OCRIT1) IFLAG=1
C
C         boundary block type 5
C
            ELSEIF (JTBB(I4).EQ.(JTBB(I4-1)-1).AND.
     1          JTBB(I4).EQ.JTBB(I4+1)) THEN
              OCRIT1=XFACE(IX)+(0.8*XSTEP(IX))
              OCRIT2=YFACE(IY)+(0.8*YSTEP(IY))
              IF (XPIN.GE.OCRIT1.AND.YPIN.GE.OCRIT2) IFLAG=1
C
C         boundary block type 6
C
            ELSEIF (JTBB(I4).EQ.JTBB(I4-1).AND.
     1          JTBB(I4).EQ.(JTBB(I4+1)-1)) THEN
              OCRIT1=XFACE(IX)+(0.2*XSTEP(IX))
              OCRIT2=YFACE(IY)+(0.8*YSTEP(IY))
              IF (XPIN.LE.OCRIT1.AND.YPIN.GE.OCRIT2) IFLAG=1
C
C         boundary block type 7
C
            ELSEIF (JTBB(I4).EQ.(JTBB(I4-1)+1).AND.
     1          JTBB(I4).EQ.(JTBB(I4+1)-1)) THEN
              OCRIT1=XFACE(IX)+(0.2*XSTEP(IX))
              IF (XPIN.LE.OCRIT1) IFLAG=1
C
C         boundary block type 8
C
            ELSEIF (JTBB(I4).EQ.(JTBB(I4-1)+1).AND.
     1          JTBB(I4).EQ.JTBB(I4+1)) THEN
              OCRIT1=XFACE(IX)+(0.2*XSTEP(IX))
              IF (XPIN.LE.OCRIT1) IFLAG=1
              OCRIT2=YFACE(IY)+(0.8*YSTEP(IY))
              IF (YPIN.GE.OCRIT2) IFLAG=1
C
C         boundary block type 9
C
            ELSEIF (I4.EQ.NTBB) THEN
              OCRIT1=XFACE(IX)+(0.8*XSTEP(IX))
              IF (XPIN.GE.OCRIT1) IFLAG=1
              OCRIT2=YFACE(IY)+(0.8*YSTEP(IY))
              IF (YPIN.GE.OCRIT2) IFLAG=1
            ENDIF
          ENDIF
 9030 CONTINUE
C
C       next, check the bottom boundary
C
      DO 9040 I5=1,NBBB
C
```

```
C        is the particle in a boundary block
C
           IF (IX.EQ.IBBB(I5).AND.IY.EQ.JBBB(I5)) THEN
C
C        the numbering system below applies to the bottom boundary
C
C                        5            6
C                        |            |  7
C                       [x][x][x][x][x] /
C                       [x]          [x]
C            1-  [x][x][x][x] \       [x][x][x][x] -9
C                  |     |   4        |
C                  2     3            8
C
C          boundary block type 1
C
             IF (I5.EQ.1) THEN
               OCRIT1=XFACE(IX)+(0.2*XSTEP(IX))
               IF (YPIN.LE.OCRIT1) IFLAG=1
               OCRIT2=YFACE(IY)+(0.2*YSTEP(IY))
               IF (YPIN.LE.OCRIT2) IFLAG=1
C
C          boundary block type 2
C
             ELSEIF (JBBB(I5).EQ.JBBB(I5-1).AND.
     1           JBBB(I5).EQ.JBBB(I5+1)) THEN
               OCRIT1=YFACE(IY)+(0.2*YSTEP(IY))
               IF (YPIN.LE.OCRIT1) IFLAG=1
C
C          boundary block type 3
C
             ELSEIF (JBBB(I5).EQ.JBBB(I5-1).AND.
     1           JBBB(I5).EQ.(JBBB(I5+1)-1)) THEN
               OCRIT1=XFACE(IX)+(0.8*XSTEP(IX))
               IF (XPIN.GE.OCRIT1) IFLAG=1
               OCRIT2=YFACE(IY)+(0.2*YSTEP(IY))
               IF (YPIN.LE.OCRIT2) IFLAG=1
C
C          boundary block type 4
C
             ELSEIF (JBBB(I5).EQ.(JBBB(I5-1)+1).AND.
     1           JBBB(I5).EQ.(JBBB(I5-1)-1)) THEN
               OCRIT1=XFACE(IX)+(0.8*XSTEP(IX))
               IF (XPIN.GE.OCRIT1) IFLAG=1
C
C          boundary block type 5
C
             ELSEIF (JBBB(I5).EQ.(JBBB(I5-1)+1).AND.
     1           JBBB(I5).EQ.JBBB(I5+1)) THEN
               OCRIT1=XFACE(IX)+(0.8*XSTEP(IX))
               OCRIT2=YFACE(IY)+(0.2*YSTEP(IY))
               IF (XPIN.GE.OCRIT1.AND.YPIN.LE.OCRIT2) IFLAG=1
C
C          boundary block type 6
C
             ELSEIF (JBBB(I5).EQ.JBBB(I5-1).AND.
     1           JBBB(I5).EQ.(JBBB(I5+1)+1)) THEN
               OCRIT1=XFACE(IX)+(0.2*XSTEP(IX))
               OCRIT2=YFACE(IY)+(0.2*YSTEP(IY))
               IF (XPIN.LE.OCRIT1.AND.YPIN.LE.OCRIT2) IFLAG=1
C
C          boundary block type 7
C
             ELSEIF (JBBB(I5).EQ.(JBBB(I5-1)-1).AND.
     1           JBBB(I5).EQ.(JBBB(I5+1)+1)) THEN
               OCRIT1=XFACE(IX)+(0.2*XSTEP(IX))
               IF (XPIN.LE.OCRIT1) IFLAG=1
C
C          boundary block type 8
C
             ELSEIF (JBBB(I5).EQ.(JBBB(I5-1)-1).AND.
     1           JBBB(I5).EQ.JBBB(I5+1)) THEN
               OCRIT1=XFACE(IX)+(0.2*XSTEP(IX))
               OCRIT2=YFACE(IY)+(0.2*YSTEP(IY))
               IF (XPIN.LE.OCRIT1.AND.YPIN.LE.OCRIT2) IFLAG=1
C
C          boundary block type 9
C
             ELSEIF (I5.EQ.NBBB) THEN
               OCRIT1=XFACE(IX)+(0.8*XSTEP(IX))
               IF (XPIN.GE.OCRIT1) IFLAG=1
               OCRIT2=YFACE(IY)+(0.2*YSTEP(IY))
               IF (YPIN.LE.OCRIT2) IFLAG=1
             ENDIF
           ENDIF
 9040 CONTINUE
C
C        lastly, check the right boundary
C
      DO 9050 I6=1,NRBB
C
C        is the particle in a boundary block
C
           IF (IX.EQ.IRBB(I6).AND.IY.EQ.JRBB(I6)) THEN
C
C        the numbering system below applies to the right boundary
C
C                    [x] -9
C              7     [x]
C                \   [x]
C           6-  [x][x][x] -8
C               [x]
C               [x]
C               [x]
C           5-  [x][x][x] -3
C                 /  [x]
C               4    [x] -2
C                    [x] -1
C
C          boundary block type 1
C
             IF (I6.EQ.1) THEN
               OCRIT1=XFACE(IX)+(0.8*XSTEP(IX))
               IF (XPIN.GE.OCRIT1) IFLAG=1
               OCRIT2=YFACE(IY)+(0.2*YSTEP(IY))
               IF (YPIN.LE.OCRIT2) IFLAG=1
C
C          boundary block type 2
C
             ELSEIF (IRBB(I6).EQ.IRBB(I6-1).AND.
     1           IRBB(I6).EQ.IRBB(I6+1)) THEN
               OCRIT1=XFACE(IX)+(0.8*XSTEP(IX))
               IF (XPIN.GE.OCRIT1) IFLAG=1
C
C          boundary block type 3
C
             ELSEIF (IRBB(I6).EQ.IRBB(I6-1) AND.
     1           IRBB(I6).EQ.(IRBB(I6+1)+1)) THEN
               OCRIT1=XFACE(IX)+(0.8*XSTEP(IX))
               IF (XPIN.GE.OCRIT1) IFLAG=1
               OCRIT2=YFACE(IY)+(0.8*YSTEP(IY))
               IF (YPIN.GE.OCRIT2) IFLAG=1
C
C          boundary block type 4
C
             ELSEIF (IRBB(I6).EQ.(IRBB(I6-1)-1).AND.
     1           IRBB(I6).EQ.(IRBB(I6+1)-1)) THEN
               OCRIT1=YFACE(IY)+(0.8*YSTEP(IY))
               IF (YPIN.GE.OCRIT1) IFLAG=1
C
C          boundary block type 5
C
             ELSEIF (IRBB(I6).EQ.(IRBB(I6-1)-1).AND.
     1           IRBB(I6).EQ.IRBB(I6+1)) THEN
               OCRIT1=XFACE(IX)+(0.8*XSTEP(IX))
               OCRIT2=YFACE(IY)+(0.8*YSTEP(IY))
               IF (XPIN.GE.OCRIT1.AND.YPIN.GE.OCRIT2) IFLAG=1
C
C          boundary block type 6
C
             ELSEIF (IRBB(I6).EQ.IRBB(I6-1).AND.
     1           IRBB(I6).EQ.(IRBB(I6+1)-1)) THEN
               OCRIT1=XFACE(IX)+(0.8*XSTEP(IX))
               OCRIT2=YFACE(IY)+(0.2*YSTEP(IY))
               IF (XPIN.GE.OCRIT1.AND.YPIN.LE.OCRIT2) IFLAG=1
C
C          boundary block type 7
C
             ELSEIF (IRBB(I6).EQ.(IRBB(I6-1)+1) AND
     1           IRBB(I6).EQ.(IRBB(I6+1)-1)) THEN
               OCRIT1=YFACE(IY)+(0.2*YSTEP(IY))
               IF (YPIN.LE.OCRIT1) IFLAG=1
C
C          boundary block type 8
C
             ELSEIF (IRBB(I6).EQ.(IRBB(I6-1)+1).AND.
     1           IRBB(I6).EQ.IRBB(I6+1)) THEN
               OCRIT1=XFACE(IX)+(0.8*XSTEP(IX))
               IF (XPIN.GE.OCRIT1) IFLAG=1
               OCRIT2=YFACE(IY)+(0.2*YSTEP(IY))
               IF (YPIN.LE.OCRIT2) IFLAG=1
C
C          boundary block type 9
C
             ELSEIF (I6.EQ.NRBB) THEN
               OCRIT1=XFACE(IX)+(0.8*XSTEP(IX))
               IF (XPIN.GE.OCRIT1) IFLAG=1
               OCRIT2=YFACE(IY)+(0.8*YSTEP(IY))
               IF (YPIN.GE.OCRIT2) IFLAG=1
             ENDIF
           ENDIF
 9050 CONTINUE
C
C        send back the new particle location to the main routine
C
      XPI=XPIN
      YPI=YPIN
      RETURN
      END
C
C
C        RAN3 generates a random number with mean 0.0 and
C        standard deviation 1.0.  Set IDUM to any negative
C        number to initialize or re-initialize the sequence
C
      FUNCTION RAN3(IDUM)
      IMPLICIT REAL*8 (A-H,O-Z)
      PARAMETER (MBIG=1000000000,MSEED=161803398,MZ=0,FAC=1./MBIG)
      INTEGER MA(55)
      SAVE IFF,INEXT,INEXTP,MA
      DATA IFF /0/
      IF (IDUM.LT.0 .OR. IFF.EQ.0) THEN
            IFF=1
            MJ=MSEED-IABS(IDUM)
            MJ=MOD(MJ,MBIG)
            MA(55)=MJ
            MK=1
            DO 11 I=1,54
              II=MOD(21*I,55)
              MA(II)=MK
              MK=MJ-MK
              IF (MK.LT.MZ) MK=MK+MBIG
              MJ=MA(II)
 11     CONTINUE
            DO 13 K=1,4
              DO 12 I=1,55
                MA(I)=MA(I)-MA(1+MOD(I+30,55))
                IF (MA(I).LT.MZ) MA(I)=MA(I)+MBIG
 12         CONTINUE
 13     CONTINUE
            INEXT=0
            INEXTP=31
            IDUM=1
      ENDIF
      INEXT=INEXT+1
      IF (INEXT.EQ.56) INEXT=1
      INEXTP=INEXTP+1
      IF (INEXTP.EQ.56) INEXTP=1
      MJ=MA(INEXT)-MA(INEXTP)
      IF (MJ.LT.MZ) MJ=MJ+MBIG
      MA(INEXT)=MJ
      RAN3=FLOAT(MJ)*FAC
      RETURN
      END
```

```
C
C       subroutine OUTPUT sends particle tracks to an
C       output surfer file (RWALK.BLN)
C
      SUBROUTINE OUTPUT(NPART,XPO,YPO,NPO)
      IMPLICIT REAL*8(A-H,O-Z)
      DIMENSION XPO(200,201),YPO(200,201),NPO(200)
      OPEN (21,FILE='rwapc.bln',STATUS='UNKNOWN')
      DO 10000 I=1,NPART
           WRITE (21,10500) NPO(I)
           DO 10001 J=1,NPO(I)
             WRITE (21,10501) XPO(I,J),YPO(I,J)
10001   CONTINUE
10000 CONTINUE
10500 FORMAT(I5)
10501 FORMAT(2X,F9.2,2X,F9.2)
      RETURN
      END
```

APPENDIX III

FORTRAN CODE

CZAREA.FOR

"CZAREA.FOR"

```
      PROGRAM CZAREA
C
C       * This is a program to determine the area of a capture
C       * zone by the method laid out in the CRC Handbook
C
C                                  D.J. Miln Harvey, Feb 1998
C
      IMPLICIT REAL*8 (A-H,O-Z)
      DIMENSION XPOINT(500),YPOINT(500)
C
C       * open input SURFER *.bln file
C
      OPEN(UNIT=20,FILE='input.bln',STATUS='OLD')
C
C       * read input for WHPA information and determine
C       * the Minimum and Maximum points in the capture zone
C
      READ(20,1000) NP
      NPM1=NP-1
      DO 100 I1=1,NP
        READ(20,*) XPOINT(I1),YPOINT(I1)
  100 CONTINUE
C
C       * calculate the products of x and y
C
C       * PROD1 = X(i) * Y(i+1)
C       * PROD2 = Y(i) * X(i+1)
C
      SUM1=0.0
      SUM2=0.0
      DO 200 I2=1,NPM1
        PROD1=XPOINT(I2)*YPOINT(I2+1)
        PROD2=YPOINT(I2)*XPOINT(I2+1)
        SUM1=SUM1+PROD1
        SUM2=SUM2+PROD2
  200 CONTINUE
C
C       * AREA = 0.5 * [SUM(PROD1) - SUM(PROD2)]
C
      AREA=(SUM1-SUM2)*0.5
      WRITE(*,*)
      WRITE(*,*)
      WRITE(*,1001) AREA
      WRITE(*,*)
 1000 FORMAT(I5)
 1001 FORMAT(2X,'The area of the capture zone is:',F12.1,' sq.ft.')
      END
```

APPENDIX IV

FORTRAN CODE

UNIFORM.FOR

"UNIFORM.FOR"

```
      PROGRAM UNIFORM
C
C
C       * This is a program to generate the dividing
C       * streamline for a groundwater pumping well
C       * using the uniform flow equation and delineates
C       * a t-year capture zone for it
C
C                                  D.J. Miln Harvey, Jun 1997
C
      CHARACTER*80 FHEAD
      REAL RKH,DEPTH,RI,QWELL,XWELL,YWELL,AREG,A1,TTIME,POROS,WSDEP
      DIMENSION XTEMP(23),YTEMP(23),XOUT(23),YOUT(23)
C
C       * open input and output files
C
      OPEN(UNIT=20,FILE='ufe.in',STATUS='OLD')
      OPEN(UNIT=21,FILE='ufe.bln',STATUS='UNKNOWN')
C
C       * set model constants
C
      PI=3.1415926536
C
C       * read input data from 'ufe.in'
C
      READ(20,800) FHEAD
      READ(20,801) RKH
      READ(20,801) DEPTH
      READ(20,802) RI
      READ(20,801) QWELL
      READ(20,803) XWELL
      READ(20,803) YWELL
      READ(20,801) AREG
      READ(20,801) TTIME
      READ(20,803) POROS
      READ(20,801) WSDEP
C
C       * initialize data arrays to zero
C
      DO 100 I=1,23
        XTEMP(I)=0.0
        YTEMP(I)=0.0
        XOUT(I)=0.0
        YOUT(I)=0.0
  100 CONTINUE
C
C
C       * determine the UFE coordinates of the dividing streamline
C
C       * the stagnation point
C
C
      XSTAG=-QWELL/(2.0*PI*RKH*DEPTH*RI)
C
C       * then the boundary limit for the Y-direction
C
      YBOUND=QWELL/(2.0*RKH*DEPTH*RI)
C
C       * split the y-direction up into 11 intervals
C
      YTEMP(1)=0.92*YBOUND
      YTEMP(2)=0.88*YBOUND
      YTEMP(3)=0.84*YBOUND
      YTEMP(4)=0.80*YBOUND
      YTEMP(5)=0.72*YBOUND
      YTEMP(6)=0.64*YBOUND
      YTEMP(7)=0.56*YBOUND
      YTEMP(8)=0.48*YBOUND
      YTEMP(9)=0.40*YBOUND
      YTEMP(10)=0.24*YBOUND
      YTEMP(11)=0.08*YBOUND
      YTEMP(12)=0.0
      YTEMP(13)=-YTEMP(11)
      YTEMP(14)=-YTEMP(10)
      YTEMP(15)=-YTEMP(9)
      YTEMP(16)=-YTEMP(8)
      YTEMP(17)=-YTEMP(7)
      YTEMP(18)=-YTEMP(6)
      YTEMP(19)=-YTEMP(5)
      YTEMP(20)=-YTEMP(4)
      YTEMP(21)=-YTEMP(3)
      YTEMP(22)=-YTEMP(2)
      YTEMP(23)=-YTEMP(1)
C
C       * determine the (x,y) points for the dividing streamline
C
      DO 200 I1=1,11
        XTEMP(I1)=-YTEMP(I1)/TAN(2.0*PI*RKH*DEPTH*RI*YTEMP(I1)/QWELL)
  200 CONTINUE
      XTEMP(12)=XSTAG
      DO 250 I2=13,23
        XTEMP(I2)=-YTEMP(I2)/TAN(2.0*PI*RKH*DEPTH*RI*YTEMP(I2)/QWELL)
  250 CONTINUE
C
C
C       * determine the upgradient 10 year extent of the capture zone
C       * by comparing the distance upgradient in the x direction to the
C       * x coordinates of the streamline points
C
C
      UPGRDX=(QWELL*TTIME/(PI*POROS*WSDEP))**0.50
      IF(UPGRDX.GE.XTEMP(1)) THEN
        DY1=YTEMP(1)-YTEMP(2)
        DX1=XTEMP(1)-XTEMP(2)
        XDIFF=UPGRDX-XTEMP(2)
        SLOPE1=DY1/DX1
        XTEMP(1)=UPGRDX
        XTEMP(23)=XTEMP(1)
        YTEMP(1)=YTEMP(2)+(SLOPE1*XDIFF)
        YTEMP(23)=-YTEMP(1)
      ELSEIF(UPGRDX.GE.XTEMP(2).AND.UPGRDX.LT.XTEMP(1)) THEN
        DY1=YTEMP(1)-YTEMP(2)
        DX1=XTEMP(1)-XTEMP(2)
        XDIFF=UPGRDX-XTEMP(2)
        SLOPE1=DY1/DX1
        XTEMP(1)=UPGRDX
        XTEMP(23)=XTEMP(1)
        YTEMP(1)=YTEMP(2)+SLOPE1*XDIFF
        YTEMP(23)=-YTEMP(1)
      ELSEIF(UPGRDX.GE.XTEMP(3).AND.UPGRDX.LT.XTEMP(2)) THEN
        DY1=YTEMP(2)-YTEMP(3)
        DX1=XTEMP(2)-XTEMP(3)
        XDIFF=UPGRDX-XTEMP(3)
        SLOPE1=DY1/DX1
        XTEMP(1)=UPGRDX
        XTEMP(23)=XTEMP(1)
        YTEMP(1)=YTEMP(3)+SLOPE1*XDIFF
        YTEMP(23)=-YTEMP(1)
        XTEMP(2)=(XTEMP(1)+XTEMP(3))/2.0
        XTEMP(22)=XTEMP(2)
        YTEMP(2)=(YTEMP(1)+YTEMP(3))/2.0
        YTEMP(22)=-YTEMP(2)
      ELSEIF(UPGRDX.GE.XTEMP(4).AND.UPGRDX.LT.XTEMP(3)) THEN
        DY1=YTEMP(3)-YTEMP(4)
        DX1=XTEMP(3)-XTEMP(4)
        XDIFF=UPGRDX-XTEMP(4)
        SLOPE1=DY1/DX1
        XTEMP(1)=UPGRDX
        XTEMP(23)=XTEMP(1)
        YTEMP(1)=YTEMP(3)+SLOPE1*XDIFF
        YTEMP(23)=-YTEMP(1)
        XTEMP(2)=(XTEMP(1)+XTEMP(3))/2.0
        XTEMP(22)=XTEMP(2)
        YTEMP(2)=(YTEMP(1)+YTEMP(3))/2.0
        YTEMP(22)=-YTEMP(2)
        XTEMP(3)=XTEMP(4)
        XTEMP(21)=XTEMP(3)
        YTEMP(3)=YTEMP(4)
        YTEMP(21)=-YTEMP(3)
        XTEMP(4)=(XTEMP(4)+XTEMP(5))/2.0
        XTEMP(20)=XTEMP(4)
        YTEMP(4)=(YTEMP(4)+YTEMP(5))/2.0
        YTEMP(20)=-YTEMP(4)
      ELSE
        WRITE(*,*)
        WRITE(*,*) ' **** Something wrong with the capture ****'
        WRITE(*,*) ' **** zones parameters you have chosen ****'
        WRITE(*,*)
        WRITE(*,*) ' **** Abnormal Termination of UFE.EXE  ****'
        WRITE(*,*)
        STOP
      ENDIF
C
C
C       * determine the output points with respect to the center of the
C       * well by finding the magnitude of the distance, the angle from
C       * the well to the point and adding the regional flow angle
C
C
      DO 300 I3=1,23
        D1=(ABS(XTEMP(I3))**2.0+ABS(YTEMP(I3))**2.0)**0.50
        IF(XTEMP(I3).EQ.0.0.AND.YTEMP(I3).GT.0.0) THEN
          A1=90.0
        ELSEIF(XTEMP(I3).LT.0.0.AND.YTEMP(I3).GT.0.0) THEN
          A1=(ATAN(YTEMP(I3)/XTEMP(I3)))*180.0/PI)+180.0
        ELSEIF(XTEMP(I3).LT.0.0.AND.YTEMP(I3).EQ.0.0) THEN
          A1=180.0
        ELSEIF(XTEMP(I3).LT.0.0.AND.YTEMP(I3).LT.0.0) THEN
          A1=(ATAN(YTEMP(I3)/XTEMP(I3)))*180.0/PI)+180.0
        ELSEIF(XTEMP(I3).EQ.0.0.AND.YTEMP(I3).LT.0.0) THEN
          A1=270.0
        ELSEIF(XTEMP(I3).GT.0.0.AND.YTEMP(I3).LT.0.0) THEN
          A1=(ATAN(YTEMP(I3)/XTEMP(I3)))*180.0/PI)+360.0
        ELSE
          A1=ATAN(YTEMP(I3)/XTEMP(I3)))*180.0/PI
        ENDIF
C
C
C       * add the u.f.e angle to the angle of the regional gradient
C
C
        A1=A1+AREG
        IF(A1.GE.360.0) A1=A1-360.0
C
C       * determine the new position of point (x,y)
C
        IF(A1.EQ.0.0) THEN
          XOUT(I3)=D1+XWELL
          YOUT(I3)=YWELL
        ELSEIF(A1.GT.0.0.AND.A1.LT.90.0) THEN
          XOUT(I3)=(D1*COS(A1*PI/180.0))+XWELL
          YOUT(I3)=(D1*SIN(A1*PI/180.0))+YWELL
        ELSEIF(A1.EQ.90.0) THEN
          XOUT(I3)=XWELL
          YOUT(I3)=D1+YWELL
        ELSEIF(A1.GT.90.AND.A1.LT.180.0) THEN
          XOUT(I3)=(D1*COS(A1*PI/180.0))+XWELL
          YOUT(I3)=(D1*SIN(A1*PI/180.0))+YWELL
        ELSEIF(A1.EQ.180.0) THEN
          XOUT(I3)=XWELL-D1
          YOUT(I3)=YWELL
        ELSEIF(A1.GT.180.0.AND.A1.LT.270.0) THEN
          XOUT(I3)=(D1*COS(A1*PI/180.0))+XWELL
          YOUT(I3)=(D1*SIN(A1*PI/180.0))+YWELL
        ELSEIF(A1.EQ.270) THEN
          XOUT(I3)=XWELL
          YOUT(I3)=YWELL-D1
        ELSE
          XOUT(I3)=(D1*COS(A1*PI/180.0))+XWELL
          YOUT(I3)=(D1*SIN(A1*PI/180.0))+YWELL
        ENDIF
  300 CONTINUE
C
C       * print the results out to a SURFER file
C
      NUMPTS=24
      WRITE(21,804) NUMPTS
      DO 400 I4=1,23
        WRITE(21,805) XOUT(I4),YOUT(I4)
  400 CONTINUE
      WRITE(21,805) XOUT(1),YOUT(1)
C
C       * formating statements
C
  800 FORMAT(A80)
  801 FORMAT(F10.1)
```

```
  802 FORMAT(F10.4)
  803 FORMAT(F10.2)
  804 FORMAT(I5)
  805 FORMAT(1X,F10.2,2X,F10.2)
C
C
C
      WRITE(*,*)
      WRITE(*,*) '  ***** Normal Termination of UPE.EXE ***** '
      WRITE(*,*)
      STOP
      END
```

APPENDIX V

FORTRAN CODE

CZSTAT.FOR

"CZSTAT.FOR"

```
C
C     This is a program to statistically analyze the
C     capture zone boundaries produced by CAPZON and
C     uncertainty analysis simulation
C
C                                   D.J. Miln Harvey, June 1998
C
C       CZBPX(300,150) = capture zone boundary point input
C       CZBPY(300,150) = capture zone boundary point input
C       300 = the number of capture zones analyzed
C       150 = the number of points in each capture zone
C       180 = the number of transects (every 2 degrees)
C       BPX(300,200) = output CZs from intersection points
C       BPY(300,200) = output CZs from intersection points
C       200 = number of intersection points with transects
C       DIST(200,300) = distance from center of mass to
C                       intersection point with output CZ
C       CZ50X(182) = 50th percentile capture zone
C       CZ50Y(182) = 50th percentile capture zone
C       ZOCX(182) = zone of certainty (ZOC)
C       ZOCY(182) = zone of certainty (ZOC)
C       ZOUX(182) = zone of uncertainty (ZOU)
C       ZOUY(182) = zone of uncertainty (ZOU)
C       CZ95X(182) = 95th percentile capture zone
C       CZ95Y(182) = 95th percentile capture zone
C
      IMPLICIT REAL*8(A-H,O-Z)
      COMMON /POINTS/ CZBPX,CZBPY
      INTEGER NBPTS(300)
      DIMENSION CZBPX(300,150),CZBPY(300,150),CZ50X(182),
     1          CZ50Y(182),CZAREA(300),ZOCX(182),ZOCY(182),
     2          ZOUX(182),ZOUY(182),CZ95X(182),CZ95Y(182)
C
C   first, get input information from external files
C
      CALL INPUT(NUMCZ,NBPTS)
C
C   determine the average capture zone boundary (50th percentile)
C   and the pdf of distances away from the center of wellfield mass
C
      CALL FIFTY(NUMCZ,NBPTS,CZ50X,CZ50Y,CZ95X,CZ95Y,
     1           ZOCX,ZOCY,ZOUX,ZOUY)
C
C   calculate the area of each of the N capture zones and the
C   50th percentile capture zone
C
      CALL AREA(NUMCZ,NBPTS,CZAREA,CZ50X,CZ50Y,AREA50,
     1          ZOCX,ZOCY,ZOUX,ZOUY,AZOC,AZOU)
C
C   calculate the risk cost associated with the uncertainty in the
C   capture zone analysis technique and its input parameter values
C
      CALL DECISION(NUMCZ,CZAREA,AREA50,DANAL)
C
C   determine the uncertainty in the input capture zones
C
      CALL UNCERT(NUMCZ,CZAREA,AZOC,AZOU,VARCZ,UNCZ)
C
C   send statistical information to output files
C
      CALL OUTPUT(NUMCZ,CZ50X,CZ50Y,CZAREA,AREA50,DANAL,
     1            ZOCX,ZOCY,ZOUX,ZOUY,VARCZ,UNCZ,
     2            CZ95X,CZ95Y)
C
C
      WRITE(*,*)
      WRITE(*,*) ' ******   Termination of CZSTAT   ****** '
      WRITE(*,*)
      WRITE(*,*)
      END
C
C   ******************************************************
C   *                                                    *
C   *                                                    *
C   *          *****  subroutines  *****                 *
C   *                                                    *
C   *                                                    *
C   ******************************************************
C
C     subroutine INPUT gets input capture zone
C     information from an external file (czstat.in)
C
      SUBROUTINE INPUT(NUMCZ,NBPTS)
      IMPLICIT REAL*8(A-H,O-Z)
      COMMON /POINTS/ CZBPX,CZBPY
      DIMENSION CZBPX(300,150),CZBPY(300,150)
      INTEGER NBPTS(300)
C
      OPEN(UNIT=20,FILE='czstat.in',STATUS='OLD')
C
C   read in capture zone boundary lines into a 2 dimensional array
C
C   read in the number of capture zone boudaries
C   from the first line of the input cumulative capture zone file
C
      READ(20,1500) NUMCZ
      WRITE(*,*)
      WRITE(*,*) ' *******   Program CZSTAT   ******* '
      WRITE(*,*)
C
C   read capture zone points from input file
C
      DO 1000 I1=1,NUMCZ
        READ(20,1500) NBPTS(I1)
        DO 1001 I2=1,NBPTS(I1)
          READ(20,*) CZBPX(I1,I2),CZBPY(I1,I2)
 1001   CONTINUE
 1000 CONTINUE
C
 1500 FORMAT(I8)
      RETURN
      END
C
C     subroutine FIFTY determines the 5,50 and 95th percentile CZ
C     and the zone of certainty (ZOC) and zone of uncertainty (ZOU)
C
      SUBROUTINE FIFTY(NUMCZ,NBPTS,CZ50X,CZ50Y,CZ95X,CZ95Y,
     1                 ZOCX,ZOCY,ZOUX,ZOUY)
      IMPLICIT REAL*8(A-H,O-Z)
      COMMON /POINTS/ CZBPX,CZBPY
      DIMENSION CZBPX(300,150),CZBPY(300,150),BPX(300,200),
     1     BPY(300,200),DIST(200,300),CZ50X(182),CZ50Y(182),
     2     ATMP(150),ZOCX(182),ZOCY(182),ZOUX(182),ZOUY(182),
     3     CZ95X(182),CZ95Y(182)
      INTEGER NBPTS(300)
      LOGICAL SORTED
C
C   open a file to output a pdf of the distance of each
C   capture zone away from the center of mass
C
      OPEN(UNIT=23,FILE='czpdf.dat',STATUS='UNKNOWN')
C
C   set subroutine constants
C
      PI=3.1415926536
C
C   determine center of mass of capture zone endpoints
C
      ICENT=0
      XWSUM=0.0
      YWSUM=0.0
      DO 2000 I3=1,NUMCZ
        DO 2040 I4=1,NBPTS(I3)
          ICENT=ICENT+1
          XWSUM=XWSUM+CZBPX(I3,I4)
          YWSUM=YWSUM+CZBPY(I3,I4)
 2040   CONTINUE
 2000 CONTINUE
      CENTX=XWSUM/FLOAT(ICENT)
      CENTY=YWSUM/FLOAT(ICENT)
C
C   for each capture zone
C
      DO 2001 JMH1=1,NUMCZ
C
        WRITE(*,2501) JMH1
C
C   for each capture zone point determine its angle
C   with respect to the center of mass and
C   save it into an array for further analysis
C
        IEND=NBPTS(JMH1)-1
        AMIN=361.0
        AMAX=0.0
        DO 2002 JMH2=1,IEND
          X1=(CZBPX(JMH1,JMH2)-CENTX)
          Y1=(CZBPY(JMH1,JMH2)-CENTY)
          IF(X1.EQ.0.0) X1=0.000001
          ARAD=ATAN(Y1/X1)
          ANGLE=(ARAD*180.0/PI)
          IF(Y1.GT.0.0.AND.X1.LT.0.0) ANGLE=180.0+ANGLE
          IF(Y1.EQ.0.0.AND.X1.LT.0.0) ANGLE=180.0
          IF(Y1.LT.0.0.AND.X1.LT.0.0) ANGLE=180.0+ANGLE
          IF(Y1.LT.0.0.AND.X1.GT.0.0) ANGLE=360.0+ANGLE
          ATMP(JMH2)=ANGLE
          IF(ANGLE.LT.AMIN) THEN
            AMIN=ANGLE
            IMIN=JMH2
          ENDIF
          IF(ANGLE.GT.AMAX) THEN
            AMAX=ANGLE
            IMAX=JMH2
          ENDIF
 2002   CONTINUE
        ATMP(IEND+1)=ATMP(1)
C
C   for each radial transect from 0 to 360 degrees compare
C   the transect angle to the angle of each capture zone point
C
        ANGLE1=-1.0
        DO 2003 JMHJ=1,180
          ANGLE1=(ANGLE1+2.0)
C
C   determine the two points on either side of the transect
C   line based on their angular position w.r.t ANGLE1
C
          IP1=0
          IP2=0
          DO 2004 JMH4=1,IEND
            IF(ATMP(JMH4).LT.ANGLE1.AND.
     1         ATMP(JMH4+1).GT.ANGLE1) THEN
              IP1=JMH4
              IP2=JMH4+1
            ENDIF
 2004     CONTINUE
          IF (IP1.EQ.0.AND.IP2.EQ.0) THEN
            IP1=IMAX
            IP2=IMIN
          ENDIF
          XP1=CZBPX(JMH1,IP1)-CENTX
          YP1=CZBPY(JMH1,IP1)-CENTY
          XP2=CZBPX(JMH1,IP2)-CENTX
          YP2=CZBPY(JMH1,IP2)-CENTY
C
C   determine the radian measure of ANGLE1
C
          IF(ANGLE1.GT.90.0.AND.ANGLE1.LT.270.0) THEN
            ARAD1=(ANGLE1-180.0)*PI/180.0
          ELSEIF(ANGLE1.GT.270.0) THEN
            ARAD1=(ANGLE1-360.0)*PI/180.0
          ELSE
            ARAD1=ANGLE1*PI/180.0
          ENDIF
C
C   the intercept for the transect angle is (0,0)
C
          SLOPE1=TAN(ARAD1)
```

```
          B1=0.0
C
C   determine the slope and intercept of (XP1,YP1) (XP2,YP2)
C
          DY2=(YP2-YP1)
          DX2=(XP2-XP1)
          IF (DX2.EQ.0.0) DX2=0.000001
          SLOPE2=DY2/DX2
          B2=YP1-(SLOPE2*XP1)
          DSLOPE=(SLOPE1-SLOPE2)
          IF (DSLOPE.EQ.0.0) DSLOPE=0.000001
          XINT=B2/DSLOPE
          YINT=SLOPE1*XINT
C
C   save this point in an array for further statistical analysis
C
          BPX(JMH1,JMH3)=XINT
          BPY(JMH1,JMH3)=YINT
 2003   CONTINUE
 2001 CONTINUE
C
C   analyze the capture zones statistically
C   ---------------------------------------
C
C   start by looking at each of the 180 radial transects, calculate
C   the distance from center of mass to the each boundary point,
C   and find the 50th percentile capture zone boundary
C
      WRITE(*,*)
      WRITE(*,*) '  Determining the statistical capture zones'
      WRITE(*,*)
C
      XNUMCZ=FLOAT(NUMCZ)
C
      TMP5=XNUMCZ*0.05
      TMP95=XNUMCZ*0.95
      R95TH=NINT(TMP95)
      I95TH=REAL(R95TH)
C
      TMP50=XNUMCZ*0.50
      TMP50A=ANINT(TMP50)
      DIFF50=ABS(TMP50-TMP50A)
      IF (DIFF50.NE.0.0) THEN
          I50TH=REAL(TMP50)+1
      ELSE
          I50TH=REAL(TMP50)
      ENDIF
C
C   determine the distance from the center of mass
C
      DO 2026 JMH20=1,180
        DO 2027 JMH21=1,NUMCZ
          DIST(JMH20,JMH21)=(ABS(BPX(JMH21,JMH20))**2.0+
     &                       ABS(BPY(JMH21,JMH20))**2.0)**0.50
 2027   CONTINUE
C
C   bubble sort the distances away from the center of mass
C
        NCZM1=(NUMCZ-1)
        SORTED=.FALSE.
 2028   IF (.NOT.SORTED) THEN
          SORTED=.TRUE.
          DO 2029 JMH23=1,NCZM1
            IF (DIST(JMH20,JMH23).GT.DIST(JMH20,JMH23+1)) THEN
              TEMP1=DIST(JMH20,JMH23)
              TEMP2=BPX(JMH23,JMH20)
              TEMP3=BPY(JMH23,JMH20)
              DIST(JMH20,JMH23)=DIST(JMH20,JMH23+1)
              BPX(JMH23,JMH20)=BPX(JMH23+1,JMH20)
              BPY(JMH23,JMH20)=BPY(JMH23+1,JMH20)
              DIST(JMH20,JMH23+1)=TEMP1
              BPX(JMH23+1,JMH20)=TEMP2
              BPY(JMH23+1,JMH20)=TEMP3
              SORTED=.FALSE.
            ENDIF
 2029     CONTINUE
          GOTO 2028
        ENDIF
C
C   send the distances from the 1st capture zone to an output
C   file which is a probability density function of distance
C
        IF(JMH20.EQ.1) THEN
           DO 2030 JMH30=1,NCZM1
             WRITE(23,2502) JMH30,DIST(1,JMH30)
 2030      CONTINUE
        ENDIF
C
C   choose the 50th percentile values for each of the 180
C   transect lines, and save them in an output array
C
        CZ50X(JMH20)=BPX(I50TH,JMH20)+CENTX
        CZ50Y(JMH20)=BPY(I50TH,JMH20)+CENTY
        ZOCX(JMH20)=BPX(1,JMH20)+CENTX
        ZOCY(JMH20)=BPY(1,JMH20)+CENTY
        ZOUX(JMH20)=BPX(NUMCZ,JMH20)+CENTX
        ZOUY(JMH20)=BPY(NUMCZ,JMH20)+CENTY
        CZ95X(JMH20)=BPX(I95TH,JMH20)+CENTX
        CZ95Y(JMH20)=BPY(I95TH,JMH20)+CENTY
 2026 CONTINUE
C
C   formatting information
C
 2501 FORMAT(5X,'Analyzing capture zone ',I5)
 2502 FORMAT(2X,I3,2X,F10.2)
      RETURN
      END
C
C     subroutine AREA determines the area of each capture zone
C                 and the area of the average capture zone (50%)
C
      SUBROUTINE AREA(NUMCZ,NBPTS,CZAREA,CZ50X,CZ50Y,AREA50,
     1                ZOCX,ZOCY,ZOUX,ZOUY,AZOC,AZOU)
C
C   CZAREA(I)  = area of the Ith capture zone
C   AREA50     = area of the 50 percentile capture zone
C
      IMPLICIT REAL*8 (A-H,O-Z)
      COMMON /POINTS/ CZBPX,CZBPY
      DIMENSION CZBPX(300,150),CZBPY(300,150),CZ50X(182),
     1          CZ50Y(182),CZAREA(300),ZOCX(182),ZOCY(182),
     2          ZOUX(182),ZOUY(182)
      INTEGER NBPTS(300)
C
C   calculate the products of x and y
C
C   PROD1 = X(i) * Y(i+1)
C   PROD2 = Y(i) * X(i+1)
C
      DO 3000 I1=1,NUMCZ
        SUM1=0.0
        SUM2=0.0
        NP=NBPTS(I1)-1
        DO 3001 I2=1,NP
          PROD1=CZBPX(I1,I2)*CZBPY(I1,I2+1)
          PROD2=CZBPY(I1,I2)*CZBPX(I1,I2+1)
          SUM1=SUM1+PROD1
          SUM2=SUM2+PROD2
 3001   CONTINUE
C
C   AREA = 0.5 * [SUM(PROD1) - SUM(PROD2)]
C
        CZAREA(I1)=(SUM1-SUM2)*0.5
 3000 CONTINUE
C
C   calculate the area of the 50th percentile capture zone
C
      SUM1=0.0
      SUM2=0.0
      DO 3002 I3=1,180
        PROD1=CZ50X(I3)*CZ50Y(I3+1)
        PROD2=CZ50Y(I3)*CZ50X(I3+1)
        SUM1=SUM1+PROD1
        SUM2=SUM2+PROD2
 3002 CONTINUE
C
C   AREA = 0.5 * [SUM(PROD1) - SUM(PROD2)]
C
      AREA50=(SUM1-SUM2)*0.50
C
C   calculate the area of the ZOC and ZOU
C
      SUM1=0.0
      SUM2=0.0
      DO 3003 I4=1,180
        PROD1=ZOCX(I4)*ZOCY(I4+1)
        PROD2=ZOCY(I4)*ZOCX(I4+1)
        SUM1=SUM1+PROD1
        SUM2=SUM2+PROD2
 3003 CONTINUE
      AZOC=(SUM1-SUM2)*0.5
C
      SUM1=0.0
      SUM2=0.0
      DO 3004 I5=1,180
        PROD1=ZOUX(I5)*ZOUY(I5+1)
        PROD2=ZOUY(I5)*ZOUX(I5+1)
        SUM1=SUM1+PROD1
        SUM2=SUM2+PROD2
 3004 CONTINUE
      AZOU=(SUM1-SUM2)*0.5
C
      RETURN
      END
C
C     subroutine DECISION determines the cost of using the
C     current estimates of input parameter values to
C     calculate capture zones using numerical modeling
C
      SUBROUTINE DECISION(NUMCZ,CZAREA,AREA50,DANAL)
      IMPLICIT REAL*8(A-H,O-Z)
      DIMENSION CZAREA(300)
C
C   sum the differences between the uncertainty areas
C   and the 50th percentile capture zone area
C
      SUMDIF=0.0
      XNCZ=FLOAT(NUMCZ)
      DO 4000 I1=1,NUMCZ
         DAREA=ABS(CZAREA(I1)-AREA50)
         SUMDIF=SUMDIF+DAREA
 4000 CONTINUE
      DANAL=(SUMDIF/XNCZ)/43560.0
      RETURN
      END
C
C     subroutine UNCERT determines the variance in
C     the estimate of capture zone area, var(A), and
C     the uncertainty (U) in capture zone area
C
      SUBROUTINE UNCERT(NUMCZ,CZAREA,AZOC,AZOU,VARCZ,UNCZ)
      IMPLICIT REAL*8(A-H,O-Z)
      DIMENSION CZAREA(300)
C
C   determine the variance in CZAREA(I)
C
      XNCZ=FLOAT(NUMCZ)
      XNCZM1=XNCZ-1.0
      SUMCZ=0.0
      SUMCZ2=0.0
C
      DO 5000 I0=1,NUMCZ
        SUMCZ=SUMCZ+CZAREA(I0)
        SUMCZ2=SUMCZ2+(CZAREA(I0)*CZAREA(I0))
 5000 CONTINUE
C
      VARCZ=(SUMCZ2-(SUMCZ*SUMCZ/XNCZ))/XNCZM1
C
```

```
C   determine the uncertainty (U)
C
      UNCZ=(1.0-(AZOC/AZOU))*100.0
C
      RETURN
      END



C
C     subroutine OUTPUT sends the statistical information to
C     several output files:
C     ---------------------------
C     CZSTAT.BLN - the 5th,50th and 95th percentile capture zones
C     CZSTAT.OUT - the text format output file
C     ZOC.BLN    - the zone of certainty capture zone
C     ZOU.BLN    - the zone of uncertainty capture zone
C     CZ95.BLN   - the 95th percentile capture zone
C
      SUBROUTINE OUTPUT(NUMCZ,CZ50X,CZ50Y,CZAREA,AREA50,DANAL,
     1                  ZOCX,ZOCY,ZOUX,ZOUY,VARCZ,UNCZ,
     2                  CZ95X,CZ95Y)
      IMPLICIT REAL*8(A-H,O-Z)
      DIMENSION CZ50X(182),CZ50Y(182),CZAREA(300),ZOCX(182),
     1          ZOCY(182),ZOUX(182),ZOUY(182),
     2          CZ95X(182),CZ95Y(182)
C
C   first open up the output files
C
      OPEN(UNIT=21,FILE='cz50.bln',STATUS='UNKNOWN')
      OPEN(UNIT=22,FILE='czstat.out',STATUS='UNKNOWN')
      OPEN(UNIT=24,FILE='zoc.bln',STATUS='UNKNOWN')
      OPEN(UNIT=25,FILE='zou.bln',STATUS='UNKNOWN')
      OPEN(UNIT=26,FILE='cz95.bln',STATUS='UNKNOWN')
C
C   output the 50th and 95th percentile capture zones
C   to CZ50.BLN and CZ95.BLN
C
      NPOUT=181
C
      WRITE(21,6500) NPOUT
      DO 6000 IO=1,180
        WRITE(21,6501) CZ50X(IO),CZ50Y(IO)
 6000 CONTINUE
      WRITE(21,6501) CZ50X(1),CZ50Y(1)
C
      WRITE(26,6500) NPOUT
      DO 6001 I1=1,180
        WRITE(26,6501) CZ95X(I1),CZ95Y(I1)
 6001 CONTINUE
      WRITE(26,6501) CZ95X(1),CZ95Y(1)
C
C   write capture zone areas to CZSTAT.OUT
C
      WRITE(22,*) 'Output from Uncertainty Analysis of CZ Modeling '
      WRITE(22,*)
      WRITE(22,*) '   CZ      Capture Zone Area   '
      WRITE(22,*) '   #       (sq.ft.)     (Ac)   '
      WRITE(22,*) '  ---  ---------------  -------  '
      WRITE(22,*)
      DO 6003 I3=1,NUMCZ
        ACRES=CZAREA(I3)/43560.0
        WRITE(22,6502) I3,CZAREA(I3),ACRES
 6003 CONTINUE
C
C   write the area of the 50th % CZ to output
C
      WRITE(22,*)
      WRITE(22,6503) AREA50
      WRITE(22,*)
C
C   write the cost of risk to the output file
C
      WRITE(22,*)
      WRITE(22,6504) DANAL
      WRITE(22,*)
C
C   write the variance of CZ modeling to the output file
C
      WRITE(22,*)
      WRITE(22,6505) VARCZ
      WRITE(22,*)
C
C   write the uncertainty (U) to the output file
C
      WRITE(22,*)
      WRITE(22,6506) UNCZ
      WRITE(22,*)
C
C   write the ZOC and ZOU capture zones to output
C
      WRITE(24,6500) NPOUT
      WRITE(25,6500) NPOUT
      DO 6004 I4=1,180
        WRITE(24,6501) ZOCX(I4),ZOCY(I4)
        WRITE(25,6501) ZOUX(I4),ZOUY(I4)
 6004 CONTINUE
      WRITE(24,6501) ZOCX(1),ZOCY(1)
      WRITE(25,6501) ZOUX(1),ZOUY(1)
C
C   formatting information
C
 6500 FORMAT(I5)
 6501 FORMAT(2X,F9.2,2X,F9.2)
 6502 FORMAT(2X,I3,2X,F12.1,5X,F7.1)
 6503 FORMAT(2X,'The area of the average capture zone is',F12.1)
 6504 FORMAT(2X,'The area of uncertainty in CZ modeling is ',
     1       F12.2,' acres')
 6505 FORMAT(2X,'The variance in capture zone areas is ',F17.1)
 6506 FORMAT(2X,'The uncertainty (U) in CZ modeling is ',F6.2)
      RETURN
      END
```